# GEOCHEMICAL CHARACTERIZATION OF MUDFLAT AND MANGROVE SEDIMENTS IN ZUARI ESTUARY

Ph.D THESIS

By
**Cheryl A. Noronha e D'Mello**
M.Sc.

JULY, 2016

# GEOCHEMICAL CHARACTERIZATION OF MUDFLAT AND MANGROVE SEDIMENTS IN ZUARI ESTUARY

THESIS

SUBMITTED TO THE GOA UNIVERSITY FOR THE AWARD OF THE DEGREE OF DOCTOR OF PHILOSOPHY

IN

MARINE SCIENCES

BY

**CHERYL A. NORONHA E D'MELLO**
M.Sc.

RESEARCH GUIDE

**PROF. G. N. NAYAK**

Department of Marine Sciences,
Goa University,
Taleigao, Goa, India -403206

JULY 2016

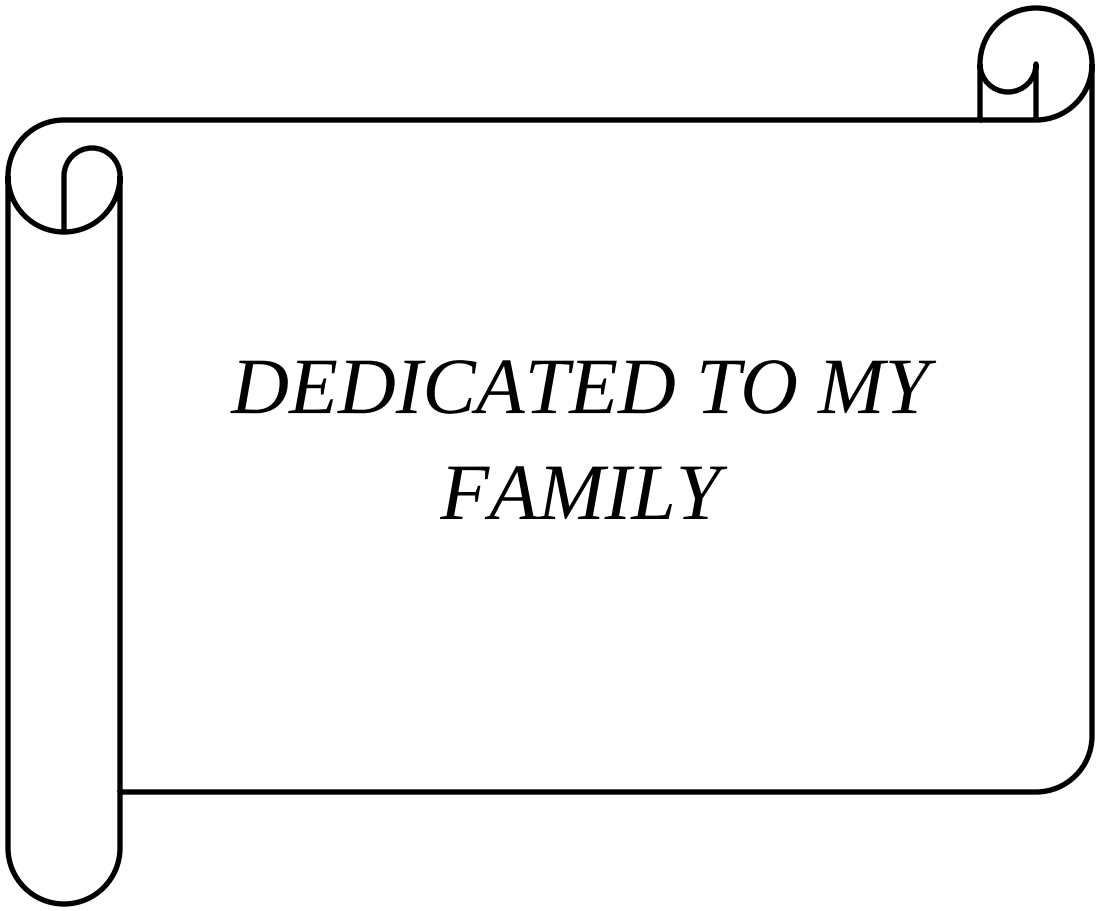
*DEDICATED TO MY FAMILY*

## STATEMENT

As required under the University ordinance OB.9.9 (iv), I state that the present thesis entitled "**GEOCHEMICAL CHARACTERIZATION OF MUDFLAT AND MANGROVE SEDIMENTS IN ZUARI ESTUARY**" is my original contribution and the same has not been submitted on any other previous occasion. To the best of my knowledge, the present study is the first comprehensive work of its kind from the area mentioned.

The literature related to the problem investigated has been cited. Due acknowledgements have been made wherever facilities and suggestions have been availed of.

Place: Goa University

Date : 19th April 2017

Mrs. Cheryl A. Noronha e D'Mello

## CERTIFICATE

This is to certify that the thesis entitled, "**GEOCHEMICAL CHARACTERIZATION OF MUDFLAT AND MANGROVE SEDIMENTS IN ZUARI ESTUARY**", submitted by Mrs. Cheryl A. Noronha e D'Mello for the award of the Degree of Doctor of Philosophy in Marine Science is based on her original studies carried out by her under my supervision. The thesis or any part thereof has not been previously submitted for any other degree, diploma, associateship, fellowship or similar titles in any universities or institutions. This thesis represents independent work carried out by the student.

Place: Goa University

Date: 19th April 2017

Prof. G. N. Nayak
(Research Guide)
Department of Marine Sciences,
Goa University, Goa

**Acknowledgements**

First and foremost, I would like to express my sincere gratitude to my research guide and supervisor Prof. G. N. Nayak, whose expertise, understanding, and patience, added considerably to my research experience. His systematic guidance helped me in all the times of research and in writing of this thesis. I would like to thank him for encouraging my work with many insightful discussions and suggestions, and the great effort he put into training me in the scientific field.

I would also like to thank the FRC members, Dr. N. B. Bhosle, retired Scientist, NIO, Goa; Prof. M. K. Janarthanam, Dean of the faculty of life sciences and environment; Prof. C. U. Rivonkar, Head of the Department of Marine Sciences and Prof. G. N. Nayak, for their encouragement, insightful comments, and thought provoking questions.

I wish to acknowledge Dr. S. R. Shetye, Vice Chancellor of Goa University and Prof. Y. V. Reddy, Registrar and their subordinates for their support and administrative help throughout the Ph.D. program. I also wish to thank Prof. Dileep Deobagkar, former Vice Chancellor of Goa University and Prof. V. P. Kamat, former Registrar, for their support and encouragement.

I am grateful to Dr. S.W.A. Naqvi, Director, NIO, Goa for permitting me to carry out some of the analysis at the institute. My sincere thanks go to Dr. V. P. Rao, Scientist, NIO, Goa, for assistance in the clay mineralogy analysis and Dr. Pratima Kessarkar, Scientist, NIO, Goa, for providing assistance in magnetic susceptibility measurements. Further, I wish to thank Dr. S. Kurian, Dr. Lidita Khandeparkar, Dr. Lina Fernandes Scientists, NIO, Goa and technical officers Mr. Girish Prabhu and Mr. B. G. Naik for their co-operation, support and suggestions during the analysis. I also wish to thank Dr. Sangeeta Jadhav, Dr. R. Shynu and A. Prajith, NIO, Goa for their help and support during the analysis.

My sincere thanks go to the faculty of department of Marine Sciences, Goa University, Prof. C. U. Rivonkar, Prof. H. B. Menon, Dr. S. Upadhyay, Prof. V.M. Matta and Dr. A. Can, for their encouragement.

I wish to acknowledge the non-teaching staff of the department of Marine Sciences, Mr. Yeshwant Naik, Mr. Samrat Gaonkar, Mr. Shatrugan Shetgaonakar, Mr. Ratnakar Naik, Ms. Reena Tari, Mrs. Mangal and Mrs. Concessao as well as the former staff, Mr. Ashok Parab and Mr. Rosario for their help and support. I also wish to thank Prof. Savita Kerkar, Head of the Department of Biotechnology, Prof. U.D. Muraleedharan, former Head of the Department of Biotechnology, Prof. B. F. Rodrigues, Head of the Department of Botany and non-teaching staff Mr. Redualdo Serrao, Mr. Ulhas and Mr. Martin from the Department of Biotechnology for their kind help.

I am also grateful to my colleagues in research, Dr. Deepti Dessai, Dr. Lina Fernandes, Dr, Ratnaprabha Siraswar, Dr. Samida Volvoikar, Dr. Anant Pande, Mr. Maheshwar Nasnodkar, Ms. Maria Fernandes, Ms. Purnima Bejugam, Ms. Shabnam Choudhary, Mrs. Janhavi Kamat, Ms. Tanu Hoskatta, Dr. Vinay Padte, Dr. Mahableshwar Hegde, Mr. Dinesh Velip, Ms. Vijaylaxmi Parwar, Ms. Mithila Bhat, Ms. Samiksha Prabhudessai, Ms. Sahita Desai, Mr. Ganesh Hegde, Mr. Shrivardhan Hulswar, Ms. Neha Shaikh, Dr. Nutan Sangekar, Dr. Shilpa Shirodkar, Dr. Renosh Remanan, Mr. Santosh Nulageri, Ms. Veloisa Mascharenhas, Mr. Vinit Lotlikar, Mr. Satyam Shirvoikar, Mr. Abhilash Nair, Mr. Vineel Deshpande, Mrs. Soniya Khedekar, Ms. Sweety Halarnekar, Ms. Cynthia Gaonkar, Ms. Kalpana Dhiman, Mrs. Nita Rane, Mrs. Nila Sankpal, Mr. Joshua D'Mello, Ms. Richita Naik, Mrs. Jesly Araujo, Mrs. Puja Naik, Mrs. Renu Paropkari and Mr. Siddesh Nagoji for their support during my Ph.D. research work.

Moreover, I specially thank Ms. Maria Fernandes, Mr. Maheshwar Nasnodkar, Ms. Purnima Bejugam, Ms. Tanu Hoskatta, Ms. Queenie Dias, Mr. Gautam Lolienkar, Mr. Akshay Parab, Mr. Amogh Mahavarkar, Mr. Sunil and Mr. Rajesh for their willing assistance during sampling. I also thank the people of Goa for providing information about the study area, helping us at the sampling locations as well as in collecting the sediment samples and for their hospitality during the field work.

Most importantly, none of this would have been possible without the love and patience of my family. My immediate family, to whom this thesis is dedicated to, has been a constant source of love, concern, support and strength all these years. I would like to express my heart-felt gratitude

to my family. My extended family has aided and encouraged me throughout this endeavor. Finally, there are my friends. We were not only able to support each other by deliberating over our problems and findings, but also happily by talking about things including research.

In conclusion, I recognize that this research would not have been possible without the financial assistance of the University Grants Commission Maulana Azad National Fellowship and the Goa University, Goa, and express my gratitude to these agencies.

Above all I thank almighty God for granting health, strength and wisdom, to undertake and complete this research work successfully.

Mrs. Cheryl A. Noronha e D'Mello

**Table of contents**

**List of tables**

**List of figures**

## Preface

An estuary is a dynamic environment in which sediment's received from various sources interact under the influence of different processes. The estuary comprises of the main channel, the intertidal areas like mudflats and wetland vegetation such as mangroves that act as enormous natural filters removing nutrients, pollutants and retain then in sediments. Metals received from the weathering of rocks from catchment area, the sea, and anthropogenic sources, are incorporated into sediments of mangroves and mudflats. The metals further are transformed, due to biogeochemical processes or are buried, forming a part of the sediment record. The metals accumulated within estuarine sediments can reach toxic levels and involve in bioaccumulation processes and uptake into the food chain. The assessment of metals in estuarine sediments is therefore, of prime importance as sediments act as a sink and a useful indicator of a long and medium term flux in the coastal zone.

The present study was carried out to understand the abundance and distribution of metals in sediments and the role of physicochemical and geochemical processes influencing the distribution of metals in the Zuari estuary, West coast of India, so as to apply them in the perspective of global environmental issues. Further, an attempt was made to study the concentration of metals in soft tissue of selected biota associated with sediments and to establish a relation between bioavailability of metals in sediments and bioaccumulation of metals in biota. The study is focused on the tracing the source of metals entering into the estuary, understanding their geochemical transformation in the estuary, their mobility and their uptake by estuarine biota.

The first chapter introduces the different aspects of an estuary, relating to definition and classification of estuaries and the various physical, chemical and biological processes that occur within the estuaries. Further, a brief outline is provided on the importance of estuarine sub-environments of interest i.e. mangroves and mudflats and the nature of the depositional environments. In addition, the different components of the estuarine sediments are presented with emphasis on metals. The chemical speciation of metals in the five sedimentary fractions and the bioavailability of metals are discussed with reference to uptake of metals by sediment

associated biota. Additionally, recent literature review is presented followed by the objectives of the study and the description of the study area. `

The next chapter describes the detailed analytical methodology for various sediment parameters, components and metals in sediment and biota that were used to achieve the objectives of the study. The details of the sampling and subsampling procedure and the standard analytical techniques are described along with the necessary operational precautions.

The third chapter describes the results of the various sedimentological and geochemical parameters that were analyzed. The results and discussions are divided in to three subsections. In the first section, the results of the sampling carried out during the premonsoon season of 2011 using sediment cores are discussed under two subsections of mangrove and mudflats. The sediment cores were analyzed for pH, grain size, clay mineralogy, magnetic susceptibility and bulk metals and metals in the clay fraction. The sedimentological parameters were used to interpret the distribution of metals in the sediments. Further, the sediment quality was assessed using the enrichment factor and geoaccumulation index. Speciation of metals was also carried out with depth to understand the mobility and bioavailability of the metals. Further the toxicity risk to sediment biota was assessed using standard reference tables and risk assessment code. In addition, the sediment components and metals abundance were compared with respect to mangroves and mudflats. The second section describes the results of the analysis of surface samples that were collected during the premonsoon, monsoon and post monsoon seasons. The variations in sediment parameters, bulk metal abundance and speciation of metals and their toxicity risk during the three different seasons were discussed. In the third section, the results of the sedimentological and geochemical parameters of sediments collected in the premonsoon season of 2015 after the imposition of a mining ban in 2012 were discussed and compare with the 2011 data set.

The fourth chapter deals with the bioaccumulation of metals by mangrove plants using pneumatophores and by sediment associated molluscs. The bioconcentration factor and biota sediment accumulation factor was calculated to understand the metal bioaccumulation ability and

identification of probable bioindicators. The fifth chapter provides a summary of the study along with conclusions. Lastly, the references are listed in alphabetical order.

# *Chapter 1*

# *Introduction*

## 1.1 Introduction

The coastal zone is characterized by a variety of landforms out of which estuaries have received considerable attention due to large land-sea interaction mechanisms (Bianchi, 2006; Buddemeier et al., 2008). Estuaries are complex and dynamic aquatic environments, where fresh water from river mixes with rhythmically intruding seawater of completely different composition. Estuaries are major nutrient suppliers to coastal oceans, breeding and nursery grounds for marine organisms and a potential fishery habitat. They act as transportation routes and also recreational places for humans (Yu et al., 2010; Liu et al., 2003).

The word “Estuary" is derived from the Latin "aestus", meaning the tide (American Geological Institute, 1960), and implies that tidal mixing is a pronounced process in estuarine environments. Cameron and Pritchard (1963) and Pritchard (1967) defined an estuary as a semi-enclosed and coastal body of water, with free communication to the ocean, and within which ocean water is diluted by freshwater derived from land. Kjerfve and Magill (1989) later defined an estuary as an inland river valley or section of the coastal plain, drowned as the sea invaded the lower course of a river during the Holocene sea-level rise, containing sea water measurably diluted by land drainage, affected by tides, and usually shallower than 20 m.

Freshwater inflow plays a key role in carrying continental material from the watershed to the estuary and in balancing effects of tidal inputs of saltwater and of evaporation in the estuary (Hedges et al., 1997). Physical, chemical, and biological interactions between terrestrial and coastal systems profoundly affect the transport and fate of material in to the estuary (Ip et al., 2007). Material is carried in, from the land via rivers and from the sea by the tides (Figure 1.1).

Waves and tides carry coarse marine sediments from the seabed to an estuary. Meanwhile, rivers carry finer sediments into the estuary. Tidal currents provide the steady supply of energy that causes sediment movement into and out of estuaries. Waves and swell at the entrances to estuaries can stir up large amounts of sediment, which move into the estuary by the incoming tide. Fresh river water floats over seawater. So when sediment-laden floodwaters enter an estuary, the finer suspended particles may be flushed out to sea quite quickly. But heavier particles sink to the bottom as the flow meets salt water. This results in

greater sediment deposition in the estuary. In addition, suspended and particulate material is removed on changes of physicochemical properties on interaction of fresh water and seawater.

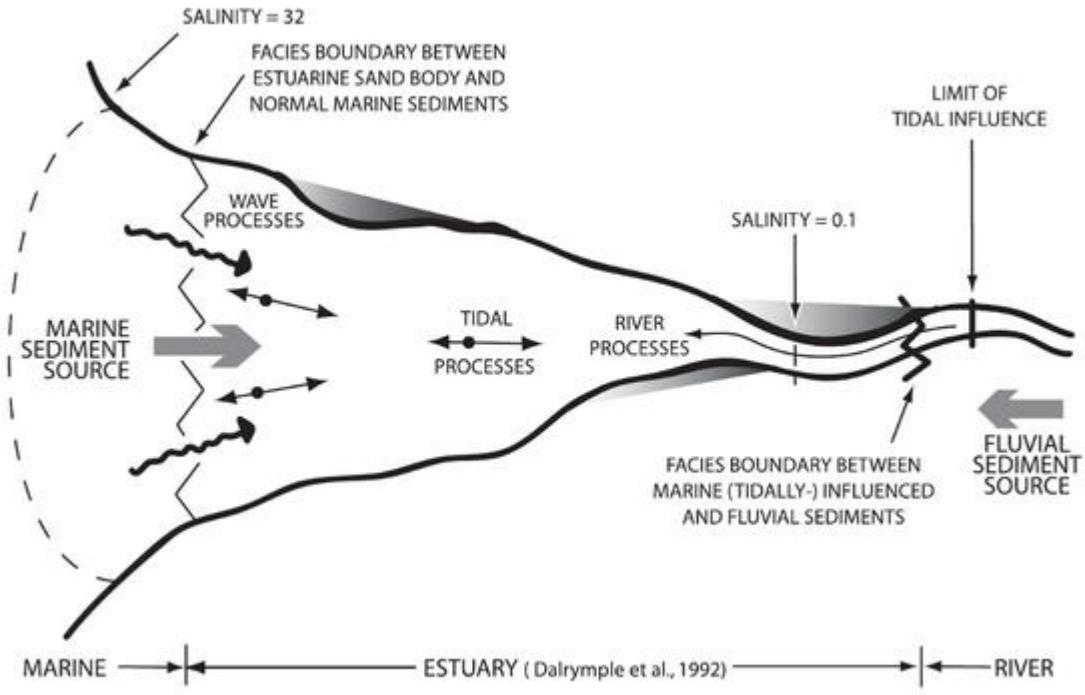


Figure 1.1: Classic estuarine zonation depicted from the head region where fluvial processes dominate, to the mid- and mouth regions where tidal and wave processes are dominant controlling physical forces, respectively. Differences in the intensities and sources of physical forcing throughout the estuary also result in the formation of distinct sediment facies. (Dalrymple et al., 1992; Bianchi, 2006)

Although all estuaries are analogous, in that they are semi-enclosed bodies of brackish water, a multiple criteria are used to classify them. According to their geological characteristics or geomorphology, estuaries are classified as coastal-plain estuaries, bar-built estuaries or lagoons, fjord-type estuaries, and tectonically caused estuaries (Pritchard, 1952; Valle-Levinson, 2010). Coastal-plain estuaries were formed by the gradual rise of sea level following the last glacial period, 10,000 to 15,000 years ago. They are typically wide (around several kilometers) and shallow (around 10 m), with large width/depth aspect ratio. Bar-built estuaries are semi-enclosed embayments with the formation of a sand bar or spit between the coast and the ocean created as a result of littoral drift. Fjords are found in high latitudes where glacial activity is intense. They are portrayed by an elongated, deep channel with a sill that is related to a moraine of either a currently active or an extinct glacier. Tectonic estuaries

were formed by earthquakes and fractures of the Earth's crust that generated faults in the regions near the ocean, causing the crust to sink and form a hollow basin that is filled by the ocean.

Further, based on stratification and circulation, estuaries have also been classified as salt wedge estuaries, vertically homogeneous estuaries and partially mixed estuaries. A salt-wedge estuary is highly stratified and has minimal mixing wherein the seawater forms a wedge, thickest at the seaward end, tapering to a very thin layer at the landward limit. The vertically homogenous estuary occurs when the river flow is low and strong tidal currents eliminate the vertical layering of fresh water floating above denser seawater. The saline water and fresh water tend to mix vertically, and at times laterally as well. Intermediate estuaries are partially mixed and exhibit circulation patterns that are somewhere between the salt-wedge and vertically homogenous estuaries wherein the deeper water layers remain more saline than the upper layers.

On the basis of water balance, estuaries are classified into three types: positive, inverse and low-in flow estuaries. In positive estuaries, freshwater additions from river discharge, rain and melting ice exceed freshwater losses from evaporation or freezing and a longitudinal density gradient established. Inverse estuaries are found in arid regions where loss of freshwater from evaporation exceeds freshwater additions from precipitation and the river discharge scarce into these systems. Low-inflow estuaries also occur in regions with high evaporation rates but with a small influence from river discharge.

Based on tidal range, Hayes (1975) defined three types of estuaries: microtidal, mesotidal and macrotidal estuaries. Microtidal estuaries have a tidal range less than 2 m and are dominate by wind and wave action. The principal forms of deposition are river and flood deltas, wave built features such as spits, bars, beaches, and storm deposits. Mesotidal estuaries have a tidal range between 2 m and 4 m. Macrotidal estuaries have a tidal range greater than 4 m and are generally have a broad and funnel shaped mouth with linear sand bodies occupying the central portion and extensive tidal flats and salt marshes bordering the coasts

Estuaries contain many different habitats such as shallow open waters, sandy beaches, salt marshes mud and sand flats, rocky shores, mangrove forests, seagrass beds, river deltas and tidal pools. Out of these, mangrove and mudflats have received considerable attention as they

are very effective in coastal protection, respond to sea level changes and offer an important habitat for wildlife, food and recreation.

Mangroves are a diverse group of trees, palms, shrubs, vines and ferns that have the ability to thrive in waterlogged saline soils that are subjected to regular flooding by tides. The global mangrove area is estimated to cover l00000 $km^2$ to 230000 $km^2$ of sheltered coastal intertidal land which is <0.2% of the global land surface area (Bunt, 1992; Snedaker, 1984; Jennerjahn and Ittekkot, 1997) and accounts for approximately 75% of coastal vegetation (Linden and Jernelov, 1980). They are highly specialized plants that have developed specialized adaptations to the unique environmental conditions in which they are found. Mangrove forests are typically found in the tropical and sub-tropical latitudes, lying between the land and the sea in sheltered coastal areas that are subjected to tidal influence and are among the most productive ecosystems (Kathiresan and Bingham, 2001; Kathiresan, 2002). The mangrove ecosystems play an important role in carbon, nitrogen, phosphorus, and sulfur cycles, in addition to providing protection to coastal areas from waves and storms (Meng et al., 2016). Mangroves are known for being sites for sediment deposition and are associated carbon and nutrients (Eyre, 1993; Furukawa and Wolanski, 1996). The mangroves trap sediment by their complex aerial root structure and are an important sink for suspended sediments and thus function as land builders (Woodroffe, 1992; Wolanski et al., 1992; Wolanski 1994, 1995; Furukawa et al., 1997). Mangroves tend to accelerate the sedimentation process with the annual sedimentation rate in mangroves ranging from 1 to 8 mm (Bird and Barson, l977; Woodroffe, l992). In addition, they are vital habitats for aquatic organisms, birds and other terrestrial animals. The mangrove trees supply large amounts of organic matter, which is consumed by many small aquatic animals. These organisms provide food for larger fish and other animals. Mangroves also help to maintain water quality by filtering the silt from runoff and recycling nutrients.

Mudflats are coastal wetlands formed in sheltered shores where greater amounts of sediments, detritus are deposited by the rivers or tides. They are frequently associated with estuaries, and are usually situated adjacent to mangroves and comprise around 7 % of total coastal shelf areas (Stutz and Pikey, 2002). Intertidal mudflats play a critical role in the estuarine exchange of marine and continental supplies of nutrients and sediments. The mudflat habitat represents a transition from subtidal sediment areas that are successively flooded and uncovered by tides and/ or river discharge variations (Deloffre et al., 2005,

2007). Mudflats are the interface between the flood plain and the main river channel, and are characterized by a cross-shore slope typically separated into two specific environments: the shore in the upper part of the mudflat that flooded during high spring tides; and the tidal flat that is the lower part of the mudflat and has an upper limit corresponding to the highest sea level reached during the mean tidal range (Jaud et al., 2016). The sediments consist mainly of fine particles, mostly in the silt and clay fraction. Little oxygen penetrates through the cohesive sediments, and an anoxic layer is often present within millimeters of the sediment surface. Mudflats generally support very little vegetation other than green algae. Their biodiversity centers on the range of invertebrates living in the sediment which are biologically productive. The intertidal mudflats support communities characterized by polychaetes, bivalves and oligochaetes and large numbers of birds and fish. Mudflats provide an important nursery and feeding ground for many fish species.

The characteristics of an estuary are determined by the dynamics of various processes and the sediment sources. Material is imported from the river and its catchments, and sea into the estuary where the transformation of material takes place. Post transformation, a part of the material such as a particulate matter is retained in the estuary in sediments whereas the dissolved material is exported to the sea (Turner and Riddle, 2001). The main sediment sources of an estuary are from existing base material, terrigenous material held in the catchment and sand transported from the open-coast marine environment. In addition particulate and dissolved matter composed of organic and inorganic material is added in to the estuary that may be supplied naturally or from anthropogenic sources. The distribution of the sediments within an estuary is regulated by interactions between the available sediments, bottom morphology and flow hydrodynamics (Frey and Howard, 1986). The dynamics of sediment transport depend on the water circulation, salinity, biological interaction, and sediment type (Wang and Andutta, 2013). The interaction among cohesive sediments (mud) is different from that of non-cohesive sediments (sand). Cohesive sediments may aggregate, forming flocs by the flocculation process caused by chemical or biological interaction. Flocculation increases the settling velocity of sediment particles. Chemical flocculation is started by salinity, ions that attach to the small mud particles, cause electronic forces between the particles, which start aggregating and thus forming a larger mud floc. In contrast, “Biological flocculation” is caused by bacteria and plankton that produce exopolymer and binds mud particles leading to formation of extremely large flocs of ~1000 µm in size (Wolanski et al., 2012).

Sediments that are transported by the estuarine waters typically cover a range of sizes from less than 0.002 mm to more than 4 mm, with the finer sizes dominant in most estuaries. Estuarine sand is typically composed of quartz, although other minerals such as feldspar or various heavy minerals such as magnetite may be present depending on the sediment source. The fine sediments in estuaries are mixtures of inorganic minerals, organic materials, and biochemicals. Mineral grains usually consist of clays such as montmorillonite, illite, and kaolinite and chlorite, and non-clay minerals like quartz and carbonate. Organic materials comprise of biogenic detritus and microorganisms (McNally and Mehta, 2004).

The estuarine system is mainly an area of deposition and acts as an important sink for metals in the environment. Metals are supplied to the estuary by natural factors such as chemical leaching of bedrocks, water drainage basins, and runoff from banks while the discharge of urban and industrial waste water, combustion of fossil fuels, mining and smelting operations, waste disposal and transportation activities are the important anthropogenic sources of the metal pollutants (Abdullah et al., 1999; Shazili et al., 2006; Dragun et al., 2009; Pardo et al., 1990; Zhou et al., 2008). Metals brought into the estuary are transferred from solution to sediments by adsorption onto suspended particulate matter, and are deposited with relatively short lag times and tend to get trapped and accumulate in the sediments (Spencer et al., 2003). The distribution and accumulation of metals are influenced by the sediment texture, mineralogical components and physical transport (Buccolieri et al., 2006; Marchand et al., 2006). The metals get assimilated in the sediment along with organic matter, Fe/Mn oxides, sulphide, and clay and thus undergo alterations in their speciation due to geochemical modifications by processes such as dissolution, precipitation, sorption and complexation when discharged into the estuary and form several reactive components (Lim et al., 2012). The sediment characteristics such as pH, cation exchange capacity, organic matter content, redox conditions, chloride content and salinity determine metal sorption and precipitation processes, which are associated to the metal mobility, bioavailability and potential toxicity (Du Laing et al., 2002). The organic matter content in the sediments leads to relatively higher metal accumulation (Zhong et al., 2006). In addition, sediment grain size substantially influences the metal concentration in the estuarine sediments as the clay fractions that have a high specific surface area, favor adsorption processes (Thuy et al., 2000). Following deposition and burial, metals become subject to a variety of physical, chemical and biological processes which may mix and remobilize the metals into the water column (Lee and Cundy,

2001) or may be immobilized in the sediments for long periods of time and undergo compaction and diagenesis.

The chemical speciation of metals in sediments involves the identification and quantification of the different forms or phases of the metal present in the sediments and provides advanced information on the potential availability of metals to biota under various environmental conditions (Álvarez-Iglesias and Rubio, 2009; Fytianos and Lourantou, 2004; Gao et al., 2008; Rauret et al., 1998). The fractionation procedure can indicate the propensity for metals to be remobilized and can help distinguish those metals having a lithogenic origin from those with an anthropogenic origin (Förstner et al., 1990; Korfali and Jurdi, 2011). Tessier et al. (1979) devised a fractionation procedure which defined the desired partitioning of trace metals into fractions that are likely to be affected by various environmental conditions i.e. exchangeable, bound to carbonates, bound to iron and manganese oxides, organic matter/sulfide bound and the residual fraction. The metals in the exchangeable fraction are likely to be affected by sorption-desorption processes such as weakly bound to clays, hydrated oxides of iron and manganese and humic acids while the metals in the carbonate fractions can be associated with sediment carbonates and this fraction is susceptible to changes of pH. Together the exchangeable and carbonate fractions are known as the labile fraction (Perin et al., 1985). The third fraction of sediment consists of metals bound to iron and manganese oxides and these oxides are excellent scavengers for trace metals (Gutierrez, 2000) and are thermodynamically unstable under anoxic conditions. The fourth fraction consists of trace metals bound to various forms of organic matter such as detritus, humic and fulvic acids etc, through complexation and peptization phenomenon. A large amount of sulfides are also leached into this fraction. Under oxidizing conditions in natural waters, the degradation of organic matter leads to the release of soluble trace metals. The residual fraction of the sediments consists of primary and secondary minerals which may retain trace metals within their crystal structure and are not released easily into solution. The first four fractions are known as the bioavailable fraction as they exhibit mobility and are potentially available for uptake by organisms. The mobile fractions introduced by anthropogenic activities remain bound to the exchangeable, the carbonate and the easily reducible phases (Nair, 1992). The sediment-associated metals have the potential to be ecotoxic due to their mobility and bioavailability, and this in turn affects both ecosystems and life through a process of bioaccumulation and biomagnification, respectively (Buccolieri et al., 2006; Ip et al., 2007). Thus, evaluating metal speciation can provide detailed information about the

origin, mobilization, contamination risks, biological availability and toxicity of metals (Yang et al., 2014).

As sediments are often the final repository of metals, accumulation of high concentrations of metals can present a risk to organisms (Casado-Martinez et al., 2013). Metals normally occurring in nature are not harmful to the environment, because they play an essential role in tissue metabolism and growth of plants and animals (Amundsen et al., 1997). However, metals like Cu, Zn, Fe, Co, Mo, Ni, Si, and Sn become predominantly toxic when their level exceeds the limit, and V, Cd, Pb, and Hg are prominently classified as toxic because of their detrimental effect even at low concentrations (Michael, 2010). Marine organisms can accumulate metals in their tissues that may threaten the health of organisms higher in the food chain through trophic transfer to terrestrial, estuarine and eventually coastal species that become prey for oceanic predators and humans (Boyle et al., 2008; Cheung and Wang, 2008). Metals are ingested of metal-enriched sediment and suspended particles during feeding, and by uptake from solution (Luoma, 1983). The ecological risk posed by metal-contaminated sediments depends strongly on the sediment characteristics, specific chemical forms of the metals, influencing their availability to aquatic organisms (bioavailability) and the ability of these organisms to accumulate (bioaccumulation) or remove metals. The efficiency of bioaccumulation via sediment ingestion is dependent on geochemical characteristics of the sediment. Various accumulation patterns have been described regulating the uptake of metals defined by the balance between uptake and excretion rates (Luoma et al., 2008; Rainbow, 2002) and by detoxification processes usually involving proteins such as metallothioneins (Casado – Martinez et al., 2010; Greim and Snyder, 2008; Walker et al., 2012).

Thus, the analysis of estuarine sediments offers certain advantages. The surface sediment often exchanges with suspended materials, thereby affecting the release of metals to the overlying water (Zvinowanda et al., 2009). As a result, the top few centimeters of the sediments reflect the continuously changing present-day degree of contamination, whereas the bottom sediments record its history (Seshan et al., 2010). Therefore, the metal concentration in sediment core profiles give information on the weathering processes and post- depositional mobility of metals (Subramanian and Mohanchandran, 1994).

## 1.2 Literature review

Table 1.1 Literature survey of the research studies carried out of late in India and other regions of the world

| Authors | Parameters analyzed | Observations |
|---|---|---|
| Prajith et al., 2016 | Grain size, organic carbon, major elements and trace metals, speciation of metals | Major elements and trace metals were analyzed in sediment cores of the Mandovi estuary to investigate their distribution, provenance and early diagenesis. The results showed that the sediment texture ranged from clayey silts to sand-dominated sediments and the organic carbon content was higher in fine-grained sediments. The contribution metals Ti, V, Cr and Zr to the sediments were probably from the laterites of the hinterland and abundant Fe and Mn in the estuary were due to the anthropogenic activities on the shore. The trace metals were redistributed in the organic-rich sediments due to early diagenetic processes. In addition, the sediments showed significant pollution by Mn and Cr and the high Mn content is susceptible to be mobilized along with redox-sensitive metals under reducing conditions. |
| Prajith et al., 2015 | Grain size, organic carbon, magnetic parameters, Fe and Mn | The magnetic properties of sediments were examined in 7 gravity cores that were collected along transect of the Mandovi estuary, to understand sediment provenance and pollution. The magnetic parameters indicated that hematite and goethite dominated in the sediments of the upper/middle estuary and magnetite-dominated in the sediments of the lower estuary/bay and the two sediment types were discernible because of the |

| | | |
|---|---|---|
| | | deposition of abundant ore material in the upper/middle estuary whereas detrital sediment were deposited in the lower estuary/bay. The enrichment factor and the index of geo-accumulation of metals indicated significant to strong pollution by Fe and Mn in the upper/middle estuary. |
| Kessarkar et al., 2015 | Magnetic parameters | The environmental magnetic properties of sediments of the Mandovi and Zuari estuaries and the adjacent shelf were investigated. The study revealed that the magnetic susceptibility (χlf) and saturation isothermal remanent magnetization (SIRM) values of sediments were highest in upstream and, decreased gradually towards the downstream region of the estuary and were lowest on the adjacent shelf. The χlf values of the Mandovi estuary were two to four folds higher than those in the Zuari. In addition, the sediments of these two estuaries showed the enrichment of older magnetite after the mining ban. |
| Rao et al., 2015 | Grain size, clay minerals, Sr- Nd isotopes | The clay mineralogy and Sr-Nd isotopes of the suspended particulate matter (SPM) and the bottom sediments in the Mandovi and Zuari estuaries were investigated to determine the provenance and role of estuarine processes on their distribution. It was reported that kaolinite and illite followed by minor gibbsite, goethite and chlorite are the intense chemical weathering products of the laterites in the hinterland whereas smectite may have formed in the coastal plains. The high $^{87}Sr/^{86}Sr$ ratios at river end stations of both estuaries indicated intense chemical weathering of the hinterland laterites while the ƐNd |

| | | |
|---|---|---|
| | | values indicated the influence of lateritic weathering and anthropogenic contribution of ore material to the SPM and the bottom sediments of both the estuaries. |
| Venkatramanan et al., 2015 | Salinity, grain size, organic matter, speciation of metals in sediments | A study was carried out to estimate the concentrations of the metals Fe, Mn, Cr, Cu, Co, Ni, Pb and Zn in surface sediments from the Tirumalairajan river estuary with an aim to investigate their speciation, the effects of grain size, physico-chemical parameters and organic matter, to trace the metal source and to understand the seasonal variation and the geochemical accumulative phase of the metals. The results revealed that metals were higher in the residual fraction and were thus derived mainly from geogenic origin in addition to minor contribution from anthropogenic origin. The fine sediments and organic matter acted as efficient scavengers for metals and the metal concentrations posed a low environmental risk. |
| Kumar and Ramanathan, 2015 | Grain size, speciation of metals | The study was conducted to highlight the distribution of trace metals in the mangrove sediments of the Sundarbans in India and Bangladesh using a speciation technique to document the bioavailability and the environmental hazards associated with the operationally defined chemical forms of trace metals. The results indicated the dominance of anthropogenic activity and the lack of freshwater flow affected the speciation profile of trace metals in the mangrove sediments. |

| | | |
|---|---|---|
| Birch et al., 2015 | Fine nutritive roots, leaves and pneumatophores, metals | The study was carried out to determine the remediation effectiveness of a former Pb-contaminated industrial site in Homebush Bay in the Sydney estuary (Australia) through the sampling of intertidal sediments and mangrove (Avicennia marina) tissues (fine nutritive roots, pneumatophores, and leaves). The results indicated that since remediation carried out 6 years ago, the metal concentrations in the surficial sediment have increased which may have been sourced either from the surface/ subsurface water from the catchment or more likely the remobilized contaminated sediments from the un-remediated regions. The results also indicated that with increasing surficial sediment metal concentrations, the metal levels in mangrove tissue are likely to increase over time. |
| Fernandes and Nayak, 2015 | Grain size, organic carbon, speciation of metals | Sediment cores collected from mudflat environments of the Swarna and Gurpur estuaries, India were studied to understand the bioavailability of metals in sediments and their probable toxicity. Most trace metals in both the cores were mainly from lithogenic source and the metal speciation indicated that Mn, Ni, Cu and Co concentrations in Gurpur estuary indicated anthropogenic additions in recent years whereas in Swarna estuary most metals exhibited diagenetic remobilization and diffusion to the water column from surface sediments. |
| Veerasingam et al., 2015 | Grain size, trace metals, scanning electron microscopy | The concentrations of trace metals (Fe, Mn, Cu, Cr, Co, Pb and Zn) in three sediment cores were analyzed to assess the depositional trends of metals and their respective contamination levels in the Mandovi estuary, west coast of India. The |

| | | |
|---|---|---|
| | | enrichment of trace metals suggested an excess of anthropogenic loadings (including mining activities) occurred lately. Scanning electron microscope images of core sediments distinguished the shape, size and structure of particles derived from lithogenic and anthropogenic sources. The geo-accumulation index (Igeo) values indicated that Mandovi estuary sediments are 'moderately polluted' with Pb, and 'unpolluted to moderately polluted' with Fe, Mn, Cu, Cr, Co and Zn. |
| da Silva et al., 2014 | Grain size, cation exchange capacity, organic matter, pH, speciation of metals in sediments | The study was carried out on mangrove sediments of the Tibiri River Estuary, Brazil to evaluate the three geochemical fractions of trace metals (Cd, Cr, Cu, Ni, Pb and Zn) in sediments i.e. the exchangeable/acid-soluble, reducible and oxidizable fractions and to assess the risks of trace metals using the TEL/PEL and ERL/ERM guide values for the protection of the aquatic life. The results demonstrated that metal levels were below TEL (Threshold effect level) and ERL (effect range low) ranges and was associated with occasional adverse biological effects for the aquatic life. |
| He et al., 2014 | Mangrove leaves and stems, metals | Heavy metals in mangrove sediments and plants were assessed in the Futian mangrove forest of Shenzhen, China to evaluate the characteristics of heavy metal contamination, that included essential elements (Cu and Zn) and non-essential elements (Cr, Ni, As, Cd, Pb and Hg). The results indicated that the heavy metals Cd, As, Pb and Hg contents were higher than the background values in sediments while in mangrove plants' leaves and stems, concentrations of Cu, Zn and As were |

| | | |
|---|---|---|
| | | higher. The high heavy metal concentrations in sediments and low levels in leaves and stems indicated that mangrove plants actively avoided the uptake of heavy metals even when sediment metal concentrations are high. The high bioconcentration factors for Cr implied its potential use as a temporal Cr contamination indicator in sediments. |
| Chakraborty et al., 2014 (a) | Sediment grain size, total carbon, total nitrogen, metals in mangrove sediments and roots, kinetic speciation of Ni and Cu in the mangrove sediments | Kinetic speciation study was carried out to determine the concentrations of labile metal-complexes and their dissociation rate constants in the mangrove sediments of the Divar Island in Goa, India to establish a linkage between chemical speciation of copper and nickel and their bioavailability in the mangrove ecosystem. It was found that the bioaccumulation of both the metals gradually increased with the increase in concentrations of the labile metal complexes and their dissociation rate constants in the mangrove sediments. In addition, the concentration of labile metal complexes and their dissociation rate constants in mangrove sediment can be a useful indicator of their bioavailability. |
| Chakraborty et al., 2014 (b) | Metals in sediments | This review comprehended the changes in metal contamination levels with time in surface estuarine sediments around India. This study indicated that estuarine sediments from the east coast of India were comparatively less contaminated by metals than the west coast. In addition, the sediments of estuaries that were located near major cities were found to be more contaminated by metals. An improvement in estuarine sediment quality over time around India was noted. |

| | | |
|---|---|---|
| Zhang et al., 2014 | Acid volatile sulfides, organic fraction, sediment texture, pH, heavy metals, redox potential, salinity, nutrients, benthic organisms, hydrological kinetic conditions, temperature, geographic position, adsorption time | The mechanisms of sediment properties such as the acid-volatile sulfides, organic matter, texture and geology, organism behaviors influencing the bioavailability of metals were analyzed in this review. It was noted that under anoxic conditions, AVS reduced the solubility and toxicity of metals, while organic matter, Fe–Mn oxides, clay or silt stabilized heavy metals in conditions of elevated oxidative–reductive potential. Factors including the variation of pH, redox potential, aging, nutrition and the behavior of benthic organisms in sediment also largely alter metals mobility and distribution. |
| Fernandes and Nayak, 2014 | Sediment pH, sediment texture, organic carbon, total phosphorus, total nitrogen, metals and their speciation | The study assessed the concentration, distribution and speciation of metals (Fe, Mn, Cu, Pb, Co, Zn and Cr) in intertidal sediments of Mumbai. The results revealed the significant role of organic matter and grain size as metal carriers. Based on the metal concentrations and the various sediment quality guidelines employed, the Ulhas estuary displayed greater metal contamination levels as compared to the Thane creek. However, the speciation results indicated a high percentage of metals in the residual fraction of both the sites that suggested a low risk to the aquatic biota of the region, except for Mn in sediments of Thane creek. |
| Volvoikar and Nayak, 2014 | Grain size, organic carbon, metals in bulk sediments and the clay fraction of sediments | Sediment cores from the intertidal mudflats of Vaitarna estuary, west coast of India were studied to investigate the distribution of sediment texture, organic carbon, metals (Fe, Mn, Al, Cu, Zn, Co, Ni, Pb) in bulk sediments and clay-sized fraction (<2 |

| | | |
|---|---|---|
| | | microns). The results demonstrated that Fe-Mn oxy-hydroxides controlled the distribution of most metals in the core collected towards the lower middle estuary and the mouth. The greater deposition of metals in the clay fraction in recent times was due to increased marine inundation that caused greater flocculation and deposition of metals and finer clay particles. The metals associated with the clay fraction were least affected by anthropogenic activities while the metals that showed enrichment in the bulk sediments implied the association of metals with the coarser sediment particles and Fe-Mn oxy-hydroxides, thus indicating their anthropogenic additions along with lithogenic inputs. |
| Kathiresan et al., 2014 | Metals in sediments, mangrove bark, root and leaves | The study was carried out to analyze the concentrations of 12 micro-nutrients (Al, B, Cd, Co, Cr, Cu, Fe, Mg, Mn, Ni, Pb, and Zn) in various plant parts of *Avicennia marina* and its rhizosphere soil of the south east coast of India. The sediments held more levels of metals than plant parts, but within the permissible limits of concentration. The bark and root accumulated higher concentrations of trace elements than other plant parts. The essential elements accumulated in higher concentrations in mature mangrove forest while non-essential elements accumulated high metal concentrations in the industrially polluted mangroves. |
| Birch et al., 2014 | Oyster tissue, metals, sediments, SPM | The study aimed to deduce the relationship between metals in sediments and metal bioaccumulation in oyster tissues in the Sydney estuary, Australia. The SPM and surficial sediment contained high Cu, Pb |

| | | |
|---|---|---|
| | | and Zn concentration. The oyster tissue metal content varied greatly at a single locality over temporal scales of years. The Oyster tissue was found to exceed consumption levels for Cu. It was proposed that the bioaccumulation of metals in oyster tissue is a useful indicator of anthropogenic influence in estuaries. |
| Nath et al., 2014 | Metals in sediments, pneumatophores, bioavailability | Heavy metal concentrations in pneumatophore tissues and ambient sediments from Sydney Estuary, Australia were investigated to assess the bio-indication potential of *Avicennia marina*. The results indicated that the metal concentrations in sediment were mostly above the Australian interim sediment quality guidelines and the enrichment factors indicated "very severe" modification of sediment. High bioconcentration factors were observed for Cu and Ni in comparison with other metals (As, Cd, Co, Cr, Pb and Zn). In addition, a strong, positive relationship between metals in sediments and pneumatophores suggested the potential use of these tissues as a bio-indicator of estuarine contamination and that metals are entering the biotic environment. The study further highlighted the positive role of mangroves in metal sequestration from sediments and the water column and thus protecting the estuarine environments from pollution. |
| Kesavan et al., 2013 | Metals in sediments, shells and tissues of molluscs. | The concentration of metals (Cd, Co, Cu, Fe, Mg, Mn, Pb, Zn) were analyzed in sediments, shells and tissues of molluscs i.e. *Meretrix meretrix*, *Crassostrea madrasensi*s and *Cerithidea cingulata* from the Uppanar Estuary, southeast coast of India. |

| | | |
|---|---|---|
| | | The results demonstrated that the concentrations of the heavy metals analyzed exhibited spatial variations in sediments, tissues and shells. The concentration of heavy metals in the tissue was higher than the shell. Furthermore, it was proposed that oysters are particularly recommended as biomonitors over bivalves, due to their strong accumulation patterns for many metals, their large size and their local abundance whereas the bivalves assimilate metals from solution and suspended material. |
| Shynu et al., 2013 | Suspended particulate matter, salinity, rare earth elements, major elements | The concentrations of Al, Fe, Mn and rare earth elements (REE) were measured in suspended particulate matter (SPM) and surficial sediments from the Zuari estuary and the adjacent shelf to understand their distribution, provenance and estuarine processes. The results indicated that the REE of SPM/sediment is dominated by Fe, Mn ore dust and, its distribution along transect is influenced by the estuarine turbidity maximum (ETM). The ETM and seasonal circulation in the estuary controlled the mixing and the advective transport of particulates to the shelf during monsoon and into the estuary during dry season. This study indicated that the sediment contribution to the shelf from tropical, minor rivers is controlled by the hydrodynamic conditions in the estuaries. |
| Singh et al., 2013 | Grain size, organic carbon, major elements and metals | This study presented the variation in sediment components and metal distributions between three cores collected from three mudflats of the Zuari estuary. The cores collected from upper middle estuarine mudflats showed higher values of finer |

| | | |
|---|---|---|
| | | fractions, TOC and metals, than the core collected near the river mouth. Mn, Ca, and to some extent with Fe and Zn in sediments were likely of local anthropogenic inputs. Overall, the highest concentrations of metals were found in the upper middle estuarine mudflats and may be attributed to the nearby mining zone and the transportation of ore by barges in these water courses. In the lower estuarine core, the diagenetic signal was masked by the high input of Fe and Mn. The enrichment factors revealed a high degree of metal contamination in sediments. |
| Rumisha et al., 2012 | Organic matter, sediments grain size, metal analysis in sediments and molluscan tissues | The effects of trace metal pollution on the community structure of soft bottom molluscs were investigated in intertidal areas of the Dar es Salaam coast, Tanzania. The result revealed that the community structure of the soft bottom molluscs along the Dar es Salaam coast was influenced by trace metals pollution. The soft bottom molluscs exhibited species-specific responses to specific contaminants wherein the gastropods *L. aberrans*, *A. fortis and A. ovata* were very sensitive to trace metals pollution whereas the gastropod *M. honkeri* was tolerant to As and other trace metals. The study also revealed that soft bottom molluscs exhibited species-specific responses to specific contaminants due to the different capabilities in accumulating and regulating toxicants. |
| Palpandi and Kesavan, 2012 | Metals in sediments and gastropod shell and tissue. | The objective of the study was to estimate the levels of the metals Fe, Al, Mg, Mn, Cd, Cu, Pb, Zn, Cr and Ni in mangrove sediments of the Vellar estuary, Southeast coast of India and shells and soft |

| | | |
|---|---|---|
| | | tissues of the mangrove gastropod *Nerita crepidularia.* It was found that *N. crepidularia* accumulated higher concentrations of heavy metals than the ambient environment and Cu and Mn, in particular and suggested that the organism may therefore be used as a biomonitor of certain heavy metals in mangrove environment. |
| Gupta and Singh, 2011 | Metals in Molluscs | The objective of this study was to understand the use of different species of molluscs as cosmopolitan bioindicators for heavy metal pollution in aquatic ecosystems. The review described the potential ecological effects of rising levels of heavy metals concentrations in the environment due to their highly bioaccumulative nature, persistent behavior, and higher toxicity and bioamagnification capabilities. They proposed that molluscs reflect the high degree of environmental contamination by heavy metals and are useful bioindicator tools. The metals burden in molluscs may reflect the concentrations of metals in the surrounding water and sediment, and may thus be an indication of the quality of the surrounding environment. |
| Fernandes et al., 2011 | pH, sediment components, total organic carbon, total nitrogen, total phosphorus , $^{210}$Pb and metals | Two sediment cores were collected from the intertidal regions of Manori creek near Mumbai, India and were analyzed to understand the distribution of selected elements and to identify the controlling factors, thereby determining the depositional environment of the region. The results indicated that the metal associations reflected the differences in the depositional environments of the sediments and factors such as low energy, mechanical processes, bioturbation, salinity, pH, |

| | | |
|---|---|---|
| | | sediment components and organic matter content in sediments influenced the mobility of metals and their distribution. In addition, it was reported that the inner area of the estuary received a greater input of organic matter from terrestrial as well as domestic and industrial discharges, whereas sediments near the mouth had typical marine organic matter composition as inferred from the C:N ratio. The concentration of metals near the mouth was also low, that indicated the concentrations were diluted by the mixing of freshwater and seawater. |
| Dessai et al., 2009 | Salinity , total suspended matter, grain size, organic carbon, metals in sediments, magnetic susceptibility parameters | Metals (Fe, Mn, Cr, Cu, Zn and Co) and sediment components in the surface sediments of Zuari estuary in three different seasons were analyzed to understand the various sources and factors controlling the abundance and distribution of the metals. In addition, the total suspended matter (TSM) concentration and salinity of near surface and bottom waters were measured. The results indicated that the concentration of most of the metals were higher during the pre-monsoon season. Further, high concentrations were noted at lower middle and lower estuary and also at few stations at the upstream end. Salinity, distribution of TSM, size of the sediment, organic matter, geomorphological setup, fresh water input from land and release of industrial waste within the estuary played a major role in the distribution and concentration of metals. The magnetic measurements indicated the dominance of haematite like minerals that aided in understanding the source |

| | | |
|---|---|---|
| | | and depositional processes. |
| Dessai and Nayak, 2009 | Grain size, organic carbon, bulk metals and speciation of metals in sediments. | Surface sediments from Zuari estuary, Goa were analyzed by a sequential procedure for metals Fe, Mn, Cu, Zn, Cr and Co to determine their distribution the in five geochemical phases. The total metal content, sand, silt, clay and organic carbon were also determined of the surface sediments. The results indicated an enrichment of metals probably due to anthropogenic inputs. The results obtained from the sequential procedure showed that Mn and Co were potentially bioavailable indicating their importance in toxicity whereas metals Fe, Cu, Zn and Cr were high in the residual phase. Further, it was reported that the main source of metals to the estuary was mining and its associated activities in the study area. |

### 1.3 Objectives

Earlier studies have focused on the sediment distribution, transport and geochemistry within the estuarine channel using suspended particulate matter, surface sediments and mudflat cores of the Zuari estuary. Further research is necessary to provide information on the distribution of metals and their speciation in the sediment to understand the deposition, migration and accumulation mechanisms, their bioavailability, bioaccumulation and toxicity to organisms associated with the sediments. Therefore, a comprehensive multi proxy approach analysis was carried out to understand the processes occurring in the estuary, specifically in the mangroves and mudflats as these depositional environments are sinks as well as sources for many metals, natural as well as anthropogenic. The present study was carried out along transect of the Zuari estuary with the following objectives:

1. To study the abundance and distribution of metals in sediments and to understand the role of physicochemical and geochemical parameters influencing the distribution of metals.

2. To study the concentration of metals in soft tissue of selected biota associated with sediments.

3. To establish a relation between bioavailability of metals in sediments and bioaccumulation of metals in biota.

### 1.4 Study area

The Zuari estuary is located on the west coast of India, is classified as a tide-dominated, coastal plain estuary and geomorphologically as drowned river valley estuary (Murty et al., 1976). The estuary has a basin area of 973 $km^2$, catchment area of around 550 $km^2$ and tidal range of 2.3 (Singh et al., 2013) with surface run off of 2247.4 MCM (Kessarkar et al., 2015). The Zuari River originates in Hemad– Barshem in the Western Ghats and is about 70 km in length. The hinterland of Zuari is covered by rocks of the Dharwar Super Group of the Archaean Proterozoic age represented by metamorphosed basic and acid volcanic rocks and sediments at the base, overlain by greywacke suite of rocks, which in turn, is followed by pyroclasts and tuffs with the associated chaemogenic precipitates of lime, manganese and iron and again overlain by greywacke suite of rocks (Gokul et al., 1985; Dessai et al., 2009). Most of these formations have been lateritized, with original unweathered rocks exposed only in coastal headlands, along steep slopes of high hills or in manmade cuttings like quarries, road cuts, and railway tunnels (Fernandes, 2009) The hinterland rocks of the Zuari estuary are subjected to intense chemical weathering under humid tropical climate conditions. Two thirds of the area in Goa is covered by laterite (Nayak, 2002), that has been formed after extensive leaching of other elements and due to the concentration of iron and aluminum. Alluvial and loamy soils are found along the riverbanks and are rich in minerals and humus. River flow dominates during monsoon, but in the remaining period, tidal flow dominates and the lower estuary becomes an extension of the sea (Shetye et al., 2007). The Cumbharjua canal of length around 17 km connects the Mandovi and Zuari at distances of 14 and 11 km, respectively, from their mouths. The catchment areas of the adjacent Mandovi and the Zuari estuaries are known for open cast mining of ferromanganese ores. The mined ore is stored in stacks on the river banks for loading onto barges that transport the ores to the Mormugao harbor located at the southern bank of the Zuari and loaded onto larger ships. Around 15 million tons of iron and manganese ore was transported annually along these rivers to the

nearby Mormugao harbor in 1990's (Satyanarayana and Sen Gupta, 1996) which increased to around 50 million tons in 2010's. The ore stored for transportation at different points on the shores of the estuary gets eroded and flushed into the estuaries during heavy monsoon rains and part of the ore and/or dust ultimately gets accumulated in the estuaries and is incorporated into sediments (Shynu et al., 2012; Alagarsamy, 2006; Dessai et al., 2009). The Cumbharjua canal adds much of the mining material to the Zuari during the monsoons and ebb tide (Dessai and Nayak, 2009). Iron ore was mined from the banded iron formations of Goa, India, and transported through the Mandovi and Zuari estuaries for six decades until the ban on mining from September 2012. Mining in Goa has resulted in an environmental threat, though that was first felt in the year 1978, as a consequence 287 mining concessions/leases were terminated in the year 2012, that led to a complete ban on mining (Nayak, 2002; Kessarkar et al., 2015). In addition to mining discharges, several jetties, barge building and repairing industries, constructions, industrial and domestic waste discharges along the estuary also release large amounts of organic and inorganic contaminants to the estuary. The estuary has a prominent cover of mangroves, the composition and configuration of which varies as per the salinity gradient from the mouth of the river to upstream (Misra and Vethamony, 2015). The mangroves are subjected to increased pressure due to increasing amount of urbanization in recent times. There are also prominent mudflats environments that extend from the lower estuarine region to the upper middle estuarine region of the Zuari estuary at the fringes of the mangroves.

# *Chapter 2*

# *Materials and Methods*

## 2.1 Introduction

Sampling is the process or technique of selecting a representative part of a field site in a particular environment for the purpose of determining parameters or characteristics of the entire environment. The sampling strategy is critically important and should be undertaken with caution in order to represent the sampling site and achieve the objectives. Maintaining the integrity of the collected sample is of primary concern as the way in which sediment samples are collected, processed, transported, and stored might alter metal complexation, bioavailability and concentration by introducing contaminants to the sample or by changing the physical, chemical, or biological characteristics of the sample. Choosing the most appropriate sampling device and technique depends on: (1) the purpose of the sampling; (2) the location of the sediment sample; and (3) the characteristics of the sediment sample. Further, techniques and materials should be selected to minimize sources of contamination and variation, and sample treatment prior to analysis should be as consistent as possible.

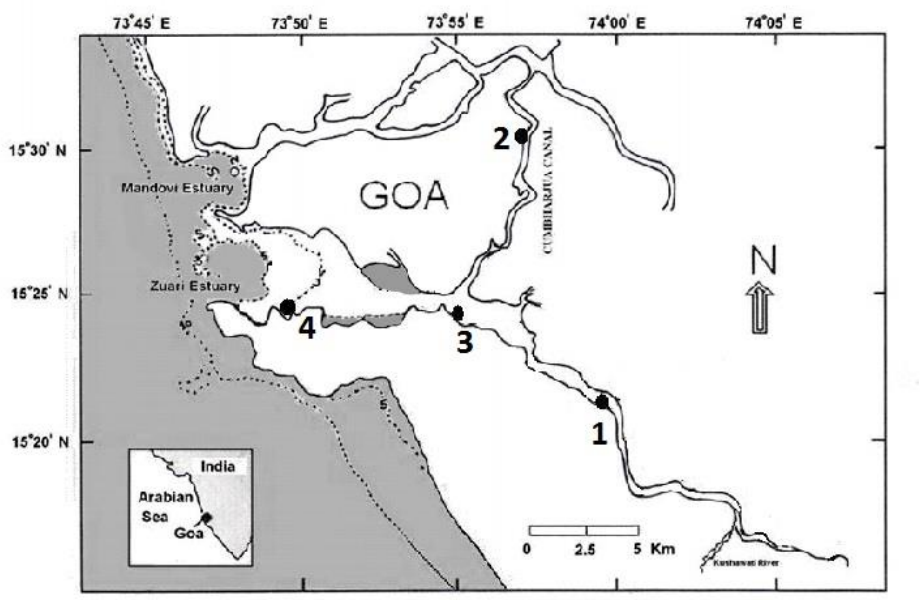


Figure 2.1: Sampling locations of sediment cores collected from the Zuari estuary. S1 - Upper middle estuary (Borim), S2 - Cumbharjua Canal, S3 - Lower middle Estuary (Cortalim) and S4 - Lower Estuary (Chicalim).

For the present study, sediment cores were collected from mudflat and mangrove environments from the upper middle-S1 (Borim), lower middle-S3 (Cortalim), lower estuarine-S4 (Chicalim) regions of the Zuari estuary and from mangrove environment of

adjoining Cumbharjua canal-S2 (Figure 2.1). Precautions were taken to avoid contamination of sediment samples during collection and handling and a systematic procedure for the analysis of the sediments was followed. All the apparatus were cleaned with acid and distilled water prior to collection and analysis Analytical grade reagents and standards were used in all the analysis. The procedure adopted on the collection, handling, and analysis of sediment and biological samples collected from the study area and the details of the protocol followed is given in figure 2.2.

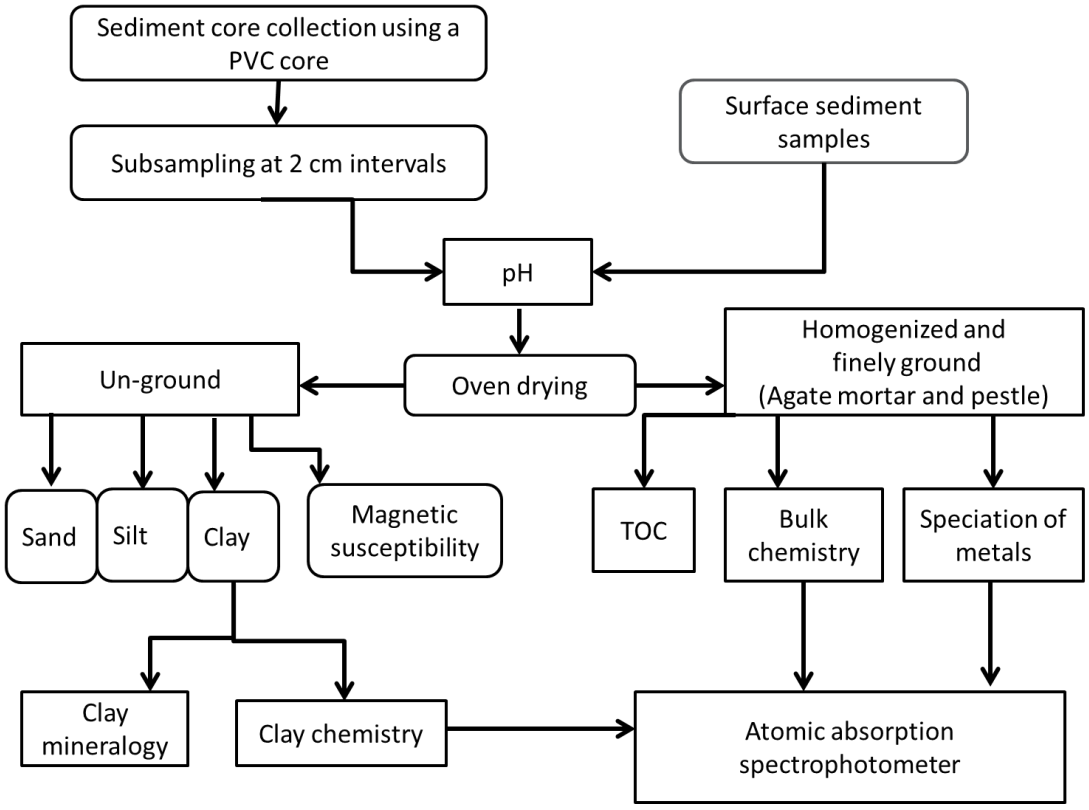


Figure 2.2: Schematic flowchart of steps followed in processing of sediment samples for metal analysis by Atomic absorption spectrophotometer.

**2.2 Field survey: Sediment core sample collection and sub sampling.**

Sediment cores were collected from intertidal mudflats and mangroves of the Zuari estuary in three planned periods: (1) premonsoon season collection of long (24-54 cm) sediment cores in May 2011, (2) Seasonal sampling of surface samples representing premonsoon (May 2011), monsoon (September 2011) and post monsoon seasons (January 2012) and (3) premonsoon season collection of short 10 cm sediment cores and biota in May 2015.

The sampling locations were positioned using a hand held Global positioning system (GPS) and fixed along the estuary for all subsequent sample collections. The sediment cores were collected during the low tide when the intertidal region was well exposed using a pre-cleaned handheld PVC corer. The sediment cores were then sub-sampled at 2 cm intervals with the help of plastic knife and transferred into clean and labeled plastic bags with care taken to avoid metal contamination. The packed sub samples were then store in an ice box and transported to the laboratory.

In the first sampling of sediment cores during premonsoon season, a total of seven cores were collected that varied in length from 24 cm to 54 cm. The details of the cores are presented in table 2.1.

In the second seasonal sampling, surface samples (0-2 cm) were collected from the specified locations by inserting the PVC corer in the sediments and the surface sediment up to 2 cm was sectioned and collected.

In the third sampling in premonsoon season of 2015, short cores of 10 cm were collected from the above specified locations and sectioned at 2 cm intervals. Additionally, sediment associated organisms and mangrove pneumatophores were collected from the four locations.

Table 2.1: Details of sediment cores and sampling locations of premonsoon sampling of 2011.

| Sampling location | Name of place | Estuarine zonation | Sub-environment | GPS location | Core length (cm) |
|---|---|---|---|---|---|
| S1 | Borim | Upper middle estuary | Mudflat | 15º20’44.10’’N 74º00’16.83”E | 44 |
| | | | Mangrove | 15º20’43.92”N 74º00’16.70”E | 34 |
| S2 | Cumbharjua canal | Cumbharjua canal | Mangrove | 15º30’14.90”N 73º56’50.05”E | 54 |
| S3 | Cortalim | Lower middle estuary | Mudflat | 15º23’54.74”N 73º55’30.21”E | 42 |

| | | | | | |
|---|---|---|---|---|---|
| | | | Mangrove | 15º23’54.99”N 73º55’30.86”E | 40 |
| S4 | Chicalim | Lower estuary | Mudflat | 15º24’01.07”N 73º50’47.36”E | 30 |
| | | | Mangrove | 15º23’56.94”N 73º50’47.88”E | 24 |

### 2.3 Laboratory analysis

#### 2.3.1 pH

The pH of each sub sample was measured using a Themo Orion 420A+ pH/mV/ temperature meter with temperature compensation. The pH meter was calibrated using a three point calibration using freshly prepared buffer solutions of 4.01, 7.00 and 10.1. The pH was measured by inserting the electrode into the sediment subsamples and the pH was noted from the digital meter display.

#### 2.3.2 Sediment components (sand, silt and clay) analysis

The percentage of sand, silt and clay in the sediment subsamples was determined by the procedure proposed by Folk (1974). Sand, silt, and clay fractions contain particles whose diameters range from 2000 to 62.5 µm, 62.5 to 3.91 µm, and less than 3.91 µm, respectively. About 15 g of each dried subsample were placed in a beaker with 1000 ml of distilled water. The samples were lightly disaggregated with a glass stirring rod. The sediments were then allowed to settle and after 24 hours the overlying water was decanted. This step was repeated at least 4 to 5 times to remove salinity that was tested using a solution of $AgNO_3$. 10 ml of 10 % sodium hexametaphosphate (calgon) was added to dissociate the clay particles because of the unbalanced electrostatic charges on most clay particles that will cause the clay particles to aggregate or flocculate in suspensions, unless a dispersant is added to inhibit flocculation. After 24 hours, 5 ml of 30 % Hydrogen peroxide was added to oxidize the organic matter. The sediment was wet sieved on a 63 µ screen to separate the sand and mud (silt and clay) fractions. The sand fraction was collected in a pre-weighed 100 ml beaker and dried in an oven at 60 ºC. Grain size of the mud fraction was determined in a constant

temperature room by pipette technique which is based on settling velocities of particles calculated from Stokes' Law wherein a particle falling freely through a quiescent fluid will cease to accelerate when the frictional force exerted on the particle by the fluid exactly balances the downward force of gravity on the particle. The velocity of the particle under these conditions is called the settling velocity. The solution with mud in the cylinder was homogenized using a stirrer and stirring time was noted. A pipette withdrawal of 25 ml was taken at time corresponding to time intervals (Table 2.2) of 8Φ by inserting the pipette up to 10cm depth from the solution level in the cylinder. The pipetted solution was then transferred into a pre-weighed 100 ml beaker and dried in an oven at 60 ºC. The oven dried beakers containing sand and silt were then weighed and the percentage of sand, silt and clay was determined and calculated as follows

Sand (%) = (Weight of sand/ Total weight of sediment) * 100

Clay (%) = [((Weight of clay* 1000 / 25) - 1) / Total weight of sediment)] * 100

Silt (%) = 100 – (Sand % + Clay %)

Table 2.2: Time schedule used for pipette analysis

| Size Φ | Depth to which pipette was inserted (cm) | Time after which suspension was pipetted out (Hours: Minutes: Seconds) | | | | |
|---|---|---|---|---|---|---|
| | | 28 ºC | 29 ºC | 30 ºC | 31 ºC | 32 ºC |
| 4 | 20 | 00:00:48 | 00:00:46 | 00:00:46 | 00:00:44 | 00:00:44 |
| 5 | 10 | 00:01:36 | 00:01:34 | 00:01:32 | 00:01:29 | 00:01:28 |
| 6 | 10 | 00:06:25 | 00:06:15 | 00:06:06 | 00:06:57 | 00:05:52 |
| 7 | 10 | 00:25:40 | 00:25:02 | 00:24:25 | 00:24:49 | 00:23:27 |
| 8 | 10 | 01:42:45 | 01:40:13 | 01:37:42 | 01:37:15 | 01:33:51 |
| 9 | 10 | 06:30:00 | 06:40:40 | 06:32:50 | 06:32:10 | 06:11:30 |
| 10 | 10 | 27:06:00 | 26:30:00 | -- | -- | -- |

### 2.3.3 Clay minerals analysis

The method of Rao and Rao (1995) was adopted for the analysis of clay minerals. The procedure for separation of clay sediment fraction is the same as that for pipette analysis. The clay suspension was pipetted out at 10 cm depth to a 100 ml beaker at 9 Φ from the 1000 ml cylinder containing the mud suspension. 5 ml of glacial acetic acid and 10 ml hydrogen peroxide was added to render the clay free of carbonates and organic matter and stirred well. The contents of the beaker were allowed to settle for 24 hours. The clear solution above the settled clay was decanted and distilled water was added. Addition of distilled water followed by decantation was repeated several times to free the clay from excess reagents. Slides for analysis of clay minerals were prepared by pipetting 1 ml of the concentrated clay suspension onto a pre-numbered glass slide and uniformly spreading it across the slide. Extreme care was taken to obtain uniform distribution of clay and to avoid size sorting. The slides were further air dried and preserved in a box away from moisture till further analysis. For analysis by X-ray diffractometer, the slides were processed by exposing them to ethylene glycol vapors at 100 ºC for 1 hour in a glass desiccator. The slides were then scanned on a Rigaku X-ray diffractometer (Ultima IV) apparatus using nickel- filtered CuKα as target and scanning between 3 º to 30 º 2Θ at 1.2º 2Θ / min. Clay minerals were then identified and quantified following the semi-quantitative method of Biscaye (1965). The clay mineral analyses were carried out in the sedimentology laboratory of the National Institute of Oceanography (NIO), Goa.

### 2.3.4 Magnetic susceptibility measurements

For the measuring of magnetic susceptibility, a known weight of sediment sample was packed in a 10 cc plastic sample container, which was wrapped with a plastic film to reduce the possibility of cross contamination and generally to keep the sediment immobile within the sample container while handling the sample. The containers with the packing material are pre-measured for mass and susceptibility and the values were corrected.

A Bartington MS2 system was used for magnetic susceptibility measurements. The high (4.7 kHz) and low (0.47 kHz) frequency measurements were determined using a dual frequency Bartington MS2 susceptibility meter. Magnetic susceptibility (χ) measurements of very weak samples were carried out employing the more sensitive Agico's Kappabridge KLY-4S

instrument. Frequency dependent susceptibility ($\chi_{fd}$%) was calculated using the formula ($\chi_{lf}$-$\chi_{hf}$)/ $\chi_{hf}$ *100 where $\chi_{lf}$ is magnetic susceptibility at low frequency and $\chi_{hf}$ is susceptibility at high frequency.

Anhysteretic remanence magnetization (ARM) was imparted in a steady 0.05 Mt field superimposed over decreasing alternating field from 100 mT to 0 mT using a Molspin A.F. demagnetizer. ARM created within the sample was then measured using a Molspin spinner magnetometer.

Isothermal remnant magnetization (IRM) was acquired by first exposing the samples to series of successively larger fields along one direction and then in the opposite direction (backfields -20mT, -30mT, -40mT, -100mT, -200mT and -300mT) using a Pulse magnetizer (Magnetic measurement Ltd.). After each forward and reverse field (DC magnetization), samples were measured using the Molspin spinner magnetometer. The IRM at 3T is referred as the saturation isothermal remnant magnetization (SIRM).

Using the above parameters various other parameters were calculated in terms of magnetic concentration, mineralogy and grain size as summarized by Thomson and Oldfied (1986) and Oldfield (1999). The descriptions of different parameters are presented in table 2.3.

Table 2.3: Magnetic susceptibility parameters, their definitions and implications

| Magnetic parameters | Definitions/ formulas | Implications |
|---|---|---|
| 1.Magnetic susceptibility $\chi$ ($10^{-8}$ $m^3$/ kg) | It indicates the degree of magnetization of a material in response to an applied magnetic field.<br>$\chi = M/H$<br>Where M is the magnetization of the material and<br>H is the magnetic field strength. | Proportional to the concentration of magnetic minerals. |
| 2. Frequency | Variation in $\chi$ between low (0.47 | Used to detect the presence of ultrafine (<0.03 μm) |

| | | |
|---|---|---|
| dependent susceptibility, $\chi_{fd}$ (%) | kHz) and high (4.7 kHz) frequency. Defined as ($\chi_{lf}$ -$\chi_{hf}$/$\chi_{lf}$) x 100 where $\chi_{lf}$ is the susceptibility at low frequency and $\chi_{hf}$ is the susceptibility at high frequency. | superparamagnetic ferrimagnetic minerals occurring as crystals produced largely by biochemical processes |
| 3.Isothermal remanent magnetization, IRM (10-5 Am2/kg-1) | Magnetization acquired instantaneously in an external field | Proportional to the concentration of magnetic minerals. |
| 4.Anhysteretic remanent magnetization, ARM ($10^{-5}Am^2/kg$) | Magnetization acquired by the combined effects of a large alternating field and a small DC field | ARM gives an estimation of the concentration and presence of fine grain minerals. |
| 5. Susceptibility of ARM, $\chi_{ARM}$ ($10^{-8}m^3/kg$-1) | It is a form of normalized ARM for the strength of a steady field | Proportional to the concentration of magnetic minerals of stable single domain size range |
| 6. Saturation isothermal remanent magnetization , SIRM ($10^{-5}$ $Am^2/kg$) | It is measured as the highest volume of magnetic remanence that can be produced in a sample by applying a very high field | It is a characteristic of mineral type and concentration. |
| 7. S-ratio (%) | It is defined as IRM (-300 mT)/SIRM. | S-ratio provides a measure of the relative proportions of ferrimagnetic and antiferromagnetic minerals (high ratio = relatively high proportion of magnetite) |
| 8. $\chi_{ARM}/\chi$ | It is the ratio of the susceptibility of Anhysteretic remnant magnetization to magnetic susceptibility. | Indicative of magnetic grain size of ferrimagnetic minerals High values indicate significant stable single domain (magnetite) grains. |
| 9. $\chi_{ARM}$/ SIRM | It is the ratio of the susceptibility of | Indicative of magnetic grain |

| | | |
|---|---|---|
| ($10^{-3}$ $A^{-1}$ m) | Anhysteretic remnant magnetization to Saturation isothermal remnant magnetization. | size |

### 2.3.5 Total organic carbon estimation

An estimate of total organic carbon (TOC) was used to assess the amount of organic matter in sediments. The total organic carbon percentage in sediments was determined following the chromic acid wet oxidation method protocol of Walkley and Black (1934). The method is based on the principle wherein oxidisable matter in the sediment is oxidised by 1 N $K_2Cr_2O_7$ solution. The reaction is assisted by the heat generated when two volumes of $H_2SO_4$ are mixed with one volume of the dichromate. The remaining dichromate is titrated with ferrous ammonium sulfate. The titre is inversely related to the amount of Carbon present in the sediment sample.

Prior to analysis, all glassware was rinsed with chromic acid and distilled water, followed by drying in an oven. 0.5 g of sediment was weighed on a digital 4 decimal weighing balance and transferred to a 500 ml conical flask. 10 ml of 1 N $K_2Cr_2O_7$ solution was added to the flask using a graduated burette followed by 20 ml of concentrated $H_2SO_4$ with silver sulfate ($AgSO_4$) to prevent oxidation of chloride ions. The flask was gently swirled for 1 minute to mix the contents and allowed to react for 30 minutes. After 30 minutes, 200 ml of distilled water was added to the flask, followed by 10 ml of 85 % phosphoric acid ($H_3PO_4$) and 0.2 g of Sodium Fluoride (NaF). The solution was then back-titrated with 0.5 N Ferrous ammonium sulfate solution using diphenylamine as an indicator to a one-dropt end point (brilliant green). Standardization blank was run following the same procedure.

The percentage of organic carbon was calculated as follows:

$$TOC\ \% = 10\ (1-T/S) * F$$

Where S= Volume in ml of Ferrous ammonium sulfate used in blank titration

T= Volume in ml of Potassium dichromate used in sample titration

F=Factor which is derived as

F= (1.0N)*12/4000 * 100/ Sample weight

=0.6

where sample weight is 0.5 g and 12/4000 is the milli equivalent weight of Carbon.

### 2.3.6 Analysis of bulk sediment chemistry

For analysis of total/bulk metal concentrations in sediments, sediment samples were digested by the total decomposition procedure using strong acids HF, $HClO_4$ and $HNO_3$ given by Jarvis and Jarvis (1985). 0.2 g of oven dried sediments were homogenized and weighed on an electronic weighing balance and transferred to pre-cleaned Teflon beakers. To this, 10 ml of acid mixture i.e. HF: $HNO_3$:$HClO_4$ in the ratio 7:3:1 was slowly added to avoid excessive frothing and was completely dried on an electric hot plate at 150 ºC. After drying, 5 ml of the acid mixture was added and dried on the hot plate for 1 hour. 2 ml of concentrated $HNO_3$ was then added followed by complete drying. After ensuing complete drying and the resultant residue was dissolved in10 ml of 1:1 $HNO_3$ and the clear solution was transferred into an acid washed 50 ml volumetric flask and diluted up to the mark with millique water. The digested sediment extracts were then analyzed using an Atomic Absorption spectrophotometer (Flame AAS). Sediment standard reference 2702 obtained from National Institute of Standards and Technology (NIST) was digested following the same procedure.

### 2.3.7 Clay fraction chemistry analysis

The clay fraction of sediments was separated using the pipette technique at 9 Φ as described in section 2.3.2. The clay fraction was collected in a 500 ml beaker after pipetting the clay suspension from the cylinder containing the mud suspension by inserting the pipette at 10 cm depth. The collected clay suspension was allowed to settle for 24 hours followed by oven drying at 60 ºC. The dried clay was then collected and stored in plastic vials. 0.2 g of the dried clay was then digested following the procedure for digestion of bulk sediments as described in section 2.3.6 and metals were analyzed using an flame AAS.

### 2.3.8 Speciation of metals

An analytical procedure developed by Tessier et al. (1979) involving sequential chemical extractions of sediments for the partitioning of trace metals into five fractions: exchangeable, bound to carbonates, bound to Fe-Mn oxides, bound to organic matter/ sulfides, and residual was employed. The speciation of metals in sediments furnishes detailed information about the origin, mode of occurrence, biological and physicochemical availability, mobilization, and

transport of trace metals. The following steps were followed for extraction of each of the five phases/ fractions.

**(i) Exchangeable fraction (F1):** Exchangeable metals are a measure of those traces metals which are released most readily to the environment. This fraction involves weakly adsorbed metals retained on the solid surface by relatively weak electrostatic interaction, metals that can be released by ion-exchangeable processes. Exchangeable fraction can be released by the action of cations such as K, Ca, Mg or $NH_4$ displacing metals weakly bond electrostatistically organic or inorganic sites. The common reagents used for the extraction of metals in this fraction are $MgCl_2$ or sodium acetate.

1 g of dried ground sediment was weighed and transferred into plastic capped tubes. 8 ml of magnesium chloride solution (1 M $MgCl_2$, pH 7.0) was added and the sediment was extracted at room temperature for 1 h with continuous agitation. The sediment suspension was centrifuged at 8000 rpm for 10 minutes and the supernatant was collected for analysis of metals. The residue was washed with millique water and decanted.

**(ii) Bound to Carbonates (F2):** The carbonate fraction is a loosely bound phase and bound to changes with environmental factors such as pH. This fraction is sensitive to pH changes, and metal release is achieved through dissolution of a fraction of the solid material at pH close to 5.0. The most popular reagent used for the extraction of trace metals from carbonates phases in sediments is 1 M sodium acetate adjusted to pH 5.0 with acetic acid.

Metals in the residue from step (i) were leached at room temperature with 8 mL of 1M Sodium acetate (NaOAc) adjusted to pH 5.0 with acetic acid (HOAc). Continuous agitation was maintained and the time necessary for complete extraction was evaluated. The suspension was centrifuged at 8000 rpm for 10 minutes and the supernatant was collected for analysis of metals. The residue was then washed with millique water and decanted.

**(iii) Bound to Fe-Mn Oxides (F3):** This phase is referred to as sink for heavy metals. The scavenging of metals by the oxides, present as coating on mineral surfaces or as fine discrete particle can occur as a combination of the precipitation, adsorption, surface complex

formation and ion exchange. Hydroxylamine, oxalic acid and dithionite are the most commonly used reagents to extract metals associated with this phase.

The residue from step (ii) was extracted with 20 mL of 0.04 M Hydroxylamine hydrochloride ($NH_20H$-HCl) in 25% (v/v) acetic acid (HOAc) at 96 ± 3 ºC with occasional agitation for 5 hours. The suspension was centrifuged at 8000 rpm for 10 minutes and the supernatant was collected for analysis of metals. The residue was then washed with millique water and decanted.

**(iv) Bound to Organic Matter/ Sulfides (F4):** In organic phase, metals bound to this phase are assumed to stay in the sediment for longer periods but may be immobilized by decomposition process. Under oxidizing conditions, degradation of organic matter can lead to a release of soluble trace metals bound to this component. The extracts obtained during this step also contain metals bound to sulfides. The most commonly used reagent for the extraction of metals in organic phases is hydrogen peroxide with ammonium acetate re-adsorption or precipitation of released metals

To the residue from step (iii), 3 mL of 0.02 M $HN0_3$ and 5 mL of 30% $H_2O_2$ adjusted to pH 2 with $HN0_3$ were added and the mixture was heated to 85 ± 2 ºC for 2 h with occasional agitation. A second 3 ml aliquot of 30 % $H_2O_2$ (pH 2 with $HNO_3$) was then added and the sample was heated again to 65 ± 2 ºC for 3 h with intermittent agitation. After cooling, 5 mL of 3.2 M ammonium acetate $NH_4OAc$ in 20 % (v/v) $HN0_3$ was added and the sample was diluted to 20 ml and agitated continuously for 30 min. The addition of ammonium acetate ($NH_4OAc$) is designed to prevent adsorption of extracted metals onto the oxidized sediment. The suspension was centrifuged at 8000 rpm for 10 minutes and the supernatant was collected for analysis of metals. The residue was then washed with millique water and decanted.

**(v) Residual (F5):** Metals in the residual fraction are associated with the silicate matrix and are resistant metals bound to primary and secondary minerals in the crystalline lattice. Its destruction is achieved by digestion with strong acids, such as HF, $HClO_4$, HCl and $HNO_3$.
The residue from step (iv) was then transferred into a teflon beaker and oven dried at 60 ºC. The residue was further digested using a HF-$HNO_3$-$HClO_4$ mixture following the procedure for total/ bulk metal analysis.

The extracts from the five steps described above were then aspirated into an AAS for analysis of metals. The first four fractions are known as the bioavailable fractions and the first two fractions are knows as the labile fractions.

### 2.4 Sampling of biota

Sediment associated organisms and mangrove pneumatophores were collected from the specified sampling locations during the premonsoon season in 2015. From each sampling location, Gastropod organisms which were easily available on the surface and subsurface were handpicked from the sediments and transferred into clean polythene bags and stored in an ice box. The organisms were washed with distilled water to remove dirt and sediments particles that adhered to the organisms. The organisms were then identified and refrigerated at - 23 ºC in plastic zip log bags until further analysis.

Mature pneumatophores were randomly collected surrounding the sediment core. Mangrove pneumatophores of *Avicennia officinalis* were collected at locations S1, S2 and S3, whereas pneumatophores of *Sonneritia alba* was collected at S4. Pneumatophores were cut at the sediment surface with a stainless steel knife at each sediment core site. Three strands of pneumatophores were pooled together to make one sample for each core site. Pneumatophore samples were stored in a zip-lock plastic bag and transferred to an ice box and transported to the laboratory for preservation at 4 °C until further processing. The schematic diagram for processing of biota samples to study bioaccumulation of metals is presented in figure 2.3.

#### 2.4.1 Metals in sediment associated organism's tissues

The frozen samples were brought to room temperature. Gastropod shells were opened by breaking their shells. A pair of stainless steel forceps was used to dislodge and to remove the soft tissues from the shell. The tissue of each sub sample was oven dried in a glass petri dish to a constant weight at 60 ºC for 72 hours (Ferreira et al., 2004). The dried samples were pulverized together into fine powder using a porcelain mortar and pestle. The digestion of the tissue was carried out by taking 0.5 g of tissue sample in a Teflon beaker with 2 ml of $HNO_3$ and 1 ml of $HClO_4$ at 120 ºC for 3 hours. The digest was diluted with millique water and the final volume was made up to 25 ml in a glass volumetric flask and stored in pre-cleaned

plastic bottles (Yüzereroglu et al., 2010). Metals in the extracts were then analyzed using the AAS.

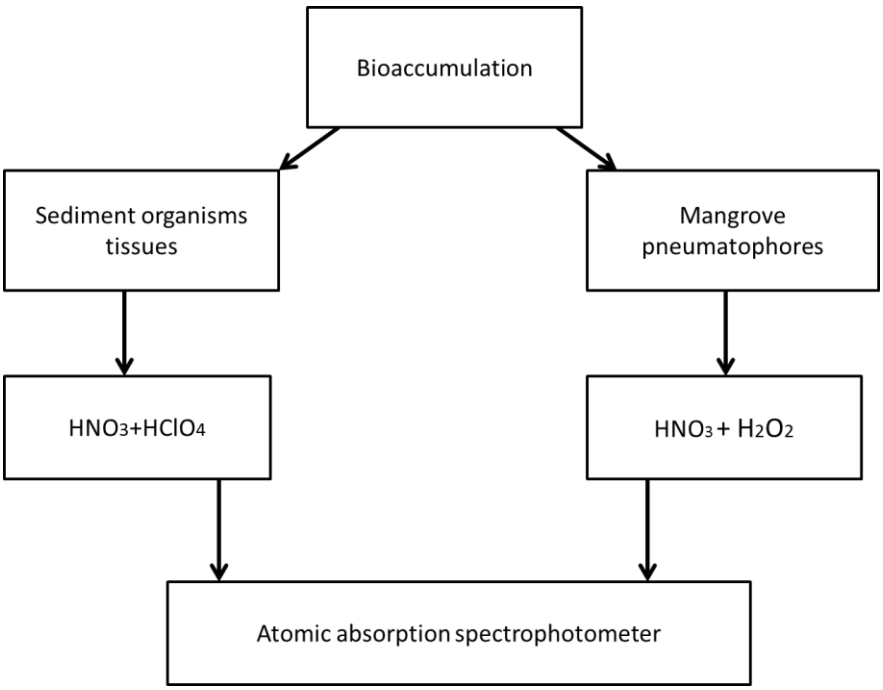


Figure 2.3: Schematic flowchart of steps followed in processing of biota samples for metal analysis by Atomic absorption spectrophotometer.

### 2.4.2 Metals in mangrove pneumatophores

The collected pneumatophores were washed with distilled water to remove dirt and sediment particles, and dried in an oven at 60 °C for 24 h. Oven-dried samples were ground to fine powder using a porcelain mortar and pestle and kept in a plastic container for chemical analysis (Nath et al., 2014). The digestion of dried pneumatophore samples was carried out by adding $HNO_3$ and $H_2O_2$ in teflon beakers at 90 ºC for 2 hours. The digested extracts were then diluted to 25 ml with millique water and were analyzed using AAS (MacFarlane and Burchette, 2002).

## 2.5 Atomic Absorption Spectrophotometry

The digested bulk sediment, clay fraction, sediment fractions, gastropod tissue and pneumatophore extracts were analyzed for metals using a Varian AA240FS flame atomic absorption spectrometry (AAS) with an air/acetylene flame for all metals at specific wavelengths. The bulk sediment and clay extracts were analyzed for Al, Fe, Mn , Cr, Co, Ni, Cu and Zn whereas sediment fractions were analyzed for metals, Fe, Mn, Cr, Co, Cu and Zn. Biota samples i.e. organism tissue and pneumatophore fraction were analyzed for metals Fe, Mn, Cr, Co, Ni, Cu and Zn. The accuracy of the analytical method was obtained by the standard reference 2702 from National Institute of Standards and Technology (NIST). The average recoveries and ± standard deviations found for metals Fe, Mn, Cr, Co, Ni, Cu and Zn, were 89±12, 91±15, ±14, 74±12, 86±16, 82±15, and 84±16 respectively. Precision was monitored by running triplicates after every ten samples and the relative standard deviation was generally <6 % for major and trace elements. Analytical grade reagents and standards were used in all the analysis

## 2.6 Data processing

### 2.6.1. Ternary diagram, Isocon diagram and statistical analysis

To understand the hydrodynamic conditions in which sediments have been deposited, the data of the cores were plotted on a ternary diagram by Pejrup (1988). According to his classification, lines of constant clay content of the mud fraction (smaller than 4 phi) are drawn to divide the triangle. The finest part of the mud fraction (smaller than 4 phi) of estuarine sediments very often has a constant textural composition, because these small grain sizes occur in the water as part of sediment flocs. The percentage of this flocculated grain size population in the mud fraction of estuarine sediment can therefore be used as a simple indicator of the hydrodynamic conditions under which deposition took place. Sections labelled I to IV, (Figure 2.4) which indicate increasingly high energy hydrodynamic conditions. The sediments are classified according to their sand content into four sections, A to D. The triangle is thus divided into 16 sections, each of which can be named by a letter indicating the type of sediment and a number indicating the hydrodynamic conditions during deposition (Shi, 1992). Section I represents calm conditions, II – relatively calm conditions, III- relatively violent conditions and IV- violent conditions. In this scheme, class A-IV designates the highest, class D-I the lowest energy regime.

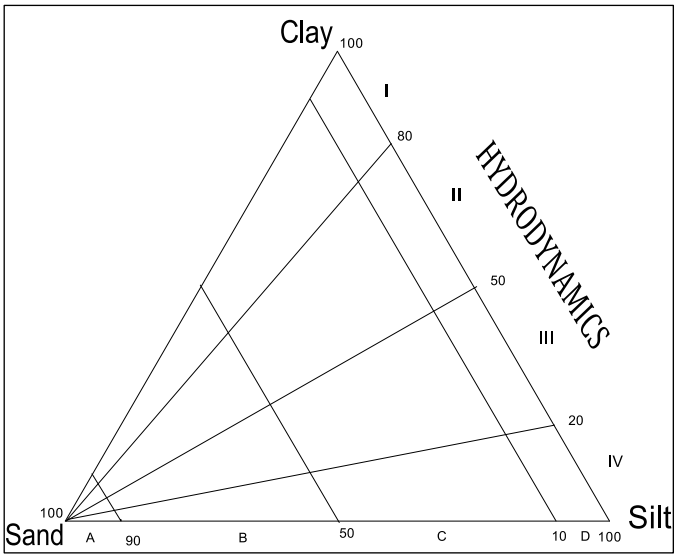


Figure 2.4: Ternary diagram proposed by Pejrup, 1988

Isocon diagram proposed by Grant (1986) was used to compare sediment component and metal abundance with respect to mudflats and mangroves and metal abundance with respect to bulk sediments and clay fraction.

Statistical Pearson's (two-tailed) correlation and principal component analyses (PCA) were carried out on sediment components and metals for the studied cores by using the software SPSS 17.

### 2.6.2 Sediment quality assessment

Enrichment factor (EF) was used to differentiate between the metals originating from anthropogenic activities and those from natural procedure, and to assess the degree of anthropogenic influence. Enrichment factor was computed to evaluate metal enrichment in sediments using the equation "EF= $(M_{sed}/R_{sed})/ (M_{bk}/R_{bk})$" where $(M_{sed}/R_{sed})$ is the ratio of heavy metal concentration $(M_{sed})$ to that of the reference element $(R_{sed})$ in sediment and $(M_{bk}/R_{bk})$ is the same ratio in the natural background (Huu et al., 2010). Aluminum was used as reference element to counter balance lithogenic influences of granulometric and mineralogical variations of sediments (Qi et al., 2010). EF values ranging from 0.5 to 2 can be considered to be similar to that of the sediments unaffected by any human activities and thus are in the range of natural variability, and EF values over 2.0 represent enrichment and contamination of heavy metal in the sediment resulted by the significant anthropogenic inputs.

Geo-accumulation index- Igeo (Muller, 1979) was computed to assess the level of metal contamination in sediments using the equation "Igeo= $Log_2$ (Cn/1.5Bn)" where Cn is the concentration of the metal in the sample and Bn is the background metal concentration in average shale (Turekian and Wedepohl, 1961). Igeo values are categorized based on level of pollution into seven classes viz. "Very strongly polluted"-Igeo class 6 (Igeo >5); "Strong to very strong"-Igeo class 5 (Igeo 4–5); "Strongly polluted"-Igeo class 4 (Igeo 3–4); "Moderately to strongly polluted"-Igeo class 3 (Igeo 2–3); "Moderately polluted"-Igeo class 2 (Igeo 1–2); "Unpolluted to moderately polluted—Igeo class 1 (Igeo 0–1) and "Unpolluted"-Igeo class 0 (Igeo < 0).

Concentration of metals in the bioavailable fractions (sum of first four fractions) and bulk sediments was compared with the sediment quality values (SQV) following screening quick reference table (SQUIRT) (Table 2.4) developed by NOAA (Buchman, 1999) and labile fractions (exchangeable and carbonate) was compared with the Risk Assessment Code- RAC (Perin et al., 1985) to explain the toxicity level of the metals (Table 2.5).

Table 2.4 Screening Quick Reference table for metals in marine sediments (Buchman, 1999)

| Metal | Threshold Effect level (TEL) | Effects range level (ERL) | Probable Effects level (PEL) | Effects Range Median (ERM) | Apparent Effects Threshold (AET) |
|---|---|---|---|---|---|
| Fe | NA | NA | NA | NA | 22 % / 22000 ppm (Neanthes) |
| Mn | NA | NA | NA | NA | 260 (Neanthes) |
| Cr | 52.30 | 81.00 | 160.00 | 370.00 | 62 (Neanthes) |
| Co | NA | NA | NA | NA | 10 (Neanthes) |
| Ni | 15.90 | 20.90 | 42.80 | 51.60 | 110 (Echinoderm larvae) |
| Cu | 18.70 | 34.00 | 108.00 | 270.00 | 390 (Microtox and Oyster Larve) |
| Zn | 124.00 | 150.00 | 271.00 | 410.00 | 410 (Infaunal community) |

*All values are in ppm or indicated otherwise

| Sediment guidelines | |
|---|---|
| Threshold Effect level (TEL) | Maximum concentrations at which no toxic effects are observed |
| Effects range level(ERL) | $10^{th}$ percentile values in effects or toxicity may begin to be observed in sensitive species. |
| Probable Effects level(PEL) | Lower limit of concentrations at which toxic effects are observed |
| Effects Range Median(ERM) | $50^{th}$ percentile value in effects |
| Apparent Effects Threshold (AET) | Concentrations above which adverse biological impacts are observed. |

Table 2.5: Classification of risk assessment code (RAC) by Perin et al. (1985)-.

| RAC | Criteria (%) |
|---|---|
| No risk | < 1 |
| Low risk | 1-10 |
| Medium risk | 11-30 |
| High risk | 31-50 |
| Very high risk | > 50 |

**2.6.3 Bioaccumulation tools to estimate uptake of metals by biota.**

Biosediment accumulation factor (BSAF) was used to investigate the capability of the sediment associated organisms to accumulate heavy metal from the environment and hereby, suggesting its possibility as biomonitor for heavy metals. BSAF was calculated to assess the bioaccumulation of metals by organisms. BSAF was calculated using the equation

"BSAF = Cx/ Cs"

where Cx and Cs are metal concentrations in biota and sediments, respectively (Szefer et al., 1999). If the BSAF >1, bioaccumulation is considered to reach threshold with respect to contamination. Based on the values calculated, the gastropod could be classified into a few

groups such as macro concentrator (BSAF >2), micro concentrator (1< BSAF <2) or de-concentrator (BSAF <1) as proposed by Dallinger (1993).

Bioconcentration Factor (BCF) was computed on similar lines to BSAF, to assess metal accumulation in pneumatophores relative to environmental loadings using the equation "BCF= metal concentration in pneumatophore/ Metal concentration in sediments" (MacFarlane et al., 2007).

# *Chapter 3*

# *Results and Discussions*

**Section 3.1: Sediment cores collected in premonsoon of 2011.**

**3.1A Mangroves**

**3.1. A.1 Sediment components (pH, sand, silt, clay and total organic carbon)**

The range and average values of sediment pH, grain size, and total organic carbon within the mangroves of the Zuari estuary are presented in table 3.1.1 (a). The sediment core collected from the upper middle region (S1) of the Zuari estuary (Borim) during premonsoon season in 2011 was with length 34 cm. The sediments were of near neutral pH and clay was the dominant sediment size fraction followed by silt and sand. The pH in this core ranged from 6.12 to 7.54 (average 7.09). The sand content ranged from 0.49 % to 6.14 % (average 2.28 %), whereas silt ranged from 22.52 % to 48.41 % (average 36.8 %) and clay ranged from 48.00 % to 71.68 % (average 60.92 %). Total organic carbon (TOC) ranged from 2.50 % to 3.53 % (average 2.85 %) in the mangrove sediments of S1. In sediment core of length 54 cm collected from the mangrove sub-environment of the Cumbharjua canal (S2) during the premonsoon season, the pH was weakly acidic ranging from 5.9 to 6.5 (average 6.19). The sand content ranged from 2.28 % to 13.85 % (average 5.82 %). Silt was the dominant sediment component in this core and ranged from 24.51 % to 69.39 % (average 48.55 %). The clay percentage in the core ranged between 26.90 % and 61.64 % (average 45.64 %) and the TOC varied from 1.64 % to 2.96 % (average 2.13 %). In sediment core collected from the Cortalim representing the lower middle estuarine mangroves (S3) was with 40 cm in length and the sediment pH was of near neutral nature, ranging from 6.44 to 6.94 (average 6.65). Clay was the dominant fraction in the sediments followed by silt and sand. Sand percentage ranged from 0.46 % to 2.17 % (average 1.04 %). Silt percentage ranged between 29.38 % and 55.13 % (average 37.01 %) whereas clay ranged from 43.52 % to 68.88 % (average 61.95 %). TOC in core S3 ranged between 1.31 % and 3.18 % (average value of 2.52 %). The sediment core collected from Chicalim mangrove region represented the lower estuary (S4) was of 24 cm length. The pH of the sediments was near neutral, ranging from 6.73 to 7.01 (average 6.86). The dominant sediment fraction in this core was sand that ranged between 29.98 % and 84.74 % (average 57.5 %). Silt content in the core sediments ranged between 3.21 and 44.05 % (average 19.88 %). Clay percentage however, was higher than silt, but less than sand and ranged between 7.68 % and 34.88 % (average of 22.61 %) and the TOC content ranged between 0.37 % and 1.99 % (average of 1.26 %).

The distribution of sediment components with depth in cores S1, S2, S3 and S4 are presented in figure 3.1.1. The sediment components in core S1 exhibited distinct distribution patterns. The pH was relatively constant with depth except at 8 cm where the profile showed a decreased peak. Sand distribution in core S1 showed percentages above average up to 26 cm from bottom, followed by constant percentages below the average towards the surface. Silt and clay distribution patterns compensated each other with fluctuations. The distribution of TOC with depth in core S1 was constant up to 20 cm and showed an increased peak at 14 cm that corresponded to the higher clay values followed by lower than average TOC values up to the surface. In core S2, the pH exhibited a constant distribution pattern with depth. The sand percentage decreased from the core base to 22 cm followed by an increase towards the surface. The clay values decreased towards the surface and was compensated by an increase in silt with fluctuating trends. The TOC percentage was constant up to 26 cm followed by an increased peak at 24 cm. The distribution of pH in core S3 was relatively constant with depth with minor peaks at 26 cm, 20 cm and 12 cm. The distribution of sand, silt and clay percentages showed little variation with depth. The sand percentage showed a uniform distribution pattern towards the surface from the base of the core. The distribution of silt was constant towards the surface with the exception of higher silt percentages at 40 cm, 32 cm, 16 cm and 8cm. The clay distributions compensated silt. TOC in core S3 showed higher than average but constant values from the base of the core up to 24 cm. Further above, values showed large fluctuations with an overall decreasing trend. In core S4, the pH showed a uniform distribution with depth. The sand content decreased towards the surface and that was compensated by an increase in silt percentage. The clay percentage gradually increased towards the surface along with silt. In core S4 collected from the lower estuarine region, large amount of calcareous material was noted in the deeper portion. The higher sand percentage in the lower part may have been the result of the presence of coarse calcareous sand, gastropods shells, and bivalves (Welle et al., 2004). The TOC percentage increased towards the surface along with the finer sediments.

Table 3.1.1: Range and average values of sediment components (a), clay minerals (b) and magnetic susceptibility parameters (c) in sediment cores S1, S2, S3 and S4.

| | | | **S1** | | **S2** | | **S3** | | **S4** | |
|---|---|---|---|---|---|---|---|---|---|---|
| | | Parameters | Average | Range | Average | Range | Average | Range | Average | Range |
| (a) | Sediment components | pH | 7.09 | 6.12 -7.54 | 6.19 | 5.9-6.5 | 6.65 | 6.44-6.94 | 6.86 | 6.73-7.01 |
| | | Sand (%) | 2.28 | 0.49-6.14 | 5.82 | 2.28-13.85 | 1.04 | 0.46-2.17 | 57.5 | 29.98-84.74 |
| | | Silt (%) | 36.8 | 22.52-48.41 | 48.55 | 24.51-69.39 | 37.01 | 29.38.-55.13 | 19.88 | 3.21-44.05 |
| | | Clay (%) | 60.92 | 48.00-71.68 | 45.64 | 26.90-61.64 | 61.95 | 43.52-68.88 | 22.61 | 7.68-34.88 |
| | | TOC (%) | 2.85 | 2.50-3.53 | 2.13 | 1.64-2.96 | 2.52 | 1.31-3.18 | 1.26 | 0.37-1.99 |
| (b) | Clay minerals | Smectite (%) | 20.88 | 13.43-27.27 | 12.66 | 10.53-14.29 | 15.25 | 10.98-19.30 | 22.86 | 17.36-31.58 |
| | | Illite (%) | 17.22 | 13.26-20.90 | 27.75 | 21.05-37.62 | 22.39 | 16.18-26.94 | 19.46 | 15.79-22.22 |
| | | Kaolinite (%) | 55.33 | 49.79-60.42 | 54.03 | 44.55-63.76 | 55.27 | 50.32-66.59 | 52.84 | 40.60-58.48 |
| | | Chlorite (%) | 6.58 | 5.25-8.29 | 5.57 | 3.50-7.42 | 7.08 | 5.13-10.50 | 4.84 | 2.51-7.31 |
| (c) | Magnetic Susceptibility parameters | $\chi_{lf}$ ($10^{-8}$ $m^3$ $kg^{-1}$) | 229 | 152- 406 | 265 | 226 - 323 | 148 | 128 - 161 | 145 | 53.27- 267 |
| | | $\chi_{ARM}$ ($10^{-8}$ $m^3$ $kg^{-1}$ ) | 1008 | 792 -1106 | 944 | 796- 1118 | 986 | 823-1143 | 542 | 229-840 |
| | | SIRM ($10^{-5}$ $Am^2$ $kg^{-1}$) | 2212 | 1532 - 4701 | 3757 | 2919- 5387 | 1384 | 1293- 1486 | 1646 | 518-2982 |
| | | $\chi_{ARM}/\chi_{lf}$ | 4.70 | 2.66-5.45 | 3.58 | 2.96 -4.08 | 6.67 | 6.27-7.08 | 3.84 | 2.98-4.64 |
| | | $\chi_{ARM}$/SIRM ($10^{-3}$ $A^{-1}m$ ) | 0.51 | 0.23 -0.67 | 0.26 | 0.18-0.31 | 0.71 | 0.64-0.78 | 0.34 | 0.26- 0.44 |
| | | $\chi_{fd}$ (%) | 7.04 | 1.24 -10.84 | 4.45 | 3.45-5.45 | 7.03 | 4.28-9.47 | 4.81 | 2.95-7.95 |
| | | Sratio (%) | 90.44 | 87.75-93.55 | 87.76 | 85.98-89.28 | 89.98 | 88.81- 91.85 | 89.08 | 84.73- 91.48 |

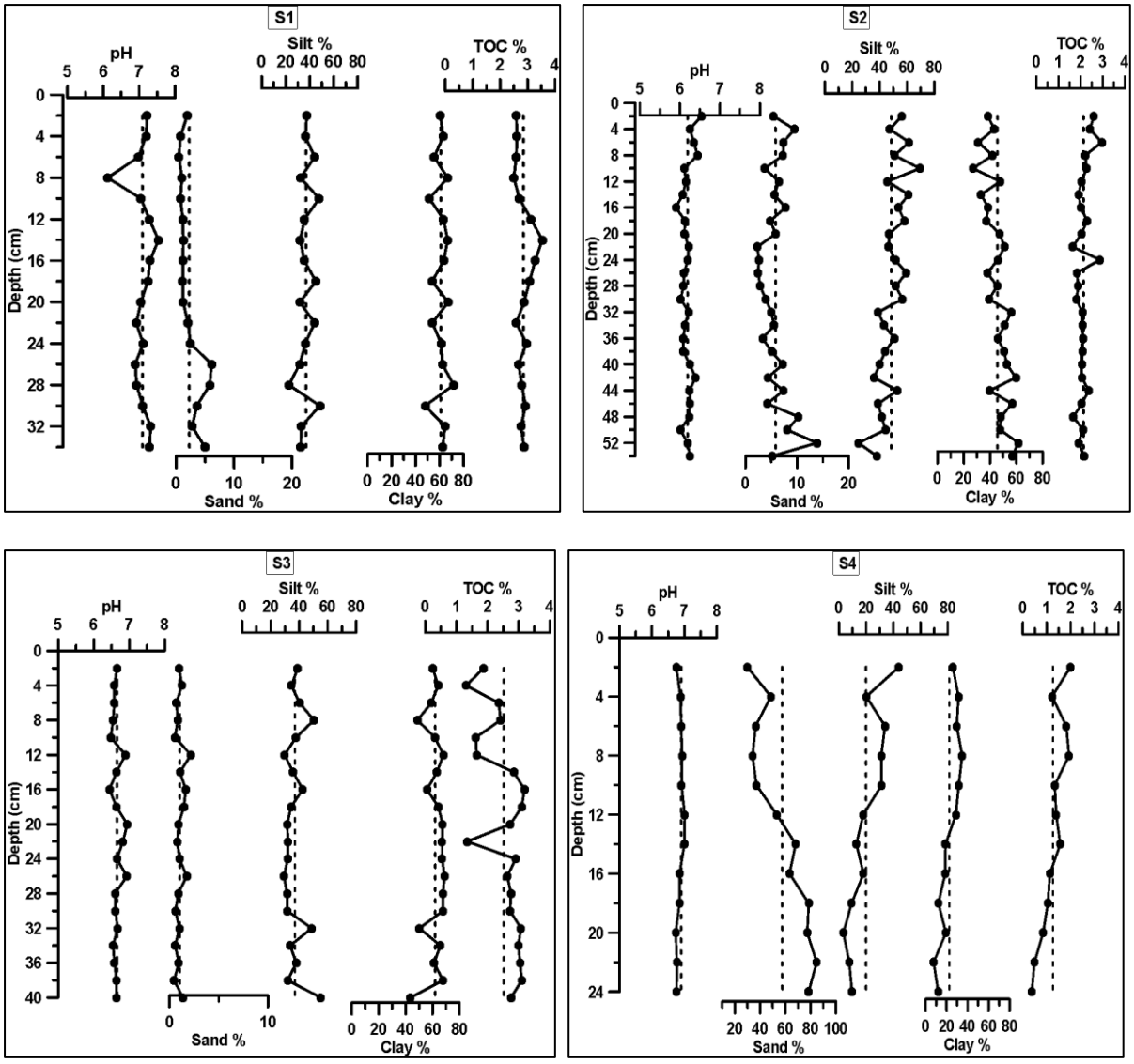


Figure 3.1.1: Distribution of sediment components with depth in mangrove cores S1, S2, S3 and S4.

The sediments exhibited wide variations in grain size at different sampling stations of the Zuari estuary. The percentage of the coarser sediment decreased towards the upper middle estuary with a corresponding increase in finer sediment. The high sand content in the lower estuary sediments was due to the higher hydrodynamic conditions prevailing owing to high energy waves that prevented the accumulation of finer sediments. High silt content was observed in the canal sediments whereas clay was notably higher in the lower middle estuarine sediments. Overall, clay and silt dominated the sediments collected from the upper middle, lower middle estuary and Cumbharjua canal. Thus, the high-energy conditions in the lower estuary caused the finer sediments carry in suspension and deposited at places where

hydrodynamic conditions were quiet. When the distributions of the sediment components with depth, amongst the stations, are considered, the lower middle estuary seems to maintain uniform hydrodynamic conditions with time as shown by constant distribution trends of sediment components. The higher sand in the lower part of the cores collected from the upper middle estuary, Cumbharjua canal and the lower estuary indicated that higher energy hydrodynamic conditions prevailed in the past compared to recent years.

The accumulation of organic matter in estuarine mangrove sediments is controlled by several factors that include organic matter sources, sedimentation rate, preservation potential and the decomposition rate of organic materials (Yang et al., 2011). The high TOC percentage in the core collected from the upper middle estuary that coincided with high clay was attributed to the enhanced adsorption of organic carbon onto the clay minerals in the low salinity regimes (Akhil et al., 2013). The increased TOC percentage along with silt in the upper sections of the core in the Cumbharjua canal may be due to the rapid burial of organic matter. Rapid sedimentation and burial can enhance TOC preservation that is accomplished by a high influx of inorganic detritus, biogenic inorganic sediment or organic material (Waples, 2013). The higher TOC in the lower part of the sediment core of the lower middle estuary might have been caused either by the additional supply of terrestrial organic matter, better preservation or increased surface water productivity (Wahyudi and Minagawa, 1997).

Further, to understand the hydrodynamic conditions in which sediments were deposited, the ternary diagram of sand, silt and clay proposed by Pejrup (1988) was employed (Figure 3.1.2). The data of sediment samples of core S1 and S3 fell in section IID indicating the sediments were deposited under relatively calm conditions. The sediments of mangrove core S2 fell in sections IID and IIID revealing the sediments were deposited under relatively calm to relatively violent depositional conditions. The sediments of core S4 however, fell in sections IIB, IIC and IIIC suggesting varying hydrodynamic environments, with time at this location.

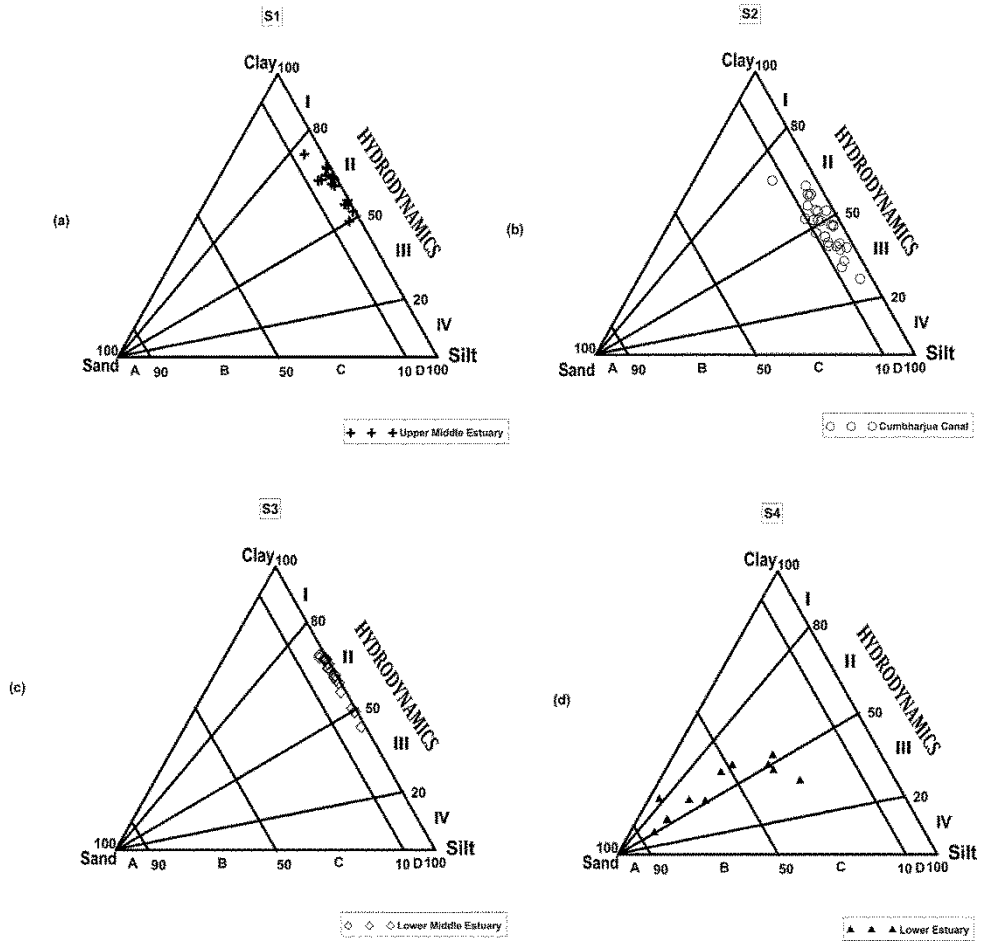


Figure 3.1.2: Ternary plots of sand, silt and clay as proposed by Pejrup (1988) for mangrove sediment cores S1, S2, S3 and S4.

### 3.1.A.2 Clay mineralogy

Clay minerals in mangrove environments are derived from continental sources and also possibly through authigenic processes. They are involved in typical soil formation processes and have an important role in nutrient dynamics and the behavior of toxic compounds, such as metals and organic pollutants, due to adsorption on the large specific surface area of clays.

The sediments of the Zuari estuarine mangroves are largely comprised of fine-grained sediments that are composed mainly of clay minerals and amorphous material. The composition and relative abundance of the clay minerals are controlled by their source rocks and weathering conditions. Their distribution in the estuary is controlled by depositional processes, the circulation patterns and the settling of clay minerals in response to the salinity and energy conditions (Rao and Rao, 1995). Selected subsamples of the mangrove cores were

subjected to clay mineral analysis using X-ray Diffraction and the range and average values obtained are presented in table 3.1.1(b). The clay mineral assemblage of the Zuari estuary was comprised of kaolinite, smectite, chlorite and illite. Kaolinite was the major clay mineral at all stations along the estuary followed by illite, smectite and chlorite.

In the mangrove sediment core S1, the percentages of smectite ranged between 13.43 % and 27.27 % (average 20.88%), illite ranged between 13.26 % and 20.90 % (average 17.22 %), kaolinite ranged between 49.79 % and 60.42 % (average 55.33 %) and chlorite ranged between 5.25 % and 8.29 % (average 6.58 %). The sediment core S2 collected from the Cumbharjua canal showed smectite percentages that ranged between 10.53 % and 14.29 % (average 12.66 %), illite ranged between 21.05 % and 37.62 % (average 27.75 %), kaolinite ranged between 44.55 % and 63.76 % (average 54.03 %) and chlorite ranged between 3.50 % and 7.42 % (5.57 %). The clay minerals composition of the sediments collected from the lower middle estuarine mangrove core S3 consisted of smectite that ranged between 10.98 % and 19.30 % (average 15.25 %), illite ranged between 16.18 % and 26.94 % (average 22.39 %), kaolinite ranged between 50.32 % and 66.59 % (average 55.27 %) and chlorite ranged between 5.13 % and 10.50 % (average 7.08 %). In the case of the lower estuarine mangrove sediment core S4, smectite content ranged between 17.36 % and 31.58 % (average 22.86 %), illite ranged between 15.79 % and 22.22 % (average 19.46 %), kaolinite ranged between 40.60 % and 58.48 % (average 52.84 %) and chlorite ranged between 2.51 % and 7.31 % (average 4.84 %).

In the distribution of clay minerals with depth (Figure 3.1.3), in the sediment core S1 collected from the upper middle estuary, smectite percentage decreased from the base of the core up to 14 cm and then increased towards the surface. Illite increased up to 10 cm and then decreased towards the surface. Kaolinite showed opposite distribution pattern to smectite and chlorite exhibited opposite distribution pattern to illite. In the clay mineral distributions in core S2 with depth, smectite displayed little variation, illite showed a fluctuating distribution pattern with a decrease in percentage from the base of the core up to 22 cm followed by an increase up to 10 cm and further decreased and then constant values along the average towards the surface. Kaolinite exhibited an opposite distribution pattern to illite. Smectite and chlorite percentages decreased up to 18 cm followed by fluctuations around the average line towards the surface.

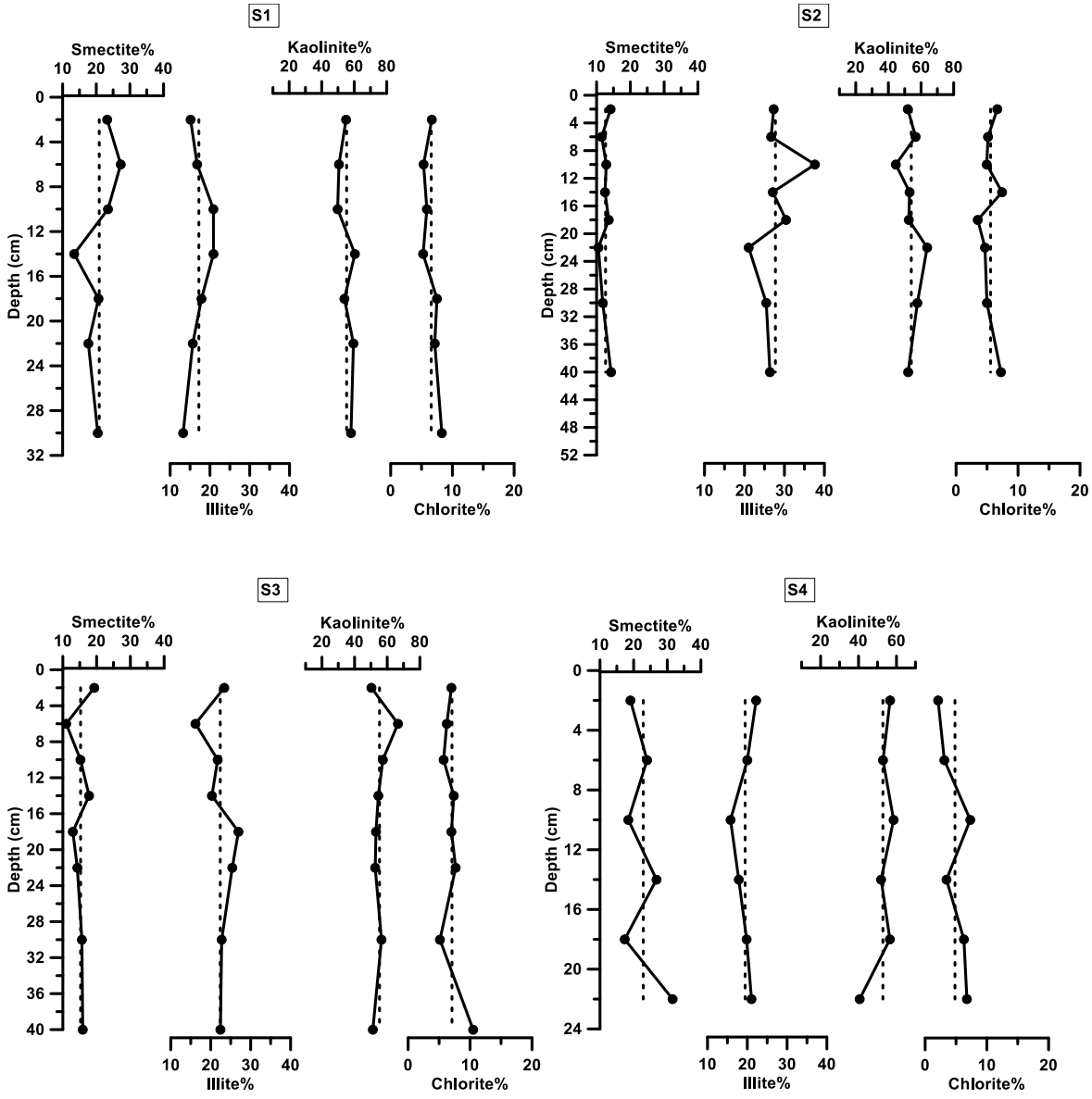


Figure 3.1.3: Distribution of clay minerals in the mangrove sediment cores S1, S2, S3, and S4.

In the distribution of clay mineral with depth of the lower middle estuarine mangrove core S3, smectite exhibited near uniform distribution up to 18 cm followed by fluctuating distribution towards the surface. The illite showed a minor increase up to 18 cm followed by a fluctuating distribution towards the surface similar to smectite. Kaolinite values were constant with depth except for a minor positive peak at 6 cm. Chlorite values decreased up to 30 cm from the base of the core followed by a uniform distribution towards the surface. Overall, clay minerals showed minor variations in their distributions with depth in this core. From the distribution of clay minerals with depth in core S4, smectite showed a fluctuating

trend with overall decrease towards the surface. Illite showed a minor decrease up to 10 cm followed by an increase towards the surface. Kaolinite percentage increased up to 18 cm followed by a steady distribution pattern towards the surface. Chlorite percentages decreased towards the surface with minor fluctuations.

Clay minerals are good indicators of the source area, weathering intensity and maturity of modern marine and fluvial sediments. As the distance from the source area increases, the sediments present a clay mineral assemblage that might have changed in relation to transport, deposition, remobilization and inputs from tributaries (Guyot et al., 2007). Abundant kaolinite reflected intense chemical weathering of the rocks along the drainage basin under humid tropical conditions in the catchment area and marks well developed leached soils and mature sediments. Feuillet and Fleischer (1980) stated that the estuarine circulation exerts the dominant influence on the clay mineral distribution. Average clay mineral percentages in the mangrove sediments indicated that smectite was abundant in core S4, illite in core S2, kaolinite in core S1 and chlorite in core S3. Smectite being the finest clay and flocculated at higher salinity explained the higher smectite concentration in the lower estuarine core. A decrease of kaolinite from the upstream regions towards downstream was noted in Zuari estuary within the mangrove sediments. The higher values of kaolinite in the upper middle estuarine sediments have resulted from its characteristic flocculation at low salinity. Furthermore, the relatively low kaolinite content in the Cumbharjua canal, as compared to the upper middle and lower middle estuarine sediments, suggested that the Cumbharjua canal does not make a strong impact with respect to addition of kaolinite but may have supplied a considerable amount of illite to the Zuari estuary. However, minor amounts of Illite and chlorite seem to be added as products of weathering of rocks from the catchment area. The smectite percentage was also high in sediments of the upper middle estuary. Smectite as a weathering product of the lithological formations in coastal plains and transported into the Zuari estuary during the monsoon season was reported by Kessarkar et al. (2013). However, Bukhari and Nayak (1996) have interpreted higher smectite near the mouth as input from sea side as weathering products of coastal basalts. The input of smectite from the seaside was possible as continental shelf sediments off Goa contain high smectite (Rao and Rao, 1995).

The clay mineral distributions at each station as a whole did not show much variation with depth that suggested little change in source in the catchment area. However, smectite and to some extent illite showed opposite distribution patterns to that of kaolinite. This distribution

pattern implied an authigenic transformation process likely taking place, from kaolinite to Fe-illite/glauconite, through transitory kaolinite - smectite and illite - smectite phases in the mangrove sediments. The reaction is triggered by high Fe activity in solution generated by dissolution of Fe oxides and pyrite present in the sediment, at approximately neutral pH and high salt content in the water (Pugliese-Andrade et al., 2014). Thus, the clay mineral assemblage reflected the weathering conditions in the catchment area, in addition to the transportation and depositional processes occurring in the mangrove environments.

### 3.1.A.3 Magnetic susceptibility

The magnetic parameters that determine the concentration of magnetic minerals are magnetic susceptibility ($\chi_{lf}$), saturation isothermal remnant magnetization (SIRM) and susceptibility of anhysteretic remnant magnetization ($\chi_{ARM}$). These parameters increase in denomination as the concentration of magnetic material in sediment increases. S-ratio was used as a mineral dependent parameter and values of S-ratio near 100 % indicate a high proportion of magnetite, whereas lower values indicate an increasing amount of haematite and goethite. The magnetic grain size is denoted by the frequency dependent susceptibility ($\chi_{fd}$) and the ratios $\chi_{ARM}$/ $\chi_{lf}$ and $\chi_{ARM}$/SIRM. Higher values of these parameters reflect more Stable Single Domain (SSD) grains and lower values reflect more Multi-Domain (MD) or Super-Paramagnetic (SP) grains (Dessai et al., 2009; Singh et al., 2013). The range and average values of magnetic susceptibility parameters in mangrove sediments are presented in table 3.1.1(c).

The magnetic mineral concentration parameters, $\chi_{lf}$ values of the core S1 collected from the upper middle estuarine mangroves varied distinctly from 152 $\times10^{-8}$ $m^3$ $kg^{-1}$ to 406 $\times10^{-8}$ $m^3$ $kg^{-1}$ (average 228.60 $\times10^{-8}$ $m^3$ $kg^{-1}$), $\chi_{ARM}$ values ranged from 792 $\times10^{-8}$ $m^3$ $kg^{-1}$ to 1106 $\times10^{-8}$ $m^3$ $kg^{-1}$ (average 1008 $\times10^{-8}$ $m^3$ $kg^{-1}$) and SIRM values ranged from 1532 $\times10^{-5}$ $Am^2$ $kg^{-1}$ to 4701 $\times10^{-5}$ $Am^2$ $kg^{-1}$ (average of 2212$\times10^{-5}$ $Am^2$ $kg^{-1}$). The inter-parameter ratios of $\chi_{ARM}$ / $\chi_{lf}$, $\chi_{ARM}$ /SIRM vary with magnetic grain size and are used to assess the relative change in the concentrations of fine magnetic grain sizes (Peters and Dekkers, 2003; Maher, 1988). The $\chi_{ARM}$ / $\chi_{lf}$ ratio ranged from 2.66 to 5.45 (average of 4.70) whereas the $\chi_{ARM}$ /SIRM ratio ranged from 0.23$\times10^{-3}$ $A^{-1}m$ to 0.67$\times10^{-3}$ $A^{-1}m$ (average 0.51$\times10^{-3}$ $A^{-1}m$). $\chi_{fd}$, a parameter that is a measure of the concentration of ultra-fine magnetic grains in the SP or SSD size

range that are produced during pedogenesis, in core S1 ranged from 1.24 % to 10.84 % (average 7.04 %). The S-ratio % of core S1 ranged from 87.75 % to 93.55 % (average 90.44 %). In the sediment core S2 collected from the Cumbharjua canal, the $\chi_{lf}$ values ranged from 226 $\times 10^{-8}$ $m^3$ $kg^{-1}$ to 321 $\times 10^{-8}$ $m^3$ $kg^{-1}$ (average 264.85$\times 10^{-8}$ $m^3$ $kg^{-1}$), $\chi_{ARM}$ values ranged between 796 $\times 10^{-8}$ $m^3$ $kg^{-1}$ and 1118$\times 10^{-8}$ $m^3$ $kg^{-1}$ (average 944$\times 10^{-8}$ $m^3$ $kg^{-1}$) and SIRM values ranged from 2919$\times 10^{-5}$ $Am^2$ $kg^{-1}$ to 5387 $\times 10^{-5}$ $Am^2$ $kg^{-1}$ (average of 3757$\times 10^{-5}$ $Am^2$ $kg^{-1}$). The ratio of $\chi_{ARM}$ / $\chi_{lf}$ varied between 2.96 and 4.08 (average 3.58) whereas the ratio of $\chi_{ARM}$ /SIRM in the core ranged between 0.18 $\times 10^{-3}$ $A^{-1}m$ and 0.31 $\times 10^{-3}$ $A^{-1}m$ (average 0.26$\times 10^{-3}$ $A^{-1}m$) and $\chi_{fd}$ in core S2 ranged from 3.45 % to 5.45 % (average 4.45 %) and the S-ratio varied between 85.98 % to 89.28 % (average 87.76 %). In the mangrove sediment core S3 collected from the lower middle estuary magnetic susceptibility parameters, $\chi_{lf}$ ranged from 128 $\times 10^{-8}$ $m^3$ $kg^{-1}$ to 161 $\times 10^{-8}$ $m^3$ $kg^{-1}$ (average 147$\times 10^{-8}$ $m^3$ $kg^{-1}$), $\chi_{ARM}$ varied between 823$\times 10^{-8}$ $m^3$ $kg^{-1}$ and 1143$\times 10^{-8}$ $m^3$ $kg^{-1}$ (average 986$\times 10^{-8}$ $m^3$ $kg^{-1}$) and SIRM ranged from 1293$\times 10^{-5}$ $Am^2$ $kg^{-1}$ to 1486$\times 10^{-5}$ $Am^2$ $kg^{-1}$ (average 1384$\times 10^{-5}$ $Am^2$ $kg^{-1}$). The values of the ratio of $\chi_{ARM}$ / $\chi_{lf}$ varied between 6.27 and 7.08 (average of 6.67) and $\chi_{ARM}$ /SIRM values ranged from 0.64$\times 10^{-3}$ $A^{-1}m$ to 0.78$\times 10^{-3}$ $A^{-1}m$ (average 0.71$\times 10^{-3}$ $A^{-1}m$). $\chi_{fd}$ values ranged from 4.28 % to 9.47 % (average 7.03) and S-ratio varied from 88.81 % to 91.85 % (average 89.98 %). In the lower estuary core S4, the magnetic susceptibility measurements of $\chi lf$ varied from 53.27$\times 10^{-8}$ $m^3$ $kg^{-1}$ to 267$\times 10^{-8}$ $m^3$ $kg^{-1}$ (average 145.39$\times 10^{-8}$ $m^3$ $kg^{-1}$), $\chi_{ARM}$ ranged from 229$\times 10^{-8}$ $m^3$ $kg^{-1}$ to 840$\times 10^{-8}$ $m^3$ $kg^{-1}$ (average 542$\times 10^{-8}$ $m^3$ $kg^{-1}$) and SIRM varied from 518$\times 10^{-5}$ $Am^2$ $kg^{-1}$ to 2982$\times 10^{-5}$ $Am^2$ $kg^{-1}$ (average 1646$\times 10^{-5}$ $Am^2$ $kg^{-1}$). The magnetic grain size distribution parameters $\chi_{ARM}$ / $\chi_{lf}$ values varied from 2.98 to 4.64 (average 3.84), $\chi_{ARM}$ /SIRM values ranged from 0.26$\times 10^{-3}$ $A^{-1}m$ to 0.44$\times 10^{-3}$ $A^{-1}m$ (average 0.34$\times 10^{-3}$ $A^{-1}m$) and $\chi_{fd}$ values ranged from 2.95 % to 7.95 % (average 4.81 %). S-ratio values in the core range from 84.73 % to 91.48 % (average 89.08 %).

The distribution of magnetic susceptibility parameters with depth in core sediment S1 showed that the $\chi_{lf,}$ $\chi_{ARM,}$ and SIRM values decreased up to 14 cm from the core base followed by a constant distribution pattern towards the surface. The ratios of $\chi_{ARM}$ / $\chi_{lf}$, $\chi_{ARM}$ /SIRM and $\chi_{fd}$% increased towards the surface but showed lower values at the surface, than at 6 cm, and $\chi_{ARM}$ /SIRM and $\chi_{fd}$% exhibited a decreased peak at 14 cm. S-ratio values decreased from the base of the core up to 14 cm followed by an increase towards the surface. A decrease at 14 cm was noted for most magnetic susceptibility parameters i.e. magnetic concentration, grain size and mineralogy. In sediment core S2, the distribution of $\chi_{lf,}$ $\chi_{ARM}$ and SIRM with depth

exhibited higher values from 40 cm to 22 cm followed by a sharp decrease up to 18 cm and constant values towards the surface. The profiles of $\chi_{ARM}$ / $\chi_{lf}$, $\chi_{ARM}$ /SIRM and $\chi_{fd}$ showed a similar distribution trend i.e. a minor decrease from 40 cm to 22 cm followed by constant distribution towards the surface. The distribution of S-ratio exhibited a decreasing trend up to 18 cm followed by an increase towards the surface. The distribution of magnetic susceptibility parameters with depth in core S3 revealed that the magnetic mineral concentration parameters $\chi_{lf}$ and SIRM exhibited a uniform distribution pattern with depth whereas $\chi_{ARM}$ distribution showed minor variations around the average. $\chi_{ARM}$ / $\chi_{lf}$ and $\chi_{ARM}$ /SIRM showed values slightly higher than average below 22 cm followed by constant distribution pattern towards the surface whereas $\chi_{fd}$ exhibited constant distribution pattern up to 14 cm followed by fluctuating distribution towards the surface. The S-ratio showed little variation in its distribution with a decrease up to 30 cm followed by constant distribution pattern towards the surface with a minor decreased peak at 10 cm. Overall the magnetic susceptibility parameters showed little variation in distributions with depth in the lower middle estuarine region. The variation in the vertical distribution of magnetic parameters in core S4 revealed that concentration dependent parameters $\chi_{lf}$, $\chi_{ARM}$ and SIRM values to increase towards the surface of the core. Magnetic grain size distribution parameters $\chi_{ARM}$ / $\chi_{lf}$, $\chi_{ARM}$ /SIRM and $\chi_{fd}$ displayed similar distribution trends i.e. increase up to 30 cm followed by decrease towards the surface. The S-ratio increased up to 14 cm from the base of the core followed by relatively constant values above average towards the surface.

The mean values of the magnetic parameters and inter-parametric ratios for the four sediment cores collected from the mangroves of the Zuari estuary indicated the presence of magnetite and hematite in the sediments. High $\chi_{lf}$ values were noted in the upper middle estuary and the Cumbharjua canal which decreased towards the downstream regions of the estuary. The SIRM values were high in the upper middle estuary and the Cumbharjua canal than the downstream regions of the estuary. Thus, the high magnetic susceptibility values in the upper middle estuary indicated the presence of ferromagnetic minerals such as magnetite. $\chi_{fd,}$ is a measure of the concentration of ultra-fine magnetic grains in the Super-Paramagnetic (SP) or SSD size range and is produced during pedogenesis (Maher and Taylor, 1988). $\chi_{fd,}$ showed low values at S2 and S4 (4.45% to 4.81 %) suggesting that much of the material in these regions was derived from natural sources with some contribution from the mining material and ship building activities in the lower estuary. The ratios of $\chi_{ARM}$ / $\chi_{lf}$ and $\chi_{ARM}$ /SIRM are used to interpret magnetic grain size. Higher $\chi_{ARM}/\chi_{lf}$ value reflects more Stable Single

Domain (SSD) grains and lower values reflect more Multi-Domain (MD) or Super-Paramagnetic (SP) grains. The average $\chi_{ARM}$ / $\chi_{lf}$ values decreased in the order of S3 > S1> S4>S2 which indicated the presence of SSD grains at S3, S1 and S4 whereas S2 may have some amount of MD or SP grains. The low average values of grain size parameters at S2 suggested the association of higher concentrations of mineral with the coarser grains indicating that the control was detrital as well as authigenic components (Sangode et al., 2001). According to Dearing et al. (1997), a $\chi_{ARM}$ /SIRM value of <20 $\times 10^{-5}$ $Am^{-1}$ indicated MD + PSD grains and values between 20 and $90\times10^{-5}$ $Am^{-1}$ suggested coarse SSD grains. From the average values of $\chi_{ARM}$ /SIRM of the four locations, it was noted that the Zuari estuary had a higher amount of coarse SSD grains. A plot of $\chi_{fd}$ % versus $\chi_{ARM}$ /SIRM with superimposed threshold values allowed estimates of the proportions of frequency dependent SP and non-SP grains (Maher and Taylor, 1988; Dearing et al., 1997; Sandeep et al., 2010).

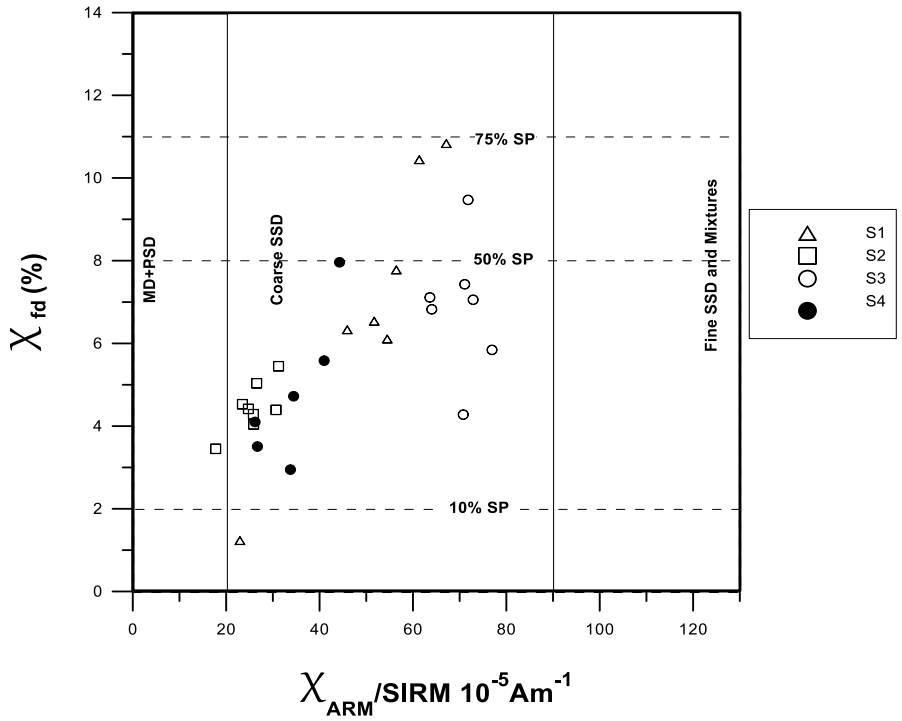


Figure 3.1.4: Plot of $\chi_{fd}$ % versus $\chi_{ARM}$ /SIRM for mangrove sediments from the Zuari estuary.

The plot of $\chi_{fd}$ versus $\chi_{ARM}$/SIRM (Figure 3.1.4) showed wide variations in magnetic grain size ranging from MD + PSD, coarse SSD and indicated the overall coarse SSD nature of the sediments of the Zuari estuary. A higher proportion of SP grains were noted in S1 followed by S3. The sediments of the Cumbharjua canal however, had some contribution from the MD+ PSD grains suggesting some inputs from mining activities. From the IRM acquisition

curves (Figure 3.1.5) it was observed that the Cumbharjua canal S2 and the upper middle estuary S1 have high IRM values that suggested contributions from the mining area to the estuarine regions. The iron ore mining areas are located in the catchment area of Mandovi and Zuari estuaries with storing and loading points of iron ore in the upstream region. During the monsoon months some material from mining and stored ore dumps are released to the estuary. Among the mines, two third of iron ore mining activities come under the Mandovi river watershed (Pathak et al., 1988). Further, in the case of Mandovi estuary, a major drainage area comes through quartzsericite schist and phyllite with banded iron formations, which could add magnetic minerals to the estuary. The Cumbharjua canal connects the Mandovi and the Zuari estuaries and during monsoon water flows from the Mandovi to the Zuari estuary. Therefore, a part of the magnetic material that was supplied to the Mandovi estuary consequently was accumulated in the Cumbharjua canal mangrove sediments. The higher IRM values of the lower estuarine mangrove sediments than the lower middle estuary could be due to hematite weathering into more magnetic soils containing maghemite (Allan et al., 1988) or formation of ferritized iron crust during lateritic weathering (Mathé et al., 1997). Additionally, shipbuilding activities in the lower estuary may have contributed to the higher IRM values.

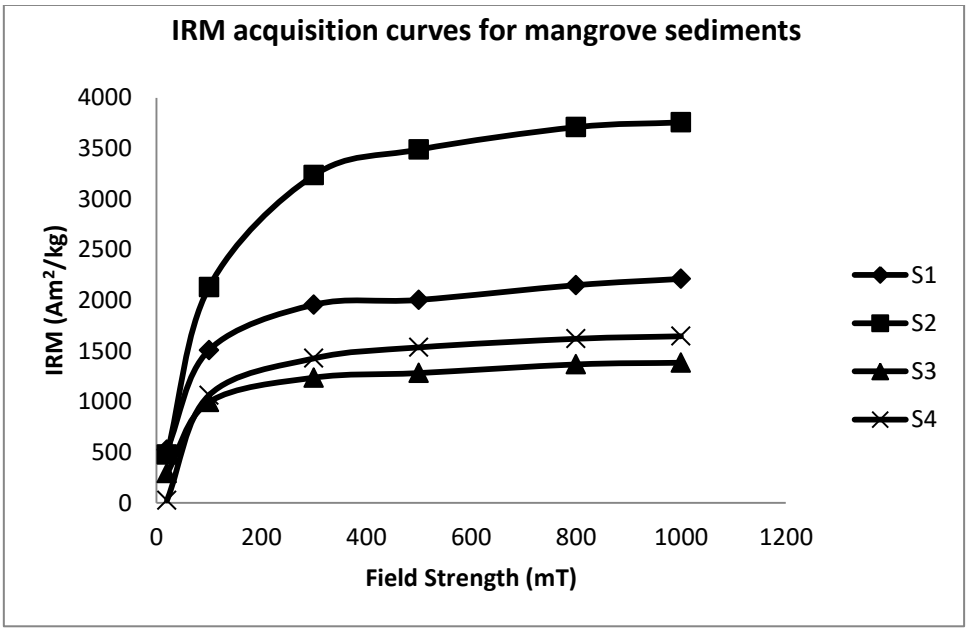


Figure 3.1.5: IRM acquisition curves of mangrove sediments collected from the Zuari estuary.

The S-ratio which is an indicator of mineral type was relatively higher in the upper middle estuary followed by the lower middle and lower estuary (S1, S3 and S4 ~ 90 %) and lowest in the Cumbharjua canal (88 %). High S-ratios are associated with magnetite and low S-ratios are associated with hematite and exhibit high Fe content in the spectrum (Kessarkar et al., 2015). The high S-ratio (~90 %) observed suggested the presence of magnetite; however, the S-ratio also suggested the presence of hematite in the sediments that was indicated by the IRM acquisition curves that revealed most samples were not saturated even at 1T. Thus, the sediments in the estuary were a mixture of magnetite and hematite.

From the distribution of magnetic susceptibility parameters with depth in the four sediment cores (Figure 3.1.6), minor variations with depth were observed. In core S1, a decrease in magnetic concentration parameters along with increasing grain size parameters suggested the higher magnetic susceptibility and S- ratio in the lower part of the core, which may be due to coarse SP grains and indicated the dominance of magnetite with relative increase in hematite towards the surface. The increase in the S-ratio values above 14 cm towards the surface suggested the increase of magnetite. In the core collected from the Cumbharjua canal, the lower part of the core (40 cm to 22 cm) had higher content of magnetic material of the coarser grain size with decreasing content of magnetite. The upper part of the core showed little variations in the distributions of magnetic parameters and S-ratio values increased that suggested the increasing amount of magnetite towards the surface. Little variation with depth was observed in the lower middle estuarine core in the distribution of magnetic parameters suggesting the stability of the depositional environment. Increase in magnetic concentration in the lower estuary, along with decrease in grain size parameters indicated the presence of coarse magnetic grains towards the surface. $\chi_{lf}$ reflects the concentration of magnetic material largely associated with terrigenous supply. Its low values in core S1 (10 cm to 2 cm) and core S2 (22 cm to 2 cm) reflected decrease in terrigenous input of sediments. However, in core S4, the increase in $\chi$lf values indicated increase in detrital supply of sediments.

Liu et al. (2004) identified four stages of sediments that correspond to the effects of progressive early diagenesis. Stage 1 is least affected by diagenesis with high concentrations of detrital magnetite and hematite. Stage 2 shows the presence of pyrite and decreasing concentrations of detrital magnetite. Stage 3 is marked by a progressive loss of hematite with depth and minimum magnetite and stage 4 with enhanced concentrations of authigenic magnetic minerals such as greigite or pyrrhotite.

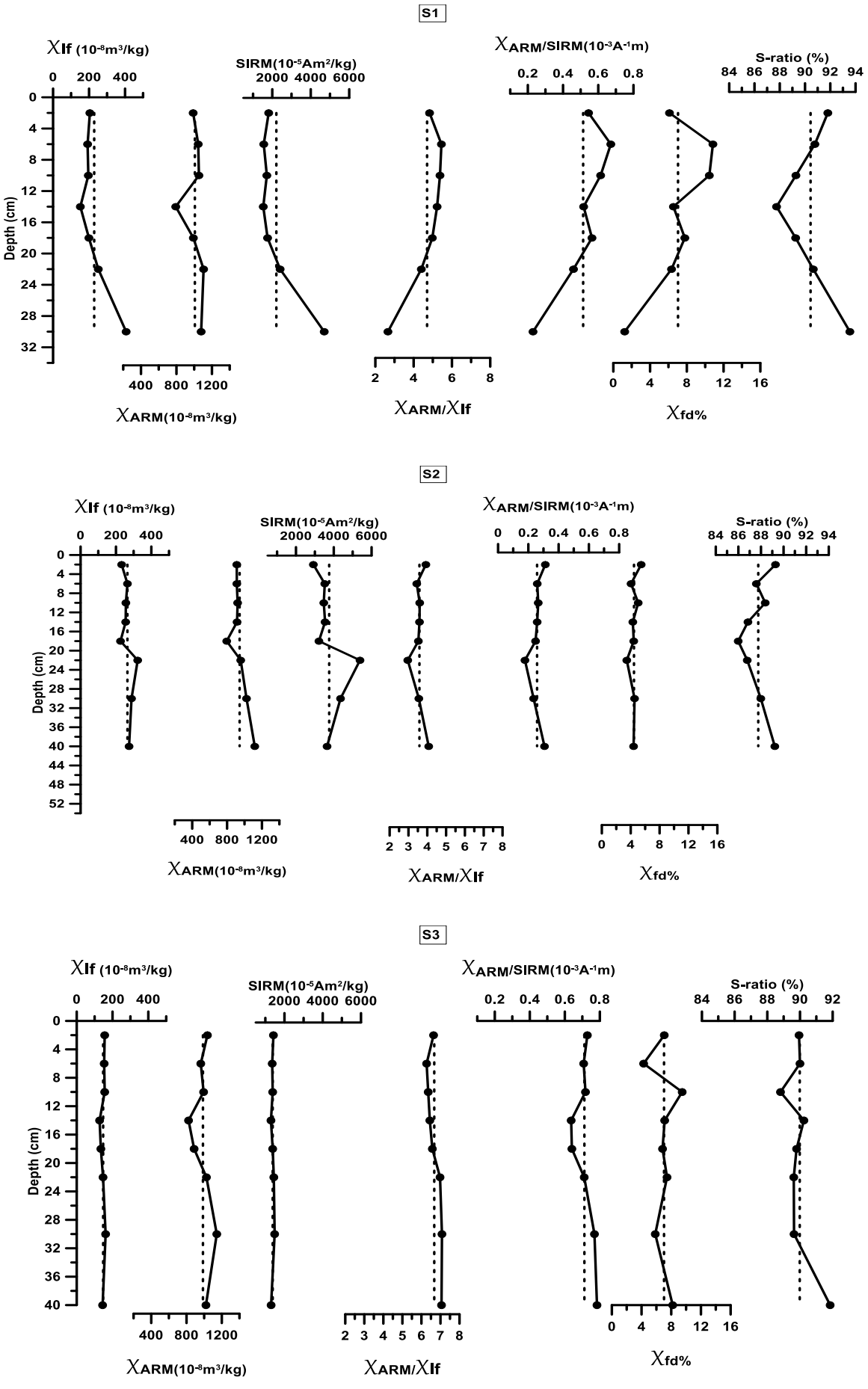
S1
χlf (10⁻⁸m³/kg)
SIRM(10⁻⁵Am²/kg)
χARM/SIRM(10⁻³A⁻¹m)
S-ratio (%)
Depth (cm)
χARM(10⁻⁸m³/kg)
χARM/χlf
χfd%
S2
χlf (10⁻⁸m³/kg)
SIRM(10⁻⁵Am²/kg)
χARM/SIRM(10⁻³A⁻¹m)
S-ratio (%)
Depth (cm)
χARM(10⁻⁸m³/kg)
χARM/χlf
χfd%
S3
χlf (10⁻⁸m³/kg)
SIRM(10⁻⁵Am²/kg)
χARM/SIRM(10⁻³A⁻¹m)
S-ratio (%)
Depth (cm)
χARM(10⁻⁸m³/kg)
χARM/χlf
χfd%

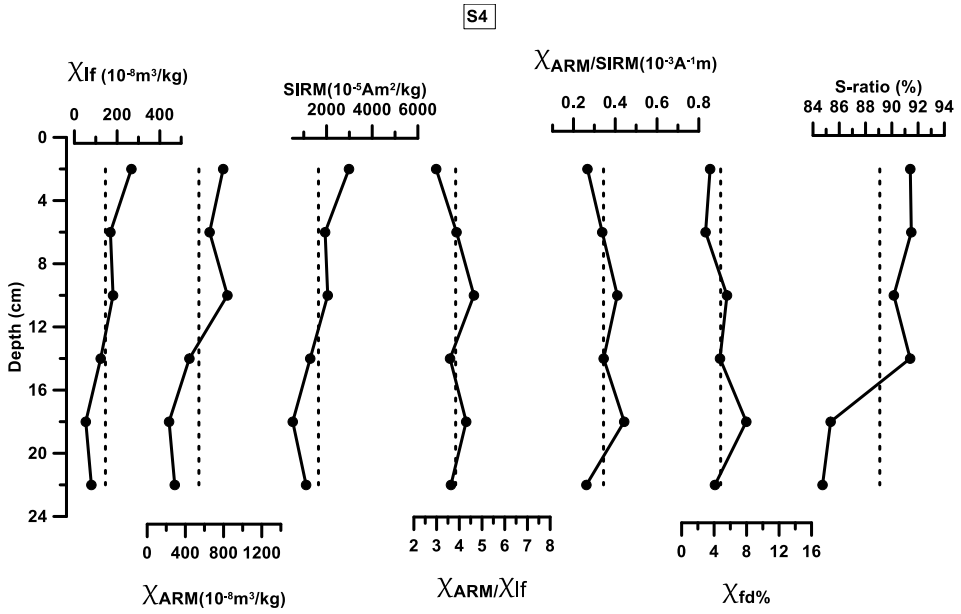


Figure 3.1.6: Distribution of magnetic susceptibility parameters with depth in cores mangrove sediment cores S1, S2, S3, and S4.

A decreased peak of all the parameters, namely magnetic concentration, grain size and mineralogy in sediments of core S1 at 14 cm indicated stage 2 diagenesis. High TOC at 14 cm may have favored reductive diagenesis and dissolution of magnetic minerals. The high S-ratios in lower portion of the core and surface sediments indicated that the ferrimagnetic material was the dominant component. The low values of $\chi_{ARM}$, $\chi_{ARM}$ / $\chi_{lf}$ and $\chi_{ARM}$ /SIRM at 10 cm indicated that the fine grained ferrimagnetic components are selectively dissolved during early diagenesis (Karlin, 1990) leaving a residue of coarse grained lithogenic magnetites (Rolph et al., 2004).

### 3.1.A.4 Geochemistry of sediments

### 3.1.A.4a Metals in bulk sediments

The range and average values of metals in the bulk sediments of mangrove cores S1, S2, S3 and S4 are presented in table 3.1.2.

The metal content in the sediment core S1 showed that major elements Al % varied from 7.28 % to 11.24 % (average 8.75 %), Fe % ranged from 9.26% to 12.47 % (average 10.84 %) and

Mn concentration varied between 4132 ppm and 6793 ppm (average 5181 ppm). Trace metals Cr, Co, Ni, Cu and Zn ranged from 228 ppm to 405 ppm (average 274 ppm), 14.00 ppm to 27.75 ppm (average 21.75 ppm), 33.75 ppm to 58.00 ppm (average 41.78 ppm), 34.50 ppm to 59.25 ppm (average 45.9 ppm) and 122 ppm to 187 ppm (average 144 ppm ) respectively. In sediment core S2 collected from the Cumbharjua canal, Al, Fe and Mn ranged from 6.64 % to 10.73 % (average 8.38 %), 11.20 % to 20.89 % (average 14.53 %) and 2049 ppm to 8134 ppm (average 5122 ppm) respectively. The trace metal concentrations of Cr, Co, Ni, Cu and Zn ranged from 175 ppm to 428 ppm (average 271 ppm), 18.50 ppm to 30.75 ppm (average 22.85 ppm), 36.50 ppm to 73.75 ppm (average 47.15 ppm), 30.50 ppm to 50.00 ppm (average 36.26 ppm) and 85.50 ppm to 194 ppm (average104 ppm) respectively. The lower middle estuarine sediment core S3 showed that, Al, Fe and Mn concentrations ranged from 10.28 % to 15.80 % (average 11.59 %), 8.57 % to 12.10 % (average 10.54 %) and 1281 ppm to 4004 ppm (average 2138 ppm) respectively. Trace metals Cr, Co, Ni, Cu and Zn concentrations ranged from 210 ppm to 494 ppm (average 318 ppm), 17.75 ppm to 27.75 ppm (average 23.23 ppm), 35.75 ppm to 49.50 ppm (average 44.33 ppm) , 33.50 ppm to 52.25 ppm (average 42.11 ppm) and 117 ppm to 153 ppm (average 127 ppm) respectively. In the lower estuarine core sediment S4, major elements Al, Fe and Mn ranged from 3.63 % to 9.94 % (average 6.33 %), 7.25 % to 10.35 % (average 9.15 %) and 448 ppm to 2286 ppm (average 1153 ppm). Trace metals Cr, Co, Ni, Cu and Zn concentrations varied from 216 ppm to 542 ppm (average 336 ppm), 2.25 ppm to 29.50 ppm (average 19.98 ppm), 18.75 ppm to 39.50 ppm (average 27.6 ppm), 18.75 ppm to 37.75 ppm (average 26.92 ppm) and 46.25 ppm to 119.50 ppm (average 79.63 ppm).

The distribution of metals with depth in the four-mangrove sediment cores are presented in figure 3.1.7. In the distribution of major and trace metals in core S1 with depth, Al showed a near uniform distribution with minor increase from 34 cm to 12 cm followed by constant distribution pattern toward the surface. Fe also exhibited a near uniform distribution with minor positive peaks at 26 cm and negative peak at 24 cm. Mn concentrations decreased from 34 cm to 14 cm with a peak at 22 cm followed by constant distribution towards the surface. Cr, Co, Ni, Cu, and Zn showed similar distribution trends to Fe with common peaks around 26 cm and 24 cm depth. The similar distribution trends of Cr, Co, Ni, Cu, and Zn with Fe suggested the adsorption of metals onto Fe oxides. However, peak values at 10 cm for most of the trace metals along with Mn indicated their diagenetic enrichment in the sedimentary column. Co, Ni, Cu showed slightly increased concentrations at the surface.

Table 3.1.2: Range and average values of metals in bulk sediments (a) and metals in the clay fraction (b) in mangrove sediment cores S1, S2, S3, and S4 of the Zuari estuary.

| | | | S1 | | S2 | | S3 | | S4 | |
|---|---|---|---|---|---|---|---|---|---|---|
| | | Metals | Average | Range | Average | Range | Average | Range | Average | Range |
| (a) | Metals in bulk sediment | Al (%) | 8.75 | 7.28-11.24 | 8.38 | 6.64-10.73 | 11.59 | 10.28-15.80 | 6.33 | 3.63-9.94 |
| | | Fe (%) | 10.84 | 9.26-12.47 | 14.53 | 11.20-20.89 | 10.54 | 8.57-12.10 | 9.15 | 7.25-10.35 |
| | | Mn (ppm) | 5181 | 4132-6793 | 5123 | 2049-8134 | 2138 | 1281-4004 | 1153 | 448-2286 |
| | | Cr (ppm) | 274 | 228-405 | 271 | 175-428 | 318 | 210-494 | 336 | 216-542 |
| | | Co (ppm) | 21.75 | 14.00-27.75 | 22.85 | 18.50-30.75 | 23.23 | 17.75-27.75 | 19.98 | 2.25-29.50 |
| | | Ni (ppm) | 41.78 | 33.75-58.00 | 47.15 | 36.50-73.75 | 44.33 | 35.75-49.50 | 27.6 | 18.75-39.50 |
| | | Cu (ppm) | 45.9 | 34.50-59.25 | 36.26 | 30.50-50.00 | 42.11 | 33.50-52.25 | 26.92 | 18.75-37.75 |
| | | Zn (ppm) | 144 | 122-187 | 104 | 85.50-194 | 127 | 117-153 | 79.63 | 46.25-120 |
| (b) | Metals in clay fraction | Al (%) | 11.18 | 10.62-11.64 | 15.33 | 13.31-17.52 | 8.84 | 6.96-10.74 | 7.68 | 4.36-10.76 |
| | | Fe (%) | 7.76 | 6.83-8.43 | 8.81 | 8.13-9.88 | 7.18 | 6.49-7.65 | 5.23 | 3.25-6.37 |
| | | Mn (ppm) | 6409 | 5683-6747 | 5459 | 4327-6266 | 3217 | 1804-5043 | 2045 | 438-3302 |
| | | Cr (ppm) | 454 | 328-521 | 410 | 348-583 | 731 | 689-797 | 700 | 566-785 |
| | | Co (ppm) | 29.54 | 19.50-39.50 | 36.56 | 31.50-45.75 | 19.97 | 11.25-30.25 | 18.13 | 10.25-28.50 |
| | | Ni (ppm) | 153 | 125-180 | 117 | 97.75-157 | 158 | 135-184 | 52.21 | 42.00-62.25 |
| | | Cu (ppm) | 197 | 177-213 | 217 | 166-297 | 198 | 178-226 | 170 | 153-208 |
| | | Zn (ppm) | 527 | 148-1076 | 355 | 128-1023 | 438 | 135-810 | 327 | 123-689 |

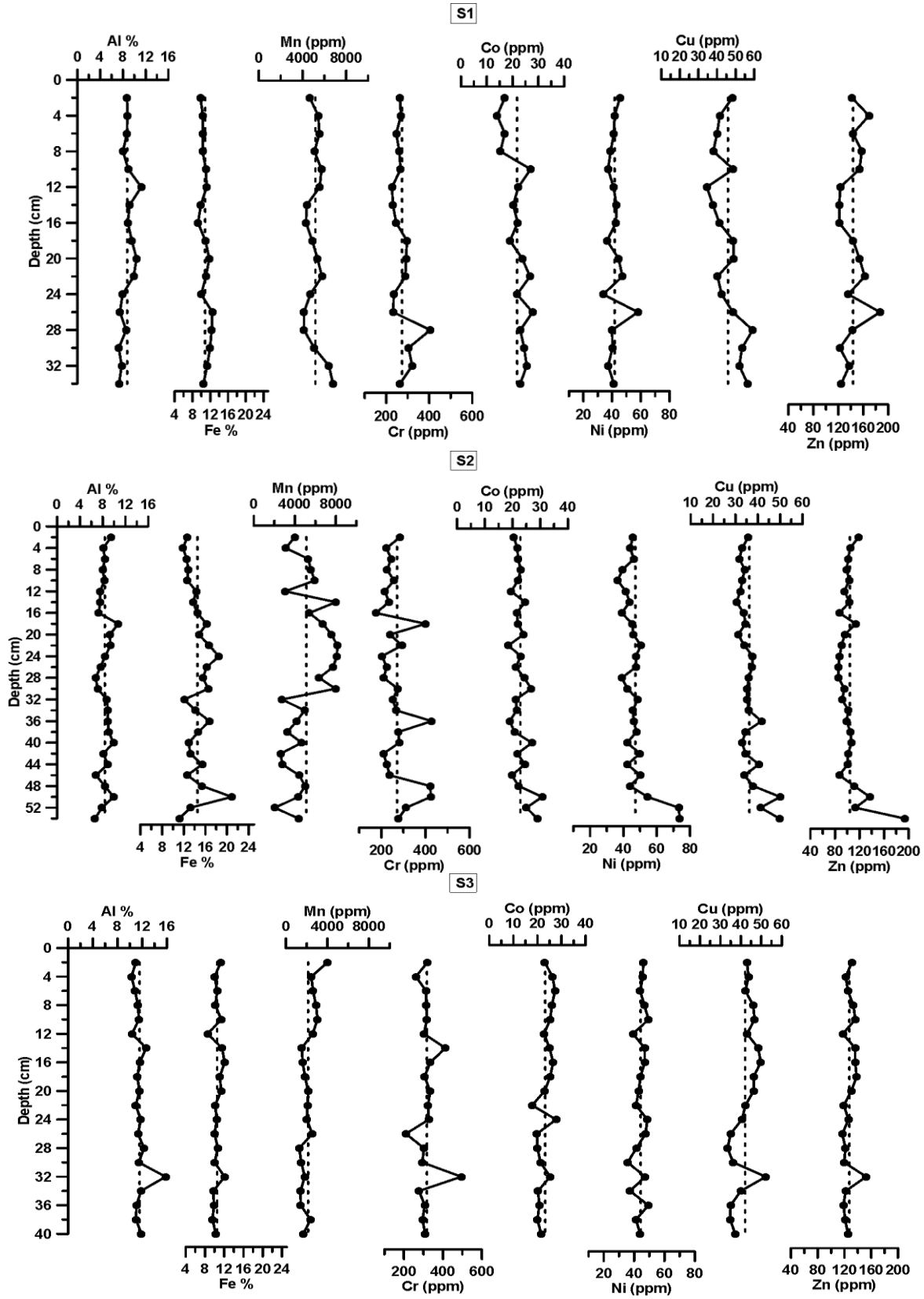
S1
Al %
Mn (ppm)
Co (ppm)
Cu (ppm)
Depth (cm)
Fe %
Cr (ppm)
Ni (ppm)
Zn (ppm)
S2
Al %
Mn (ppm)
Co (ppm)
Cu (ppm)
Depth (cm)
Fe %
Cr (ppm)
Ni (ppm)
Zn (ppm)
S3
Al %
Mn (ppm)
Co (ppm)
Cu (ppm)
Depth (cm)
Fe %
Cr (ppm)
Ni (ppm)
Zn (ppm)

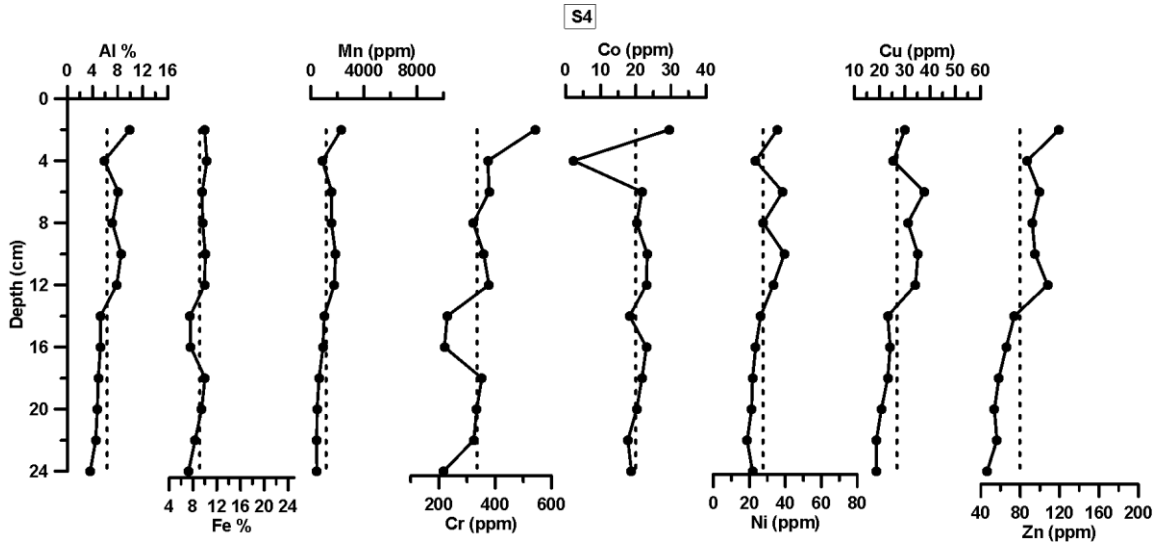


Figure 3.1.7: Distribution of bulk metals Fe, Mn, Cr, Co, Ni, Cu and Zn with depth in mangrove sediment cores S1, S2, S3 and S4.

In core S2, when the distribution of metals was considered with depth, Al displayed a constant distribution trend towards the surface with minor fluctuations around the average. Fe and Mn showed resemblance in their distribution patterns with an increasing trend up to 22 cm followed by a decreasing trend towards the surface. The peaks at 30 cm and 24 cm in the profiles of Fe and Mn suggested their diagenetic mobilization. Trace metals Cr, Co, Ni, Cu and Zn exhibited high concentrations in the lower part of the core (54 cm to 46 cm) with higher peak at 50 cm that agreed with Al and Fe. Cr, Ni, Cu and Zn showed slight increase near the surface. The depth profile of metals in core S3 showed uniform distribution patterns for major elements Al and Fe with depth. Mn increased between 12 cm to 0 cm indicating recent inputs. Most of the trace metals Cr, Co, Ni, and Zn displayed uniform distribution patterns with depth similar to Al and Fe. The concentration of Cu increased up to 14 cm from the bottom of the core. Overall, no large variations in concentrations with depth were observed except for Mn and Cu. Most of the metals showed a positive peak at 32 cm and negative peak at 12 cm depth. The distribution of metals with depth in sediment core S4 showed that Al, Fe, and Mn concentrations increased towards the surface. Trace metals Cr, Ni, Cu and Zn closely followed the distribution of Al, Fe and Mn in the vertical distribution suggesting their association with aluminosilicates and Fe-Mn oxides.

Further, Pearson's correlation analysis was carried out to understand the association of metals with the sediment components to ascertain the factors that govern their distribution in the sediments of the estuary and the results are presented in table 3.1.3. The range and average values showed considerable spatial variations in the distribution of metals. High average values of Mn, Cu, and Zn were noted in core S1, Fe and Ni in the core S2, Al and Co in core S3 and Cr in core S4 sediments.

The trends and associations observed in the sediment cores indicated different sedimentary processes operated at the four locations. In the upper middle estuary (S1), the highest concentrations of Mn, Cu and Zn were noted which implied the proximity of their source to the sampling location. The similar distribution trends of Cr, Co, Ni and Cu with Fe and their positive correlation with sand suggested the formation of Fe oxides coating on the sand particles. The trace metals must have adsorbed onto the Fe-oxide surfaces and/or may be present as silicates in rock fragment or heavy minerals (d'Anglejan et al., 1990). Burdige (1993) reported that iron and manganese oxides take up a variety of transition elements and heavy metals, either by adsorption to the oxide surface or by direct incorporation into the crystal structure. The distribution of Fe and Mn in estuarine sediments was affected by variations in several physicochemical factors like salinity, pH, Eh along the estuary. Low salinity in the upper reaches of the estuary must have caused the flocculation of Fe oxides along with the adsorbed trace metals. All trace metals in core S1 showed poor correlation with Al indicating their different source may be anthropogenic or different depositional process. However, peak values of metals at 10 cm for most of the trace metals along with Mn indicated their diagenetic re-mobilization in the sedimentary column (Jenne, 1968; Turekian, 1977). Thus, the distribution of most trace metals in this core was influenced by adsorption onto Fe-oxides and flocculation in low salinity.

Highest concentrations of Fe and Ni were recorded in sediment core S2 collected from the Cumbharjua canal. Mn in the Cumbharjua canal sediments was either associated with the silt-sized particles or may have occurred in the form of detrital mining particles that was implied by the significant correlation of Mn with silt. Further, Fe and Mn showed synchronous distribution with depth in this core reflecting similarity in their redox behaviors and the peak at 30 cm suggested their diagenetic enrichment. The high concentration of trace metals in the lower part of the core (54 cm to 50 cm), along with Al, Fe and Mn peak indicated lithogenic input. The significant association of Cr with Al and Fe implied a detrital source for Cr.

Table 3.1.3: Pearson's correlation coefficients of sediment components and bulk metals of mangrove cores S1 (a), S2 (b), S3 (c) and S4 (d) of the Zuari estuary.

(a)

**Correlations-S1**

| | pH | Sand | Silt | Clay | TOC | Al | Fe | Mn | Cr | Co | Ni | Cu | Zn | |
|---|---|---|---|---|---|---|---|---|---|---|---|---|---|---|
| pH | 1.00 | | | | | | | | | | | | | |
| Sand | -0.04 | 1.00 | | | | | | | | | | | | |
| Silt | 0.07 | -0.45 | 1.00 | | | | | | | | | | | |
| Clay | -0.07 | 0.21 | -0.97** | 1.00 | | | | | | | | | | |
| TOC | 0.65** | -0.11 | -0.11 | 0.15 | 1.00 | | | | | | | | | |
| Al | 0.19 | -0.56 | 0.07 | 0.08 | 0.26 | 1.00 | | | | | | | | N=17 |
| Fe | -0.19 | 0.59* | -0.13 | -0.03 | -0.23 | -0.04 | 1.00 | | | | | | | |
| Mn | 0.09 | -0.15 | 0.26 | -0.24 | -0.28 | 0.00 | -0.01 | 1.00 | | | | | | |
| Cr | -0.11 | 0.39 | -0.24 | 0.15 | -0.22 | -0.10 | 0.53* | 0.00 | 1.00 | | | | | |
| Co | 0.15 | 0.49* | 0.05 | -0.20 | 0.11 | -0.06 | 0.59* | 0.12 | 0.18 | 1.00 | | | | |
| Ni | -0.08 | 0.38 | -0.19 | 0.10 | -0.17 | 0.00 | 0.31 | -0.29 | -0.22 | 0.27 | 1.00 | | | |
| Cu | 0.10 | 0.69** | -0.16 | -0.02 | -0.18 | -0.49* | 0.53* | 0.10 | 0.70** | 0.39 | -0.03 | 1.00 | | |
| Zn | -0.53** | 0.12 | -0.03 | 0.00 | -0.68** | -0.05 | 0.37 | -0.10 | 0.02 | 0.05 | 0.52* | -0.01 | 1.00 | |

(b)

**Correlations- S2**

| | pH | Sand | Silt | Clay | TOC | Al | Fe | Mn | Cr | Co | Ni | Cu | Zn | |
|---|---|---|---|---|---|---|---|---|---|---|---|---|---|---|
| pH | 1.00 | | | | | | | | | | | | | |
| Sand | 0.10 | 1.00 | | | | | | | | | | | | |
| Silt | -0.16 | -0.44* | 1.00 | | | | | | | | | | | |
| Clay | 0.15 | 0.18 | -0.96** | 1.00 | | | | | | | | | | |
| TOC | 0.42* | 0.00 | 0.32 | -0.35 | 1.00 | | | | | | | | | |
| Al | 0.11 | 0.05 | 0.05 | -0.07 | 0.22 | 1.00 | | | | | | | | N=27 |
| Fe | -0.50** | -0.23 | 0.16 | -0.11 | -0.14 | 0.32 | 1.00 | | | | | | | |
| Mn | -0.32 | -0.52** | 0.58** | -0.47* | -0.12 | -0.03 | 0.41* | 1.00 | | | | | | |
| Cr | -0.11 | 0.19 | -0.14 | 0.09 | -0.19 | 0.52** | 0.42* | -0.08 | 1.00 | | | | | |
| Co | -0.18 | 0.29 | -0.15 | 0.08 | -0.03 | -0.03 | 0.18 | 0.04 | 0.16 | 1.00 | | | | |
| Ni | 0.11 | 0.30 | -0.64** | 0.61** | -0.08 | -0.12 | -0.10 | -0.30 | 0.24 | 0.36 | 1.00 | | | |
| Cu | -0.10 | 0.15 | -0.34 | 0.33 | -0.03 | 0.00 | 0.35 | -0.26 | 0.49* | 0.56** | 0.65** | 1.00 | | |
| Zn | 0.15 | 0.24 | -0.26 | 0.21 | 0.08 | 0.02 | -0.17 | -0.25 | 0.37 | 0.59** | 0.66** | 0.69** | 1.00 | |

(c)

**Correlations-S3**

| | pH | Sand | Silt | Clay | TOC | Al | Fe | Mn | Cr | Co | Ni | Cu | Zn | |
|---|---|---|---|---|---|---|---|---|---|---|---|---|---|---|
| | 1.00 | | | | | | | | | | | | | |
| Sand | 0.39 | 1.00 | | | | | | | | | | | | |
| Silt | -0.42 | -0.02 | 1.00 | | | | | | | | | | | |
| Clay | 0.40 | -0.04 | -1.00** | 1.00 | | | | | | | | | | |
| TOC | -0.19 | -0.07 | 0.16 | -0.15 | 1.00 | | | | | | | | | |
| Al | -0.08 | -0.14 | 0.39 | -0.39 | 0.47* | 1.00 | | | | | | | | |
| Fe | -0.28 | -0.12 | 0.34 | -0.33 | 0.27 | 0.58** | 1.00 | | | | | | | N=20 |
| Mn | 0.13 | 0.01 | 0.06 | -0.06 | -0.60** | -0.36 | -0.02 | 1.00 | | | | | | |
| Cr | -0.12 | -0.14 | 0.42 | -0.41 | 0.23 | 0.80** | 0.63** | -0.17 | 1.00 | | | | | |
| Co | -0.40 | 0.12 | 0.33 | -0.34 | 0.02 | 0.12 | 0.46* | 0.22 | 0.34 | 1.00 | | | | |
| Ni | -0.20 | 0.14 | 0.35 | -0.36 | 0.03 | 0.19 | 0.49* | 0.27 | 0.24 | .510* | 1.00 | | | |
| Cu | -0.13 | 0.15 | 0.34 | -0.35 | -0.11 | 0.37 | 0.65** | 0.18 | 0.66** | 0.66** | 0.34 | 1.00 | | |
| Zn | -0.29 | -0.04 | 0.53* | -0.53* | 0.26 | 0.69** | 0.83** | 0.07 | 0.78** | 0.59** | 0.45* | 0.82** | 1.00 | |

(d)

**Correlations- S4**

| | pH | Sand | Silt | Clay | TOC | Al | Fe | Mn | Cr | Co | Ni | Cu | Zn | |
|---|---|---|---|---|---|---|---|---|---|---|---|---|---|---|
| | 1.00 | | | | | | | | | | | | | |
| Sand | -0.34 | 1.00 | | | | | | | | | | | | |
| Silt | 0.18 | -0.95** | 1.00 | | | | | | | | | | | |
| Clay | 0.51 | -0.90** | 0.72** | 1.00 | | | | | | | | | | |
| TOC | 0.49 | -0.86** | 0.82** | 0.77** | 1.00 | | | | | | | | | |
| Al | 0.29 | -0.91** | 0.91** | 0.75** | 0.82** | 1.00 | | | | | | | | N=12 |
| Fe | 0.13 | -0.55 | 0.44 | 0.62* | 0.45 | 0.62* | 1.00 | | | | | | | |
| Mn | 0.38 | -0.90** | 0.90** | 0.74** | 0.83** | 0.98** | 0.49 | 1.00 | | | | | | |
| Cr | -0.15 | -0.59* | 0.63* | 0.42 | 0.52 | 0.77** | 0.79** | 0.65* | 1.00 | | | | | |
| Co | -0.10 | -0.19 | 0.35 | -0.06 | 0.30 | 0.44 | -0.04 | 0.49 | 0.25 | 1.00 | | | | |
| Ni | 0.40 | -0.83** | 0.82** | 0.71* | 0.71** | 0.91** | 0.46 | 0.91** | 0.53 | 0.45 | 1.00 | | | |
| Cu | 0.55 | -0.86** | 0.78** | 0.83** | 0.76** | 0.87** | 0.59* | 0.86** | 0.50 | 0.31 | 0.93** | 1.00 | | |
| Zn | 0.44 | -0.90** | 0.87** | 0.80** | 0.85** | 0.96** | 0.60* | 0.95** | 0.72** | 0.26 | 0.85** | 0.86** | 1.00 | |

However, the similar distribution trends of Co, Ni, Cu and Zn and their significant correlation implied a common source for these metals that may be anthropogenic. It is important to note that substantial amount of material from the Mandovi River is added to the Zuari via the Cumbharjua canal. Singh et al. (2013) previously reported high concentrations of trace metals in mudflats of the Zuari estuary in the upper middle and Cumbharjua canal sediments, which they have interpreted as due to the effects of the nearby mining zones and ore transportation by barges. Further, they stated that increased accumulation of Fe and Mn in the upper middle estuary and Cumbharjua canal can considerably trap trace metals that can cause damage to the sediment quality.

The lower middle estuary (S3) showed little variations in metal distribution patterns and sediment grain size suggesting not much change in sediment and metal input with time. At this location, the canal joins the Zuari estuary and facilitates mixing of the two waters and sediment. Metals associated with suspended matter may have been fully mixed and then deposited in this area thus showed the uniform distribution in the depth profiles. Zhou et al. (2004) reported similar observation earlier. The increasing trend of Mn in this core suggested recent input probably of anthropogenic origin. The similar distribution pattern and good correlation indicated that metals Cr, Co, Ni, Cu and Zn were associated with Fe oxides in the sediments. Cr and Zn, however, showed association with Al, thus indicating a lithogenic source.

Further, most of the studied metals were less concentrated at the lower estuary (S4). Mistch et al. (2009) and Sun et al. (2015) stated that the sites that are subjected to intensive tidal washing generally have lower metal concentrations, while those subjected to relatively lower energy facilitated the deposition of metal particles. In the lower estuary core, the metals were associated with the finer sediments, TOC, Al, Fe, and Mn that suggested their lithogenic source. The low concentration of metals towards the base of the core can be related to the dilution of metals by coarser sediments.

The comparison of bulk metals and clay minerals profiles revealed that in core S1 the distribution to Cr showed similar to chlorite whereas Ni showed similar to kaolinite. Zinc exhibited similar to smectite in core S2. Metals showed little association with the clay minerals in cores S3 and S4. Albee (1962) reported that in natural chlorites, small amounts of Cr do substitute Si. Mattigod et al. (1979) studied the adsorption of Ni onto kaolinite and

found that increasing ionic strength decreased adsorption of Ni. Thus, the low salinity in the upper middle estuary must have facilitating the adsorption of Ni onto kaolinite as compared to the other locations in the estuary. Further, Zinc has a high affinity to adsorb onto clay minerals due to its high ionic potential. The adsorption of Zn onto smectite was therefore, thought to occur since the swelling of smectite allows greater access to interlayer sites. Additionally, Aluminum ions are replaced from the octahedral interstices by zinc to form sauconite, a type of smectitic clay (Kolay, 2007).

Further, the distribution of metals with depth was compared with magnetic susceptibility parameters in the mangrove sediments. In core S1, Fe and Mn exhibited similar distribution with the magnetic concentration parameters suggesting the source of Fe and Mn may be anthropogenic, probably from active mining and transport of ferromanganese ores in the upstream regions of the Zuari estuary. In core S2, Fe and Mn showed similar distribution with magnetic grain size parameters with a peak at 22 cm, indicating that these metals were anthropogenically influenced by mining inputs. The trace metals Cr, Co, Cu, Zn and to some extent Ni in core S2 showed similarity to the magnetic grain size and mineralogy parameters from 40 cm to 22cm and may have been associated with the coarse grain size. In core S3, no significant association of metals along with the magnetic parameters was observed. In core S4, Fe, Mn, Cr, Ni, Cu and Zn showed similar distribution pattern to the magnetic concentration parameters that suggested that these metals have some anthropogenic influence and are probably associated with Fe-oxides. The iron ore mined in the catchment areas and transported contribute significantly to the ferrimagnetic particles of sediments resulting in enhancement of magnetic susceptibility.

The similar distribution profiles between magnetic parameters and metal concentrations revealed an understandable relation between ferrimagnetic oxides and metals. Previous studies by Schmidt et al. (2005) indicated that the correlation between magnetic susceptibility and metal contamination only exists for the polluted samples, like those that carry magnetic inclusions. Since the magnetic susceptibility of the sediments was mainly influenced by iron oxides, the association of the trace metals with these iron oxides could result in association of the metals with the magnetic parameters. Magnetic particles, in the form of fine iron oxide dusts, could have been released along with other metals from a combination of different sources and introduced into the sediments (Lu et al., 2007) and the reduction of these iron oxides can have direct influence on the recycling of metals (Burdige, 1993). Fine grains that

are known to have a high surface to volume ratio are sensitive to the active sites of iron oxides. The grain size and hence the surface area thus influence the kinetics and extent of iron oxide dissolution and mobilization of associated trace metals in sediments (Roden and Zachara, 1996; Haese et al., 1997, Dessai and Nayak, 2007). Additionally, magnetic grain size parameters did not show association with the metal concentrations indicating association of metals towards the coarser magnetic grains. Thus, the comparison between magnetic susceptibility and metal distributions indicated the role played by particle size and iron oxide in the distribution of metals.

### 3.1. A.4b Metals in the clay fraction of sediments

To understand the distribution of metals in the clay fraction of sediments, the clay fraction was separated for analysis as clay has a strong tendency to adsorb trace metals. Analysis of metals Al, Fe, Mn, Cr, Co, Ni, Cu and Zn in clay fraction was carried out for selected samples of the four mangrove cores and the range and average values are presented in table 3.1.2 (b). In sediment core S1, Al, Fe and Mn concentrations ranged from 10.62 % to 11.64 % (average 11.18 %), 6.83 % to 8.43 % (average 7.76 %) and 5683 ppm to 6747 ppm (average 6409 ppm). The trace metals Cr, Co, Ni, Cu and Zn concentrations varied from 328 ppm to 521 ppm (average 454 ppm), 19.50 ppm to 39.50 ppm (average 29.54 ppm), 125 ppm to 180 ppm (average 153 ppm), 177 ppm to 212 ppm (average 197 ppm) and 148 ppm to 1076 ppm (average 527 ppm). In sediment core S2 collected from the Cumbharjua canal, Al, Fe and Mn content ranged from 13.31 % to 17.52 % (average 15.33 %), 8.13 % to 9.88 % (average 8.81 % ), 4327 ppm to 6265 ppm (average 5459 ppm) respectively. The trace metals Cr, Co, Ni, Cu and Zn concentrations ranged from 348 ppm to 583 ppm (average 410 ppm), 31.50 ppm to 45.75 ppm (average 36.56 ppm), 97.75 ppm to 157 ppm (average 117 ppm) , 166 ppm to 297 ppm (average 217 ppm) and 128 ppm to 1025 ppm (average 355 ppm) respectively. Metals in the lower middle estuary core S3 showed that Al, Fe and Mn concentrations ranged from 6.96 % to 10.74 % (average 8.84 %), 6.49 to 7.65 % (average 7.18 %) and 1804 ppm to 5043 ppm (average 3217 ppm) respectively. Trace metal concentrations in the clay fraction of Cr, Co, Ni, Cu and Zn ranged from 689 ppm to 797 ppm (average 731 ppm), 11.25 ppm to 30.25 ppm (average 19.97 ppm), 135 ppm to 184 ppm (average 158 ppm), 178 ppm to 226 ppm (average 198 ppm) and 135 ppm to 810 ppm (average 438 ppm). The sediment core collected from the lower estuary S4, showed major metals Al, Fe and Mn in the clay fraction of sediments to range from 4.36 % to 10.76 % (average 7.68 %), 3.25 % to 6.37 % (average 5.23 %) and 440 ppm to 3302 ppm (average

2045 ppm). Trace metals Cr, Co, Ni Cu and Zn in the clay fraction of sediments ranged from 566 ppm to 785 ppm (average 700 ppm), 10.25 ppm to 28.50 ppm (average 18.13 ppm), 42.00 ppm to 62.25 ppm (average 52.21 ppm), 153 ppm to 208 ppm (average 170 ppm) and 123 ppm to 689 ppm (average 327 ppm).

The highest concentrations of Al, Fe, Co and Cu were observed in core S2; Cr, Ni and Zn in core S3 and Mn in core S1.

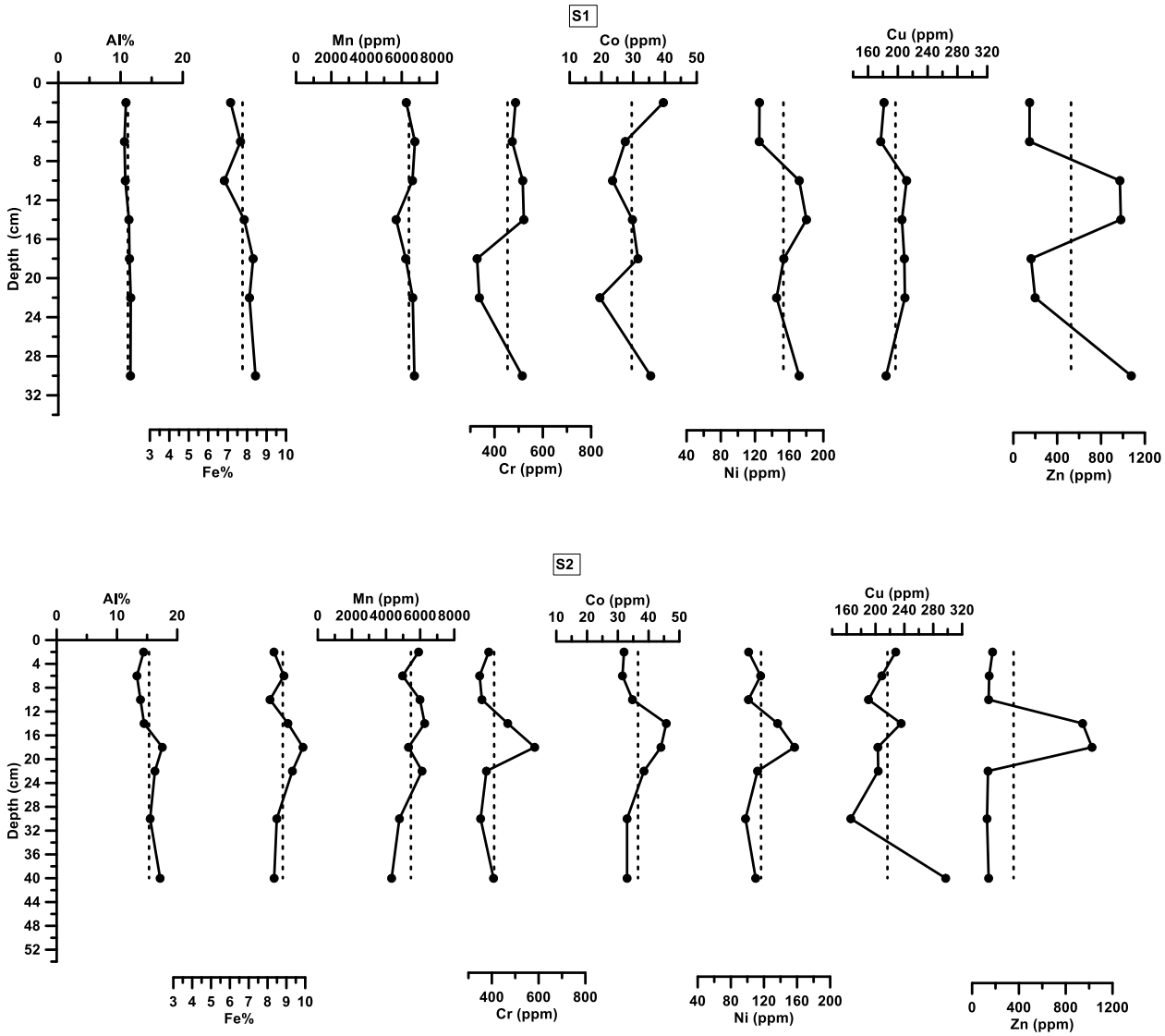

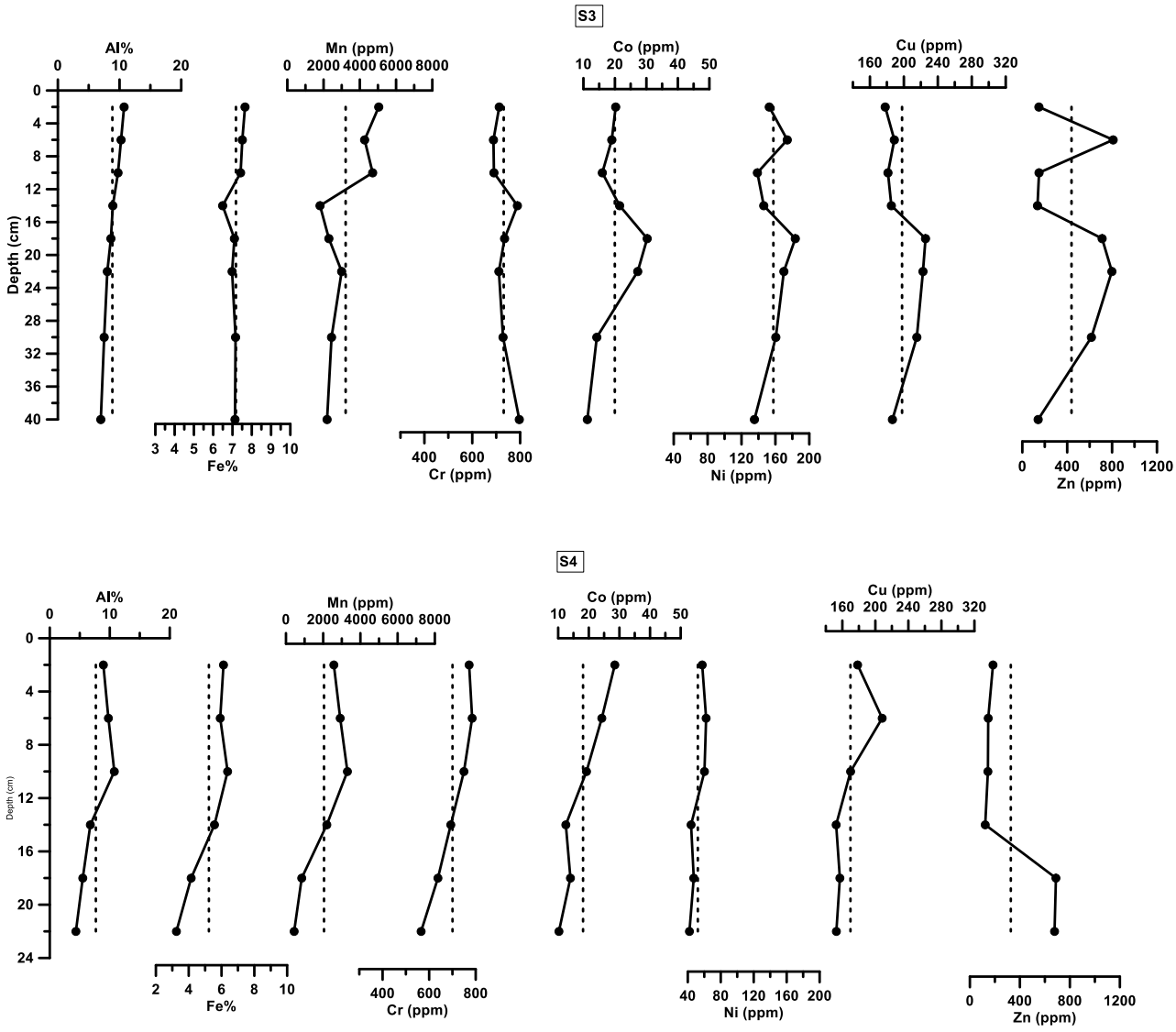


Figure 3.1.8: Distribution of metals in the clay fraction of sediments in mangrove cores S1, S2, S3 and S4.

From the distribution of metals in the clay fraction with depth presented in figure 3.1.8, metal distribution in core S1 revealed that Al showed a constant distribution trend with depth. Fe, Mn and Cu concentrations decreased towards the surface while Cr, Ni and Zn showed similar distribution trends with a decrease from the base of the core to around 22 cm followed by a peak at around 14 cm, and Co fluctuated in its distribution with a peak at 18 cm followed by higher concentration towards the surface. Overall, the lower portion of the core had high concentrations for most metals. The minor decrease in the Mn profile at 14 cm and increase around 10 cm suggested the diagenetic enrichment of Mn, similar to its distribution in the

bulk sediments. The distribution of the metals in the clay fraction with depth in core S2 revealed that the Al distribution showed a peak at 18 cm followed by decrease towards the surface. Cr, Co, Ni and Zn showed similar distribution to the profile of Fe suggesting that Fe oxides played a major role in their distribution. Mn concentrations gradually increased towards the surface whereas Cu showed a fluctuating increase towards the surface. In the distribution of metals in the clay fraction with depth in core S3, Al, Fe and Mn concentrations gradually increased towards the surface. Cr concentration decreased whereas Co, Ni, Cu and Zn showed similar distribution profiles with a common peak at 18 cm. The distribution of metals in the clay fraction of sediments with depth of the lower estuary mangrove core S4 exhibited an increase in Cr, Co, Ni and Cu towards the surface. Al, Fe and Mn increased up to 10 cm and then showed gradual decrease towards the surface. Zn showed constant value up to 18 cm followed by sharp decrease up to 14 cm and then gradual increase towards the surface.

In the core collected from the upper middle estuary, Fe exhibited similar distribution to Al with depth and Ni similar to Zn indicating that they are derived from a common source. Trace metals, Cr, Co, Ni and Zn in the Cumbharjua canal showed similar distribution to Fe and indicated that Fe oxides strongly influenced the distribution of Cr, Co, Ni and Zn and were derived from a common source. Further, the similar distribution of Al, Fe and Mn in the lower middle estuary core indicated natural source whereas the similar distributions of Co, Ni, Cu and Zn suggested a common source for these metals and were probably of detrital nature. In core collected from the lower estuary the similar distribution of trace metals Cr, Co, Ni and Cu indicated that the metals were derived from a common source whereas Zn may have been derived from a different source.

The average concentrations of metals in the clay fraction (table 3.1.2) were compared with the bulk metals using the Isocon diagram (Grant, 1986) presented in figure 3.1.9.

In core S1 and core S2, all metals showed higher concentrations in the clay fraction except for Fe. Further, in core S3, Al, Fe and Co showed higher concentrations in the bulk and other metals were higher in the clay fraction. Fe and Co in sediment core S4 showed higher concentrations in the bulk suggesting their association with the larger sized sediments. Volvoikar and Nayak (2014) reported that the clay-sized fraction of sediments represents last and stable weathering product of strong erosion of source rocks and holds metals within the

lattice structure of aluminosilicate minerals. The high content of Fe in the bulk sediments indicated Fe association with larger sediment particles like sand and silt (Roussiez et al., 2006).

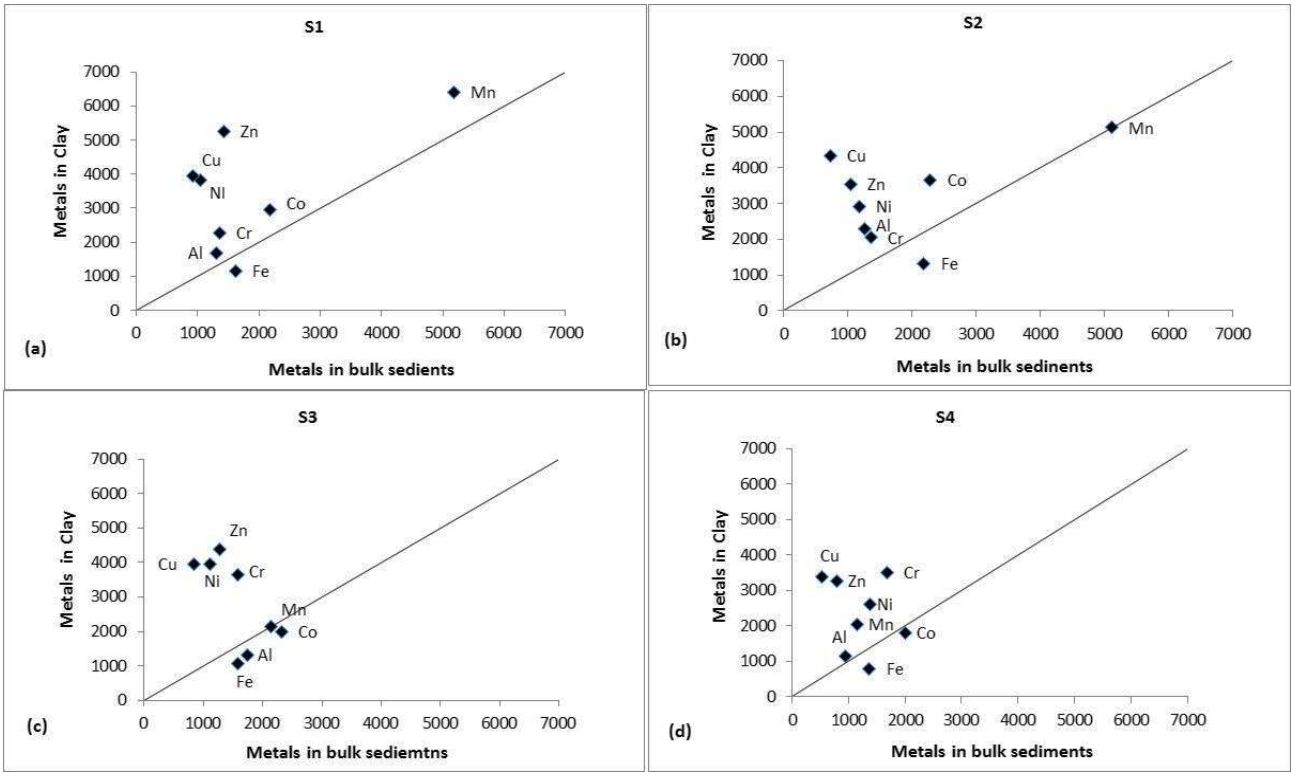


Figure 3.1.9: Isocon diagram of metals in bulk sediments versus metals in clay fraction in mangrove cores S1, S2, S3 and S4.

### 3.1.B Mudflats

Three mudflat cores were collected from the Zuari estuary, one each from the upper middle estuary M1, lower middle estuary M3 and lower estuary M4. The cores were analyzed for sediment components, clay mineralogy, magnetic susceptibility and metal chemistry and the results are presented in the following sections.

### 3.1. B.1 Sediment components (pH, sand, silt, clay and total organic carbon)

The range and average values of sediment components of mudflat cores are presented in table 3.1.4 (a).

Table 3.1.4: Range and average values of sediment components, clay mineralogy, and magnetic susceptibility parameters in mudflat cores M1, M3, and M4 of the Zuari estuary.

| | | | **M1** | | **M3** | | **M4** | |
|---|---|---|---|---|---|---|---|---|
| | | Parameters | Average | Range | Average | Range | Average | Range |
| | | pH | 6.87 | 6.47-7.34 | 7.05 | 6.78-7.38 | 7.24 | 7.00-7.43 |
| (a) | Sediment components | Sand (%) | 2.52 | 1.07- 8.55 | 1.62 | 0.35 -8.42 | 9.79 | 4.75- 16.51 |
| | | Silt (%) | 40.1 | 24.93 -47.41 | 34.47 | 23.56 -41.66 | 40.66 | 34.04 -47.55 |
| | | Clay (%) | 57.38 | 49.52-64.52 | 63.91 | 49.92 -75.92 | 49.55 | 42.84 - 57.36 |
| | | TOC (%) | 2.58 | 1.79-3.10 | 2.48 | 2.18-2.94 | 2.01 | 1.71 -2.43 |
| (b) | Clay minerals | Smectite (%) | 15.93 | 10.87 -18.80 | 16.19 | 11.11-20.00 | 31.83 | 17.87 - 50.00 |
| | | Illite (%) | 20.86 | 16.67- 23.93 | 21.12 | 17.50- 24.00 | 18.85 | 7.92 - 25.00 |
| | | Kaolinite (%) | 56.67 | 51.24- 62.21 | 55.37 | 51.99- 62.02 | 45.03 | 20.31- 62.34 |
| | | Chlorite (%) | 6.54 | 4.34- 9.63 | 7.32 | 3.61 -12.43 | 4.29 | 2.70 - 5.67 |
| (c) | Magnetic Susceptibility parameters | $\chi_{lf}$ ($10^{-8}$ $m^3$ $kg^{-1}$) | 229 | 200 - 273 | 159 | 139 -169 | 172 | 136 - 194 |
| | | $\chi_{ARM}$ ($10^{-8}$ $m^3$ $kg^{-1}$ ) | 1135 | 1086-1281 | 1025 | 925 - 1092 | 942 | 794- 1040 |
| | | SIRM ($10^{-5}$ $Am^2$ $kg^{-}$ | 2090 | 1723 - 2669 | 1402 | 1360 -1465 | 1839 | 1522- 2186 |
| | | $\chi_{ARM}/\chi_{lf}$ | 5.02 | 4.09-5.53 | 6.44 | 6.13 - 6.76 | 5.49 | 5.1- 5.84 |
| | | $\chi_{ARM}$/SIRM ($10^{-3}$ $A^{-}$ | 0.55 | 0.41-0.64 | 0.73 | 0.67- 0.78 | 0.52 | 0.46- 0.60 |
| | | $\chi_{fd}$ (%) | 6.24 | 4.04- 7.67 | 7.59 | 2.68 -9.76 | 6.60 | 2.22-12.40 |
| | | S-ratio (%) | 89.73 | 87.50-91.99 | 89.87 | 87.78 - 92.59 | 90.22 | 85.69-92.74 |

In the sediment core collected from the upper middle estuary (M1) representing the mudflat environment, the pH was near neutral in nature and ranged from 6.47 to 7.34 (average 6.87). The sediments showed that sand, silt and clay content ranged from 1.07 % to 8.55 % (average 2.52 %), 24.93 % to 47.41 % (average 40.1 %) and 49.52 % to 64.52 % (average 57.38 %) respectively. The TOC content in the mudflat core M1 ranged from 1.79 % to 3.10 % (average 2.58 %). The variation in sediment components in the lower middle estuarine region (M3) showed that the pH was near neutral and ranged from 6.78 to 7.38 (average 7.05). The sand, silt and clay content in mudflat core M3 varied from 0.35 % to 8.42 % (average 1.62 %), 23.56 % to 41.66 % (average 34.47 %) and 49.92 % to 75.92 % (average 63.91 %) respectively. TOC in core M3 ranged from 2.18 % to 2.94 % (average 2.48 %).

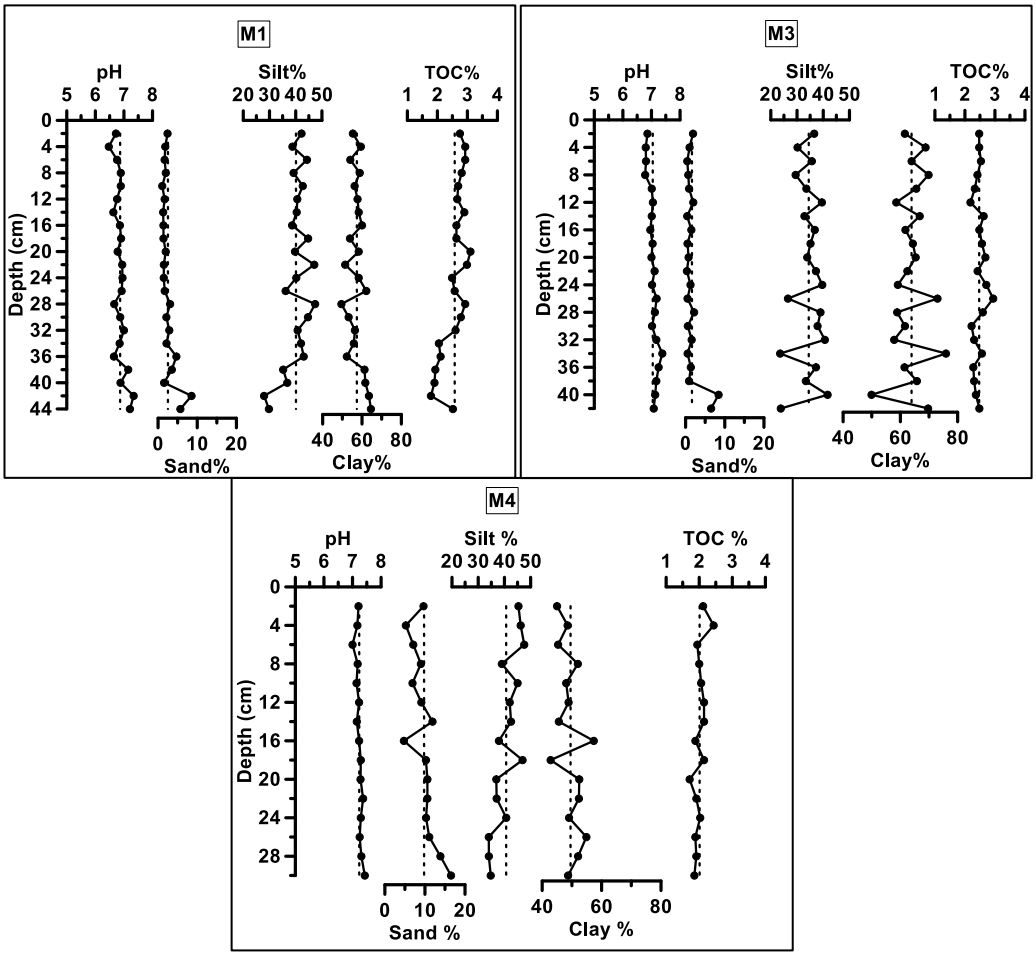


Figure 3.1.10 Distribution of sediment components with depth in mudflat sediments of core M1, M3 and M4.

In the mudflat core collected from the lower estuary (M4). The pH was weakly alkaline ranging from 7.00 to 7.43 (average 7.24). The sand, silt and clay percentages ranged from

4.75 % to 16.51 % (average 9.79 %), 34.04 % to 47.55 % (average 40.66 %) and 42.84 % to 57.36 % (average 49.55 %). The TOC content in the core ranged from 1.71 % to 2.43 % (average 2.01 %).

The distribution of sediment components with depth in cores M1, M3 and M4 are presented in figure 3.1.10. In the vertical profile of sediment components of core M1, the pH was relatively constant with depth except for a few higher values in the lower portion of the core (44 cm to 38 cm). Sand exhibited a uniform distribution pattern throughout the core with the exception of higher sand percentages in the lower part of the core (44 cm to36 cm). Silt and clay showed a complementary distribution pattern wherein silt percentage increased up to 28 cm and clay decreased up to 28 cm followed by a fluctuating distribution towards the surface. TOC showed a gradual increase towards the surface and showed some similarity to the distribution of silt. Overall clay was the dominant grain size over sand and silt. From the distribution of sediment components with depth in core M3, pH was noted to be constant with depth. Sand exhibited higher percentages in the lower portion of the core (42 cm to 40 cm) followed by uniform distribution towards the surface. Silt and clay exhibited complementary distribution patterns, with large fluctuations in their profiles, especially between 42 cm to 24 cm. This was followed by a decrease in silt percentage above 24 cm, which was compensated by an increase in clay percentage towards the surface. The TOC percentages were almost constant with depth with slightly higher percentages than average between 28 cm and 14 cm. Overall, the core was dominated by clay. The distribution of sediment components in mudflat core M4 with depth revealed that the distribution of pH in the core was relatively constant. The sand content gradually decreased towards the surface, which was compensated by an increase in silt content. The distribution of clay showed an opposite distribution to silt with large fluctuations. The TOC content showed a minor increase towards the surface above the average line and was largely associated with silt.

The range and average values revealed that the pH values recorded were among the normal range values for estuarine sediments i.e. between 5 to 7 (Caçador et al., 2004; Reddy and DeLaune, 2008). Higher pH was recorded in the lower estuary, which decreased towards the upper middle estuary due to the decreasing tidal influence towards the upstream regions. The average pH values at all stations were noted to be near neutral (7.0) which was also observed by Spetter et al. (2014) particularly in non-vegetated sediments. The mudflat sediments along the estuary were dominated by silt and clay. The lower estuary sediments had higher

percentage of sand and silt content whereas higher clay was noted in the lower middle estuary. The lower estuary is subjected to high hydrodynamics due to turbulence by waves that cause resuspension of the finer sediments, which are carried in suspension retaining the larger sediment size fractions. Activities by waves are controlled by wind direction and intensity, the water level on the mudflat, and the sediment characteristics (Deloffre et al., 2007). In all the three mudflat cores, higher sand content was noted in the lower portion of the cores, which indicated a higher energy regime prevailed during the deposition of the sediments in the past.

Highest TOC values were recorded in the upper middle estuary M1 that may be related to the high content of finer sized sediments or inputs from sewage and waste water on considering the proximity of the sampling location to a ship building industry. In addition, as the upper middle estuary has lower hydrodynamics, organic matter dissolution rates may have been lower. Organic matter is supplied to the environments from both external (i.e. terrestrial, agricultural domestic and municipal sewage) and internal (i.e. algal and microbial) sources. Benthic invertebrates and microorganisms may also contribute significant amounts of organic carbon to sediments (Reddy and DeLaune, 2008). In the core collected from the upper middle estuary, similarity of the profiles of TOC with silt suggest increasing loads of silt deposited with higher sedimentation rates must have trapped the higher TOC (Carreira et al., 2002). Finer sediments have large surface areas and tend to have associated negative charges. Therefore, on interacting with seawater, their surfaces are quickly coated with a layer of organic material (Rojas and Silva, 2005). The core collected from the lower middle estuary exhibited large fluctuations in the silt and clay profile suggesting prevailed varying depositional conditions. The profile of TOC was similar to that of clay indicating the association of organic matter with the fine sediment. In the core collected from the lower estuary, the decreasing sand content towards the surface indicated calm conditions in recent times with increase in the fine sediments and TOC.

Furthermore, by using the ternary diagram of Pejrup (1988), an understanding of the depositional conditions was attempted for the three mudflat cores (Figure 3.1.B.2). The sediments of mudflat cores M1 and M3 fell in class II (D) indicating relatively calm hydrodynamic conditions prevailed during sediment deposition. The sediments of core M4 however fell in class II (C), II (D) and III (D) indicating varying hydrodynamic conditions during deposition.

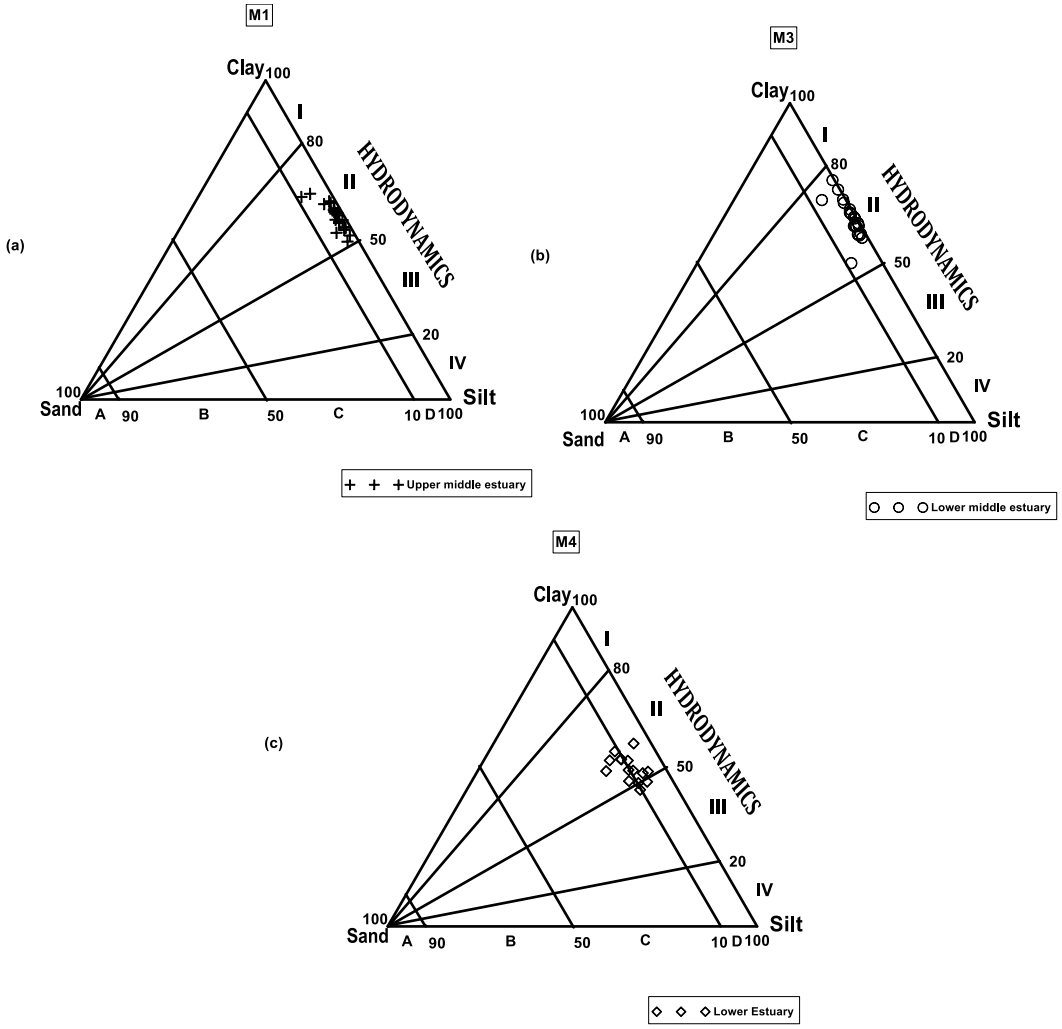


Figure 3.1.11 Ternary diagram proposed by Pejrup (1988) of sand, silt and clay of mudflat cores M1, M3 and M4.

### 3.1.B.2 Clay mineralogy

Smectite, illite, kaolinite and chlorite comprised the clay mineral assemblage of the mudflat sediments and the ranges and average values are presented in table 3.1.4 (b).

In the mudflat core M1, smectite, illite, kaolinite and chlorite percentages ranged from 10.87 % to 18.80 % (average 15.93 %), 16.67 % to 23.93 % (average 20.86 %), 51.24 % to 62.21 % (average 56.67 %) and 4.34 % to 9.63 % (average 6.54 %), respectively. In core M3 collected from the lower middle estuary, clay mineral percentages of smectite, illite, kaolinite and chlorite ranged from 11.11 % to 20.00 % (average 16.19 %), 17.50 % to 24.00 % (average 21.12 %), 51.99 % to 62.02 % (average 55.37 %) and 3.61 % to 12.43 % (average 7.32 %) respectively. The percentages of smectite, illite, kaolinite and chlorite in the core collected from the lower estuary M4, ranged from 17.87 % to 50.00 % (average 31.83 %), 7.92 % to

25.00 % (average 18.85 %), 20.31 % to 62.34 % (average 45.03 %) and 2.70 % to 5.67 % (average 4.29 %) respectively.

In the distribution profiles of clay minerals with depth (Figure 3.1.12), of core M1, all the clay minerals showed a near uniform distribution profiles with minor fluctuations at 22 cm. Smectite and illite showed similar distribution patterns, with minor decreased peak at 14 cm. Kaolinite exhibited an opposite distribution pattern to smectite and illite. Chlorite showed a positive peak at 14 cm depth. Little variations with depth were observed in the distribution clay minerals in core M3 with depth. Smectite percentages were relatively constant with depth except between 10 cm to 2 cm wherein a peak was observed at 6 cm. Illite percentage showed minor fluctuations around the average line while kaolinite exhibited an opposite distribution trend to smectite. Chlorite however, showed large variation in its distribution wherein percentages increased from the base of the core up to 18 cm followed by decrease towards the surface, except it showed an increase at the surface. The distribution of clay minerals with depth in mudflat core M4 exhibited large fluctuations and opposite trends for smectite and kaolinite. Smectite increased between 30 cm to 10 cm (except at 18 cm) followed by a decrease towards the surface whereas kaolinite decreased up to 10 cm and then increased. Illite percentages decreased towards the surface whereas chlorite percentage was constant with depth.

Kaolinite was the most abundant clay mineral in the Zuari estuary followed by illite, smectite and chlorite, except for the lower estuary where smectite was higher than illite. Kaolinite was enriched in the upper middle estuary whereas smectite was high in the lower estuary and illite and chlorite were abundant in the lower middle estuary. The transport and deposition of sediments in estuaries are complex processes with various interacting factors affecting the fate of the sediments. Clay minerals in estuary may be derived from weathering profiles on the continents called detrital clays or they may be formed during and after deposition known as diagenetic clays. Meade (1972) proposed three influencing factors that govern the distribution of clay minerals, (i) dynamic processes that circulate and mix estuarine waters, (ii) the flocculation process which increases the settling velocities of sediment particles, and (iii) properties of the particles themselves. The precipitation of clay minerals mainly depends on the flocculation, so the crystal habit of the clay minerals and geochemical environment of the depositional region are also important factors affecting the distribution of clay minerals (Yang, 1988).

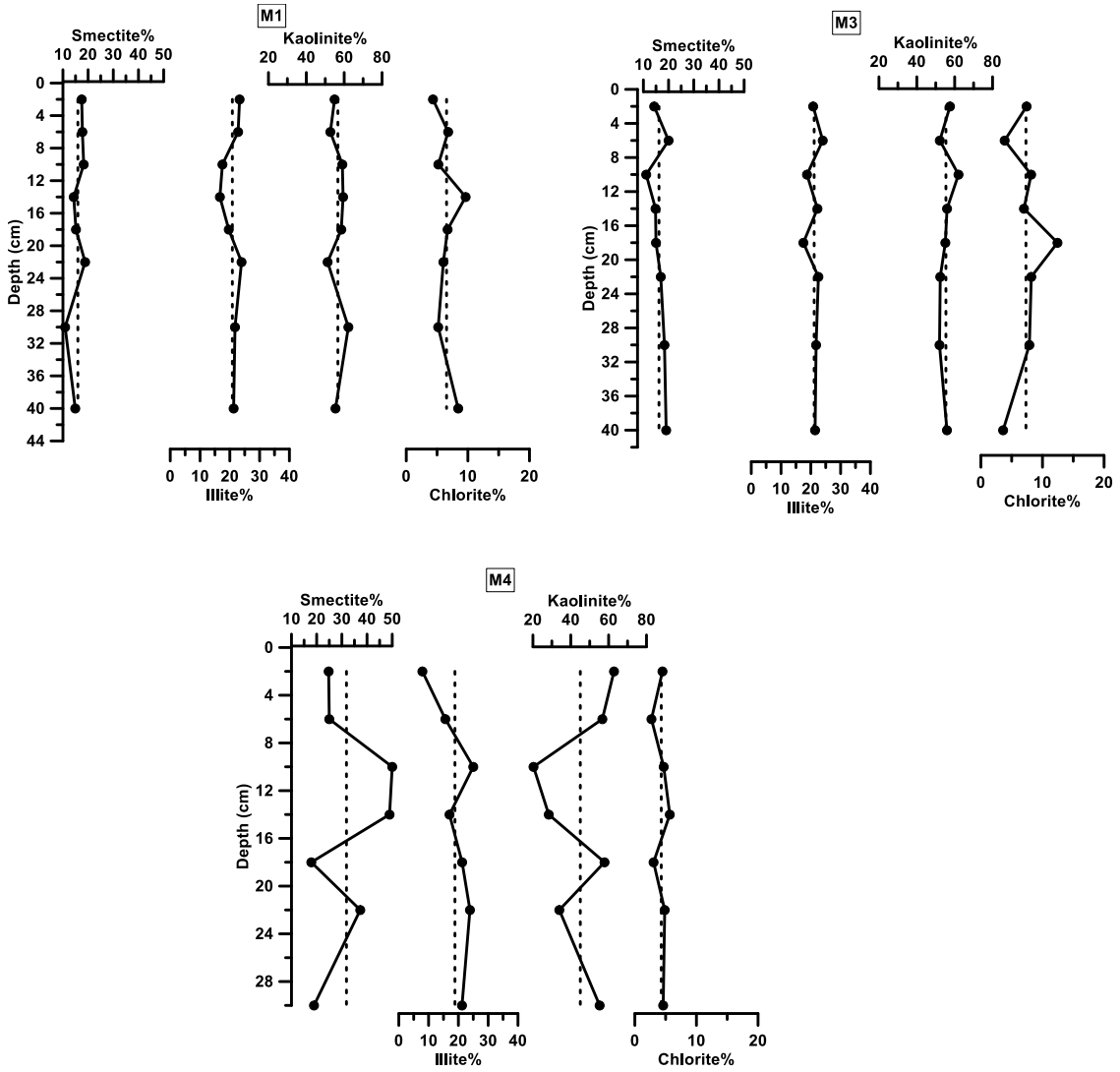


Figure 3.1.12 Distribution of clay minerals with depth in mudflat sediments of cores M1, M3 and M4.

Studies by Edzwald and O'Melia (1975) reported that illite is more stable than kaolinite so that under similar physical conditions, illite would be expected to aggregate more slowly than kaolinite and be deposited downstream of kaolinite. For any given salinity, the fresh water sediment is relatively unstable compared to downstream sediments. The lower estuary sediment is more stable than the upper estuary sediment which is more stable than the fresh water sediment. The clay deposited upstream undergone particle aggregation more rapidly than those deposited downstream. Those clays, which are relatively stable will be transported farther downstream due to slow aggregation rates before deposition can occur. As kaolinite is less stable than illite and smectite, it was deposited towards the upstream region of the estuary and hence explains the spatial variability in the abundance of the clay minerals.

Abundant smectite towards the lower estuary may have been transported from offshore regions into the estuary.

The vertical distribution of clay minerals in the mudflats of the upper middle and lower middle estuary revealed minor variations with depth that suggested little change in provenance over time. The lower estuary however, showed large variations in the clay mineral distributions mainly with respect to kaolinite and smectite that show opposite distribution patterns. The increase in smectite and peak at 10 cm in the mudflat core of the lower estuary suggested an increased seawater intrusion that transported large amount smectite into the estuary. As mudflats are more in contact with the water as compared to other intertidal sedimentary environments, the mudflats are more sensitive to the changes in flux of material and provide a more accurate record of the prevailing environmental conditions.

**3.1.B.3 Magnetic susceptibility**

The range and average values of magnetic susceptibility parameters of the mudflat cores M1, M3 and M4 are presented in table 3.1.4(c). The magnetic mineral concentration parameters $\chi_{lf}$ ,values of the mudflat core M1 collected from the upper middle estuarine mangroves markedly varied from 200 $\times 10^{-8}$ $m^3$ $kg^{-1}$ to 273 $\times 10^{-8}$ $m^3$ $kg^{-1}$ (average 229$\times 10^{-8}$ $m^3$ $kg^{-1}$), $\chi_{ARM}$ values ranged from 1085 $\times 10^{-8}$ $m^3$ $kg^{-1}$ to 1281 $\times 10^{-8}$ $m^3$ $kg^{-1}$ (average 1135 $\times 10^{-8}$ $m^3$ $kg^{-1}$) and SIRM values ranged from 1723 $\times 10^{-5}$ $Am^2$ $kg^{-1}$ to 2669 $\times 10^{-5}$ $Am^2$ $kg^{-1}$ (average of 2090 $\times 10^{-5}$ $Am^2$ $kg^{-1}$). The inter-parametric ratios of $\chi_{ARM}$ / $\chi_{lf}$, $\chi_{ARM}$ /SIRM and $\chi_{fd}$, that are indicative of magnetic grain size ranged from 4.09 to 5.53 (average of 5.02), 0.41$\times 10^{-3}$ $A^{-1}m$ to 0.64$\times 10^{-3}$ $A^{-1}m$ (average of 0.55$\times 10^{-3}$ $A^{-1}m$) and 4.04 % to 7.67 % (average 6.24 %) respectively. The S-ratio % of core M1 ranged from 87.50 % to 91.99 % (average 89.73 %). In the lower middle estuary mudflat core M3, $\chi_{lf}$ ,values ranged from 139 $\times 10^{-8}$ $m^3$ $kg^{-1}$ to 169 $\times 10^{-8}$ $m^3$ $kg^{-1}$ (average 159$\times 10^{-8}$ $m^3$ $kg^{-1}$), $\chi_{ARM}$ values ranged from 925 $\times 10^{-8}$ $m^3$ $kg^{-1}$ to 1092 $\times 10^{-8}$ $m^3$ $kg^{-1}$ (average 1025$\times 10^{-8}$ $m^3$ $kg^{-1}$) and SIRM values ranged from 1360$\times 10^{-5}$ $Am^2$ $kg^{-1}$ to 1464 $\times 10^{-5}$ $Am^2$ $kg^{-1}$ (average of 1402$\times 10^{-5}$ $Am^2$ $kg^{-1}$). The magnetic grain size parameters of $\chi_{ARM}$ / $\chi_{lf}$, $\chi_{ARM}$ /SIRM and $\chi_{fd}$, ranged from 6.13 to 6.76 (average of 6.44), 0.67$\times 10^{-3}$ $A^{-1}m$ to 0.78$\times 10^{-3}$ $A^{-1}m$ (average of 0.73$\times 10^{-3}$ $A^{-1}m$) and 2.68 % to 9.76 % (average 7.59 %) respectively. The S-ratio % of core M3 ranged from 87.78 % to 92.59 % (average 89.87 %). The core M4 of the mudflat environment of the lower estuary showed that the concentration of magnetic material parameters $\chi_{lf}$, $\chi_{ARM}$ and SIRM ranged from 136

$\times 10^{-8}$ $m^3$ $kg^{-1}$ to 194 $\times 10^{-8}$ $m^3$ $kg^{-1}$ (average $172\times 10^{-8}$ $m^3$ $kg^{-1}$), $\chi_{ARM}$ values ranged from 794 $\times 10^{-8}$ $m^3$ $kg^{-1}$ to $1041\times 10^{-8}$ $m^3$ $kg^{-1}$ (average $942\times 10^{-8}$ $m^3$ $kg^{-1}$) and SIRM values ranged from $1522\times 10^{-5}$ $Am^2$ $kg^{-1}$ to 2186 $\times 10^{-5}$ $Am^2$ $kg^{-1}$ (average of $1839\times 10^{-5}$ $Am^2$ $kg^{-1}$). The magnetic grain size parameters of $\chi_{ARM}$ / $\chi_{lf}$, $\chi_{ARM}$ /SIRM and $\chi_{fd}$ ranged from 5.1 to 5.84 (average of 5.49), $0.46\times 10^{-3}$ $A^{-1}m$ to $0.60\times 10^{-3}$ $A^{-1}m$ (average of $0.52\times 10^{-3}$ $A^{-1}m$) and 2.22 % to 12.40 % (average 6.60 %) respectively. The S-ratio of core M4 ranged from 85.69 % to 92.74 % (average 90.22 %).

In the distribution of magnetic parameters with depth (Figure 3.1.13) in core M1, concentration dependent parameters $\chi_{lf}$, $\chi_{ARM}$ and SIRM did not show much variation with depth. However, relatively higher values in the lower portion of the core (40 cm to 30 cm) as well as upper 2 cm suggested that the region received increased concentration of magnetic material. The grain size parametric ratios of $\chi_{ARM}$ / $\chi_{lf}$, $\chi_{ARM}$ /SIRM and $\chi_{fd}$ exhibited an increase from the base of the core up to 14 cm suggesting increased deposition of finer grain size magnetic material. Towards the surface, they showed decrease. The S-ratio gradually decreased towards the surface of the core indicating an increasing amount of hematite. The distribution of magnetic concentration parameters in mudflat core M3 with depth showed that $\chi$lf, $\chi_{ARM}$ and SIRM exhibited uniform distribution with depth. The grain size dependent parameters $\chi_{ARM}$ / $\chi_{lf}$, $\chi_{ARM}$ /SIRM and $\chi_{fd}$ also showed little variation with depth except for $\chi_{fd}$ wherein low value was noted at 2 cm, and high values were recorded at the bottom of the core. The S-ratio however, displayed a decrease from the base of the core up to 6 cm suggesting increase in the proportion of hematite. In the distribution of magnetic susceptibility parameters with depth in core M4, $\chi_{lf}$ values were constant with depth. $\chi_{ARM}$ and SIRM values increased towards the surface. A common decreased peak at 10 cm was noted in the profiles of magnetic concentration parameters. The inter-parametric ratios of $\chi_{ARM}$ / $\chi_{lf}$, $\chi_{ARM}$ /SIRM exhibited similar distribution pattern with a decrease in values towards the surface. $\chi_{fd}$ values however decreased up to 10 cm followed by increase towards the surface. The profile of S-ratio exhibited a fluctuating trend with depth, with a steep increase in values between 18 cm to 10 cm.

Considering the spatial variations of the magnetic susceptibility values, the upper middle estuary mudflats had a higher concentration of magnetic material as indicated from the magnetic concentration parameters $\chi_{lf}$, $\chi_{ARM}$, and SIRM. Higher amount of finer magnetic material was noted in the lower middle estuary as indicated from the grain size parameters of

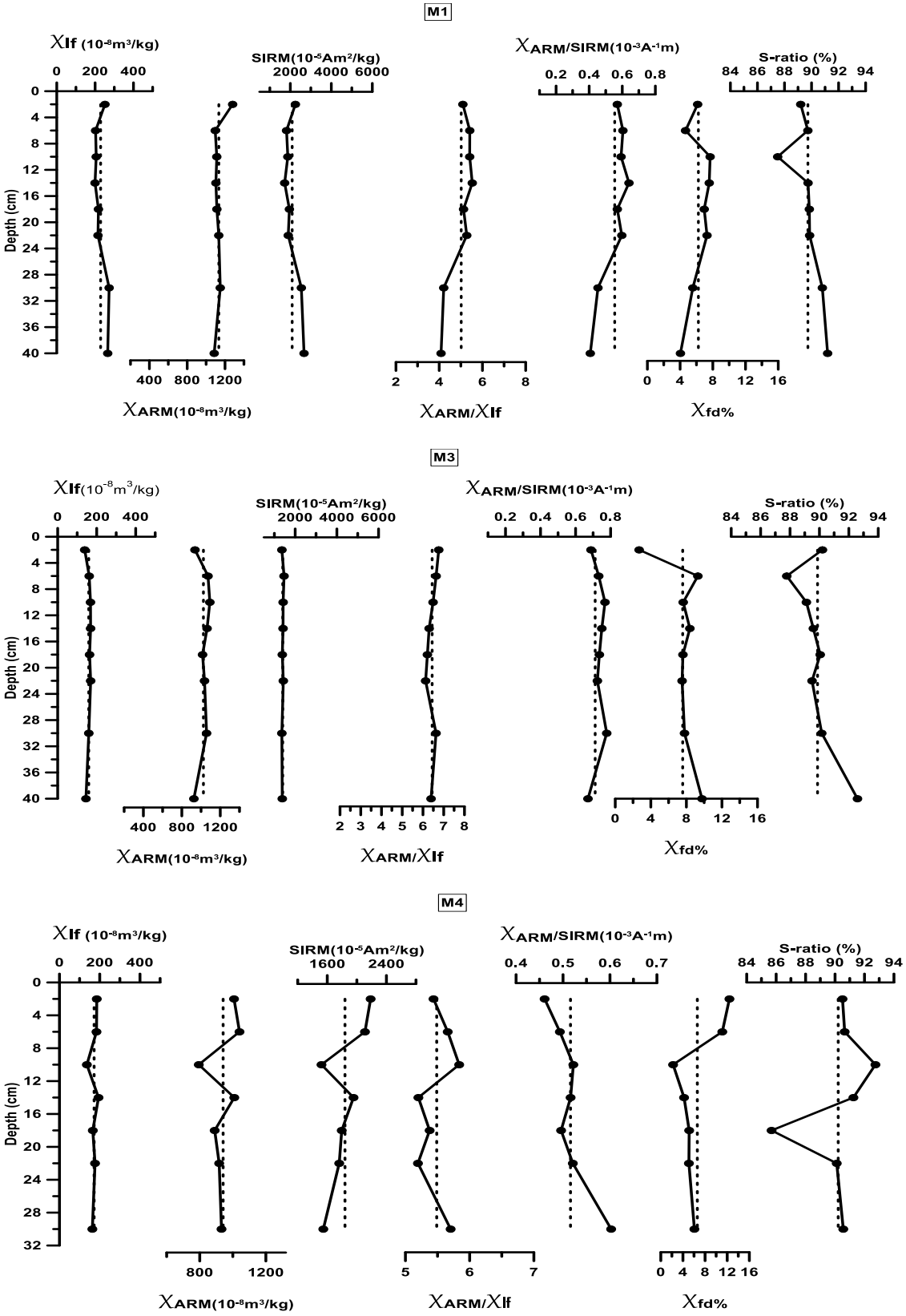


Figure 3.1.13: Distribution of magnetic susceptibility parameters with depth in mudflat sediments of cores M1, M3 and M4.

inter parametric ratios. Overall, the sediments were made up of a mixture of magnetite and hematite with slightly higher magnetite in the lower estuary. Low values of $\chi_{fd}$ at M1 and M4 indicated that these regions receive most material from natural weathering processes although there may be some contribution from mining and ship building activities. The average $\chi_{ARM}$ / $\chi_{lf}$ values decreased in the order of M3 > M4> M1 which indicated the presence of SSD grains at M3, M4 and M1. The low average values of grain size parameters in the three mudflat cores indicated the association of higher concentrations of mineral with the coarser grains, which suggested that the sediment was made up of detrital components. The average values of $\chi_{ARM}$ /SIRM in the three cores revealed that the mudflat sediments of the Zuari estuary have a higher amount of coarse SSD grains.

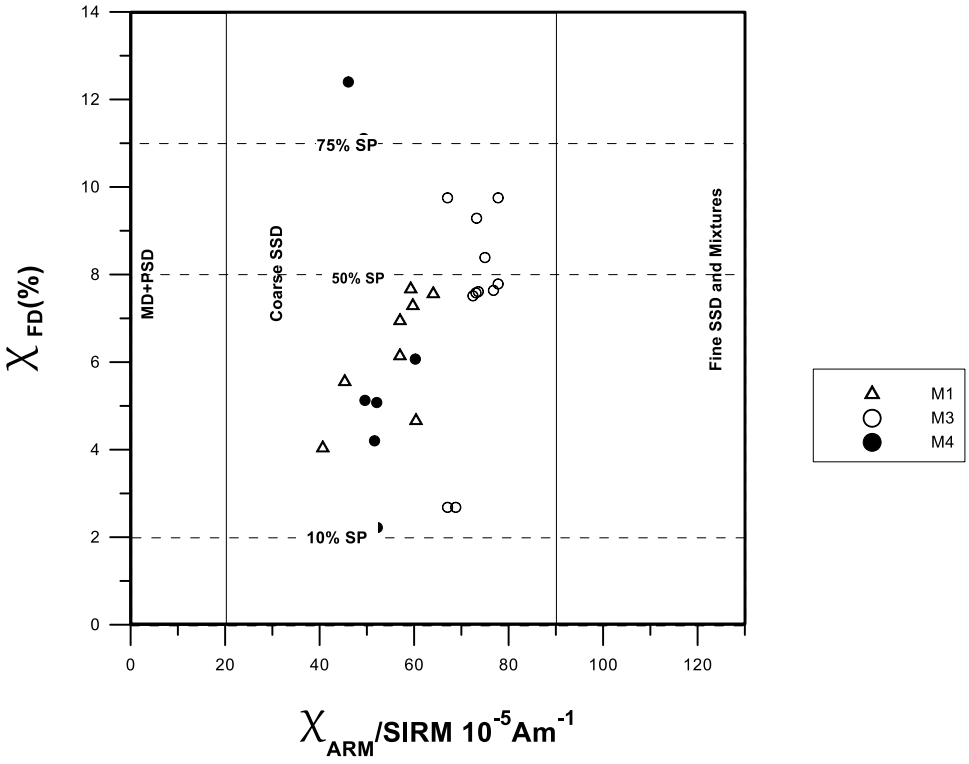


Figure 3.1.14: Plot of $\chi_{fd}$ % versus $\chi_{ARM}$ /SIRM for mudflat sediments from the Zuari estuary.

The plot of $\chi_{fd}$ versus $\chi_{ARM}$ /SIRM (Figure 3.1.14) indicated that the sediments of mudflat core M3 contained higher percentage of coarse SSD material as compared to the upper middle estuary and lower estuary, whose sediments fell between 10 % to 50 % SP grains. The coarse SSD nature of the sediments indicated that most of the material supplied to the Zuari estuary was of detrital nature.

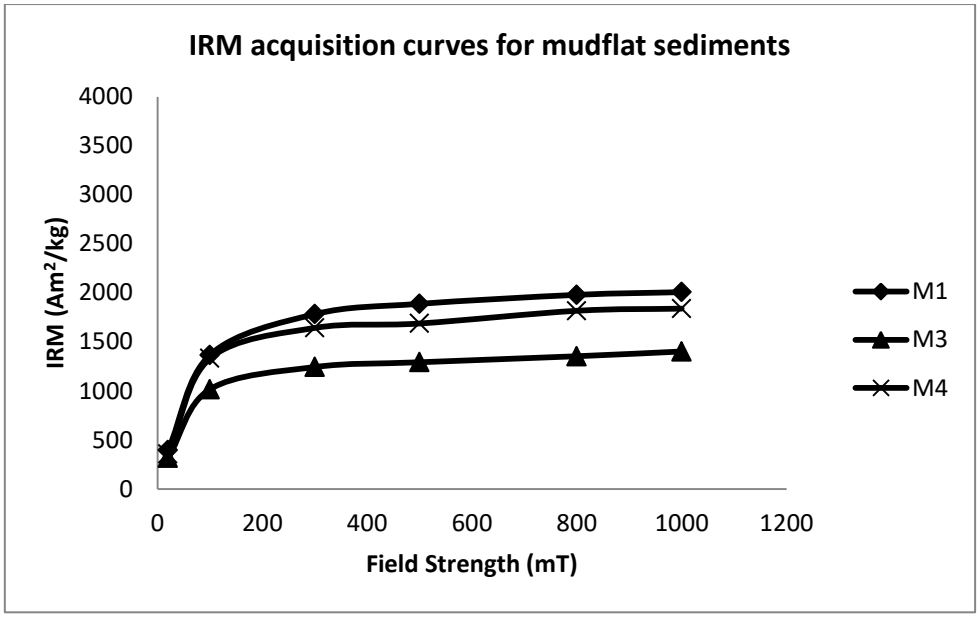


Figure 3.1.15: IRM acquisition curves of mangrove sediments collected from the Zuari estuary.

From the IRM acquisition curves (Figure 3.1.15), it was noted that the sediments of the upper middle estuary contained higher amount of magnetic material than other regions of the estuary. Additionally, the presence of hematite was noted in addition to magnetite as the IRM acquisition curves had not yet saturated at 1000 mT. Thus, higher amount of hematite was present in the upper middle estuary as compared to other regions. Further, the average S-ratio (~90 %) of the cores collected from the three regions of the estuary indicated that the sediments are of mixed nature particularly of hematite and magnetite.

In the distribution of magnetic parameters with depth, little change in magnetic susceptibility parameters of core M1, M3 and M4 suggested little change in source of magnetic materials to the estuary with time.

### 3.1.B.4 Geochemistry of sediments

In this sub-section, abundance and distribution of elements namely Al, Fe, Mn, Cr, Co, Ni, Cu, and Zn are presented in an attempt to elucidate the different processes influencing the trace element composition of the bulk and clay fraction of sediments in the estuarine, environments.

### 3.1.B.4a Metals in bulk sediments

The range and average values of metals in bulk sediment in the three mudflat cores are presented in table 3.1.5(a). In the mudflat core M1 collected from the upper middle estuary, the concentration of major elements Al, Fe and Mn ranged from 6.82 % to 12.23 % (average 8.20 %), 8.20 % to 14.59 % (average 10.50 %) and 1123 ppm to 7264 ppm (average 5341 ppm) respectively. The concentration of trace metals, Cr, Co, Ni, Cu and Zn varied from 219 ppm to 326 ppm (average 262 ppm), 18.00 ppm to 34.50 ppm (average 25.93 ppm), 38.50 ppm to 51.75 ppm (average 45.84 ppm), 32.25 ppm to 50.25 ppm (average 46.48 ppm) and 109 ppm to 173 ppm (average 136 ppm). The lower middle estuary mudflat core M3 showed the concentration of major elements, Al, Fe and Mn ranged from 8.07 % to 12.28 % (average 10.67 %), 8.30 % to 12.16 % (average 10.61 %), 2197 ppm to 4875 ppm (average 3652 ppm) respectively. Trace metal concentrations Cr, Co, Ni, Cu and Zn ranged from 261 ppm to 473 ppm (average 369 ppm), 9.50 ppm to 25.75 ppm (average 18.99 ppm), 33.00 ppm to 51.75 ppm (average 43.39 ppm), 30.75 ppm to 45.25 ppm (average 39.74 ppm) and 105 ppm to 142 ppm (average 124 ppm) respectively. The core collected from the lower estuary mudflat M4 showed that Al, Fe and Mn concentrations ranged from 8.53 % to 10.51 % (average 9.82 %), 8.94 % to 11.32 % (average 10.44 %) and 2203 ppm to 2958 ppm (average 2665 ppm) respectively. Measured concentration of trace metals Cr, Co, Ni, Cu and Zn varied from 275 ppm to 388 ppm (average 342 ppm), 26.00 ppm to 30.25 ppm (average 28.10 ppm), 36.00 ppm to 48.50 ppm (average 42.17 ppm), 32.75 ppm to 46.50 ppm (average 41.25 ppm) and 114 ppm to 151 ppm (average 129 ppm) respectively.

The distribution of metals with depth (Figure 3.1.16) in mudflat core M1 showed that Al, and Fe exhibited similar distribution patterns suggesting that their source was detrital. They exhibited a prominent peak at 26 cm and higher values at the surface. Mn concentrations increased up to 38 cm followed by near uniform distribution toward the surface. Cr exhibited a fluctuating trend around the average line with depth. Co concentrations increased gradually towards the surface, similar to the profile of TOC. Ni, Cu and Zn however, showed large fluctuations in their distributions with depth. The large fluctuating behavior of trace metals Ni, Cu and Zn suggested considerable variations in the input of these metals to the estuary. A common peak was observed at 26 cm in the profiles of Co, Cu and Zn along with Al, Fe, Mn and clay suggesting enrichment of metals with the finer sediments.

Table 3.1.5: Range and average values of metals in bulk sediments (a) and clay fraction (b) in mudflat sediments of M1, M3 and M4 of the Zuari estuary.

| | | | M1 | | M3 | | M4 | |
|---|---|---|---|---|---|---|---|---|
| | | | Average | Range | Average | Range | Average | Range |
| (a) | Metals in bulk sediments | Al % | 8.2 | 6.82-12.23 | 10.67 | 8.07-12.28 | 9.82 | 8.53-10.51 |
| | | Fe % | 10.5 | 8.20-14.59 | 10.61 | 8.30-12.16 | 10.44 | 8.94-11.32 |
| | | Mn (ppm) | 5341 | 1123-7264 | 3652 | 2197-4876 | 2665 | 2203-2958 |
| | | Cr (ppm) | 262 | 219-326 | 369 | 261-473 | 342 | 275-388 |
| | | Co(ppm) | 25.93 | 18.00-34.50 | 18.99 | 9.50-25.75 | 28.1 | 26.00-30.25 |
| | | Ni (ppm) | 45.84 | 38.50-51.75 | 43.39 | 33.00-51.75 | 42.17 | 36.00-48.50 |
| | | Cu (ppm) | 46.48 | 32.25-50.25 | 39.74 | 30.75-45.25 | 41.25 | 32.75-46.50 |
| | | Zn(ppm) | 136 | 109-173 | 124 | 105-142 | 129 | 114-150 |
| (b) | Metals in the clay fraction | Al (%) | 11.05 | 9.86-12.53 | 11.19 | 9.26-14.52 | 2.76 | 0.42-7.95 |
| | | Fe (%) | 7.75 | 6.83-8.51 | 7.21 | 6.35-8.38 | 2.24 | 0.2-7.14 |
| | | Mn (ppm) | 7121 | 6573-7618 | 4862 | 3771-5966 | 1699 | 777-3696 |
| | | Cr (ppm) | 506 | 353-575 | 659 | 501-727 | 615 | 486-791 |
| | | Co (ppm) | 33.81 | 17.25-43.75 | 23.94 | 12.00-39.00 | 13.25 | 7.00-28.00 |
| | | Ni (ppm) | 105 | 53.00-153 | 153 | 116-189 | 71.25 | 54.75-87.75 |
| | | Cu (ppm) | 184 | 161-234 | 170 | 145-179 | 117 | 87.25-174 |
| | | Zn (ppm) | 691 | 135-1064 | 757 | 428-1166 | 515 | 42.25-1717 |

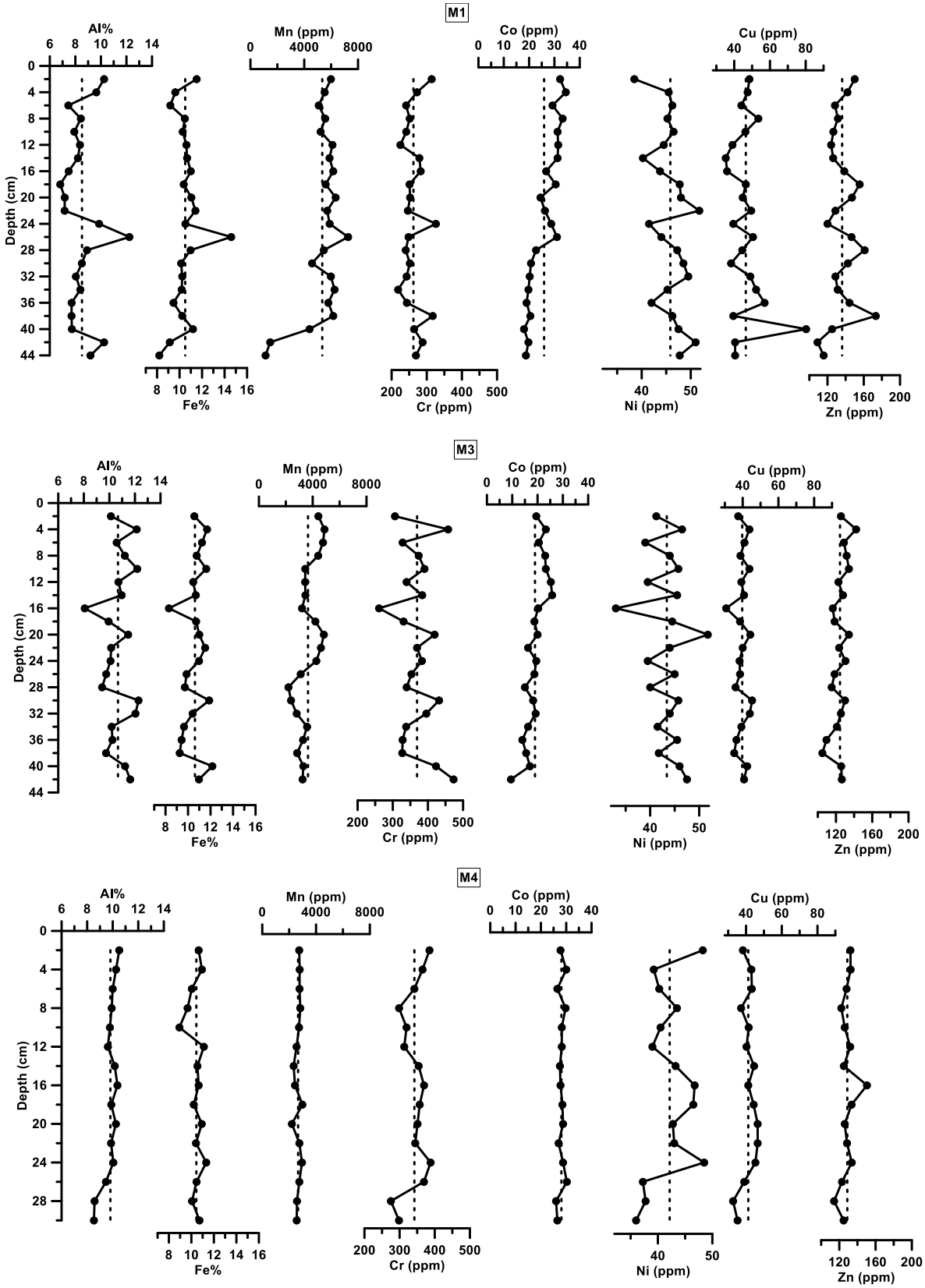


Figure 3.1.16 Distribution of bulk metals with depth in mudflat cores M1, M3 and M4.

In core M3, the distribution of metals with depth revealed that major elements Al and Fe exhibited similar distribution pattern with fluctuations and overall increase towards the surface. Mn concentrations increased towards the surface with higher values at 20 cm. Trace elements of Cr and Ni showed large fluctuations with depth. Co and Zn increased towards the surface along with Mn, whereas Cu exhibited slight increase up to 14 cm followed by constant distribution towards the surface. The distribution of metals with depth in core M4 showed that the percentage of Al exhibited minor enrichment towards the surface and higher values between 24 cm and 14 cm depth. The profile of Fe and Mn showed uniform distribution pattern except for a negative peak at 10 cm for Fe. Cr and Ni and to some extent Cu and Zn displayed similar distribution trends to Al which could indicate a detrital source for these metals. However, among them Cr and Ni showed large fluctuations.

Pearson's correlation analysis (Table 3.1.6) carried out on the data set for each of the mudflat cores, helped in understanding the source and geochemical associations of the metals. Substantial spatial and temporal variations were noted from the ranges, averages and vertical distribution profiles of the three mudflat cores. Highest concentrations of Mn, Ni, Cu and Zn were noted in the upper middle estuary; Al, Fe and Cr in the lower middle estuary and Co in the lower estuary. Most metals were accumulated in higher amounts in the middle estuary than the lower estuary due to higher estuarine hydrodynamics, which increased towards the mouth under the influence of strong waves. Metals may have been resuspended and mobilized under high hydrodynamic conditions in the lower estuary. Shiyuan et al. (1997) reported that there is a close relationship between the accumulation of heavy metals and the geomorphic features of the tidal flats in the estuary.

In the core M1 collected from the upper middle estuary mudflat, metal distributions were less influenced by sediment grain size. Fe and Mn were significantly associated indicating similarity in their redox behaviors. Fe-Mn oxides accounted for the down-core variation of metals Co and Zn in the sediments. Fe and Mn oxides are very effective scavengers for trace metals and play an important role in the remobilization processes of the adsorbed trace metals between the sediments, pore water, and overlying water (Amiard-Triquet and Rainbow, 2009). Additionally, Mn was significantly associated with the silt size particles. The fluctuating trends of Ni, Cu and Zn suggested large variations in their inputs to the estuary and their poor association to the lithogenic elements.

Table 3.1.6: Pearson's correlation coefficient of sediment components and bulk metals in mudflat cores of M1, M3 and M4.

| (a) | Correlations-M1 | | | | | | | | | | | | | |
|---|---|---|---|---|---|---|---|---|---|---|---|---|---|---|
| | | pH | Sand | Silt | Clay | TOC | Al | Fe | Mn | Cr | Co | Ni | Cu | Zn | |
| | pH | 1.00 | | | | | | | | | | | | | |
| | Sand | 0.58** | 1.00 | | | | | | | | | | | | |
| | Silt | -0.63** | -0.63** | 1.00 | | | | | | | | | | | |
| | Clay | 0.51* | 0.33 | -0.94** | 1.00 | | | | | | | | | | |
| | TOC | -0.53* | -0.54** | 0.540** | -0.42 | 1.00 | | | | | | | | | |
| | Al | 0.11 | 0.27 | -0.42 | 0.39 | -0.11 | 1.00 | | | | | | | | N=22 |
| | Fe | -0.18 | -0.48* | 0.19 | -0.02 | 0.18 | 0.37 | 1.00 | | | | | | | |
| | Mn | -0.57** | -0.74** | 0.58** | -0.38 | 0.32 | -0.10 | 0.64** | 1.00 | | | | | | |
| | Cr | 0.26 | 0.19 | -0.41 | 0.41 | -0.22 | 0.29 | -0.03 | -0.13 | 1.00 | | | | | |
| | Co | -0.47* | -0.56** | 0.26 | -0.07 | 0.61** | 0.19 | 0.33 | 0.43* | 0.07 | 1.00 | | | | |
| | Ni | 0.50* | 0.29 | -0.09 | -0.01 | -0.06 | -0.29 | -0.22 | -0.43* | -0.37 | -0.44* | 1.00 | | | |
| | Cu | -0.12 | -0.11 | 0.05 | -0.01 | -0.34 | -0.08 | 0.21 | 0.05 | -0.25 | -0.24 | 0.10 | 1.00 | | |
| | Zn | -0.30 | -0.22 | 0.36 | -0.34 | 0.12 | -0.11 | 0.33 | 0.53* | 0.10 | 0.05 | -0.15 | -0.03 | 1.00 | |

| (b) | Correlation M3 | | | | | | | | | | | | | |
|---|---|---|---|---|---|---|---|---|---|---|---|---|---|---|
| | | pH | Sand | Silt | Clay | TOC | Al | Fe | Mn | Cr | Co | Ni | Cu | Zn | |
| | pH | 1.00 | | | | | | | | | | | | | |
| | Sand | 0.13 | 1.00 | | | | | | | | | | | | |
| | Silt | -0.09 | 0.10 | 1.00 | | | | | | | | | | | |
| | Clay | 0.03 | -0.44* | -0.94** | 1.00 | | | | | | | | | | |
| | TOC | 0.00 | -0.17 | -0.39 | 0.42 | 1.00 | | | | | | | | | |
| | Al | -0.20 | 0.16 | -0.08 | 0.01 | -0.34 | 1.00 | | | | | | | | N=21 |
| | Fe | -0.37 | 0.25 | 0.13 | -0.21 | -0.14 | 0.76** | 1.00 | | | | | | | |
| | Mn | -0.56** | -0.23 | -0.13 | 0.20 | 0.25 | 0.09 | 0.37 | 1.00 | | | | | | |
| | Cr | -0.09 | 0.39 | -0.20 | 0.04 | -0.05 | 0.83** | 0.73** | 0.06 | 1.00 | | | | | |
| | Co | -0.54* | -0.43 | 0.17 | 0.00 | -0.01 | 0.19 | 0.19 | 0.33 | -0.08 | 1.00 | | | | |
| | Ni | 0.08 | 0.15 | -0.27 | 0.19 | 0.05 | 0.71** | 0.56** | 0.15 | 0.75** | -0.11 | 1.00 | | | |
| | Cu | -0.12 | 0.09 | -0.02 | -0.02 | -0.15 | 0.93** | 0.83** | 0.18 | 0.80** | 0.21 | 0.72** | 1.00 | | |
| | Zn | -0.61** | 0.00 | -0.10 | 0.09 | 0.08 | 0.70** | 0.75** | 0.53* | 0.65** | 0.50* | 0.39 | 0.73** | 1.00 | |

| (c ) | | Correlations- M4 | | | | | | | | | | | | |
|---|---|---|---|---|---|---|---|---|---|---|---|---|---|---|
| | | pH | Sand | Silt | Clay | TOC | Al | Fe | Mn | Cr | Co | Ni | Cu | Zn |
| | pH | 1.00 | | | | | | | | | | | | |
| | Sand | 0.66** | 1.00 | | | | | | | | | | | |
| | Silt | -0.67** | -0.57* | 1.00 | | | | | | | | | | |
| | Clay | 0.29 | -0.09 | -0.77** | 1.00 | | | | | | | | | |
| | TOC | -0.35 | -0.40 | 0.70** | - | 1.00 | | | | | | | | |
| | Al | -0.51 | -0.72** | 0.57* | -0.13 | 0.32 | 1.00 | | | | | | | |
| | Fe | 0.35 | 0.13 | -0.15 | 0.08 | 0.07 | 0.16 | 1.00 | | | | | | |
| | Mn | -0.06 | -0.17 | 0.38 | -0.33 | 0.40 | 0.01 | -0.21 | 1.00 | | | | | |
| | Cr | -0.17 | -0.41 | 0.34 | -0.10 | 0.22 | 0.75** | 0.46 | 0.17 | 1.00 | | | | |
| | Co | -0.16 | -0.40 | 0.10 | 0.18 | 0.33 | 0.41 | 0.11 | 0.25 | 0.39 | 1.00 | | | |
| | Ni | -0.07 | -0.33 | 0.35 | -0.17 | 0.11 | 0.72** | 0.17 | 0.21 | 0.63* | 0.12 | 1.00 | | |
| | Cu | -0.18 | -0.39 | 0.39 | -0.17 | 0.11 | 0.68** | 0.25 | -0.01 | 0.62* | 0.22 | 0.45 | 1.00 | |
| | Zn | -0.08 | -0.62* | 0.31 | 0.11 | 0.18 | 0.60* | 0.37 | 0.02 | 0.61* | 0.13 | 0.58* | 0.40 | 1.00 |

N=15

Metals in the intertidal sediments may partially originate from the weathering of parent rocks, may also stem from wastewater discharges or atmospheric deposition and are mostly retained or adsorbed by intertidal sediments of the estuary (Xue-Feng et al., 2013). Al, Fe and Mn indicated they are of mixed origins probably anthropogenic. Co however, showed association with TOC which implied that Co might have been mobilized through processes involving organic materials. The increasing distribution pattern of Co suggested recent inputs and a different source from other trace metals. The concentrations of Cr, Co, Ni, Cu and Zn along with Al above 14 cm, increased towards the surface implying detrital input of these metals in the recent past. Thus, in the upper estuarine mudflat, metal distributions were influenced by Fe and Mn and were anthropogenic in nature.

In the core M3 collected from the lower middle estuary, the influence of sediment components on metal distributions was noted to be negligible. Modification of sediments with respect to early diagenetic changes in reductive dissolution of Fe and Mn was very prominent between 22 cm to 20 cm. Under the sediment–water interface, the reductive dissolution of Mn and Fe oxides leads to the remobilization of initially bound trace elements which further can be re-adsorbed onto or co-precipitated with newly-formed Mn and Fe mineral phases (Dang et al., 2015). Cr, Ni, Cu and Zn were associated with Al and Fe. As, Al is a naturally occurring metal and its concentration is generally not influenced by anthropogenic sources (Schropp and Windom, 1988), metal associations with Al suggested a detrital source influencing metal distributions. Metal distribution patterns also exhibited constant or decreasing trends towards the surface, which suggested reduced anthropogenic inputs. Co, in a similar manner to the upper middle estuary, increased towards the surface. Thus a common source of Co may have influenced the upper middle and lower middle estuary.

The sediments of core M4 collected from the lower estuary showed little variations in the distribution pattern of metals. Metal distributions were less affected by sediment components. Association of metals Cr, Ni, Cu and Zn with Al and their significant inter-metal association suggested a detrital source. The uniform distribution of most metals suggested a constant rate of input of metals. Overall, metal distributions in this core were influenced by aluminosilicates.

On comparing the distribution profile of metals with clay minerals, no significant association was evident. This indicated that the clay mineralogy had very little influence on metal distribution and was more influenced by other sediment components and physiochemical processes. The major clay minerals of illite, kaolinite as well as chlorite weakly associated with all the investigated trace metals probably due to the weak competing strength of these clays compared with the other adsorbents and to low availability of the mobile trace metals in the system (He et al., 2012).

Additionally, an attempt was made to understand that association of metals with the magnetic material in the sediments by comparing distribution profiles. In mudflat core M1, the Cr profile showed similarity with $\chi_{ARM}$ that implied that some amount of Cr might have been anthropogenically sourced to the upper middle estuary sediments. Association of Mn and Co with the magnetic grain size parameters suggests their association with the fine grains. Scraps containing rust fragments and paints enriched in heavy metals may have settled through the water column and eventually deposited in the sediments and caused high levels of magnetic susceptibility. No significant association of metals with the magnetic susceptibility parameters were noted in core M3, that suggested that this region of the estuary subjected to low amount of the pollutant load as compared to other regions of the estuary. In core M4, Cr and Ni showed similar distribution to SIRM suggesting that Cr and Ni may be associated with some amount of ferromagnetic materials as SIRM primarily responds to the concentration of ferrimagnetic material in the sediments such as magnetite.

Magnetic particles in the sediments may be detrital derived geologically from catchment area sources; anthropogenic, if they are derived from industrial emissions and atmospheric; or biogenic in nature. The strong similarity in distribution between magnetic susceptibility and several sediment metal concentrations suggested a significant contribution to the magnetic material from anthropogenic sources (Chan et al., 1998). The ferric oxide and trace metals are associated as metals are preferentially adsorbed on to the exterior surface of Fe- oxides and precipitated to the sediments. Thus, the metals associated with the magnetic material may have been supplied anthropogenically from mining and shipbuilding discharges.

### 3.1. B.4b Metals in the clay fraction of sediments

Further, the geochemistry of the clay fraction of sediments was studied as metals have a strong tendency to associate with the fine sediments. The range and average values of metals

content in the clay fraction of cores M1, M3 and M4 are presented in Table 3.1.5(b). In the mudflat core M1, concentrations of major elements Al, Fe and Mn ranged from 9.86 % to 12.53 % (average 11.05 %), 6.83 % to 8.51 % (average 7.75 %) and 6573 ppm to 7618 ppm (average 7121 ppm). Trace metal concentrations of Cr, Co, Ni, Cu and Zn in the core ranged from 353 ppm to 575 ppm (average 506 ppm), 17.25 ppm to 43.75 ppm (average 33.81 ppm**),** 53.00 ppm to 153 ppm (average 105 ppm), 161 ppm to 234 ppm (average 184 ppm) and 135 ppm to 1064 ppm (average 691 ppm). The concentrations of major elements Al, Fe and Mn in the sediment core M3 collected from the lower middle estuary mudflat ranged from 9.26 % to 14.52 % (average 11.19 %), 6.35 % to 8.38 % (average 7.21 %) and 3771 ppm to 5966 ppm (average 4862 ppm ) respectively. Further, the trace metal concentrations of Cr, Co, Ni, Cu and Zn ranged from 501 ppm to 727 ppm (average 659 ppm), 12.00 ppm to 39.00 ppm (average 23.94 ppm), 116 ppm to 189 ppm (average 153 ppm), 145 ppm to 179 ppm (average 170 ppm) and 428 ppm to 1166 ppm (average 757 ppm) respectively. In sediment core M4 collected from the lower estuary mudflat, major elements Al, Fe and Mn concentrations ranged from 0.42 % to 7.95 % (average 2.76 %), 0.20 % to 7.14 % (average 2.24 %) and 777 ppm to 3696 ppm (average 1699 ppm) respectively. Trace metals Cr, Co, Ni, Cu and Zn concentrations ranged from 486 ppm to 791 ppm (average 615 ppm ), 7.00 ppm to 28.00 ppm (average 13.25 ppm), 54.75 ppm to 87.75 ppm (average 71.25 ppm), 87.25 ppm to 174 ppm (average 117 ppm) and 42.25 ppm to 1717 ppm (average 515 ppm).

Highest average concentration of Fe, Mn, Co and Cu was noted in the upper middle estuary mudflat, Al, Cr, Ni and Zn in the lower middle estuary mudflat and the lowest concentration of most trace metals in the clay fraction (except for Cr) was noted in the lower estuary.

From the vertical distribution of metals in the clay fractions (Figure 3.1.17) in core M1, it was observed that Al and Fe showed similar distribution trends wherein concentrations increased up to 30 cm followed by a minor decrease towards the surface. The trace metals Cr, Co, Ni, Cu and Zn exhibited similar distribution pattern among themselves and to the profiles of Al and Fe suggesting their common source that was mainly detrital. Mn concentrations showed a minor increase up to 14 cm followed by decrease towards the surface and exhibited a distribution pattern different from Al and Fe suggesting some alternative source possibly anthropogenic.

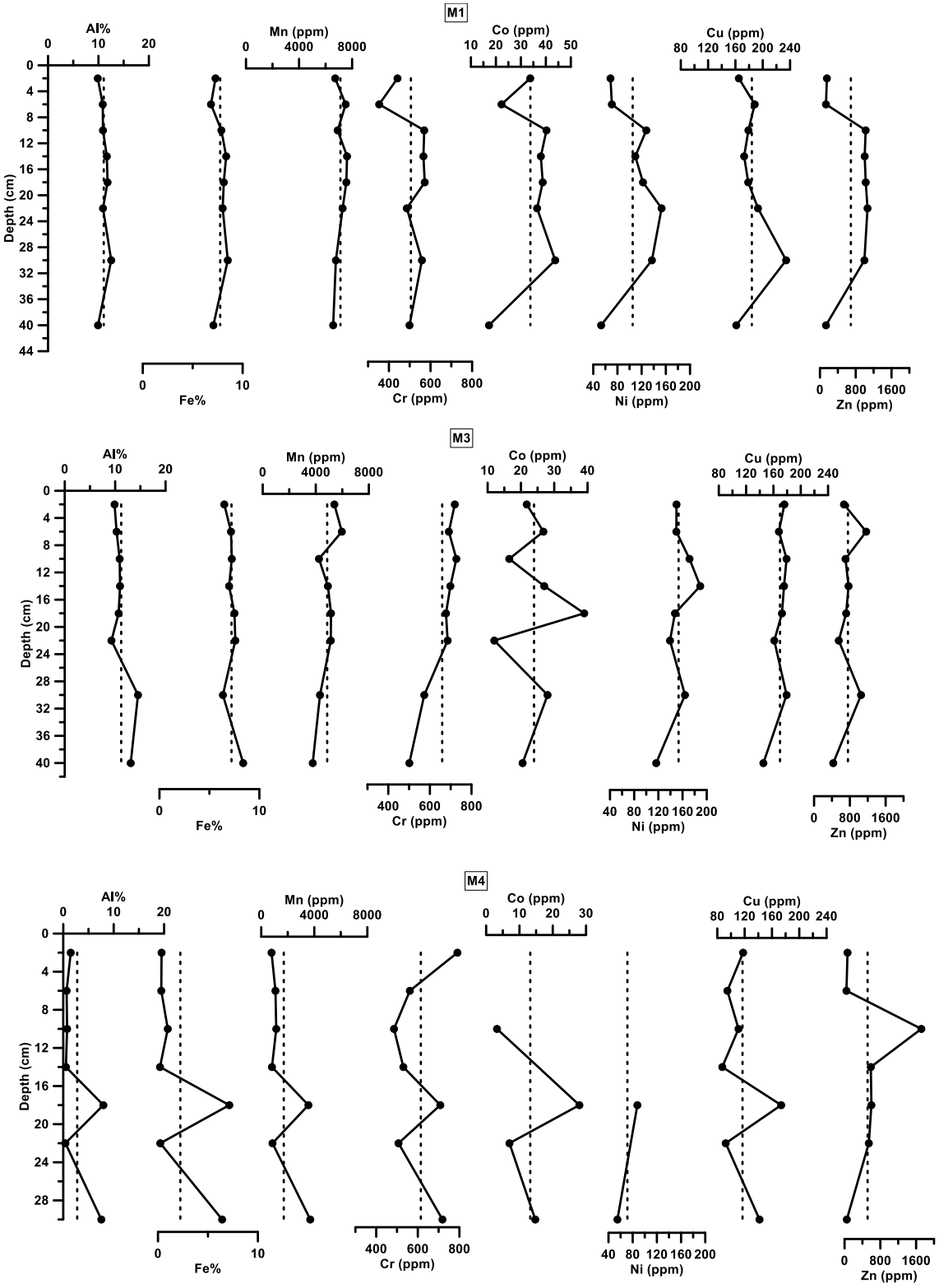


Figure 3.1.17 Distribution of metals in the clay fraction of sediments with depth in mudflat cores M1, M3 and M4.

In the vertical distribution of metals in the clay fraction of sediments of mudflat core M3, Al distribution exhibited a peak at 30 cm followed by decrease up to 22 cm and then constant

values towards the surface. Fe concentrations decreased up to 30 cm and showed near uniform distribution towards the surface. Mn concentrations gradually increased towards the surface with a prominent peak at 6 cm. The trace metals exhibited distinct distribution patterns wherein Cr gradually increased towards the surface along with Mn, while, Co exhibited a fluctuating distribution with peaks at 14 cm and 6 cm that corresponded to Mn. Ni, Cu and Zn exhibited similar distributions along with Al below 18 cm, followed by distinct distribution towards the surface that corresponded to Mn. From the vertical profile of metals in the clay fraction of mudflat core M4 showed that Al, Fe and Mn exhibited a corresponding distribution pattern with a prominent peak at 18 cm. Similar peak was noted in the profiles of Cr, Co and Cu. The concentrations of Co above 10 cm and Ni above 18 cm were below detection limits. Zn however, exhibited a peak in its distribution profile at 10 cm followed by low concentrations at the surface suggesting a difference source.

The comparison of metal profiles in clay fraction (Table 3.1.5) of core M1 revealed that all metals were associated with Al and Fe, which indicated the role of aluminosilicates and Fe-oxyhydroxides in the distribution of the trace metals. The trace metals however, were weakly associated with Mn. Similar distributions of Cr, Co, Ni and Zn suggested a common source for these metals. In core M3, all metals in the clay fraction were associated with Mn suggesting the role of Mn-oxyhydroxides in the distribution of the trace metals. Similar distributions of Ni and Cu indicated a common source for these two metals. Similar distributions of Al, Fe and Mn along with the trace metals in sediment core M4 suggested the terrigenous origin of these metals.

Further, comparison of average metal concentrations in the bulk sediments and clay fraction using the isocon diagram (Figure 3.1.18) was established. In the upper middle and lower middle estuary, concentrations of all metals except for Fe were high in the clay fraction indicating a detrital control for Al, Mn, Cr, Co, Ni, Cu and Zn and were mainly associated with aluminosilicates. Zn, Ni and Cu however, formed a group of high concentrations in the clay fraction. Further, Fe may have been associated with larger sediment particles or may have formed larger aggregates of iron oxides. In the lower estuary mudflat core M4, Cr, Ni, Cu and Zn concentrations were high in the clay fraction of sediments whereas Al, Fe, Mn and Co concentrations were higher in the bulk sediments. The association of Al, Fe and Mn with the coarse sediments suggested physically weathered coarse material or deposition of ore material in the sediments that may have come from the spillage from ore carrying barges.

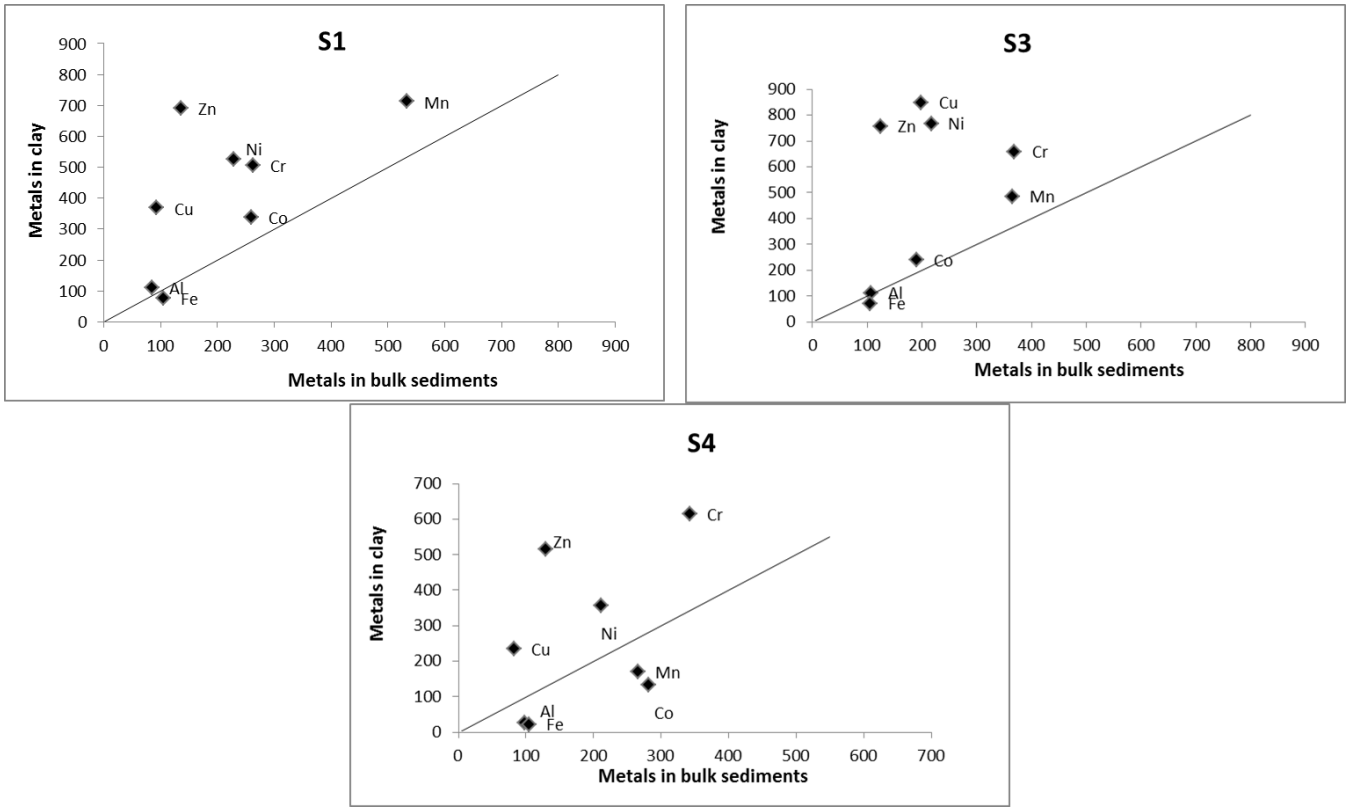


Figure 3.1.18: Isocon diagram of metals in bulk sediments versus metals in the clay fraction of mudflat cores M1, M3 and M4.

Metals are known to be more adsorbed to the smaller sediment particles especially clay than the coarser fractions. Higher concentrations of metals found in the finer sediment particles are due to the synergetic action of physical and chemical properties of the particles of each size fraction. The smaller sediment grains have a greater specific surface area than the larger grains. Also, most fine particles consist mainly of clay minerals, which have more metal binding sites than the silicate or carbonate minerals, which are the major components of coarser material in marine sediments (Campbell et al., 1988).

In general, the coarse material is an important constituent of the sediment and may represent more than 50 percent of the bulk sediment mass. Although high metal concentrations can be occasionally found in coarse sediment material (Filipek et al., 1981; Robinson, 1982), the silt and clay fractions usually contain higher metal concentrations than the sand fraction. The vicinity of land based pollution sources, which may dispose large particles with relatively high metal content through urban and industrial effluents and deposits, may lead to enhanced metal concentrations in coarse sediment material (Horowitz, 1991). Metal enrichments in

coarse sediments may be explained by the formation of coatings on the surface of the particles (Krumgalz et al., 1992) through carbonates, hydroxy-oxides and organic matter that enhance the specific surface area of particles that may lead to the increase of their adsorption capacity (Horowitz and Elrick, 1987). The coating formation may also bring about the consolidation of fine particles to the formation of larger particles with smaller specific surface area and thus, smaller adsorption capacity. The particle consolidation may also lead to an 'artificial' enhancement of metal concentrations in the coarser sediment fractions (Aloupi and Angelidis, 2002). Thus, most Fe may have been of anthropogenic origin and the associated metals like Mn, Co in the lower estuary may have led to the formation of coating around the larger sediment grains.

### 3.1.C Comparison of mangrove and mudflat core sediments in the Zuari estuary

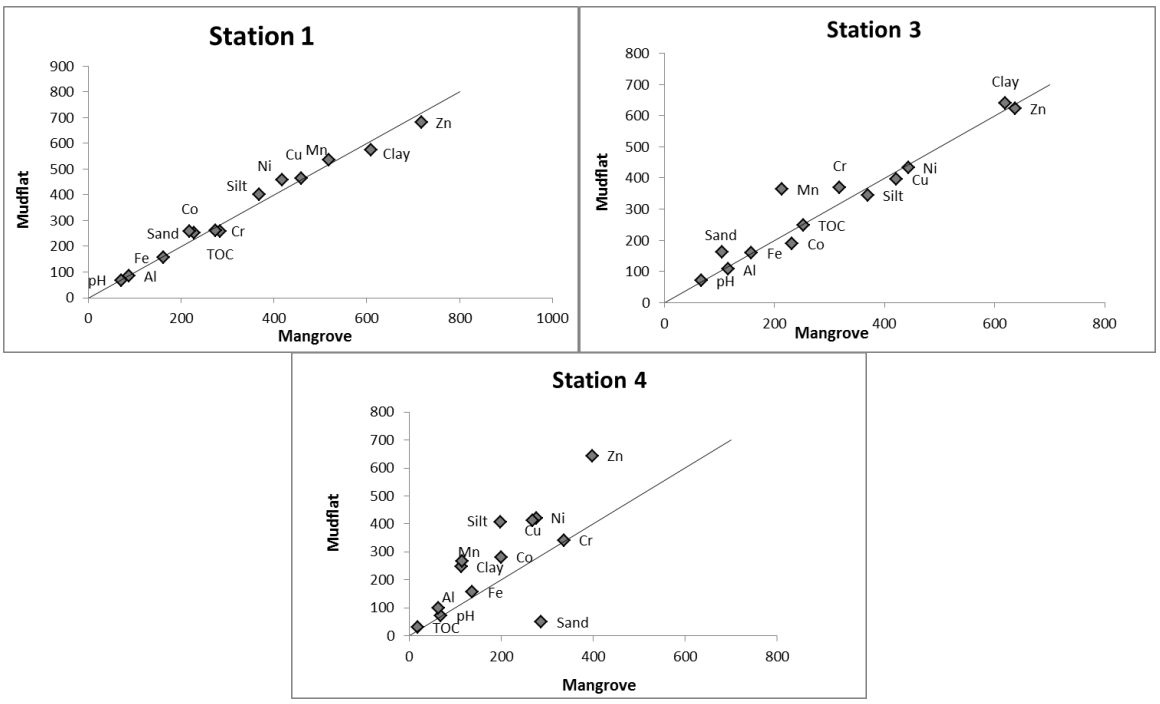


Figure 3.1.19: Isocon diagram of metals in mudflat sediments versus mangrove of sediments collected from Station 1 of the upper middle estuary, station 3 of the lower middle estuary and station 4 of the lower estuary.

A comparison of sediment components and metals in the mangrove cores with the mudflat cores collected at the sampling locations 1, 3 and 4 using the isocon diagram was made to understand the degree of metal association within each of the estuarine sub-environments and the processes controlling them.

In the upper middle estuary (station 1), the average values plotted on the isocon diagram (Figure 3.1.19) revealed higher content of sand, silt, Mn, Co, Ni and Cu in the mudflat whereas clay, TOC , Cr and Zn were higher in the mangrove. In the lower middle estuary (station 3), sand, clay, Mn and Cr were high in the mudflat whereas silt, Co, Ni, Cu and Zn were higher in the mangrove. In the lower estuary (station 4), silt, clay, TOC, Al, Fe, Mn, Co, Cu, Ni and Zn were higher in the mudflat sediments whereas sand was higher in the mangrove.

The sediments of the upper middle estuary showed less variation with respect to the sediment components and metal concentrations as most of the point fell close to the central line. Proceeding seawards, the variation in the sediment component and metals increased and with highest variation observed in the lower estuary. This difference was mainly due the geomorphic characteristics and the physical processes in the estuary. The Mormugao Bay, at the mouth of the Zuari River, is relatively large in area and is funnel-shaped with a width of 5 km at the mouth and narrows down to 1 km at the joining point of the channel. The funnel-shaped bay favors the enhancement of physical processes. Sampling location 1 was located in close proximity to the upstream region of the estuary where much of the fluvial sedimentary material is supplied. The narrow width of the canal and the less magnitude of the tidal currents in the upstream regions of the estuary facilitated quick removal of material from the water column to the sediments. Thus, less variation between the mudflats and mangrove sediment components were observed. In the mudflat, higher content of Co, Ni and Cu may be probably associated with the Fe-Mn oxyhydroxides whereas enrichment of Cr and Zn in the mangrove may be associated with Fe oxides and TOC. The mangrove sediments contain higher percentage of organic matter that may be related to the accumulation of litter within the mangrove forest (Tam and Wong, 1998). In the lower middle estuary, the relatively broader width of the channel allowed for an increased tidal magnitude and thus may have caused resuspension of sediments to the water column which facilitated sorting of material and its subsequent deposition in the intertidal regions. Higher Cr content in the mudflats may have been influenced by sand, clay, Mn-oxides whereas Co, Ni, Cu and Zn in mangroves were positively correlated with silt and thus co-precipitated together. In the lower estuary, the broad width of the bay and the high energy conditions caused turbulence due to which much of the sediments were re-suspended and transported to calmer regions. The larger grain size material got trapped in the mangroves due to the effect of the specialized network of

mangrove roots called pneumatophores that aid in trapping larger grain size particles brought in by the tide. The fine sediments along with adsorbed metals accumulated in the mudflats. Additionally the coarse calcareous material in the mangrove sediments provides little surface for adsorption of metals. The accumulation of Co, Cu, Ni and Zn in mudflats is attributed to the higher silt, clay, TOC, Al, Fe, Mn that facilitated the accumulation of metals. In the lower estuary, metals in the mudflat are associated with silt and clay particles due to the processes of adsorption and coagulation (Anithamary et al., 2012).

The transfer and the chemical stability of metal contaminants in sediments are controlled by a complex series of biogeochemical processes depending on parameters like pH, clay content, and redox potential (Vanbroekhoven et al., 2006). Mangroves are known for the high organic matter content and their sediments are favorable to reducing conditions, where metals can be immobilized in the form of sulfides or complexed with organic matter (da Silva et al., 2014). Oxidizing conditions generally increase the retention capacity of metals in sediments, while reducing conditions will generally lessen the retention capacity of metals (McLean and. Bledsoe, 1992). The decomposition of the organic matter received in the mangroves provides reducing conditions in the mangroves that causes mobility of redox sensitive elements Fe and Mn along with associated metals. These mobilized metals may either get re-precipitated at the oxidizing surface of the sedimentary column or may escape to the water column. This was evident from the marginally higher TOC content in mangroves from the isocon diagram. The mudflat habitat provides an interesting case study in metal geochemistry in a system with a high suspended particulate concentration through ebb and flood tide (Rezaie-Boroon et al., 2013). During the transition to oxidizing condition in ebb, solid iron oxide (e.g. FeOOH) will precipitate dramatically, reducing the mobility of metals, which co-precipitate with iron (Andrews et al., 2004). Thus, the mobilized metals from the mangrove sediments are trapped along with oxides of Fe and Mn in the mudflat sediments, which was evident from the higher Mn content in the mudflat sediments along with metals.

### 3.1.D Enrichment Factor and Geoaccumulation index

Enrichment factors and Geoaccumulation index were calculated to assess the extent of metal enrichment and pollution levels of the estuary. The average values of the enrichment factors are present in table 3.1.7 for mangroves and mudflats at each of the sampling locations.

Table 3.1.7 **:** Enrichment Factors of metals in mangroves (a) and mudflats (b).

(a)

| Enrichment Factor (EF)- Mangroves | | | | | | | |
|---|---|---|---|---|---|---|---|
| | Fe | Mn | Cr | Co | Ni | Cu | Zn |
| S1 | 2.13 | 5.65 | 2.82 | 1.06 | 0.57 | 0.95 | 1.4 |
| S2 | 2.97 | 5.85 | 2.87 | 1.17 | 0.67 | 0.78 | 1.06 |
| S3 | 1.55 | 1.77 | 2.43 | 0.85 | 0.45 | 0.65 | 0.93 |
| S4 | 2.61 | 1.61 | 4.88 | 1.41 | 0.52 | 0.77 | 1.06 |

(b)

| Enrichment Factor (EF)- Mudflats | | | | | | | |
|---|---|---|---|---|---|---|---|
| M1 | 2.12 | 6.05 | 2.78 | 1.3 | 0.88 | 0.99 | 1.38 |
| M3 | 1.69 | 3.24 | 3.07 | 0.75 | 0.65 | 0.66 | 0.99 |
| M4 | 1.81 | 2.56 | 3.09 | 1.21 | 0.69 | 0.75 | 1.11 |

The average enrichment factor calculated for mangrove sediments revealed that sediments at S1 and S2 were enriched by Fe, Mn and Cr; S3 by Cr and S4 by Fe and Cr. Enrichment factors of trace metals, Co, Ni, Cu and Zn at S1, S2, S3 and S4 were less than 2 and were thus in the range of natural variability. Similarly, average EF calculated for the mudflat sediments revealed Fe, Mn and Cr contaminated the sediments of M1, whereas Mn and Cr contaminated the sediments of M3 and M4. Co, Ni, Cu and Zn enrichment factors were in the range of natural variability. Overall, higher EF values for Fe and Mn among the mangrove cores was noted in the Cumbharjua canal, whereas highest EF for Cr was noted in the lower estuary mangrove sediments. In the case of mudflats, the highest EF values for Fe and Mn were obtained in S1 and Cr in S4.

Furthermore, Geoaccumulation index was calculated to assess the level of pollution by the enriched metals in the sediments of the estuary (Table 3.1.8).

The average of the geoaccumulation indices calculated for mangrove sediments revealed that sediments of S1 were moderately polluted to strongly polluted by Mn, moderately polluted by Cr and unpolluted to moderately polluted by Fe. Mangrove sediments of S2 were moderately polluted by Fe and Mn and unpolluted to moderately polluted by Cr. S3 mangrove sediments were moderately polluted by Cr and un polluted to moderately polluted by Fe and Mn. S4 sediments were moderately polluted by Cr whereas unpolluted to moderately polluted by Fe. Co, Ni, Cu and Zn geoaccumulation indices fell in “class 0” of unpolluted sediments.

Table 3.1.8 **:** Geoaccumulation index of metals in mangroves (a) and mudflats (b).

(a)

| Geoaccumulation index (Igeo)-Mangroves | | | | | | | |
|---|---|---|---|---|---|---|---|
| | Fe | Mn | Cr | Co | Ni | Cu | Zn |
| S1 | 0.61 | 2.01 | 1 | -0.42 | -0.85 | -0.57 | 0 |
| S2 | 1.02 | 1.9 | 0.97 | -0.33 | -0.69 | -0.91 | -0.47 |
| S3 | 0.57 | 0.68 | 1.22 | -0.31 | -0.76 | -0.69 | -0.17 |
| S4 | 0.36 | -0.36 | 1.27 | -0.69 | -1.49 | -1.37 | -0.9 |

(b)

| Geoaccumulation index (Igeo)-Mudflats | | | | | | | |
|---|---|---|---|---|---|---|---|
| M1 | 0.56 | 1.97 | 0.95 | -0.17 | -0.71 | -0.56 | -0.07 |
| M3 | 0.58 | 1.48 | 1.44 | -0.62 | -0.8 | -0.77 | -0.2 |
| M4 | 0.56 | 1.06 | 1.33 | -0.02 | -0.84 | -0.72 | -0.15 |

Geoaccumulation index was also calculated for the metals of the mudflats sediments. According to the established classification of the geoaccumulation index, sediments of mudflat core S1 were moderately polluted by Mn and unpolluted to moderately polluted by Fe and Cr. In the mudflat sediments of core S3 and S4, Mn and Cr were moderately polluted and unpolluted to moderately polluted by Fe. The sediment at all three mudflat location fell in "class 0" of unpolluted sediments for Co, Ni, Cu and Zn.

Overall, similar to EF in the mangroves highest Igeo values of Fe were noted in S2, Mn in S1 and Cr in S4. In the case of mudflats, highest Igeo value for Fe was noted in M3, Mn in M1 and Cr in M3. The lowest EF and Igeo was noted for Ni in the mangroves as well as mudflats.

Thus, average EF values and geoaccumulation indices of Fe, Mn and Cr indicated significant anthropogenic inputs of Fe, Mn and Cr in to the estuary. Co, Ni, Cu and Zn did not show enrichment in the estuarine sediments and are of natural origin.

The Zuari estuary receives a large input of mining material from Mandovi estuary via the Cumbharjua canal. Part of this material must have settled within the canal leading to the enrichment of Fe, Mn and Cr in the sediments. The enrichment of Fe and Mn in core S1 and Mn in core S1 was probably salinity dependent in addition to mining input. Fe and Mn is supplied to the riverine flow in reduced and soluble Fe(II) and Mn (II) state which undergoes oxidative conversion to insoluble Fe (III) and Mn (IV) state as the riverine waters encounter

saline waters (Chester and Jickells, 2012). The behavior of Fe and Mn is similar but Fe is precipitated at lower salinities compared to Mn. Dessai and Nayak (2009) noted that higher salinity of the waters was maintained from the mouth of the Zuari estuary up to slightly upstream of the Cumbharjua canal. Thus, in the upper middle estuary, much of the Fe and Mn were removed from the solution to the sediments on encountering waters of higher salinity. Cr, however, showed higher Igeo values in the lower estuary that decreased towards the upper middle estuary. Association of Cr with Fe ores was earlier reported (Bukhari, 1994) within the catchment of the Mandovi estuary that is connected to the Zuari estuary via the Cumbharjua canal. Ore processing units operate all along the banks of the estuary and these industries release associated elements to the waters of the estuary. In addition, the loading jetties in the upstream of Zuari estuary are also expected to release considerable amount of Fe, Mn and Cr. Cr may have been released as leachates from loading of mining ores and shipping activities at the Mormugao harbor located nearby and may have accumulated in the sediments. Additionally, Cr may be released from effluents from treated domestic sewage and industrial discharges and corrosion of uncoated steels from ships in the harbor at the mouth and ship building industries located along the estuary.

### 3.1.E Speciation of metals (Fe, Mn, Cr, Co, Cu and Zn)

The sequential extraction of metals within the five geochemical phases viz. exchangeable (F1), carbonate (F2), Fe-Mn oxide (Reducible- F3), organic matter/sulfide bound (Oxidisable- F4) and residual (F5) was estimated for selected sub-samples of the cores of the mangroves and mudflats of the Zuari estuary. The non-residual metals (F1 to F4) are considered to represent the bioavailable fraction of total metal content of the sediments (Loring and Hill, 1992).

#### 3.1.E.1 Mangroves

The average values of metals in the five geochemical fractions are presented in table 3.1.9 and their respective ranges are described below.

Table 3.1.9: Average values of metals in the five sedimentary fractions of the mangrove sediments and their respective % in parenthesis.

| | | **Exchangeable** | | **Carbonate** | | **Fe-Mn oxide** | | **Organic/Sulfide** | | **Residual** | |
|---|---|---|---|---|---|---|---|---|---|---|---|
| | | (ppm) | (%) | (ppm) | (%) | (ppm) | (%) | (ppm) | (%) | (ppm) | (%) |
| **Fe** | S1 | 11.76 | 0.01 | 5.80 | 0.01 | 8129 | 9.54 | 1272 | 1.48 | 76319 | 88.96 |
| | S2 | 13.34 | 0.01 | 8.95 | 0.01 | 7131 | 6.98 | 1246 | 1.23 | 95834 | 91.76 |
| | S3 | 50.12 | 0.06 | 6.98 | 0.01 | 5144 | 6.45 | 1707 | 2.26 | 72791 | 91.22 |
| | S4 | 64.62 | 0.01 | 28.5 | 0.04 | 3694 | 5.57 | 156 | 0.24 | 62849 | 94.05 |
| **Mn** | S1 | 600 | 11.10 | 1982 | 36.23 | 2165 | 39.55 | 246 | 4.48 | 469 | 8.64 |
| | S2 | 756 | 13.24 | 786 | 14.28 | 3500 | 56.36 | 286 | 4.76 | 628 | 11.36 |
| | S3 | 484 | 21.76 | 487 | 19.70 | 698 | 28.39 | 195 | 8.07 | 508 | 22.08 |
| | S4 | 83.85 | 5.45 | 263 | 18.32 | 348 | 28.79 | 150 | 11.18 | 418 | 35.63 |
| **Cr** | S1 | 1.38 | 0.64 | 0.91 | 0.43 | 11.53 | 5.39 | 12.92 | 6.05 | 189 | 87.50 |
| | S2 | 0.90 | 0.47 | 1.34 | 0.70 | 9.87 | 5.10 | 11.24 | 5.84 | 171 | 87.89 |
| | S3 | 2.22 | 1.02 | 1.05 | 0.48 | 12.87 | 5.92 | 24.88 | 11.36 | 178 | 81.22 |
| | S4 | 1.17 | 0.55 | 1.75 | 0.82 | 11.33 | 5.37 | 10.79 | 5.21 | 187 | 88.05 |
| **Co** | S1 | 1.16 | 2.42 | 1.08 | 2.23 | 9.36 | 19.73 | 3.13 | 6.62 | 33.15 | 69.00 |
| | S2 | 1.04 | 2.63 | 1.00 | 2.25 | 10.82 | 27.67 | 2.28 | 5.88 | 24.20 | 61.27 |
| | S3 | 2.11 | 4.62 | 1.32 | 2.87 | 5.94 | 12.97 | 2.65 | 5.78 | 33.80 | 73.76 |
| | S4 | 1.63 | 4.74 | 2.41 | 7.12 | 4.66 | 13.59 | 0.98 | 2.74 | 24.98 | 71.81 |
| **Cu** | S1 | 1.26 | 1.30 | 1.56 | 1.60 | 2.74 | 2.79 | 22.25 | 22.10 | 73.79 | 71.21 |
| | S2 | 1.35 | 1.46 | 1.13 | 1.23 | 2.17 | 2.35 | 11.18 | 12.27 | 85.23 | 82.68 |
| | S3 | 0.89 | 1.22 | 0.87 | 1.18 | 1.37 | 1.83 | 12.46 | 16.64 | 59.02 | 79.13 |
| | S4 | 1.09 | 2.42 | 1.29 | 3.18 | 0.63 | 1.40 | 3.58 | 7.63 | 37.87 | 85.36 |
| **Zn** | S1 | 0.61 | 0.56 | 1.64 | 1.48 | 21.26 | 19.32 | 9.69 | 8.89 | 76.72 | 69.73 |
| | S2 | 0.75 | 0.92 | 1.37 | 1.68 | 12.73 | 15.40 | 6.07 | 7.49 | 61.42 | 74.50 |
| | S3 | 1.21 | 1.19 | 1.69 | 1.56 | 13.33 | 12.48 | 6.67 | 6.57 | 84.64 | 78.20 |
| | S4 | 3.99 | 5.09 | 1.63 | 2.66 | 10.58 | 15.34 | 2.34 | 3.41 | 49.72 | 73.49 |

### 3.1.E.1a Iron

In mangrove core S1, Fe association with different fractions varied in the order of abundance F5>F3>F4>F1>F2. The concentration of Fe in the residual phase (F5) varied from 67198 ppm to 86623 ppm (average 76319 ppm) that accounted for 85 % to 91 % (average 88.96 %) when recalculated taking all the five fractions to hundred percent. Following residual, Fe was enriched in the Fe-Mn oxide bound fraction ranging from 6723 ppm to 9053 ppm (average 8129 ppm) that accounted for 7.27 % to 11.07 % (average 9.54 %). Fe in the organic/ sulfide bound fraction varied from 640 ppm to 2820 ppm (average 1272 ppm) that accounted for 0.67 % to 3.05 % (average 1.48 %) while, Fe in the exchangeable phase ranged from 0.30 ppm to 44.03 ppm (average 11.76 ppm) that accounted for 0.0003 % to 0.05 % (average 0.01 %). The lowest concentrations of Fe were associated with the carbonate phase that ranged from 1.00 ppm to 15.80 ppm (average 5.80 ppm) that accounted for 0.001 % to 0.019 % (average 0.007 %). The concentration of Fe in core S2 in different sediment fractions varied in the order of abundant F5>F3>F4>F1>F2. The concentration of Fe in the residual phase (F5) varied from 78963 ppm to 112773 ppm (average 95834 ppm) that accounted for 89 % to 95 % (average 91.76 %) when recalculated taking all five fractions to hundred percent. Following residual, Fe was enriched in the Fe-Mn oxide bound fraction ranging from 4685 ppm to 9368 ppm (average 7131 ppm) that accounted for 3.95 % to 9.21 % (average 6.98 %). Fe in the organic/ sulfide bound fraction varied from 734 ppm to 1725 ppm (average 1246 ppm) that accounted for 0.64 % to 2.00 % (average 1.23 %) while, Fe in the exchangeable phase ranged from 0.43 ppm to 55.25 ppm (average 13.34 ppm) that accounted for 0.0004 % to 0.05 % (average 0.013 %). The lowest concentrations of Fe were noted in the carbonate phase that ranged from 0.30 ppm to 60.58 ppm (average 8.95 ppm) that accounted for 0.0003 % to 0.07 % (average 0.0097 %). In core S3, the distribution of Fe was in the order of abundance F5> F3> F4>F1> F2. Fe in the residual fraction varied from 59323 ppm to 84468 ppm (average 72790 ppm) that accounted for 84 % to 94 % (average 91.22 %) when recalculated taking all five fractions to hundred percent. Fe in the Fe- Mn oxide bound fraction varied from 3803 ppm to 6375 ppm (average 5144 ppm) that accounted to 4.99 % to 7.66 % (average 6.45 %) while, Fe concentrations in the organic/ sulfide fraction ranged from 582.5 ppm to 5653.55 ppm (average 1707 ppm) that accounted for 0.64 % to 8.03 % (average 2.26 %). Less quantity of Fe was associated with the exchangeable fraction ranging from 26.40 ppm to 100.30 ppm (average 50.12 ppm) that accounted to 0.04 % to 0.12 % (average 0.06 %). The lowest concentration of Fe was in the carbonate bound fraction ranging from

0.525 ppm to 31.175 ppm (average 6.98 ppm) that accounted to 0.0005 % to 0.03 % (average 0.01 %). The concentration of Fe in core S4, varied in the order of abundance F5> F3> F4>F1> F2. Fe in the residual fraction varied from 55893 ppm to 70325 ppm (average 62849 ppm) that accounted for 92 % to 96 % (average 94.05 %) when recalculated taking all five fractions to hundred percent. Fe in the Fe- Mn oxide bound fraction varied from 3033 ppm to 4403 ppm (average 3694 ppm) that accounted to 4.12 % to 6.96 % (average 5.57 %) while, Fe concentrations in the organic/ sulfide fraction ranged from 61.73 ppm to 228 ppm (average 155.81 ppm) that accounted for 0.08 % to 0.35 % (average 0.24 %). Some amount of Fe was associated with the exchangeable fraction ranging from 26.70 ppm to 147.85 ppm (average 64.62 ppm) that accounted to 0.04 % to 0.23 % (average 0.10 %). The lowest concentration of Fe was noted in the carbonate bound fraction ranging from 1.40 ppm to 143.85 ppm (average 28.50 ppm) that accounted to 0.002 % to 0.23 % (average 0.04 %).

Overall, Fe followed the same order of abundance F5>F3>F4>F1>F2 in the four mangrove cores. Further Fe in the residual phase varied from 88.96 % to 94.05 %, highest being in core S4. Fe in the Fe-Mn oxide phase ranged from 5.57 % to 9.54 %, highest being in core S1. Fe in the organic/ sulfide fraction varied from 0.24 % to 2.26 % highest being in core S3. Fractions F1 and F2 in all the cores were less than 1 %.

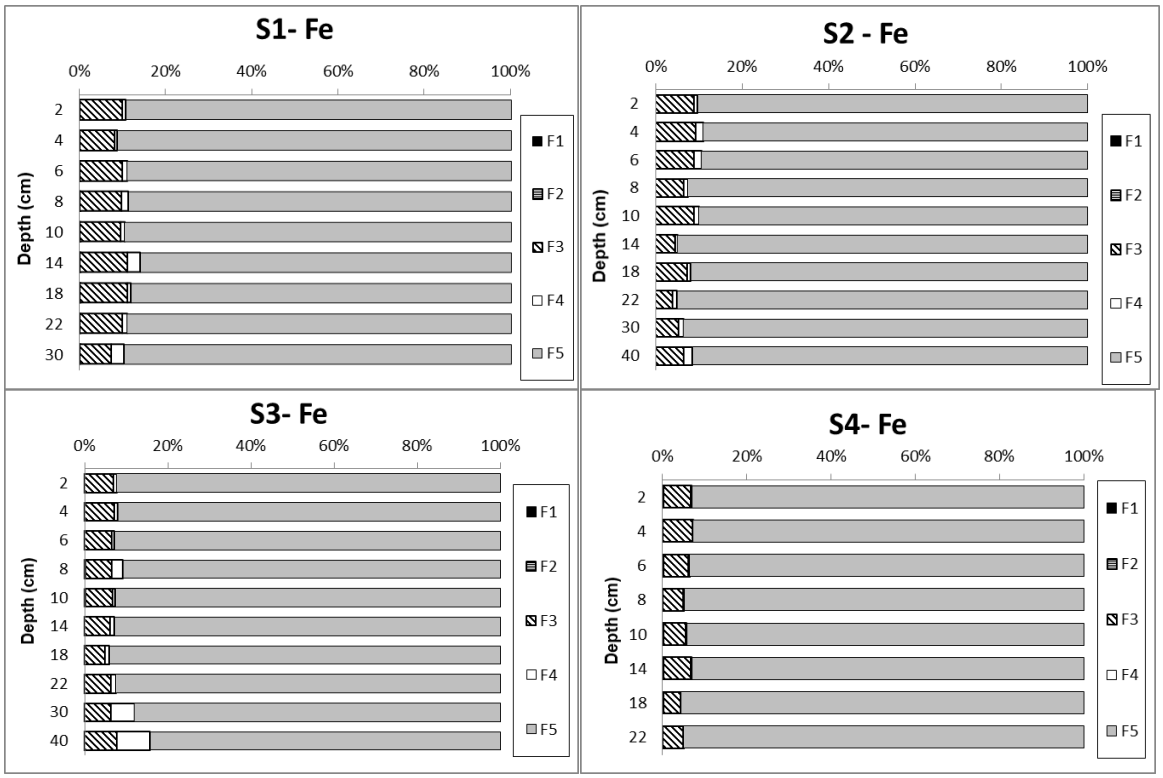


Figure 3.1.20 Speciation of Fe in cores S1, S2, S3 and S4.

From the distribution of Fe with depth in the five sediment fractions of core S1 (Figure 3.1.20) Fe in the residual fraction was highest at all depths. Next to residual, Fe was enriched in the Fe-Mn-oxide phase with highest concentrations at 14 cm. The concentration of Fe in the organic/sulfide bound phase was significant at depth 30 cm and 14 cm which suggested the formation of iron sulfides. In the distribution of Fe with depth in the five phases of core S2, the residual fraction of Fe was the dominant sedimentary fraction with depth. The concentration of Fe in the Fe-Mn oxide fraction was relatively low at depths below 14 cm. followed by higher concentrations towards the surface. Significant concentration of Fe in organic/sulfide phase was noted at depths at 40, 6 and 4 cm. The distribution of Fe with depth of core S3 showed that highest concentration was associated with the residual phase. The concentration of residual Fe at depths 40 cm and 30 cm were slightly lower than those depths towards the surface. The concentration of Fe in the Fe-Mn oxide phase did not exhibit large variations with depth. The organic/ sulfide bound Fe was higher in concentration at depth 40 cm, 30 cm and 8 cm indicating the presence of iron sulfides. Fe in the exchangeable and carbonate fraction was found to be negligible. In core S4, the distribution of Fe with depth in the different phases showed that the dominant fraction of Fe was the residual phase throughout the core. Fe in the Fe- Mn fraction exhibited increased concentrations towards the surface. Fe in fractions F4, F1 and F2 was in traces.

The data obtained showed that Fe maintained over 90 % in residual fraction, in all the four cores with depth. Iron in the residual fraction is immobile and not available to organisms as it is bound to primary and secondary minerals (Tessier et al., 1979). Highest average concentration of Fe in the Fe-Mn oxide bound fraction was noted in core S1 due to precipitation of Fe at low salinities whereas highest average concentration of Fe in the exchangeable and carbonate fractions was noted in the lower estuary. Analysis of magnetic parameters (S-ratio) indicated that high coercivity minerals such as haematite like minerals phases were dominating in the upper estuarine region and less haematite like minerals are dominating in the lower estuarine region. Dessai et al. (2009) studied the magnetic susceptibility of the surface sediments of the Zuari estuary and noted soft (magnetite like phase) and hard (haematite like phase) minerals are contributing to the sediment. The iron ore deposits of Goa are essentially of hematite and are associated with ferrogenous quartzite and phylites. The iron ore mined in the hinterland is transported and stored on the riverbanks in the upstream region. Winds and rains erode these stacks of ores into the river, carrying along with it the sediments in suspension. These suspended sediments were deposited in the estuary

causing elevated concentrations of Fe. Singh et al. (2014) found an increase in organic carbon and ferromagnetic minerals together with high sand content that suggested the possibility of more terrigenous input, which was reflected through increase in sedimentation rate. Veerasingam et al. (2015) also found polyhedral iron oxide particles in the sediments that are coarse grained iron particles of lithogenic origin derived from natural weathering processes. The transport of material from the Mandovi estuary to the Zuari estuary via the Cumbharjua canal has been reported earlier. Thus, coarse grained iron particles might have been present in the bulk sediments as discussed earlier. These lithogenic iron particles may have also constituted the residual fraction of the sediments. Thus, the higher Fe concentration in the bulk and residual phases may be due to these magnetic iron minerals. However, Singh et al. (2014) also reported the presence of fine grained ferrimagnetic minerals in mudflat sediments of the adjacent Mandovi estuary and stated that might have been derived from anthropogenic activities. Further, Veerasingam et al. (2015), studied sediment magnetic extracts of the mangrove sediments of the Mandovi estuary and found magnetic spherical iron oxides due to deposition of iron spherules from the atmosphere.

**3.1.E.1b Manganese**

Mn like Fe is a redox sensitive element and is biogeochemically reactive in the aqueous environment as it readily undergoes transformation between dissolved and particulate phases in response to physicochemical changes (Chester and Jickells, 2012). A large quantity of Mn was associated with the bioavailable fractions in the sediments of the Zuari estuary.

Mn concentrations in core S1 varied in the order of F3>F2>F1>F5>F4. Large quantity Mn was associated with the Fe-Mn oxide phase, which ranged from 1373 ppm to 2743 ppm (average 2165 ppm) that accounted for 24.75 % to 47.45 % (average 39.55 %). Considerable amount of Mn was associated with the carbonate bound phase ranging from 1413 ppm to 2728 ppm (average 1982 ppm) that accounted for 31.18 % to 49.19 % (average 36.23 %), while, Mn concentration in the exchangeable fraction ranged from 428.46 ppm to 760.35 ppm (average 600 ppm) that accounted for 7.60 % to 17.34 % (average 11.10 %). Following exchangeable Mn was associated with the residual phase with concentrations varying from 418 ppm to 538 ppm (average 469 ppm) that accounted for 7.33 % to 9.57 % (average 8.64 %). Mn was least associated with the organic / sulfide bound phase, in which the concentrations ranged from 185 ppm to 305 ppm (average 246 ppm) that accounted for 3.34 % to 5.28 % (average 4.48 %). In core S2, Mn concentrations varied in the order of

F3>F2>F1>F5>F4 similar to sediments in core S1. Highest Mn was associated with the Fe-Mn oxide phase, which ranged from 1298 ppm to 5798 ppm (average 3500 ppm) that accounted for 40.92 % to 66.86 % (average 56.36 %). Considerable amount of Mn was associated with the carbonate bound phase ranging from 568 ppm to 988 ppm (average 785.50 ppm) that accounted for 9.49 % to 25.44 % (average 14.28 %), while, Mn in the exchangeable fraction ranged from 481 ppm to 1102 ppm (average 756 ppm) that accounted for 9.36 % to 18.89 % (average 13.24 %). Following exchangeable Mn was associated with the residual phase with concentrations varying from 510 ppm to 715 ppm (average 628 ppm) that accounted for 7.58 % to 18.01 % (average 11.36 %). Mn was least associated with the organic / sulfide bound phase in which, the concentrations ranged from 128 ppm to 568 ppm (average 286 ppm) and accounted for 3.65 % to 6.54 % (average 4.76 %). Mn concentrations in the sediments core S3, varied in the order of F3>F5>F2>F1>F4. Mn was mainly associated with the Fe-Mn oxide phase, which ranged from 324 ppm to 1078 ppm (average 698 ppm) that accounted for 16.14 % to 37.04 % (average 28.39 %). Mn concentration in the residual phase varied from 453 ppm to 595 ppm (average 508 ppm) that accounted for 17.32 % to 29.18% (average 22.08 %). Considerable amount of Mn was associated with the carbonate bound phase ranging from 84.50 ppm to 774 ppm (average 487 ppm) that accounted for 4.50 % to 26.98 % (average 19.70 %), while Mn concentration in the exchangeable fraction ranged from 273 ppm to 898 ppm (average 484 ppm) that accounted for 10.79 % to 47.77 % (average 21.76 %). Mn was least associated with the organic/sulfide bound phase in which the concentrations ranged from 90.00 ppm to 318 ppm (average 195 ppm) and accounted for 4.79 % to 10.74 % (average 8.07 %). The concentration of Mn in core S4 collected from the lower estuary mangrove varied in the order of F5>F3>F2>F4>F1. Highest Mn in this core was associated with the residual phase ranging from 295 ppm to 505 ppm (average 418 ppm) that accounted for 26.39 % to 52.58 % (average 35.63 %) of total sediments considering the sum of the five fractions. Mn was largely available in the Fe-Mn oxide phase ranging from 175 ppm to 543 ppm (average 348 ppm) that accounted for 18.54 % to 40.78 % (average 28.79 %) of total sediments. Mn concentration in the carbonate fraction varied from 25.25 ppm to 496 ppm (average 263 ppm) that accounted for 4.50 % to 28.33 % (average 18.32 %) of total sediments. Mn in the organic/ sulfide bound fraction varied from 61.73 ppm to 228 ppm (average 150 ppm) that accounted for 7.69 % to 17.59 % (average 11.81 %) whereas Mn concentrations in the exchangeable fraction varied from 1.73 ppm to 178.43 ppm (average 83.85 ppm) that accounted for 0.31 % to 10.85 % (average 5.45 %).

Overall, the Fe-Mn oxide fraction was the main carrier phase (28.39 % to 56.36 %) for Mn in the sediments with highest concentrations in core S2. Considerable amounts of Mn were noted in the carbonate bound fraction (14.28 % to 36.23 %) with highest average concentrations in core S1, and in the exchangeable (5.45 % to 21.76 %) with highest average values in core S2. The concentration of Mn in the organic matter/ sulfide bound fractions was 4.48 % to 11.18 % with high average concentration in core S4. In all, a large quantity of Mn was associated with the first four extractable fractions of the sediments. Average Mn concentration in the residual fraction ranged from 8.64 % to 35.63 % with highest concentration in core S4.

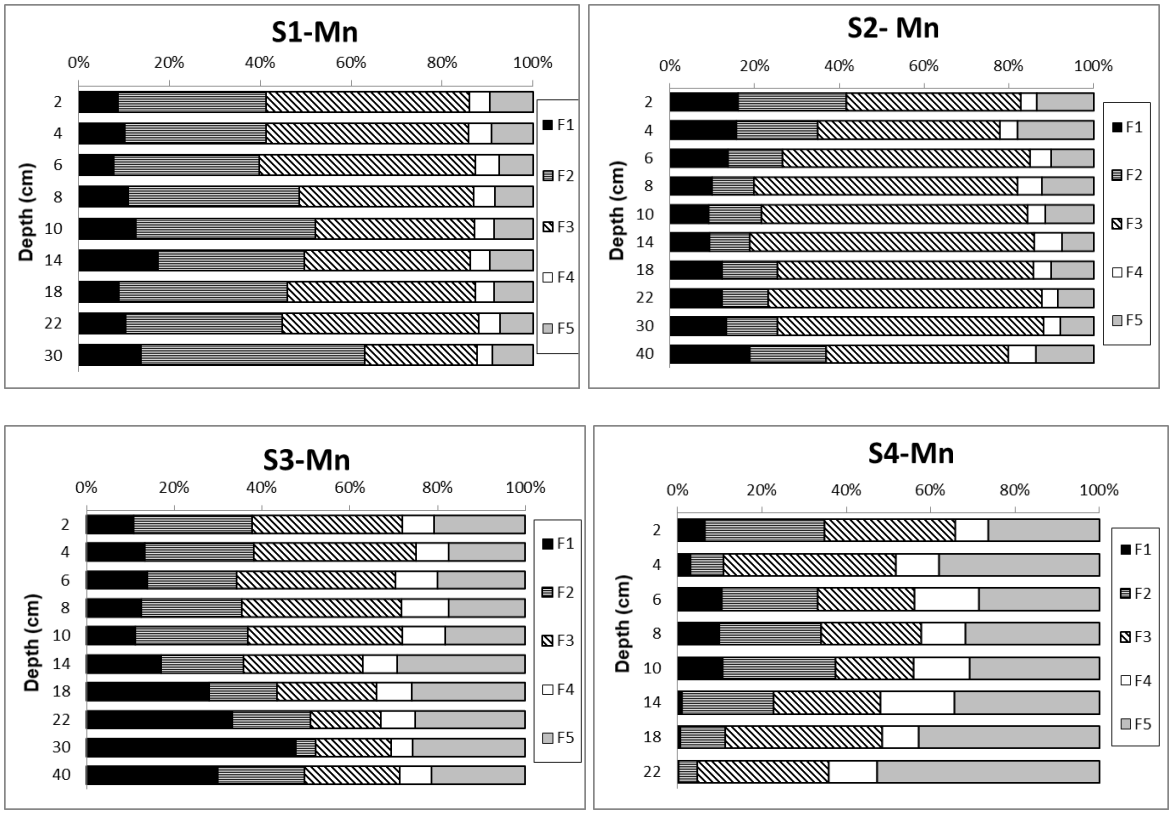


Figure 3.1.21: Speciation of Mn in cores S1, S2, S3 and S4.

The distribution of Mn with depth in the different phases of core S1 (Figure 3.1.21) showed Mn in exchangeable and carbonate bound fractions decreased towards the surface whereas the concentration in the Fe-Mn oxide phase increased. This distribution pattern indicated early diagenetic changes with a decrease in Fe-Mn oxide fraction at around 10 cm and remobilization and precipitation towards the surface as oxides. However, higher values of Mn in the exchangeable and carbonate fraction at depths 30 cm, 14 cm and 10 cm coincided with

Fe in the organic phase that may imply reductive dissolution of Fe and Mn. The distribution of Mn with depth in core S2 showed that the concentration of Mn in the Fe-Mn oxide phase increased up to 14 cm and further decreased towards the surface. Exchangeable and carbonate phases showed increase towards the surface and are available for biota as well as to diffuse to the water column. The peak in the exchangeable and carbonate phase at 40, 6 and 4 cm also correspond with the peaks of Fe in organic phase.

Large Mn variations with depth were in the five fractions in core S3. An important observation in the depth profile was that the concentration of Mn in the Fe-Mn oxide phase was low below 14 cm whereas Mn in the exchangeable phase was high which implies redox mobilization of Mn and re-precipitation towards the surface sediment layers. Mn in the carbonate phase showed increase towards the surface. In the distribution of Mn within the five fractions of core S4, Mn concentrations in the bioavailable fractions (sum of all four fractions) gradually increased towards the surface whereas Mn in the residual fractions decreased which indicated anthropogenic input of Mn. Near the surface exchangeable phase changed to Fe-Mn oxide phase allowing Mn to precipitate in high salinity zone.

Overall, the highest concentration of Mn in the Fe-Mn oxide phase was noted in the canal sediments. Highest concentrations in exchangeable and carbonate bound phases were noted in the lower middle estuary and the upper middle estuary respectively. Mn was mainly enriched in the Fe-Mn oxide bound phase as it readily forms oxides and oxyhydroxides. The carbonate fraction is a loosely bound phase and considerable quantity of Mn in the carbonate bound fraction is probably due to the similarity in ionic radii of Mn to that of calcium, which allows Mn to substitute for Ca in carbonate phase (Pedersen and Price, 1982; Zhang et al., 1988). Diagenetic modification of Mn species was observed as Manganese oxides were reduced in anoxic sediments at depth to the more soluble $Mn^{2+}$ form, which can enter the interstitial waters of the sediment (Beeftink and Rozema, 1988). The manganese enrichment seen in the younger sediments of the cores may be partly re-precipitated Mn2+, presumably in the form of insoluble oxides and hydroxides diffusing to the surface (Krupadam et al., 2006). The exchangeable phase contains loosely bound Mn, which can be easily desorbed. Mn was comparatively low in the organic/sulfide bound fraction due to weak affinity of Mn for organics (Young and Harvey, 1992) and the geochemical association of Mn as manganese oxide, manganese carbonate, organo-metallic complexes or manganese sulfide depends on

the prevailing redox condition, pH, salinity and presence of carbonate ions (Farias et al., 2007).

### 3.1. E.1c Chromium

A large quantity of Cr was associated with the residual phase in the sediments of Zuari estuary.

In core S1, Cr varied in the sequence of an abundance of F5>F4>F3>F1>F2. Large Cr concentration was found to be associated with the residual phase, which ranged from 157.95 ppm to 239.78 ppm (average 189 ppm) that accounted for 85.66 % to 89.56 % (average 87.50 %) of total sedimentary fractions. A considerable Cr concentration was found to be associated with the organic/ sulfide bound fraction, which ranged from 10.48 ppm to 14.00 ppm (average 12.92 ppm) that accounted for 4.82 % to 7.34 % (average 6.05 %) of total sediments. Cr in the Fe-Mn oxide bound fraction ranged from 9.35 ppm to 14.10 ppm (average 11.53 ppm) that accounted for 4.46 % to 7.10 % (average 5.39 %) while, a small fraction of Cr was associated with the exchangeable phase with concentrations ranging from 0.93 ppm to 2.08 ppm (average 1.38 ppm) that accounted for 0.48 % to 0.86 % (average 0.64 %). Traces of Cr were found in the carbonate bound phase with concentrations ranging from 0.78 ppm to 1.30 ppm (average 0.91 ppm) that accounted for 0.34 % to 0.72 % (average 0.43 %) of total sedimentary fractions. In the core S2 collected from the Cumbharjua canal mangrove, Cr distribution varied in the order of F5>F4>F3>F2<F1. Cr concentrations in the residual phase varied from 135.95 ppm to 207.28 ppm (average 171 ppm) that accounted for 84.24 % to 89.99 % (average 87.89 %) of the total sedimentary fractions. Cr concentration in the organic/sulfide phase ranged from 10.25 ppm to 12.60 ppm (average 11.24 ppm) that accounted for 4.98 % to 6.93 % (average 5.84 %) of the total sedimentary fractions while, Cr contents in the Fe-Mn oxide fraction ranged from 7.98 ppm to 17.20 ppm (average 9.87 ppm) that accounted for 4.01 % to 8.74 % (average 5.10 ppm). A small amount of Cr was associated with the carbonate bound fraction with concentrations ranging from 1.23 ppm to 1.45 ppm (average 1.34 ppm) that accounted for 0.61 % to 0.83 % (average 0.70 %) of the total of sedimentary fractions. Traces of Cr were found in the exchangeable phase with concentrations ranging from 0.48 ppm to 1.43 ppm (average 0.90 ppm) that accounted for 0.21 % to 0.67 % (average 0.47 %). In core S3, Cr concentrations varied in the order of abundance F5>F4>F3>F1>F2 similar to mangrove core S1. Large concentrations of Cr was associated with the residual phase which, varied between 157.10 ppm and 190.93 ppm

(average 178 ppm) that accounted for 79.12 % to 83.04 % (average 81.22 %) of the total of the five sedimentary fractions. Cr concentration in the organic / sulfide bound ranged from 20.18 ppm to 29.98 ppm (average 24.88 ppm) that accounted for 8.92 % to 13.10 % (average 11.36 %) while, Cr in the Fe-Mn oxide bound phase ranged from 9.23 ppm to 17.93 ppm (average 12.87 ppm) that accounted for 4.03 % to 8.85 % (average 5.92 %). Concentration of Cr in the exchangeable phase ranged from 1.58 ppm to 2.65 ppm (average 2.22 ppm) that accounted for 0.68 % to 1.23 % (average 1.02 %) while, Cr in the exchangeable fraction ranged from 0.75 ppm to 1.55 ppm (average 1.05 ppm) that accounted for 0.38 % to 0.77 % (average 0.48 %) of the sum of the five sedimentary fractions. The concentration of Cr in core S4 varied in the order F5>F3>F4>F2>F1 in the sediments. The concentration of Cr in the residual phase varied from 158.48 ppm to 209.68 ppm (average 187 ppm) that accounted for 84.50 % to 92.04 % (average 88.05 %) of the sum of the five sedimentary fractions. Following the residual phase, considerable amount of Cr was noted in the Fe-Mn oxide bound fraction with concentrations ranging from 9.78 ppm to 13.03 ppm (average 11.33 ppm) that accounted for 4.71 % to 6.04 % (average 5.37 %) of the sediments. The concentration of Cr in the organic/ sulfide bound fraction ranged between 4.15 ppm to 16.88 ppm (average 10.79 ppm) that accounted for 1.82 % to 8.37 % (average 5.21 %) whereas Cr in the carbonate bound fraction varied from 1.28 ppm to 2.45 ppm (average 1.75 ppm) that accounted for 0.66 % to 1.09 % (average 0.82 %). Cr was least available in the exchangeable fraction the concentrations which ranged from 0.23 ppm to 2.25 ppm (average 1.17 ppm) that accounted for 0.10 % to 1.00 % (average 0.55 %) of total sedimentary fractions.

Overall, major quantity of Cr was associated with the residual fraction followed by substantial amounts in the organic matter/ sulfide bound and Fe-Mn oxide bound fraction. The concentration of Cr in the residual phase varied from 81.22 % to 88.05 % with highest concentrations in core S4. Cr in the organic matter/ sulfide bound phase varied from 5.21 % to 11.36 % whereas, Fe-Mn oxide bound Cr concentrations varied from 5.10 % to 5.92 % with highest concentration in core S3, for both the fractions. Concentration of Cr in the exchangeable and carbonate bound fractions were below 1 % except for exchangeable Cr in core S3.

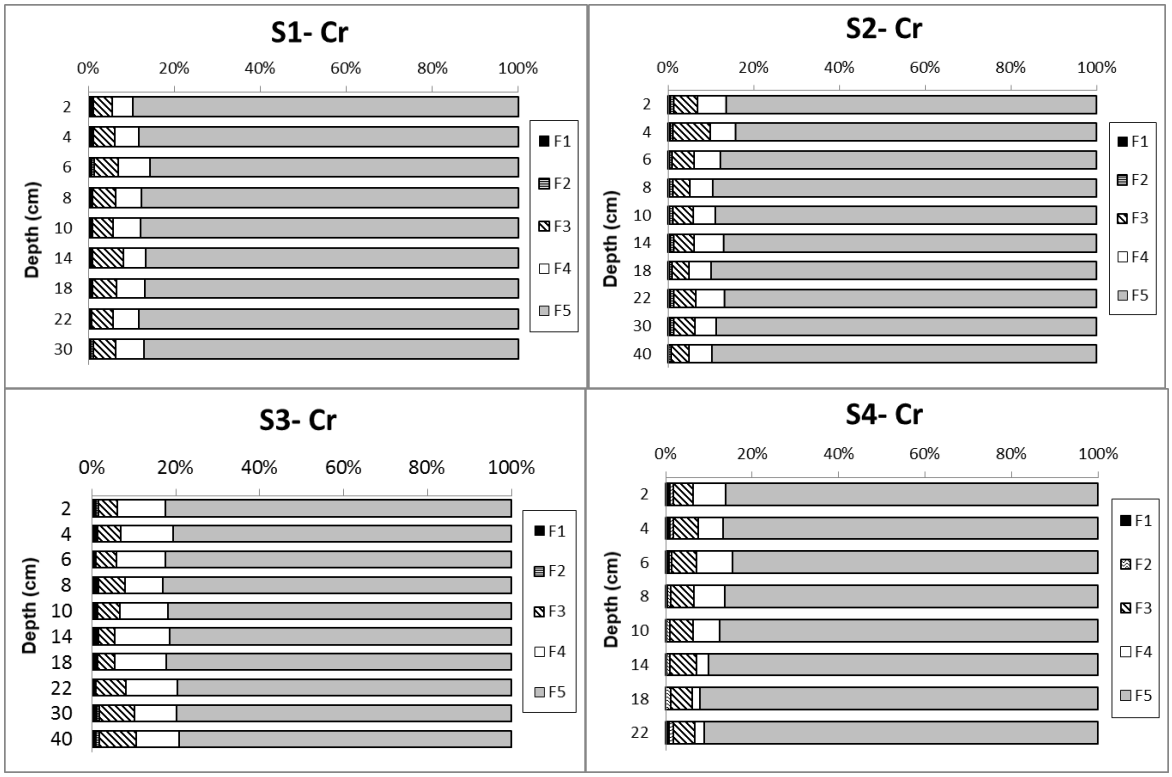


Figure 3.1.22: Speciation of Cr in cores S1, S2, S3 and S4.

In the distribution of Cr in core S1, the concentrations of Cr in the residual fraction showed little variations with depth. At depths 30 cm, 14 cm and 6 cm (Figure 3.1.22), higher concentrations of Cr was noted in the bioavailable fractions which corresponded to previously described peaks of Fe in the organic/sulfide fraction and Mn in the exchangeable and carbonate phases which may suggest redox mobilization of Cr along with Fe and Mn at these depths. The distribution of Cr with depth in the five fractions in core S2 showed that much of the Cr was associated with the residual phase and showed less variations with depth. Concentration in the bioavailable fractions showed minor enrichment in the surface layers (4 cm to 2 cm) which corresponded to high Mn in exchangeable and carbonate fractions. Thus, Mn may have affected the mobilization of Cr in the canal sediments. In core S3, Cr concentrations varied with decreasing trend of the bioavailable fractions towards the surface of the core. Concentrations of Cr in the F4 fraction was high at depths 18 and 14 cm with corresponding decrease in the Fe-Mn oxide bound fraction. Additionally, a similarity in the distribution of bioavailable phases of Cr to Fe was noted in the lower part of the core. Cr in the vertical distribution profiles in the five fractions of core S4, exhibited high concentrations in the residual phase. The concentration in the bioavailable fractions were increased towards

the surface along with Mn, which may suggest anthropogenic input of Cr and its association with Mn.

Overall, among the four cores, highest average concentration of Cr was in the residual fraction. Among the bioavailable fractions, Cr was higher in the exchangeable, Fe-Mn oxide and organic/sulfide bound fractions in the lower middle estuarine region. The higher percentage of bioavailable Cr in the lower middle estuarine region may be due to anthropogenic additions. Chromium was mainly associated with the residual phase and and hence considered to be held within the mineral matrix (Sharmin et al., 2010), therefore, it is interpreted that the concentration of Cr was largely controlled by the mineralogy and extent of weathering of source rocks. The residual fraction was followed by a considerable amount of the organic/sulfide bound fraction. Cr may have been bound to organic matter over sulfides because Cr (III) uptake by authigenic Fe-sulfides is very limited due to structural and electronic incompatibilities with pyrite and not known to form an insoluble sulfide (Huerta-Diaz and Morse, 1992; Morse and Luther, 1999). Reduced Cr (III) in anoxic sediments can easily bind to humic and fulvic acids. The concentration in the exchangeable and carbonate bound fractions was very less compared to the other three fractions.

**3.1.E.1d Cobalt**

Co in the sediments was found to be mainly associated with the residual fraction with considerable amounts in the Fe-Mn oxide and organic/ sulfide bound fractions. In mangrove core S1, the abundance of Co within the five fractions varied in the order F5> F3>F4>F1>F2. The Co concentration in the residual phase ranged from 24.10 ppm to 38.70 ppm (average 33.15 ppm) that accounted for 63.21 % to 73.54 % (average 69.00 %) of the total of the five sedimentary fractions. Co concentrations in the Fe-Mn oxide bound phase ranged from 7.43 ppm to 10.28 ppm (average 9.36 ppm) that accounted for 16.20 % to 24.19 % (average 19.73 %). A small quantity of Co was associated with the organic/ sulfide bound fraction varied between 2.85 ppm to 3.53 ppm (average 3.13 ppm) that accounted for 5.46 % to 8.35 % (average 6.62 %). Co in the exchangeable and carbonate fraction was very low, with exchangeable concentrations ranging from 0.48 ppm to 1.90 ppm (average 1.16 ppm) that accounted for 0.92 % to 3.70 % (average 2.42 %) whereas Co concentration in the carbonate bound fraction varied between 0.73 ppm to 1.55 ppm (average 1.08 ppm) that accounted for 1.49 % to 3.01 % (average 2.23 %). Co content in the sedimentary fractions in core S2 varied in the order F5>F3>F4>F1>F2. Co concentrations in the residual fraction varied between

17.45 ppm to 30.23 ppm (average 24.20 ppm) that accounted to 53.04 % to 66.60 % (average 61.27 %). Co content in the Fe-Mn oxide bound fraction ranged from 8.08 ppm to 12.78 ppm (average 10.82 ppm) that accounted for 22.52 % to 34.57 % (average 27.67 %). Minor amounts of Co were associated with the organic/ sulfide bound, exchangeable and carbonate bound fractions. Concentrations in the organic/sulfide bound fractions ranged from 1.95 ppm to 2.93 ppm (average 2.28 ppm) that accounted for 4.61 % to 7.57 % (average 5.88 %) whereas Co in the exchangeable fractions ranged from 0.60 ppm to 1.70 ppm (average 1.04 ppm) that accounted for 1.70 % to 4.11 % (average 2.63 %). Cr concentrations in the carbonate bound fractions ranged from 0.25 ppm to 1.43 ppm (average 1.00 ppm) that accounted for 0.65 % to 3.44 % (average 2.55 %) of the total of sedimentary fractions. The concentration of Co with the five sedimentary fraction in core S3, varied in the order of F5>F3>F4>F1>F2. Co content was highest in the residual fraction and ranged from 27.88 ppm to 37.08 ppm (average 33.80 ppm) that accounted for 66.69 % to 78.59 % (average 73.76 %). Co in the Fe-Mn oxide fraction ranged from 5.18 ppm to 7.08 ppm (average 5.94 ppm) that accounted for 10.97 % to 14.07 % (average 12.97 %). Concentrations of Co in the organic/sulfide bound fraction ranged from 1.95 ppm to 3.63 ppm (average 2.65 ppm) that accounted for 4.16 % to 7.78 % (average 5.78 %). The concentrations of Co were low in the exchangeable fraction that ranged from 0.95 ppm to 3.23 ppm (average 2.11 ppm) and accounted for 2.01 % to 7.72 % (average 4.62 %). Co concentrations in the carbonate bound fraction ranged from 0.90 ppm to 1.70 ppm (average 1.32 ppm) that accounted for 2.06 % to 3.83 % (average 2.87 %). In core S4, Co concentrations varied in the order of abundance F5>F3>F2>F1>F4. The concentration of Co in the residual phase varied from 19.65 ppm to 31.75 ppm (average 24.98 ppm) that accounted for 67.41 % to 78.05 % (average 71.81 %) of the total of sedimentary fractions. Co in the Fe-Mn oxide fraction ranged between 4.28 ppm and 5.15 ppm (average 4.66 ppm) that accounted for 11.97 % to 15.18 % (average 13.59 %). The concentration of Co in the carbonate bound fraction varied from 2.08 ppm to 2.85 ppm (average 2.41 ppm) that accounted for 5.47 % to 9.78 % (average 7.12 %) whereas Co concentrations in the exchangeable fraction ranged from 0.60 ppm to 2.43 ppm (average 1.63 ppm) that accounted for 1.61 % to 7.72 % (average 4.74 %). The least amount of Co in this core was associated with the organic/sulfide bound fraction that varied between 0.33 ppm and 1.53 ppm (average 0.98 ppm) that accounted for 1.10 % to 4.48 % (average 2.74 %).

In general, the concentrations of Co varied in the order of F5>F3>F4>F1>F2. Further, the Co content in the residual phase varied from 61.27 % to 73.76 %, with highest concentrations in

core S3. Co in the Fe-Mn oxide phase varied from 12.97 % to 27.67 % with highest content in core S2. The organic matter/ sulfide bound Co concentrations varied from 2.74 % to 6.62 %, highest being in core S1. Co in the exchangeable bound fractions were less that ranged between 1.04 % to 2.11 % highest being in core S3 while carbonate bound Co content varied between 1.00 % to 2.41 %, highest being in core S4.

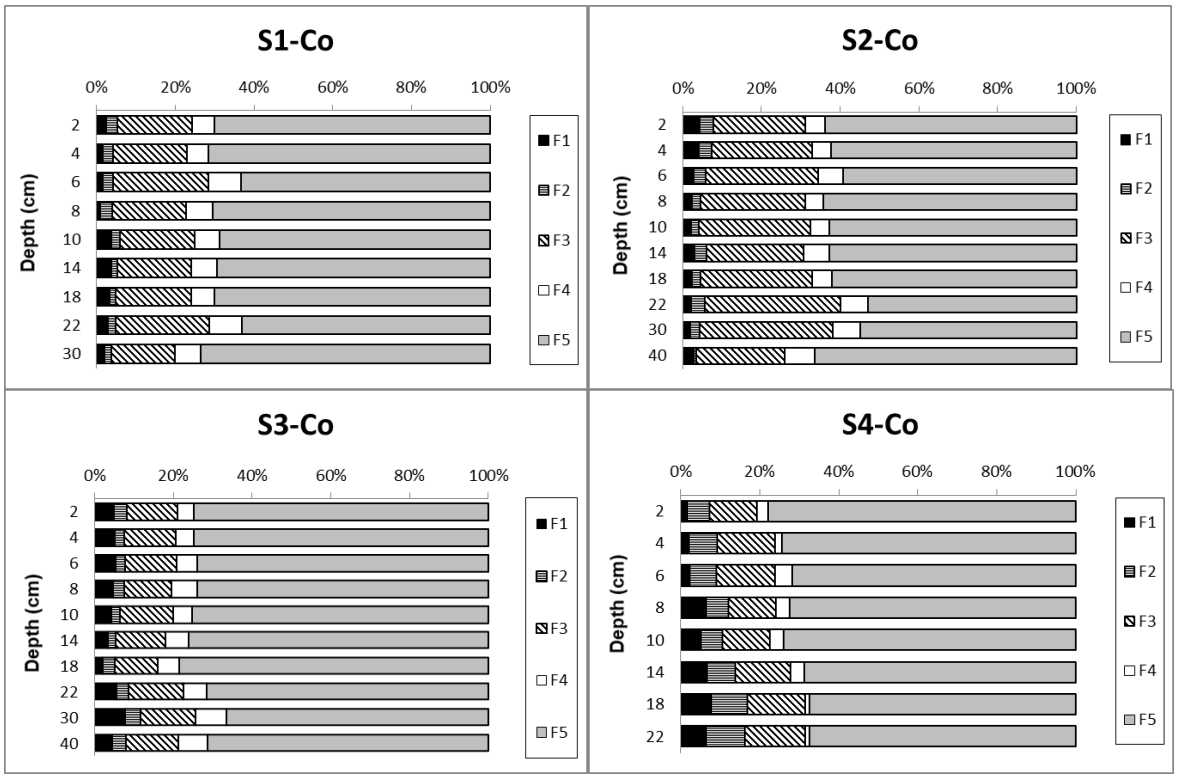


Figure 3.1.23: Speciation of Co in cores S1, S2, S3 and S4.

In the distribution of Co in the five sedimentary fractions with depth (Figure 3.1.23) of core S1 showed that the dominant phase for Co, in the residual phase, which was relatively constant with depth except at 22 cm and 6 cm, and was compensated by higher percentages of bioavailable Co mainly due to the Fe-Mn oxide bound fraction. An increase in the exchangeable fraction was observed from the base of the core up to 10 cm, which corresponded to the profile of Mn in core S1 and indicated diagenetic mobilization of Co and co-precipitation towards the surface along with Mn oxides which was noted around 6 cm. In core S2, the distribution of Co with in the five fractions showed large quantity in the residual phase, throughout the core depth with considerable amounts in the Fe-Mn oxide bound fraction. Co in the exchangeable and carbonate bound fractions increased towards the surface whereas that in the Fe-Mn oxide exhibited a minor decrease. This distribution pattern was

synonymous with the Mn speciation profile and indicated diffusion of the mobilized Co along with Mn to the water column. In the distribution of Co with depth in core S3, the dominant geochemical phase was the residual phase throughout the depth of the core. The concentration of Co in the bioavailable fractions was noted to be higher at depths from 40 cm to 22 cm, which was mainly attributed to the exchangeable, carbonate and organic/ sulfide phases. The distribution of Co in the bioavailable phases corresponds to Fe and Mn at depths from 40 cm to 22 cm that indicated diagenetic enrichment of Co along with Fe and Mn. In the lower estuary core S4, the concentration of Co was mainly associated with the residual phase, which increased towards the surface from the base of the core indicating the increased input of terrestrial derived Co in recent times. Unlike the mangrove cores of S1, S2 and S3 the profile of Co exhibited no similarities to the profile of Fe and Mn in core S4. Co in the bioavailable fractions decreased towards the surface. A high amount of Co in the exchangeable phase and carbonate phase was noted between depths 22 cm to 8 cm.

Among the four locations, the highest percentage of Co in the residual phase was found in all the locations. Fe-Mn oxide bound Co was high at core S3, organic/ sulfide bound Co at cores S1 and S2, and exchangeable and carbonate bound Co at cores S3 and S4.

The sequential extraction results of Co suggest that Fe-Mn oxides may have been the main carriers of bioavailable Co in the estuary. The mobilization of Co occurs under anoxic conditions when Fe-Mn oxides in deeper sediments dissolve and migrate upwards in the sedimentary column and gets re-precipitated with Fe and Mn as oxides when the conditions become oxic (Petersen et al., 1997). Under oxic conditions, Co co-precipitates with carbonates and/or adsorption on organic matter and freshly formed hydrous ferric oxides (Choque et al., 2013). The high content of Co in the residual fraction indicated that large quantity of Co was derived from terrestrial rocks.

### 3.1. E.1e Copper

The sequential extraction of Cu into five geochemical phases revealed that large quantity of Cu in the sediments was mainly associated with the residual phase. In core S1, the concentration of Cu varied in the order F5>F4>F3>F2>F1. Cu was found to be mainly associated with the residual phase with concentration ranging from 54.48 ppm to 146.23 ppm (average 73.79 ppm) that accounted for 63.38 % to 85.89 % (average 71.21 %) of the total of the five sedimentary fractions. Among the bioavailable fractions, Cu was largely associated

with the organic / sulfide bound fraction with concentrations ranging from 16.98 ppm to 28.43 ppm (average 22.25 ppm) that accounted for 10.91 % to 29.84 % (average 23.10 %). Cu concentration in the Fe-Mn oxide bound fraction ranged from 1.68 ppm to 3.70 ppm (average 2.74 ppm) that accounted for 1.53 % to 3.71 % (average 2.79 %). The concentration of Cu in the carbonate bound fraction ranged from 1.20 ppm to 2.10 ppm (average 1.56 ppm) that accounted for 0.90 % to 1.97 % (average 1.60 %). Least Cu was associated with the exchangeable fraction with concentrations ranging from 1.15 ppm to 1.35 ppm (average 1.26 ppm) that accounted for 0.78 % to 1.70 % (average 1.30 %) of the total of sedimentary fractions. The concentrations of Cu in core S2 sediments varied in the order of abundance F5>F4>F3>F1>F2. The residual fraction was the main carrier for Cu in the sediments with concentrations ranging from 49.50 ppm to 146.73 ppm (average 85.23 ppm) that accounted for 73.96 % to 90.89 % (average 82.68 %) of the total of the five sediment fractions. The organic/sulfide bound Cu concentration ranged between 9.23 ppm to 13.58 ppm (average 11.18 ppm) that accounted for 5.91 % to 20.28 % (average 12.27 %). The Fe-Mn oxide bound, exchangeable and carbonate bound fractions constituted for a minor amount of the bioavailable Cu. The concentration of Cu in the Fe-Mn oxide bound fraction ranged from 1.90 ppm to 2.63 ppm (average 2.17 ppm) that made up for 1.49 % to 3.09 % (average 2.35 %) whereas Cu in the exchangeable fraction ranged from 0.90 ppm to 2.43 ppm (average 1.35 ppm) that accounted for 0.78 %to 2.57 % (average 1.46 %) of the total of the sedimentary fractions. Cu was least available in the carbonate bound phase with concentration ranging from 0.78 ppm to 1.23 ppm (average 1.13 ppm) that accounted for 0.69 % to 1.65 % (average 1.23 %). In core S3, the abundance of Cu in the five geochemical fractions varied in the order F5> F4> F3> F1>F2. The concentration of Cu in the residual phase varied from 52.93 ppm to 73.58 ppm (average 59.02 ppm) that accounted for 72.20 % to 82.58 % (average 79.13 %) of the total of the five sedimentary fractions. Cu in the organic/sulfide bound phase varied from 8.98 ppm to 16.60 ppm (average 12.46 ppm) and accounted for 13.51 % to 22.65 % (average 16.64 %). A very small quantity of Cu was associated for the Fe-Mn oxide, exchangeable and carbonate bound phases. The concentration of Cu in the Fe-Mn oxide bound fraction ranged between 0.95 ppm and 1.88 ppm (average 1.37 ppm) that accounted for 1.33 % to 2.39 % (average 1.83 %) whereas the exchangeable fraction of Cu ranged from 0.58 ppm to 1.50 ppm (average 0.89 ppm) that accounted for 0.62 % to 2.10 % (average 1.22 %) of the total of the five sedimentary fractions. The concentration of Cu in the carbonate bound fraction ranged from 0.65 ppm to 1.15 ppm (average 0.87 ppm) that accounted for 0.95 % to 1.61 % (average 1.18 %) of the total sedimentary fractions. In core S4, collected from the lower

estuarine mangrove, Cu in the five geochemical fractions varied in the order F5>F4>F2>F1>F3. Major portion of Cu in the sediments was associated with the residual fraction with concentrations ranging from 25.75 ppm to 55.15 ppm (average 37.87 ppm) that accounted for 80.79 % to 90.38 % (average 85.36 %). A considerable amount of Cu was associated with the organic/sulfide bound fraction wherein concentrations ranged from 0.95 ppm to 6.63 ppm (average 3.58 ppm) that accounted for 3.22 % to 12.12 % (average 7.63 %). Cu in the carbonate fraction ranged from 1.18 ppm to 1.58 ppm (average 1.29 ppm) that accounted for 1.87 % to 5.34 % (average 3.18 %). The concentration of Cu in the exchangeable phase ranged from 0.48 ppm to 2.38 ppm (average 1.09 ppm) that accounted for 1.04 % to 4.84 % (average 2.42 %) and concentrations in the Fe-Mn bound phased ranged from 0.35 ppm to 1.20 ppm (average 0.63 ppm) that accounted for 1.07 % to 1.91 % (average 1.40 %).

Overall, Cu followed the order of abundance of F5>F4>F3>F2>F1 in most of the cores. Further, Cu in the residual fraction varied from 71.21 % to 85.36 % highest being in core S4. The organic matter/ sulfide bound Cu varied from 7.63 % to 22.10 %, highest being in core S1. Fe-Mn oxide bound Cu content ranged from 1.40 % to 2.79 % with highest concentrations in core S1. Low concentration if Cu was found in the exchangeable and carbonate fractions. Cu in the carbonate fraction varied from 0.87 % to 1.56 % with highest concentrations in core S1, while, the concentration of Cu in the exchangeable fraction ranged from 0.89 % to 1.35 %, with highest content in core S2.

In the distribution of Cu with depth (Figure 3.1.24) in core S1, the concentration of Cu in the residual phase was high at the surface than deeper sediment layers. Most of the bioavailable Cu was associated with the organic/sulfide bound fraction, which showed higher concentrations in the deeper anoxic sediments. A peak in the organic/ sulfide bound Cu was noted at 8 cm which corresponded to the enrichment of Fe in the organic/ sulfide bound phase at the same depth. Under oxic conditions, a significant fraction of Cu reaching the sediment surface may diffuse to the overlying water column by mineralization of the host organic material at the surface (Choque et al., 2013). Concentrations of Cu in the Fe-Mn oxide bound, carbonate bound and exchangeable fractions were very low and did show much variations with depth.

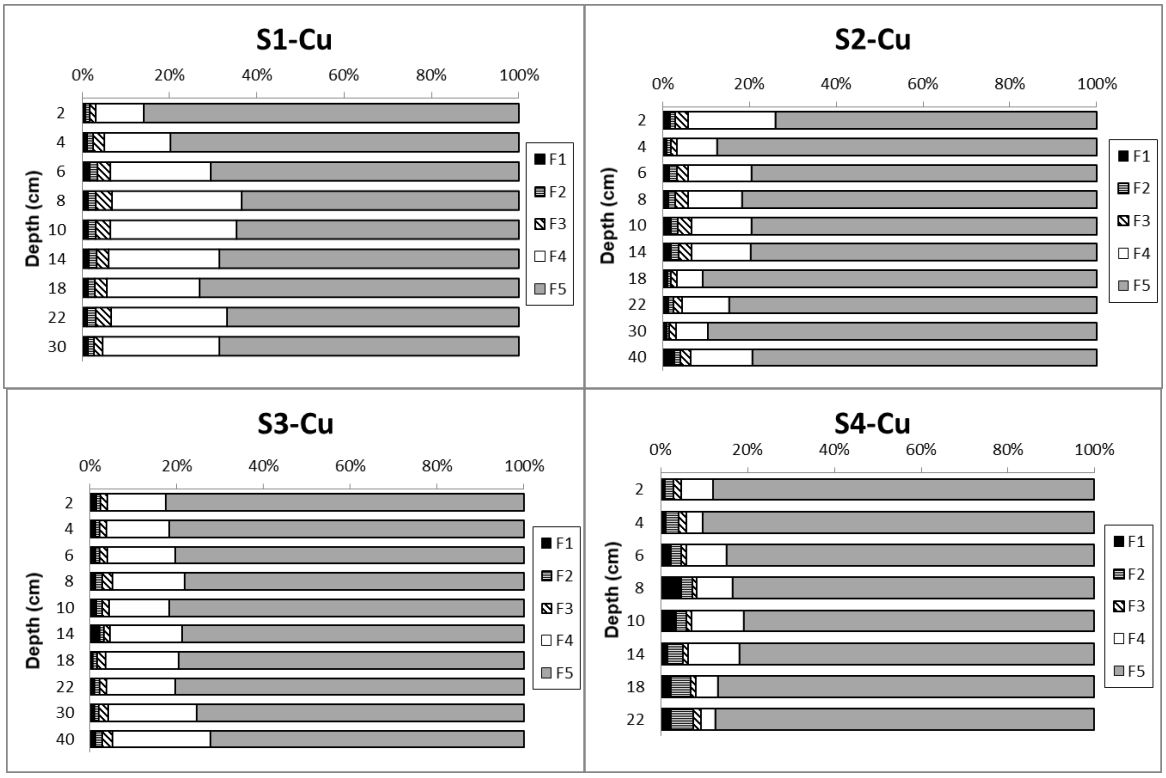


Figure 3.1.24: Speciation of Cu in cores S1, S2, S3 and S4.

The distribution of Cu with depth in the five geochemical fractions of core S2 revealed that the concentration in the residual phase was higher in the lower section of the core (30 cm to 18 cm) followed by a decrease towards the surface except at 4 cm. The concentration of Cu in the bioavailable fractions was mainly attributed to the organic/sulfide bound fraction, which decreased from the base of the core up to 18 cm. Followed by higher concentrations towards the surface (except at 4 cm). Higher Fe in organic/sulfide phase was also noted at depths at 40 cm, 6 cm, and 4 cm, which indicated the presence of sulfides at those depths. In the distribution of Cu with depth in core S3, the concentration of Cu in the residual phase increased from the base of the core towards the surface with a corresponding decrease in the bioavailable fractions. The increase in residual Cu indicated the input of detrital weathered material. The organic/sulfide fraction of Cu accounted for most of the bioavailable fractions. The high concentrations of organic/ sulfide bound Cu in the lower core may be due to the formation of insoluble Cu sulfides under anoxic conditions which decrease towards the surface oxic layers. The high concentrations in the lower layers (40 cm to 30 cm) corresponded to enriched Fe in the organic/ sulfide bound fraction at the same depths. The decrease in the organic matter bound Cu towards the surface may also be due to diffusion of Cu to the water column. The distribution of Cu with depth in core S4, large quantity of Cu

was associated with the residual fraction throughout the depth profile. The concentrations of Cu in the residual fraction decreased up to 10 cm and followed by increase towards the surface indicating lithogenic input of Cu to the recent sediments. The concentration of Cu in the organic/sulfide phase was noted to increase from the base of the core up to 10 cm followed by decrease towards the surface. The peak at 10 cm indicated formation of Cu sulfides. The low concentration of organic matter bound Cu towards the surface indicated diffusion into the water column. The enrichment of Cu with the carbonate bound fraction in the lower part of the core (22 cm to 14 cm) was possibly due to the presence of large amount of calcareous material.

Most of the bioavailable Cu in the sediments was bound to the organic matter fraction that indicated Cu in the sediment was less mobile. Copper easily forms complexes with organic matter due to the stability constant of organic Cu compounds, and is mainly transported towards the sediment surface in association with a biogenic carrier phase (Callender and Bowser, 1980; Collier and Edmond, 1984). Copper has a high affinity to humic substances (Pempkowiase et al., 1999). Under oxidizing conditions at the sediments-water interface, most of the organic bound Cu is mobilized releasing Cu into the dissolved phase. Some of this Cu migrates downward and get incorporated into sediment, but most of it gets recycled back into water column (Klinkhammer et al., 1986; Faragallah and Khalil, 2009) which explains the lower concentration of bioavailable Cu towards the surface.

### 3.1. E.1.f Zinc

Zinc in the sediments was found to be largely associated with the residual and Fe-Mn oxide bound fractions. In core S1, the concentration of Zn in the five fractions varied in the order F5>F3>F4>F2>F1. The concentration of Zn in the residual phase varied from 63.50 ppm to 103 ppm (average 76.72 ppm) that accounted for 58.26 % to 76.58 % (average 69.73 %). Among the bioavailable fractions, Zn was enriched in the Fe-Mn oxide fraction with concentration ranging from 13.60 ppm to 30.08 ppm (average 21.26 ppm) that accounted for 14.34 % to 27.59 % (average 19.32 %). The concentrations of Zn in the organic/sulfide bound phase ranged from 8.38 ppm to 12.13 ppm (average 9.69 ppm) that accounted for 6.63 % to 11.12 % (average 8.89 %). Zn concentrations in the carbonate fraction varied between 0.95 ppm and 2.60 ppm (average 1.64 ppm) that accounted for 0.92 % to 2.25 % (average 1.48 %) whereas Zn in the exchangeable fraction ranged from 0.50 ppm to 0.85 ppm (average

0.61 ppm) that accounted for 0.42 % to 0.78 % (average 0.56 %). In core S2 collected from the Cumbharjua canal, the concentration of Zn in the five fractions varied in the order F5>F3>F4>F2>F1. A large quantity of Zn was associated with residual phase, which ranged from 40.25 ppm to 73.83 ppm (average 61.42 ppm) that accounted for 70.00 % to 79.04 % (average 74.50 %). Among the bioavailable fractions, highest concentrations were noted in the Fe-Mn oxide bound phase wherein Zn ranged from 8.98 ppm to 17.05 ppm (average 12.73 ppm) that accounted for 12.54 % to 18.96 % (average 15.40 %). Considerable amount of Zn was available in the organic/ sulfide bound phase with concentrations ranging from 4.90 ppm to 8.80 ppm (average 6.07 ppm) that accounted 5.53 % to 10.58 % (average 7.49 %) of the total of the sedimentary fractions. Zn in the carbonate bound fraction ranged from 0.85 ppm to 2.10 ppm (average 1.37 ppm) that accounted for 0.89 % to 2.32 % (average 1.68 %) whereas concentration in the exchangeable fraction varied from 0.43 ppm to 2.18 ppm (average 0.75 ppm) and accounted for 0.51 % to 2.14 % (average 0.92 %). The, concentration of Zn varied in the order of F5>F3>F4>F2>F1 in core S3 collected from the lower middle estuarine region. The concentration of Zn in the residual phase ranged from 56.93 ppm to 109 ppm (average 85.64 ppm) that accounted for 71.34 % to 82.60 % (average 78.20 %). The concentration of Zn in the Fe-Mn oxide bound fraction ranged from 9.10 ppm to15.55 ppm (average 13.33 ppm) that accounted for 10.38 % to 11.61 % (average 12.48 %). Considerable amount of Zn was associated with the organic/sulfide bound phase with concentrations ranging from 4.73 ppm to 9.70 ppm (average 6.67 ppm) that accounted for 0.71 % to 2.67 % (average 1.56 %) of the total of the sediment fractions. Zn concentrations in the carbonate bound fraction ranged from 0.80 ppm to 3.13 ppm (average 1.69 ppm) that accounted for 0.71 % to 2.67 % (average 1.56 %) whereas concentrations in the exchangeable fractions ranged from 0.68 ppm to 2.45 ppm (average 1.21 ppm) that accounted for 0.57 % to 2.59 % (average 1.19 %). In core S4, the concentration of Zn in the five fractions varied in the order of F5>F3>F1>F4>F2. Zn was found to be highest in the residual phase with concentration ranging from 31.58 ppm to 79.10 ppm (average 49.72 ppm) that accounted for 66.54 % to 79.08 % (average 73.49 %) of the total of the five sedimentary fractions. The concentration of Zn in the Fe-Mn oxide fraction ranged from 5.15 ppm to 17.30 ppm (average 10.58 ppm) that accounted for 12.64 % to 19.00 % (average 15.34 %). Considerable amount of Zn was available in the exchangeable fraction with concentrations ranging from 0.23 ppm to 11.70 ppm (average 3.99 ppm) that accounted for 0.47 % to 13.74 % (average 5.09 %). The concentration of Zn in the organic/sulfide phase varied between 1.10 ppm to 3.28 ppm (average 2.34 ppm) that accounted for 2.68 % to 4.02 % (average 3.41 %) whereas

concentration in the carbonate bound fraction ranged from 0.95 ppm to 2.55 ppm (average 1.63 ppm) that accounted for 1.32 % to 4.88 % (average 2.66 %).

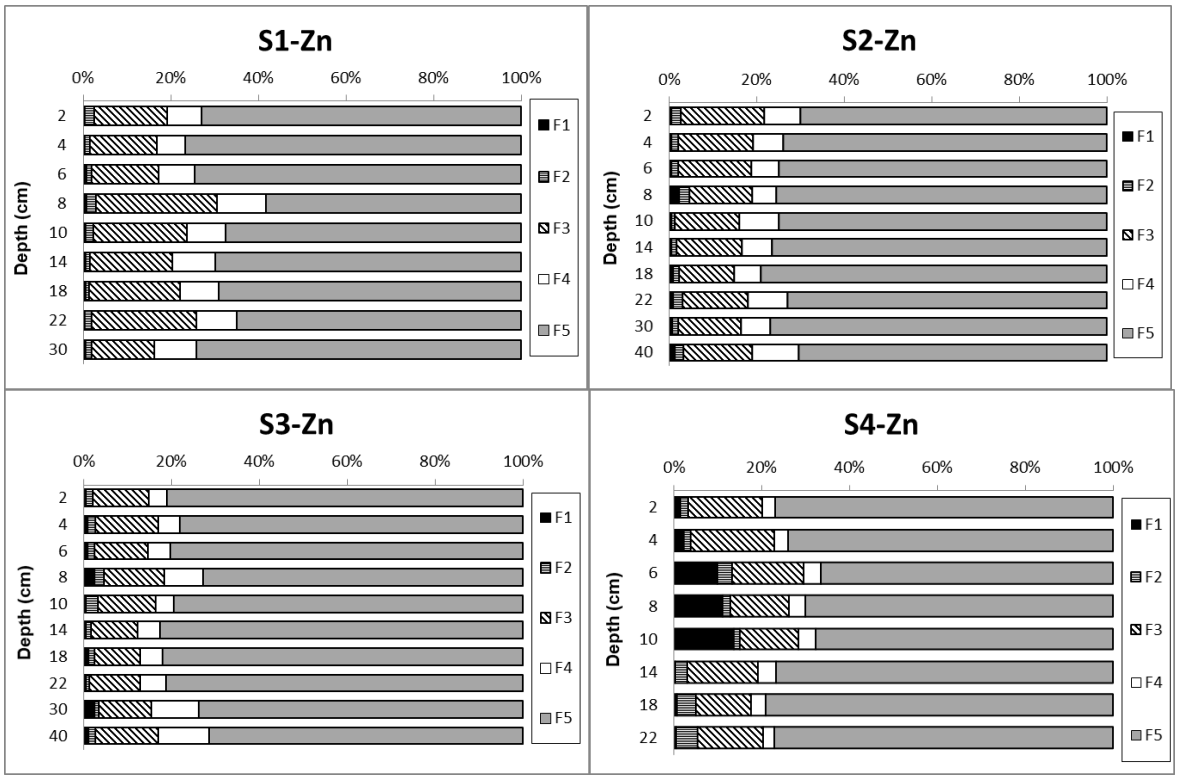


Figure 3.1.25: Speciation of Zn in cores S1, S2, S3 and S4.

Overall, Zn followed the order of abundance of F5>F3>F4>F2>F1 in most of the cores. Further, Zn in the residual fraction varied from 69.73 % to 78.20 %, highest being in core S3. Zn content in the Fe-Mn oxide bound phase varied from 12.48 % to 19.32 % with highest content noted in core S1 and organic matter/sulfide bound Zn ranged from 3.41 % to 8.89 %, highest being in core S2. Low amount of Zn was associated with the carbonate and exchangeable fractions. Zn content in the carbonate bound fraction varied from 1.48 % to 2.66 % while Zn in the exchangeable fraction ranged from 0.56 % to 5.09 %, highest concentrations for both fractions being in core S4.

The profile of Zn with depth in the five geochemical fractions is presented in figure 3.1.25. In core S1, Zn was mainly associated with the residual phase, which decreased from the base of the core up to 8 cm, followed by an increase towards the surface. The distribution of Zn in the bioavailable fractions exhibited peaks at 22 cm and 8 cm that corresponded to the profile of bioavailable Co (22 cm and 6 cm) which may indicate a common source for Co and Zn. The

Fe-Mn oxide bound fraction of Zn accounted for most of the bioavailable fraction with depth. The distribution of Zn in the Fe-Mn oxide bound fraction increased from bottom to 8 cm followed by decrease towards the surface, which was similar to the vertical distribution of Fe-Mn oxide bound Mn. This indicated that Zn was affected by the redox cycle of Mn. Zn in the organic / sulfide bound fraction exhibited lower concentrations above 8 cm, which suggested diffusion of organic bound Zn into the water column. The concentration of Zn in the exchangeable and carbonate bound fractions were negligible as compared to the other three fractions. In the distribution of five fractions of core S2, large quantity of Zn was associated with the residual phase. The concentration of Zn in the residual fraction exhibited an increase up to 18 cm followed by a decrease towards the surface. The distribution trend of residual Zn exhibited similar to residual Fe. The concentration of Zn in the Fe-Mn oxide phase accounted for most bioavailable Zn, which showed higher concentrations towards the surface similar to Fe-Mn oxide bound Fe. Considerable amount of Zn was associated the organic/ sulfide bound phase which showed higher concentrations between 40 and 22 cm. The distribution of Zn in core S3 exhibited an increase in the residual fraction towards the surface with fluctuations. The bioavailable Zn exhibited higher concentrations in the deeper sediments followed by decrease up to 14 cm and enrichment around 8 cm. The distribution pattern was similar to the bioavailable fractions of Fe and Mn. The Fe-Mn oxide and organic matter /sulfide bound fractions accounted for most of the variations of the bioavailable fractions. The distribution of Zn in the Fe-Mn oxide bound fraction was similar to the Fe-Mn oxide bound fraction of Mn whereas the distribution of the Zn in the organic matter/ sulfide bound fraction was similar to the organic/ sulfide fraction of Fe. The concentration of Zn in the carbonate and exchangeable fraction was found to be negligible as compared to the other three fractions. The distribution of Zn in the five fractions of core S4 revealed that large quantity of Zn was associated with the residual phase throughout the depth profile. The concentration of residual Zn decreased up to 6 cm from the base of the core followed by an increase towards the surface. The distribution of the bioavailable fractions of Zn with high concentrations between 14 cm and 4 cm, exhibited a similar pattern to the distribution of bioavailable Co and Mn. Between 14 cm and 4 cm, a prominent increase in the exchangeable fraction of Zn was noted which was also observed in the profiles of exchangeable Cu and Mn.

A large quantity of Zn was associated with the immobile residual fraction indicating that its major source was of detrital origin. The dominant bioavailable content of Zn was bound to the Fe-Mn (III) oxides. The Zn bound to the Fe-Mn oxides fraction had significant

association with reducible Mn and reducible Fe concentrations (Fe-Mn oxides), suggesting that Fe-Mn oxides may be the main carriers of Zn from the fluvial environment to the estuaries (Krupadam et al., 2006). Li et al. (2000) reported earlier that hydrous oxides of Fe and Mn are significant carriers for Zn in aquatic systems as the Zn adsorption onto these oxides has higher stability constants than onto carbonates (Turki, 2007).

### 3.1.E.2 Mudflats

The average values of metal concentrations in the five fractions of mudflat cores are presented in table 3.1.10 and their respective ranges are described in the text below.

### 3.1. E.2a Iron

The concentration of Fe in mudflat core M1 varied in the order of F5>F3>F4>F1>F2. The residual phase constituted major concentrations, which ranged from 63130 ppm to 73865 ppm (average 67142 ppm) that accounted for 85.82 % to 90.08 % (average 87.72 %) of the total of the sedimentary fractions (Table 3.1.10). The Fe-Mn oxide phase also accounted for considerable quantity of Fe with concentrations that ranged from 5940 ppm to 9642 ppm (average 7895 ppm) that accounted for 8.48 % to 11.20 % (average 10.29 %). The concentration of Fe in the organic/sulfide phase varied from 823 ppm to 2510 ppm (average 1498 ppm) that accounted for 1.07 % to 3.34 % (average 1.94 %) and concentrations in the exchangeable phase ranged from 17.15 ppm to 79.73 ppm (average 35.29 ppm) that accounted for 0.02 % to 0.11 % (average 0.05 %). Fe was least concentrated in the carbonate fraction wherein it varied between 0.36 ppm and 11.03 ppm (average 5.44 ppm) that accounted for 0.001 % and 0.02 % (average 0.01 %). In core M3, the concentration of Fe varied in the order of F5>F3>F4>F1>F2. The concentration of Fe in the residual fraction varied from 69318 ppm to 84723 ppm (average 79733 ppm) that accounted for 90.31 % to 93.20 % (average 92.20 %) of the total of the sedimentary fractions. This was followed by considerable amount of Fe in the Fe-Mn oxide bound fraction, which ranged from 4933 ppm to 6795 ppm (average 5757 ppm) that accounted for 6.14 % to 7.65 % (average 6.65 %). The concentration of Fe in the organic matter/ sulfide bound fractions varied from 476 ppm to 2320 ppm (average 943 ppm) that accounted for 0.56 % to 2.52 % (average 1.07 %). Fe in the exchangeable fraction ranged from 25.00 ppm to 94.03 ppm (average 60.55 ppm) that accounted for 0.03 % to 0.10 % (average 0.07 %) whereas concentration in the carbonate bound fraction ranged from 0.48 ppm to 26.25 ppm (average 9.80 ppm) that accounted for 0.001 % to 0.03 % (average 0.01 %).

Table 3.1.10: Average concentrations of metals in the five sedimentary fractions in the mudflat cores M1, M3 and M4.

| | | Exchangeable | | Carbonate | | Fe-Mn oxide | | Organic/Sulfide | | Residual | |
|---|---|---|---|---|---|---|---|---|---|---|---|
| | | (ppm) | (%) | (ppm) | (%) | (ppm) | (%) | (ppm) | (%) | (ppm) | (%) |
| Fe | M1 | 35.29 | 0.05 | 5.44 | 0.01 | 7895 | 10.29 | 1498 | 1.94 | 67142 | 87.72 |
| | M3 | 60.55 | 0.07 | 9.80 | 0.01 | 5757 | 6.65 | 943 | 1.07 | 79733 | 92.20 |
| | M4 | 97.39 | 0.20 | 22.26 | 0.04 | 4478 | 8.48 | 310 | 0.66 | 54751 | 90.62 |
| Mn | M1 | 757 | 13.71 | 1409 | 25.18 | 2366 | 42.06 | 343 | 6.14 | 712 | 12.91 |
| | M3 | 306 | 8.83 | 1064 | 26.70 | 1684 | 40.94 | 322 | 8.30 | 533 | 15.76 |
| | M4 | 99.28 | 3.38 | 860 | 29.35 | 1138 | 38.27 | 252 | 8.52 | 596 | 20.48 |
| Cr | M1 | 1.41 | 0.62 | 0.91 | 0.40 | 11.48 | 5.04 | 11.84 | 5.27 | 205 | 88.66 |
| | M3 | 1.57 | 0.55 | 1.18 | 0.42 | 11.45 | 4.07 | 22.34 | 7.95 | 251 | 87.01 |
| | M4 | 3.68 | 1.71 | 1.48 | 0.68 | 10.99 | 5.10 | 20.93 | 9.71 | 180 | 82.80 |
| Co | M1 | 1.46 | 2.97 | 2.14 | 4.36 | 9.39 | 19.08 | 3.75 | 7.64 | 32.63 | 65.95 |
| | M3 | 1.39 | 2.99 | 1.65 | 3.50 | 6.05 | 12.90 | 2.37 | 4.98 | 36.04 | 75.62 |
| | M4 | 1.99 | 4.70 | 1.55 | 3.79 | 5.51 | 13.21 | 1.61 | 3.88 | 31.29 | 74.43 |
| Cu | M1 | 1.12 | 1.27 | 1.53 | 1.73 | 3.38 | 3.79 | 24.32 | 27.14 | 59.02 | 66.08 |
| | M3 | 0.96 | 1.26 | 0.74 | 0.98 | 1.66 | 2.18 | 10.63 | 14.11 | 61.50 | 81.46 |
| | M4 | 0.47 | 0.67 | 1.11 | 1.59 | 1.19 | 1.70 | 6.71 | 9.67 | 61.07 | 86.36 |
| Zn | M1 | 0.91 | 0.89 | 1.4 | 1.36 | 19.81 | 19.18 | 10.5 | 10.19 | 70.39 | 68.37 |
| | M3 | 1.34 | 1.41 | 1.8 | 1.92 | 13.18 | 13.96 | 5.66 | 5.93 | 73.45 | 76.77 |
| | M4 | 1.64 | 1.62 | 2.14 | 2.10 | 14.74 | 14.46 | 3.86 | 3.81 | 80.25 | 78.02 |

The concentration of Fe in the five fractions varied in the order of F5>F3>F4>F1>F2 in core M4. The concentration of Fe in the residual phase varied from 16670 ppm to 66775 ppm (average 54751 ppm) that accounted for 77.30 % to 94.18 % of the total of the five sedimentary fractions. Fe content in the Fe-Mn oxide bound fraction ranged from 3418 ppm to 5363 ppm (average 4478 ppm) that accounted for 5.24 % to 19.60 % (average 8.48 %). Considerable amount of Fe was present in the organic/ sulfide bound fraction with concentrations ranging from 153.60 ppm to 564.30 ppm (average 310 ppm) that accounted for 0.27 % to 2.35 % (average 0.66 %). The concentrations in the exchangeable fraction ranged from 56.35 ppm to 154 ppm (average 97.39 ppm) that accounted for 0.09 % to 0.72 % (average 0.20 %) whereas the carbonate bound Fe concentration varied from 6.83 ppm to 63.95 ppm (average 22.26 ppm) that accounted for 0.01 % to 0.10 % (average 0.04 %).

Overall, Fe followed the same order of abundance F5>F3>F4>F1>F2 in all four mudflat cores. The Fe content in the residual fraction varied from 87.72 % to 92.20 %, highest being in core M3. The concentration of Fe in the reducible fraction ranged from 6.65 % to 10.29 %, with highest concentrations in core M1. Further, organic matter/sulfide bound Fe content in the mudflat sediments varied from 0.66 % to 1.94 %, highest being in core M1. Fe in the exchangeable and carbonate bound fractions was less than 1 % in all the mudflat cores.

From the distribution of Fe with depth in the five fractions (Figure 3.1.26) of core M1, large quantity of Fe was associated with the residual fraction, which showed uniform distribution throughout the depth profile. The concentration in the bioavailable phase was mainly attributed to the Fe-Mn oxide fraction of Fe, which also exhibited little variation with depth. However, slightly higher Fe in the organic phase was seen in the deeper sediments which decreased up to 10 cm followed by an increase at 8 cm. Fe concentration in the exchangeable and carbonate bound fractions was negligible as compared to the residual, Fe-Mn oxide bound and organic/ sulfide bound fractions. In the distribution of Fe with depth in the five fractions of core M3, the residual fraction was the dominant sedimentary fraction. The Fe-Mn oxide phase accounted for most of the bioavailable Fe and was noted to show uniform distribution with depth. The concentration of Fe in the organic matter/ sulfide bound fraction was higher at depths between 40 cm to 22 cm, which indicated the formation of Fe sulfides in the deeper anoxic sediments. The concentration of Fe in the exchangeable and carbonate bound fractions was negligible in this core also.

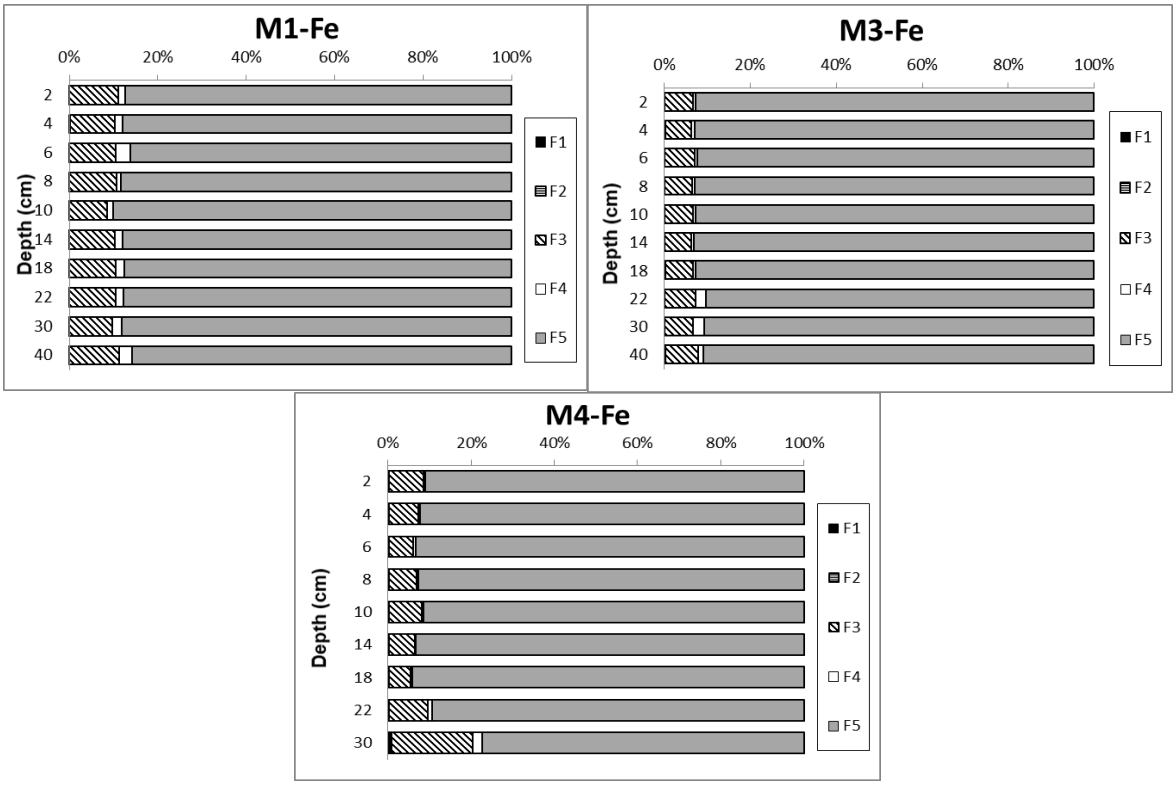


Figure 3.1.26: Speciation of Fe in cores M1, M3 and M4.

The distribution of Fe species in core M4 revealed that the residual fraction was the dominant sedimentary fraction throughout the depth profile. Lower concentrations however, were noted between 30 cm to 22 cm. The concentration of Fe in the bioavailable fractions was mainly accounted by the Fe-Mn oxide bound fraction, which exhibited higher concentrations between 30 cm to 22 cm. Higher Fe at depths 30 cm to 22 cm was also noted for the organic /sulfide bound fraction. The concentration of Fe in the exchangeable and carbonate bound phases exhibited minor variation with depth.

Overall, highest average concentrations of residual Fe was noted in all three mudflat cores. Among the bioavailable phases, slightly higher Fe-Mn oxide and organic/ sulfide bound Fe was noted in core M1. The higher Fe content in the Fe-Mn oxide and organic / sulfide bound fraction in core M1 may be due early removal of Fe from fluvial solution on encountering saline waters in the upstream regions of the estuary. The relatively higher concentration of Fe in the exchangeable and carbonate bound fractions in the lower estuary mudflat compared to the other two cores may be a result of the presence of coarse sediments with marine calcareous material which provide low binding sites for Fe. However, the concentration of Fe in the exchangeable and carbonate bound fractions accounted for <1 % in the estuarine

sediments, and this level was toxicologically insignificant to cause any adverse effect on biota (Dhanakumar et al., 2013). The fractionation study of Fe indicated that the major geochemical phases for the metals were the residual, with minor Fe and Mn oxide fractions. The high concentration of Fe in the residual phase indicated its association with the primary and secondary minerals in the sediments. Fe was mainly available in the Fe-Mn oxide phase due to its strong ability to precipitate as hydrous Fe- oxides. A small fraction of Fe was associated with organic / sulfide fraction due its ability to form iron sulfides under anoxic conditions.

### 3.1. E.2b Manganese

In core M1, the concentration of Mn varied in the order of F3>F2>F1>F5>F4. A large quantity of Mn was associated with the bioavailable fractions indicating its main source as anthropogenic. Mn mainly associated with the Fe-Mn oxide bound fraction, which ranged from 1428 ppm to 2913 ppm (average 2366 ppm) and accounted for 31.97 % to 48.94 % (average 42.06 %) of the five sedimentary fractions. Mn in the carbonate bound fraction ranged from 950 ppm to 1784 ppm (average 1409 ppm) that accounted for 19.15 % to 34.18 % (average 25.18 %). The concentration of Mn in the exchangeable fraction was relatively high i.e. from 633 ppm to 880 ppm (average 757 ppm) that accounted for 11.26 % to 19.70 % (average 13.71 %). The concentration of Mn in the residual fraction varied between 620 ppm and 792 ppm (average 712 ppm) that accounted for 10.62 % to 17.47 % (average 12.91 %) of the total of the sedimentary fractions whereas Mn concentration in the organic/ sulfide bound fraction ranged from 252.50 ppm to 422.50 ppm (average 343.00 ppm ) that accounted for 5.41 % to 6.84 % (average 6.14 %). The concentration of Mn in core M3, collected from the lower estuary mudflat sediments varied in the order of F3>F2>F5>F4>F1. The main phase for Mn in the sediments was found to be the Fe-Mn oxide fraction wherein concentrations ranged from 508 ppm to 2473 ppm (average 1684 ppm) and accounted for 27.34 % to 50.60 % (average 40.94 %) of the total of the five sedimentary fractions. A considerable amount of Mn was also associated with the carbonate bound phase wherein concentrations ranged from 327 ppm to 1450 ppm (average 1064 ppm) and accounted for 17.62% to 33.42 % (average 26.70 %). The concentration of Mn in the residual fraction ranged from 463 ppm to 598 ppm (average 533 ppm) that accounted for 10.18 % to 29.09 % (average 15.76 %) whereas the concentration of Mn in the organic/ sulfide bound fraction varied between 175 ppm to 448 ppm (average 322 ppm) that accounted for 7.19 % to 9.43 % (average 8.30 %). The least

concentration of Mn noted in the exchangeable fraction ranging from 203 ppm to 424 ppm (average 306 ppm) that accounted for 5.06 % to 16.53 % (average 8.83 %) of the total of the sedimentary fractions. In core M4, the concentration of Mn in the five fractions varied in the order F3>F2>F5>F4>F1. Large quantity of Mn was associated with the Fe-Mn oxide bound fraction that ranged from 705 ppm to 1428 ppm (average 1138 ppm) and accounted for 26.12 % to 43.61 % (average 38.27 %) of the total of the five sedimentary fractions. Mn in the carbonate bound fraction ranged from 728 ppm to 962 ppm (average 860 ppm) and accounted for 25.73 % to 35.63 % (average 29.35 %). Considerable amount of Mn was associated with the residual fraction, which ranged from 478 ppm to 708 ppm (average 596 ppm) that accounted for 14.78 % to 27.02 % (average 20.48 %). The concentration of Mn in the organic/ sulfide bound fraction ranged from 189 ppm to 490 ppm (average 252 ppm) that accounted for 6.10 % to 15.17 % (average 8.52 %) of the sediments. The lowest concentrations of Mn was associated with the exchangeable fraction which ranged from 51.65 ppm to 133 ppm (average 99.28 ppm) that accounted for 1.60 % to 4.26 % (average 3.38 %) of the total of the five sedimentary fractions.

Overall, Mn was largely concentrated in the F3 and F2 of the sediments. The concentration of Mn in the reducible fraction varied from 38.27 % to 42.06 %, highest being in core M1. Further, Mn in the carbonate bound fraction varied from 25.18 % to 29.35 % with high concentration in core M4. Mn in the exchangeable fraction varied from 3.38 % to 13.71 % with high concentrations in core M1. Organic matter/ sulfide bound Mn concentration varied from 6.14 % to 8.52 % with highest concentration in core M4. The residual Mn content of sediments varied from 12.91 % to 20.48 % highest being in core M4. In all, considerable quantity of Mn was found in the bioavailable fractions at all the three mudflat cores.

The distribution of Mn in the five fractions (Figure 3.1.27) of core M1 revealed that a large quantity of Mn was associated with the bioavailable fractions with depth. The concentration of Mn in the residual phase decreased towards the surface, which was compensated by an increase in the bioavailable fractions. The Fe-Mn oxide fraction was the main carrier phase for Mn among the bioavailable phases and the concentrations was observed to decrease up to 10 cm followed by an increase towards the surface. Mn distribution in the Fe-Mn oxide bound fraction was complemented by the carbonate bound Mn where in concentrations increased up to 10 followed by decrease towards the surface, indicating diagenetic mobilization of Mn where Fe-Mn oxides undergo dissolution in the deeper anoxic sediments

and was re-precipitated in the oxic conditions. Fe in the Fe-Mn oxide bound fraction showed similar distribution. The Mn concentration in the exchangeable phase decreased from the base of the core up to 10 cm followed by relatively higher concentrations towards the surface. The distribution of organic/sulfide bound Mn showed little variation with depth.

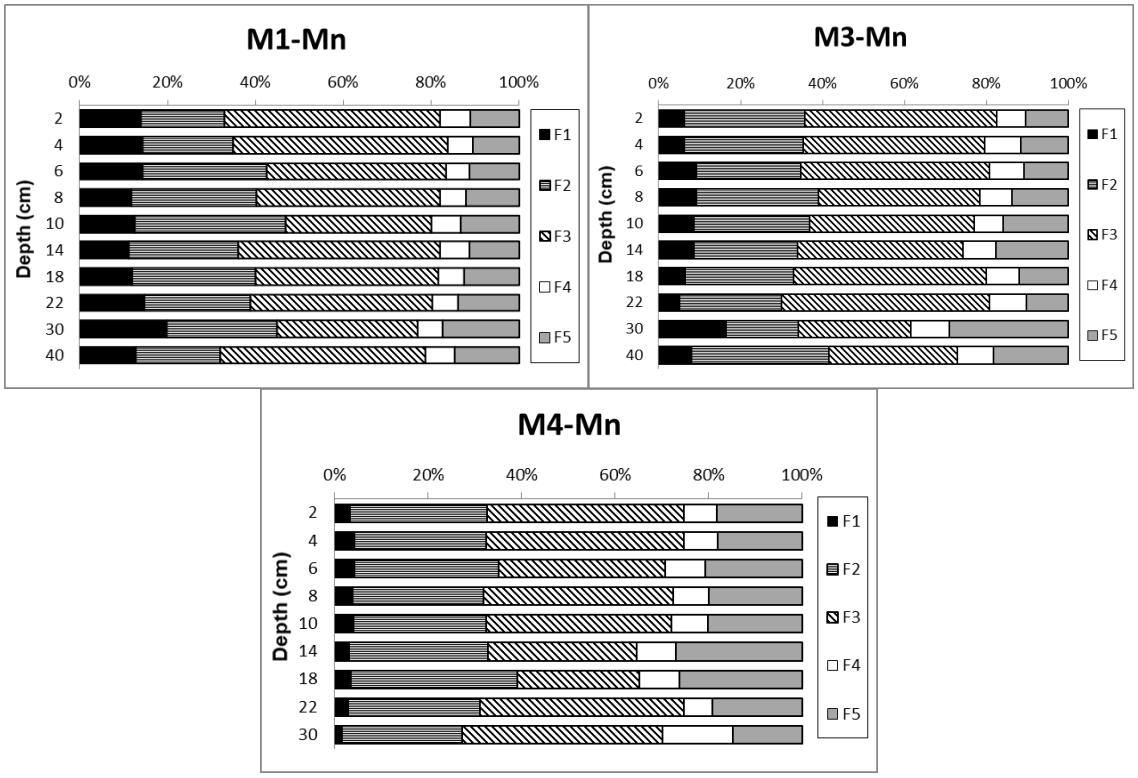


Figure 3.1.27: Speciation of Mn in cores M1, M3 and M4.

The bioavailable fractions accounted for major amount of Mn in the sediments in core M3, and increased towards the surface indicating that Mn was mainly of anthropogenic source. Large quantity of Mn was associated with the Fe-Mn oxide phase throughout the depth profile. The concentration of Mn in the Fe-Mn oxide fraction was highest at 22 cm and decreased up to 14 cm followed by an increase towards the surface. The low concentration of Fe-Mn oxide bound Mn between 40 cm and 30 cm was noted. The decrease from 22 cm up to 14 cm of Fe-Mn oxide bound Mn was compensated by an increase in the exchangeable fraction of Mn indicating redox mobilization and re-precipitation of Mn oxides towards the surface. Mn in the organic/ sulfide bound phase exhibited little variation with depth. From the distribution profile of Mn in the five geochemical phases of core M4, the concentration of Mn in the bioavailable phases increased towards the surface. Large quantity of Mn was associated with the Fe-Mn oxide bound fraction, which showed large variations with depth. The

concentration of Mn in the Fe-Mn oxide bound phase decreased from the base of the core up to 18 cm followed by an increase towards the surface but with a decrease at 6 cm. The carbonate bound fraction of Mn exhibited a complementary distribution pattern to the Fe-Mn oxide fraction of Mn with higher values at 18 cm and 6 cm. The decrease in the Fe- Mn oxide fraction at 18 cm may be attributed dissolution of Fe-Mn oxides and enrichment in the carbonate and exchangeable fractions. The concentration of Mn in the exchangeable fraction and carbonate bound fraction increased towards the surface of the core, which may facilitate diffusion of available labile Mn to the water column from the surface sediments.

Overall, highest concentrations of Mn in the bioavailable sediment fractions were noted in core S1 of the upper middle estuary compared to other cores. This enrichment was attributed to the proximity of the sampling location to the source of Mn, which is mainly a product of mining activities.

Contrasting Fe, a large proportion of Mn was found in all of the four bioavailable fractions of the three mudflat cores. Among the bioavailable phases, a considerable amount of Mn was detected in the reducible fraction (Fe-Mn oxide bound) in which Mn exists as oxides and may be released to the water if the sediment conditions become more reducing (Panda et al., 1995). In addition, in the exchangeable and carbonate bound fractions, weakly sorbed Mn retained on sediment surface by relatively weak electrostatic interactions may be released to the water column by ion-exchange processes and dissociation of Mn- carbonate phase if sediment nature become more acidic (Tessier et al., 1979; Thomas et al., 1994; Yuan et al., 2004). Thus re-working of the sediments may cause substantial release of Mn into water column. In the distribution with depth, the concentration of Mn in the bioavailable fractions increased towards the surface indicating enhanced anthropogenic inputs of Mn in recent times. Early diagenetic mobilization was also noted in the cores.

### 3.1. E.2c Chromium

The concentration of Cr in the core M1 collected from the upper middle estuary, in the five phases varied in the order F5>F4>F3>F1>F2. Large quantity of Cr was associated with the residual fraction ranged from 167 ppm to 310 ppm (average 205 ppm) that accounted for 86.63 % to 91.75 % (average 88.66 %). Considerable amount of Cr was associated with the organic matter/ sulfide bound fraction and Fe-Mn oxide bound fraction. The concentrations in

the organic matter/ sulfide bound fraction ranging from 10.80 ppm to 13.08 ppm (average 11.84 ppm) that accounted for 3.26 % to 6.77 % (average 5.27 %) whereas the concentration of Cr in the Fe-Mn oxide bound fraction ranged from 10.33 ppm to 14.45 ppm (average 11.48 ppm) that accounted for 4.27 %to 5.64 % (average 5.04 %). Low concentrations of Cr were noted in the exchangeable and carbonate bound fractions. Cr in the exchangeable fractions of Cr ranged from 1.15 ppm to 2.05 ppm (average 1.41 ppm) that accounted for 0.41 % to 0.97 % (average 0.62 %) whereas concentrations in the carbonate bound fraction ranged from 0.68 ppm to 1.08 ppm (average 0.91 ppm) that accounted for 0.29 % to 0.50 % (average 0.40 %). The concentration of Cr varied in the order of F5>F4>F3>F1>F2 in core M3. A large quantity of Cr was associated with the residual phase ranging from 184 ppm to 299 ppm (average 251 ppm) that accounted for 82.57 % and 89.93 % (average 87.01 %). The concentration of Cr in the organic matter/ sulfide bound phase ranged from 19.03 ppm to 24.13 ppm (average 22.34 ppm) that accounted for 5.99 % to 10.51 % (average 7.95 %). Cr in the Fe-Mn oxide bound fraction ranged from 9.43 ppm to 17.85 ppm (average 11.45 ppm) that accounted for 2.83 % to 6.12 % (average 4.07 %). Cr in the exchangeable fraction ranged from 0.65 ppm to 4.38 ppm (average 1.57 ppm) that accounted for 0.23 % to 1.64 % (average 0.55 %) whereas the concentration in the carbonate bound phase ranged from 0.93 ppm to 1.43 ppm (average 1.18 ppm) that accounted for 0.29 % to 0.64 % (average 0.42 %). The concentration of Cr in core M4, varied in the order F5>F4>F3>F1>F2. The residual phase was the main carrier for Cr in the sediments with concentration ranging from 150 ppm to 213 ppm (average 180 ppm) that accounted for 80.08 % to 85.24 % (average 82.80 %) of the total of the five fractions. Mn concentration in the organic matter/ sulfide bound fraction ranged from 19.60 ppm to 22.23 ppm (average 20.93 ppm) that accounted for 8.39 % to 11.12 % (average 9.71 %). Mn content in the Fe-Mn oxide bound fraction ranged from 9.70 ppm to 12.23 ppm (average 10.99 ppm) that accounted for 4.36 % to 6.16 % (average 5.10 %) of the total of the five fractions. The Cr concentration in the exchangeable fraction varied from 3.50 ppm to 3.83 ppm (average 3.68 ppm) that accounted for 1.43 % to 2.01 % (average 1.71 %) whereas the concentration in the carbonate bound fraction ranged from 1.35 ppm to 1.70 ppm (average 1.48 ppm) that accounted for 0.58 % to 0.76 % (average 0.68 %).

Overall, Cr followed the order of abundance F5>F4>F3>F1>F2 in all cores. The residual Cr content varied from 82.80 % to 88.66 %, highest being in core M1. Further, oxidisable Cr content in the sediments ranged from 5.27 % to 9.71 %, highest being in core M4. The Fe-Mn oxide bound Cr in the sediments varied from 5.04 % to 5.10 %, highest being in core M4.

Exchangeable and carbonate bound Cr was less than 1 % in the mudflat sediments, except for exchangeable Cr in core M4.

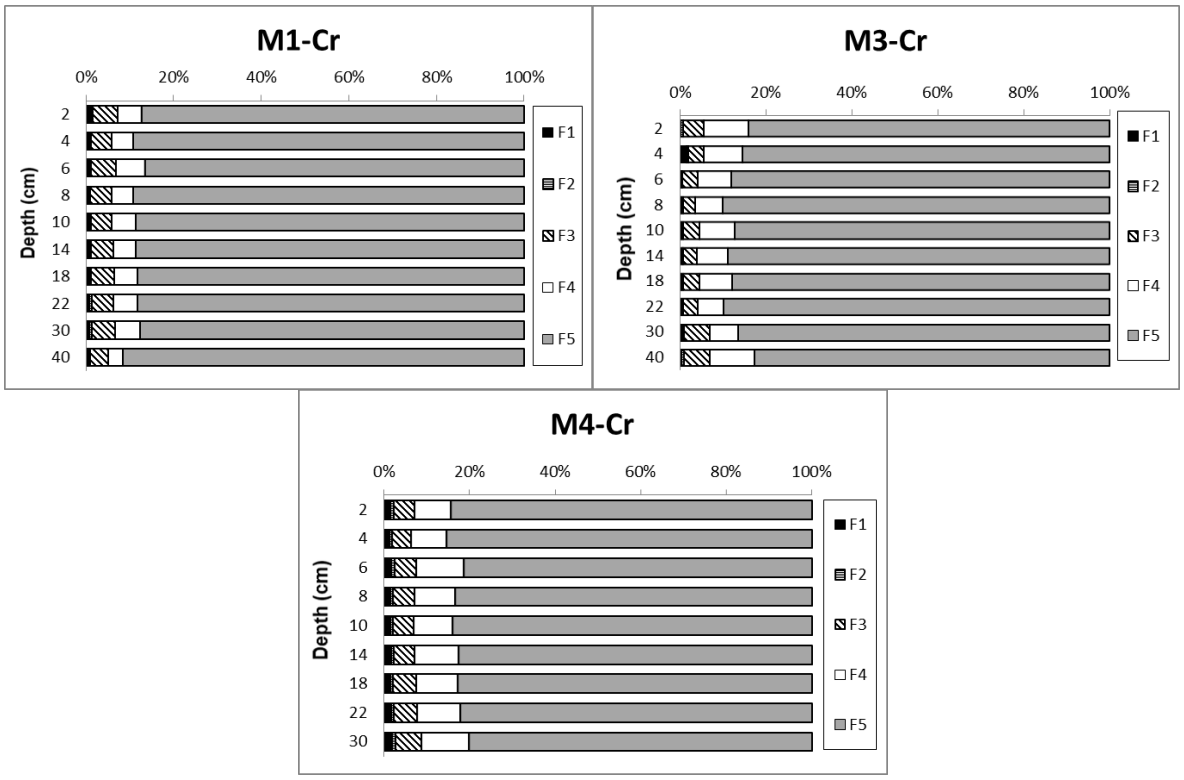


Figure 3.1.28: Speciation of Cr in cores M1, M3 and M4.

The distribution of Cr with depth in the five fractions (Figure 3.1.28) of core M1 revealed that Cr was mainly associated with the residual phase, which exhibited relatively uniform pattern with depth. The concentrations of Cr in the bioavailable phase showed little variation with depth except at 6 cm wherein minor enrichment was noted in the organic matter/ sulfide fraction, which was similar to Fe at the same depth. The distribution of Cr with depth in the five fractions of the sediments of core M3 showed that large quantity of Cr was associated with the residual fraction of sediments throughout the depth profile. The distribution of Cr in the residual phase increased from the base of the core up to 22 cm followed by constant concentrations between 22 cm to 8 cm and further decreased towards the surface. Higher Cr concentrations in the organic/sulfide bound phase was noted in the deeper sediments as well as near surface sediments. Cr distribution with depth, in the five fractions of core M4, Cr in the residual fraction increased in the surface of the sediment column with a corresponding decrease in the bioavailable organic/ sulfide bound Cr indicating the dilution of bioavailable

Cr by terrestrial derived material. Little variation in the distribution of Cr in the Fe-Mn oxide and exchangeable fraction was noted.

Between the cores, highest concentrations of Cr in the exchangeable and carbonate bound phases were noted at M4. In all the cores, however, the residual fraction was the major fraction in the sediments.

Enrichment of Cr in the oxidisable phase indicated that Cr was immobilized in the sediments as Cr-organic compounds (Lacerda et al., 1991). In the natural environment, Cr (III) can only be oxidized to Cr (VI) by Mn-oxides. In the upper middle estuary, oxidation of Cr (III) to Cr (VI) must have occurred in association with Mn-oxide. On the other hand, Fe (II) production in deeper sediments of core M1 may have led to the reduction of Cr (VI), and Cr precipitation with Fe oxide (Fendorf, 1995). However, within the anoxic organic-rich layers, Cr (VI) may have been reduced by organic matter and sulfides, inducing a lower bioavailability and toxicity of Cr (Marchand et al., 2012).

**3.1. E.2d Cobalt**

In core M1, the abundance of Co varied in the order of F5>F3>F4>F2>F1 in the sediments. Co was mainly associated with the residual fraction, which ranged from 27.79 ppm to 37.63 ppm (average 32.63 ppm) that represented 60.74 % to 69.78 % (average 65.95 %) of the total of five fractions. Considerable amount of Co was associated with the Fe-Mn oxide phase that varied between 8.25 ppm and 10.08 ppm (average 9.39 ppm) and accounted for 6.28 % to 8.97 % (average 7.64 %). Co in the organic matter / sulfide bound phase ranged from 3.43 ppm to 4.10 ppm (average 3.75 ppm) that accounted for 6.28 % to 8.97 % (average 7.64%) of the five fractions. Co concentrations in the carbonate bound fraction ranged from 1.70 ppm to 2.45 ppm (average 2.14 ppm) that accounted for 3.48 % to 5.36 % (average 4.36 %) whereas concentration in the exchangeable fraction ranged from 0.80 ppm to 2.18 ppm (average 1.46 ppm) that accounted for 1.76 % to 4.58 % (average 2.97 %) of the total of the five fractions. In core M3, the concentration of Co varied in the order of F5>F3>F4>F2>F1. A large amount of Co was present in the residual phase, which ranged from 27.70 ppm to 42.90 ppm (average 36.04 ppm) that represented 71.44 % to 79.69 % of the five fractions in the sediments. The concentration of Co in the Fe-Mn oxide phase varied between 5.35 ppm and 6.80 ppm (average 6.05 ppm) and accounted for 9.79 % to 15.51 % (average 12.90 %). Co in the organic matter/ sulfide bound fraction ranged from 1.93 ppm to 3.60 ppm (average 2.37 ppm)

that accounted for 4.11 % to 6.58 % (average 4.98 %). Co concentrations in the carbonate bound fraction ranged from 1.33 ppm to 1.88 ppm (average 1.65 ppm) that accounted for 2.90 % to 4.61 % (average 3.50 %) whereas concentrations of Co in the exchangeable fraction ranged from 0.83 ppm to 2.08 ppm (average 1.39 ppm) that accounted for 1.92 % to 5.29 % (average 2.99 %). The concentration of Co in core M4, in the five fractions varied in the order of F5>F3>F1>F4>F2. Major content of Co in the sediments of the lower estuary was associated with the residual fraction, which ranged from 25.63 ppm to 34.83 ppm (average 31.29 ppm) that represented 70.50 % to 78.28 % (average 74.43 %) of the total of the five sediment fractions. Co was mainly available in the Fe-Mn oxide phase among the bioavailable phases with concentrations ranging from 5.20 ppm to 5.78 ppm (average 5.51 ppm) that accounted for 12.08 % to 15.39 % (average 13.21 ppm). Co in the exchange able fraction ranged from 1.23 ppm to 2.88 ppm (average 1.99 ppm) that accounted for 2.82 % to 6.62 % (average 4.70 %). The Co concentration in the organic/ sulfide bound fraction ranged from 1.15 ppm to 1.85 ppm (average 1.61 ppm) that accounted for 2.65 % to 5.09 % (average 3.88 %) whereas concentration of Co in the carbonate bound fraction ranged from 0.78 ppm to 2.43 ppm (average 1.55 ppm) and accounted for 1.78 % to 6.52 % (average 3.79 %).

Overall, Co was mainly concentrated in the F5 and F3 fractions as compared to F4, F2 and F1 fractions. Residual Co content in the mudflat cores varied from 65.95 % to 75.62 %, highest being in core M3. Co in the Fe-Mn oxide fraction varied from 12.90 % to 19.08 % highest being in core M1. Organic matter/ sulfide bound Co content in the sediments ranged from 3.88 % to 7.64 % highest being in core M1. Co in the carbonate bound fraction varied from 3.50 % to 4.36 % with higher content in core M1 while, Co in the exchangeable fraction varied from 2.97 % to 4.70 % highest being in core M4.

From the distribution of Co (Figure 3.1.29) in mudflat core M1, large amount of Co in the sediments was of detrital nature. However, the increasing concentration of Co in the bioavailable fraction from the base of the core towards the surface was evident of either diagenetic remobilization or recent anthropogenic inputs into the estuary. Also, the increase in the labile fractions (exchangeable and carbonate fractions) towards the surface indicated possible diffusion of Co into the water column. The Fe-Mn oxide phase of Co increased towards the surface indicating co-precipitation of Co. The concentration of Co in the bioavailable phases increased towards the surface in core M3. The Fe-Mn oxide phase of Co accounted for major variation of the bioavailable fractions and its decrease from 22 cm to 8

cm followed by increase towards the surface was noted. Additionally, an increase in the exchangeable and carbonate bound fraction was noted from the bottom of the core up to 6 cm which indicated dissolution of Co associated with Fe-Mn oxides in the deeper parts which reprecipitated to the surface layers of the core.

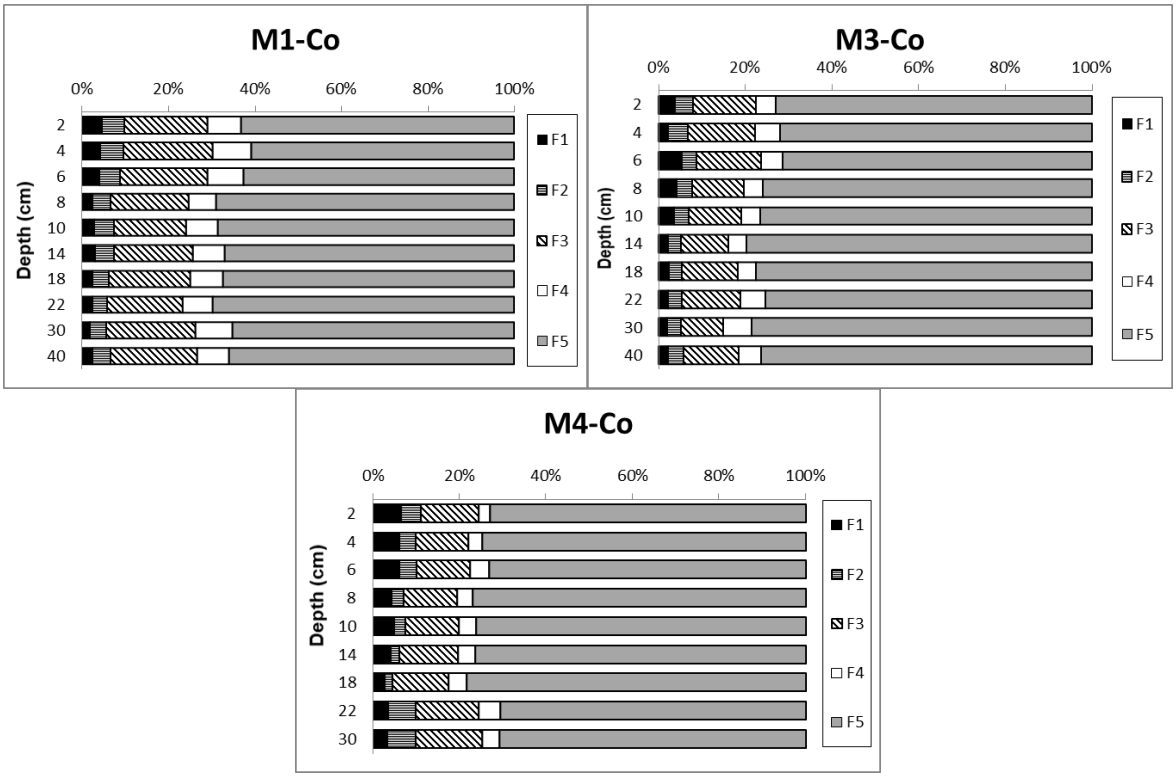


Figure 3.1.29: Speciation of Co in cores M1, M3 and M4.

In the distribution of Co in the sediments of core M4, the concentration of Co in the bioavailable fractions was low between 18 cm and 8 cm and high towards the surface, which indicated diagenetic remobilization. The similar distributions of Co with Mn, with depth indicated the strong affinity of Co with hydrous Mn oxides. The concentration of Co in the Fe-Mn oxide bound fraction was high in the lower part of the core (30 cm to 22 cm). The concentration of Co in the exchangeable and carbonate bound fractions however, gradually increased towards the surface indicating their remobilization towards the surface. The enrichment of Co in the carbonate bound phase may be due to the special affinity of Co to carbonates and its co-precipitation with its minerals (Sundaray et al., 2011). Additionally, Co in the organic matter/ sulfide bound fraction was higher between 30 cm and 22 cm which was synonymous to Fe in the organic/ sulfide fractions at the same depths and reflected the

partitioning of Co as a result of low Eh with depth along with formation of $FeS_2$ (Evans et al., 1988).

Between the three cores, higher Co in the exchangeable fraction was noted at M4, whereas Co in the carbonate bound, Fe-Mn oxide bound and organic/sulfide bound fraction was high at M1.

From the above, it was noted that the distribution and speciation of Co in sediments varied with changes in pH, ionic strength and organic matter (Mahara and Kudo, 1981). Co was precipitated to the sediments in the adsorbed state with oxides of iron and manganese or with the crystalline sediments such as aluminosilicates and goethite. The higher content of Co in the Fe-Mn oxides phase in sediments was due to adsorption of larger amount of Co to Fe-Mn oxides (McLaren et al., 1986). In deeper oxygen depleted sediment layers, the lowering of sediment redox potential and pH may have occurred which resulted in the reduction of iron and manganese oxides. Consequently, the adsorbed Co was released by dissolution of the oxides and thus increased Co mobility towards the surface and precipitation in the oxic layers along with Fe-Mn oxides (Smith and Carson, 1981, Kim et al., 2006), resulting in enrichment in the surface layers which was seen in all the three mudflat cores. Further, the considerable amount of Co in the organic/ sulfide fraction was due to the formation of complexes with fulvic and humic acids or other organic ligands but are however, less stable.

**3.1. E .2e Copper**

The concentration of Cu in the five fractions is in the order of F5>F4>F3>F2>F1 in core M1 which was collected from the upper middle estuary mudflat. Large quantity of Cu was associated with the residual fraction ranging from 52.93 ppm to 73.58 ppm (average 59.02 ppm) that accounted for 61.83 % to 72.10 % (average 66.08 %). Among the bioavailable fractions, considerable quantity of Cu was associated with the organic/ sulfide bound phases with concentrations ranging from 20.38 ppm to 33.08 ppm (average 24.32 ppm) that accounted for 21.86 % to 31.55 % (average 27.14 %). The concentration of Cu in the Fe-Mn oxide fraction ranged from 2.95 ppm to 4.20 ppm (average 3.38 ppm) that accounted for 3.34 % to 4.31 % (average 3.79 %) whereas concentrations in the carbonate fraction ranged from 1.33 ppm to 1.73 ppm (average 1.53 ppm) that accounted for 1.41 % to 1.89 % (average 1.73 %). Least amount of Cu was found in the exchangeable fraction with a range of 1.00 ppm to 1.28 ppm (average 1.12 ppm) and accounted for 1.01 % to 1.51 % (average 1.27 %) of the

total of the five fractions. The concentration of Cu in core M3 varied in the order of F5>F4>F3>F1>F2. The concentration of Cu in the residual phase ranged from 52.83 ppm to 67.98 ppm (average 61.50 ppm) that accounted for 76.23 % to 85.06 % (average 81.46 %). Considerable amount of Cu however, was found in the bioavailable phases mainly in the organic/ sulfide fraction concentrations ranged from 8.65 ppm to 13.80 ppm (average 10.63 ppm ) and accounted for 11.41 % to 19.91 % (average 14.11 %). The concentration in the Fe-Mn oxide fraction ranged from 1.18 ppm to 2.38 ppm (average 1.66 ppm) that accounted for 1.70 % to 3.08 % (average 2.18 %) whereas the concentration of Cu in the exchangeable fraction ranged from 0.53 ppm to 1.83 ppm (average 0.96 ppm) that accounted for 0.72 % to 2.37 % (average 1.26 %). Least quantity of Cu was noted in the carbonate bound fraction that ranged from 0.63 ppm to 0.88 ppm (average 0.74 ppm) and accounted for 0.86 % to 1.12 % (average 0.98 %). In core M4, the concentration of Cu varied in the order of F5>F4>F3>F2>F1. Large quantity of Cu was associated with the residual phase ranging from 50.50 ppm to 78.18 ppm (average 61.07 ppm) which accounted for 80.90 % to 89.75 % (average 86.36 %). The concentration of Cu in the organic/ sulfide bound fraction varied form 5.60 ppm to 9.00 ppm (average 6.71 ppm) that accounted for 6.83 % to 14.42 % (average 9.67 %) whereas Cu in the Fe-Mn oxide fraction ranged from 0.98 ppm to 1.60 ppm (average 1.19 ppm) that accounted for 1.41 % to 2.28 % (average 1.70 %). Cu in the carbonate bound fraction ranged from 0.98 ppm to 1.25 ppm (average 1.11 ppm) that accounted for 1.23 % to 1.99 % (average 1.59 %). Least Cu concentrations were found in the exchangeable phase, which ranged from 0.20 ppm to 0.68 ppm (average 0.47 ppm) and accounted for 0.28 % to 1.04 % (average 0.67 %).

Overall, Cu in the sediments was enriched in the F5, F4 and F3 fractions followed by low concentrations in the F2 and F1 fractions. Residual Cu in the mudflat sediments varied from 66.08 % to 86.36 %, highest being in core M4. The concentration of Cu in the organic matter/ sulfide bound fraction ranged from 9.67 % to 27.14 %, highest being in core M1. Fe-Mn oxide bound Cu content varied from 1.70 % to 3.79 %, with higher concentration in core M1. Cu content in carbonate bound and exchangeable fraction varied from 1.59 % to 1.73 % and 0.67 % to 1.72 % respectively, with higher concentrations in core M1 for both fractions.

In the distribution of Cu with depth in the five fractions of core M1 (Figure 3.1.30) Cu in the residual fraction exhibited relatively uniform distribution except for higher values at 22 cm and 14 cm. The organic/ sulfide fraction was the main repository for Cu among the

bioavailable forms. Higher Cu concentrations were noted in the lower part of the core (40 cm to 18 cm) which indicates the incorporation of Cu into iron sulfides in the oxygen depleted layers, which was similar to the enrichment of Fe in the organic/ sulfide phase in the lower part of the core. The distribution of Cu in the reducible, carbonate bound and exchangeable fraction did not exhibit much variation with depth.

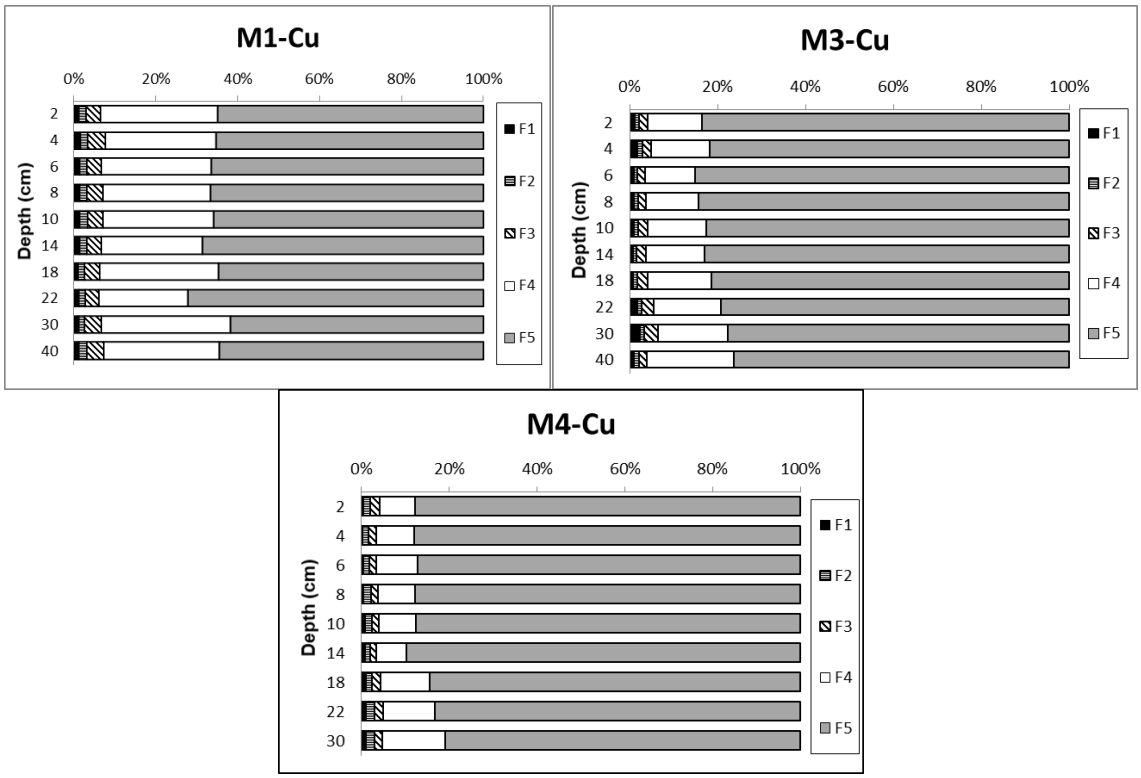


Figure 3.1.30: Speciation of Cu in cores M1, M3 and M4.

The distribution of Cu with depth in the five fractions of core M3 exhibited that the residual phase gradually increased towards the surface whereas the bioavailable Cu concentrations decreased indicating increased inputs of terrestrial weathered Cu in recent times. Considerable quantity of bioavailable Cu was attributed to the organic/ sulfide bound fraction, which exhibited higher concentration in the oxygen-depleted layers in the lower part of the core, which was similar to the distribution of oxidisable Fe, which indicated that Cu might have been co-precipitated with iron sulfides. The concentration of Cu in the reducible, carbonate bound and exchangeable fractions were negligible as compared to the residual and oxidisable fraction.

From the distributions of Cu with depth in the five fractions of core M4, Cu in the residual fractions increased towards the surface indicating the increased input of terrestrial material. Higher bioavailable Cu concentrations were noted in the deep part of the core (18 cm to 30 cm) which decreased up to 14 cm. The high concentrations of Cu in the oxidisable phase in the lower part of the core indicated the association of Cu with iron sulfides.

Overall, relatively high Cu concentration in the bioavailable phases was noted in the upper middle estuary followed by lower middle and lower estuary. The enrichment of bioavailable Cu in the upper middle estuary indicated that the source as anthropogenic probably from marine transportation and shipbuilding activities wherein Cu is employed as an active ingredient in antifouling paints for recreational and commercial vessels moored and maintained in the estuary (Burton et al., 2005). High content of Cu in the residual fraction in the estuarine system indicated that Cu was occluded within the crystal structure of recalcitrant minerals and is not available to biota or due to diagenetic processes (Tessier et al., 1979). Cu in the oxidisable fraction was due to the formation of stable organic complexes (Stumm and Morgan, 1996). Bubb et al. (1991) reported that Cu tends to have a high affinity for the clay/silt fraction. Thus, the higher proportion of Cu may be due to sorption to clay minerals (Pickering, 1986; Massolo et al., 2012). The carbonate and exchangeable fractions contained negligible concentrations of Cu.

### 3.1. E.2f Zinc

The concentration of Zn in core M1, varied in the order of abundance F5>F3>F4>F2>F1. Large proportion of Zn was associated with the residual phase ranging from 58.43 ppm to 86.35 ppm (average 70.39 ppm) that accounted for 64.36 % to 72.00 % (average 68.37 %). Considerable amount of Zn was associated with the bioavailable fractions. The concentration of Zn in the Fe-Mn oxide fraction ranged from 15.50 ppm to 26.10 ppm (average 19.81 ppm) that accounted for 16.68 % to 22.47 % (average 19.18 %) whereas, Zn in the organic/sulfide bound fractions with concentrations varying between 8.08 ppm to 12.78 ppm (average 10.50 ppm) that accounted for 9.14 % to 11.72 % (average 10.19 %). Zn in the carbonate bound fraction ranged from 0.98 ppm to 1.98 ppm (average 1.40 ppm) that accounted for 0.95 % to 1.93 % (average 1.36 %) whereas concentrations in the exchangeable fraction ranged from 0.63 ppm to 1.43 ppm (average 0.91 ppm) that accounted for 0.61 % to 1.35 % (average 0.89 %). In core M3, the concentration of Zn in the five fractions varied in the order of abundance F5>F3>F4>F2>F1. The concentrations of Zn in the residual fraction varied between 61.53

ppm to 90.47 ppm (average 73.45 ppm) that accounted for 69.79 % to 82.55 % (average 76.77 %). Among the bioavailable fractions, Zn was mainly associated with the Fe-Mn oxide fraction wherein its concentration ranged from 10.80 ppm to 14.40 ppm (average 13.18 ppm) that accounted for 9.85 % to 16.78 % (average 13.96 %). Considerable amounts of Zn were noted in the organic/ sulfide bound fraction wherein it ranged from 4.58 ppm to 8.30 ppm (average 5.66 ppm) that accounted for 4.94 % to 8.41 % (average 5.93 %). Zn in the carbonate fraction ranged from 1.23 ppm to 4.05 ppm (average 1.80 ppm) that accounted for 1.16 % to 4.51 % (average 1.92 %) whereas Zn in the exchangeable fraction ranged from 0.33 ppm to 4.05 ppm (average 1.34 ppm) that accounted for 0.40 % to 4.51 % (average 1.41 %) of the total of the five fractions. The concentration of Zn in core M4 varied in the order of F5>F3>F4>F2>F1. The residual phase contained the highest Zn concentrations among the five fractions, which ranged from 59.65 ppm to 104.78 ppm (average 80.25 ppm) that accounted for 68.01 % to 84.67 % (average 78.02 %). Among the bioavailable phases, the Fe-Mn oxide fraction was the main phase wherein Zn ranged from 11.38 ppm to 24.60 ppm (average 14.74 ppm) that accounted for 10.26 % to 20.91 % (average 14.46 %). Zn concentrations in the organic/ sulfide fraction varied between 2.98 ppm and 6.78 ppm (average 3.86 ppm) that accounted for 2.75 % to 5.76 % (average 3.81 %). The concentrations of Zn in the carbonate fraction ranged from 1.15 ppm to 4.85 ppm (average 2.14 ppm) that accounted for 0.99 % to 4.86 % (average 2.10 %) whereas concentrations in the exchangeable fraction ranged from 1.10 ppm to 2.38 ppm (average 1.64 ppm) that accounted for1.09 % to 2.35 % (average 1.62 %).

Overall, Zn followed the same order of abundance in the three mudflat cores of F5>F3>F4>F2>F1. Further, Zn in the residual fraction varied from 68.37 % to 78.02 %, highest being in core M4. The Fe-Mn oxide bound Zn in the mudflat sediments varied from 13.96 % to 19.18 % with higher concentrations in core M1. Zn content in the organic matter/ sulfide bound phase ranged from 3.81 % to 10.19 %, highest concentrations being in core M1. Low content of carbonate bound and exchangeable Zn were noted in the mudflats values varying from 1.36 % to 2.10 % and 0.89 % to 1.62 % respectively, being in core M4.

The distribution of Zn with depth (Figure 3.1.31) in five fractions of core M1 showed that Zn was mainly present in the residual phase, which exhibited a fluctuating with an overall decreasing distribution pattern towards the surface. The distribution of Zn in the bioavailable phases showed a minor increase towards the surface similar to the distribution of bioavailable

Mn, which indicated that considerable amount of Zn, may be of anthropogenic nature. In the bioavailable phases, Zn was mainly associated with the Fe-Mn oxide phase, which increased towards the surface. The distribution of Zn in the oxidisable, carbonate and exchangeable phases showed little variations with depth.

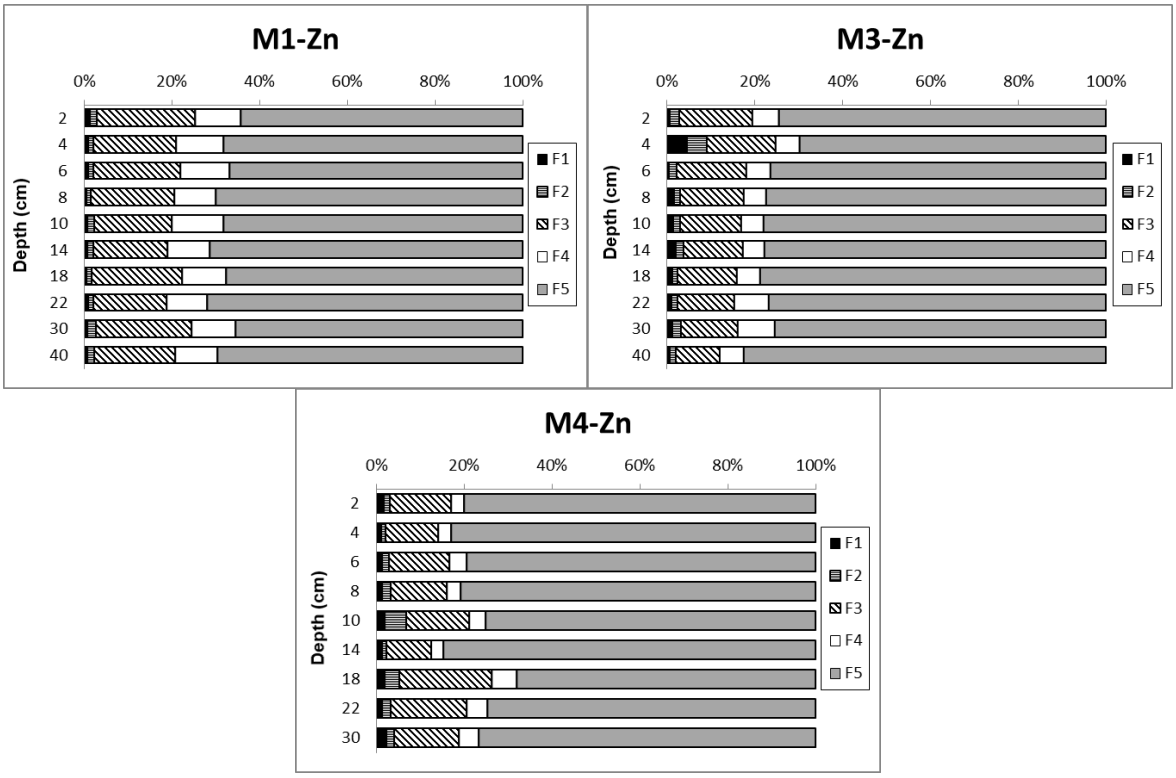


Figure 3.1.31: Speciation of Zn in cores M1, M3 and M4.

In the distribution of Zn with depth in the five fractions of core M3, the residual phase was the main carrier phase for Zn throughout the depth profile that decreased towards the surface. The distribution of Zn in the bioavailable fraction increased towards the surface similar to bioavailable Mn and indicating anthropogenic inputs in recent times. However, the increase in bioavailable Zn was attributed largely to the increase of Zn in the Fe-Mn oxide phase towards the surface. Relatively higher concentration of Zn in the oxidisable fraction was noted in the lower part of the core (30 cm to 22 cm) which similar to the observation made for Fe and indicated the formation of sulfides. Thus, there may have been dissolution of Zn oxides and sulfides around 18 cm that mobilized and co-precipitation towards the surface with the Fe-Mn oxides. The residual fraction was the dominant sediment fraction for Zn in the distribution of Zn in the five fractions of core M4, where a fluctuating distribution pattern was observed. The concentration of bioavailable Zn in sediments was accounted for by the

Fe-Mn oxide fraction wherein the Zn showed a peak at 18 cm followed by an almost uniform distribution towards the surface. This decrease from 18 to 14 cm indicated redox mobilization and increase at 10 cm indicated re-precipitation as oxides and similar to Mn and to a lesser extent Fe. Zn in the organic/ sulfide fraction showed higher concentrations in the deeper layers of the sediment core (30 cm to 18 cm) which may indicate that Zn incorporation into sulfides.

Overall, relatively higher bioavailable fractions were noted in the lower estuary. High Zn content in the reducible and oxidisable phases in the upper estuary indicated the role of Fe-Mn oxides and organic matter in the removal of Zn from the water column to sediments.

The bioavailability of Zn in sediments was thus controlled by adsorption/desorption and precipitation/dissolution mechanisms. Sorption was the dominant reaction governing transport of zinc to sediments. Zn in the bioavailable fraction was associated with Fe and Mn oxides (Lopez-Sanchez et al., 1996) due the ability of Zn to substitute for Fe in the structure of oxide minerals (Stumm and Morgan, 1996). Zn in deeper reduced sediments below 22 cm that contained sulfides might have incorporated in to sulfides. Due to anoxic conditions in deeper sediments, dissolution of Fe-Mn oxides may have occurred, which mobilized the adsorbed Zn and was thus re-precipitated near the surface in sub-oxic sediments. However, large quantity of Zn was bound to the clastic detrital fraction of sediments resulting in overall low mobility. The content of Zn in sediments therefore, depends on the chemical and mineralogical properties of the sediment such as nature of parent rocks, sediment texture, organic matter, and pH that determine the species and stability of Zn in the solid phase.

The speciation analysis of metals Fe, Mn, Cr, Co, Cu and Zn indicated that the main carrier phase for Fe, Cr, Co, Cu and Zn was the residual phase suggesting a detrital control for these metals whereas large quantity of Mn was associated with the non-residual or bioavailable fraction indicating an anthropogenic source for Mn in addition to natural source. Among the bioavailable fractions Fe, Mn, Co and Zn were mainly associated with the Fe-Mn oxide phases which may have become soluble under the changing redox conditions whereas Cr and Cu were associated with the organic matter/ sulfide fraction (except at S4 for Cr wherein higher concentrations in Fe-Mn oxide phase were noted). Sediment organic matter is important for the distribution of Cu and Cr in sediments as these metals have a strong affinity to bind to the organic phases. The abundance of Fe, Cr, Co, Cu and Zn in the residual

fractions indicated that these elements were derived from mainly from natural weathered rock sources. However, human induced activities in the catchment area of the estuary contributed a considerable amount of metals that were present in the various non residual forms due to their affinities for various components and were ultimately deposited to the sediments. Geochemical processes continue post-deposition due to changes in the physicochemical conditions in the sediments as well as that of the basin that causes mobility of the metals in the sedimentary column. Zn and Co bound to the Fe–Mn oxide fraction had significant relationship with reducible Fe and Mn suggesting that Fe–Mn oxides may be the main carriers of bioavailable Zn and Co. The present results indicated that Zn and Co have higher potentials for mobilization from the sediments than Cu and Cr supported by their higher concentration in the Fe–Mn oxide fraction.

A comparison of the total bioavailable concentrations of metals in the sediments was made in the studied mudflat and mangroves sediment core samples 1, 3 and 4 using the isocon diagram (Figure 3.1.32). At sampling location 1 of the upper middle estuary, higher bioavailable Co and Cu was noted in the mudflat core (M1) whereas Fe, Mn, Cr and Zn did not show any significant difference in the concentration between mudflat and mangrove. In the lower middle estuary, higher bioavailable Mn and Co was noted in the mudflat core M3 whereas bioavailable Cr and Cu were enriched in the mangrove. In the lower estuary, bioavailable Fe, Mn, Cr, Co, Cu and Zn was enriched in mudflat core (M4) as compared to the mangrove core.

In general at station 1, among the bioavailable fractions, metals in the exchangeable phase (Fe, Mn, Cr, Co and Zn) and organic matter/ sulfide bound (Fe, Mn, Co, Cu and Zn) were enriched in the mudflats, Fe-Mn oxide bound metals (Fe, Cr, Co, Cu) showed little difference and F2 (Mn and Zn) was enriched in the mangroves (Figure 3.1.33). The metals in the exchangeable phase are weakly adsorbed and retained on the solid surface by weak electrostatic interactions and are remobilized by adsorption-desorption reactions and lowering of pH and are released most readily to the environment (Okoro et al., 2012). Metals bound to the organic phase stay in the sediments for longer periods as the decomposition process (Kennedy et al, 1997) immobilizes them. Under oxidizing conditions, degradation of organic matter can release trace metals bound to this component. The organic fraction of metals released during the oxidisable process is associated with stable high molecular weight humic substances or sulfides. The mangrove sediments of the upper middle estuary contained high

organic matter to which metals probably bound easily and were deposited in the sediments. Earlier researchers (Clark et al., 1998; Harbison, 1986; Machado et al., 2002) noted that mangrove sediments are usually characterized by water logged anaerobic soils and have high organic matter and sulfide contents.

### 3.1.F Comparison of sediment geochemical fractions in mangroves and mudflats

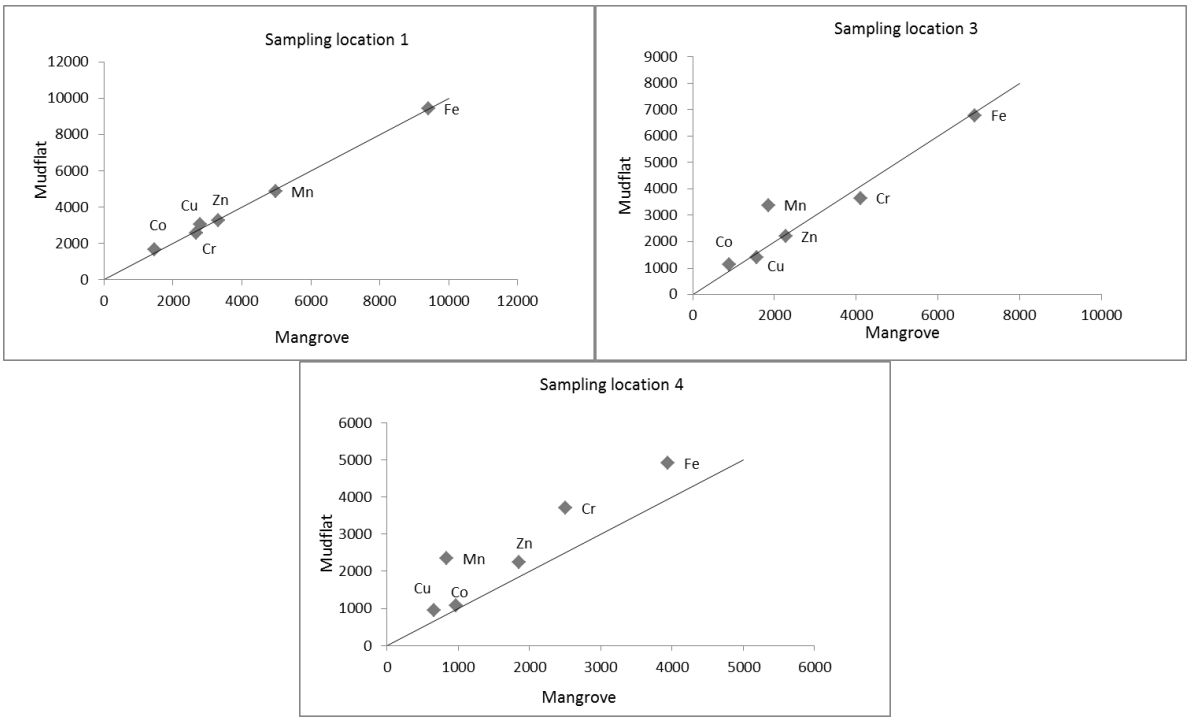


Figure 3.1.32: Isocon diagram of bioavailability of metals in mudflats versus mangroves.

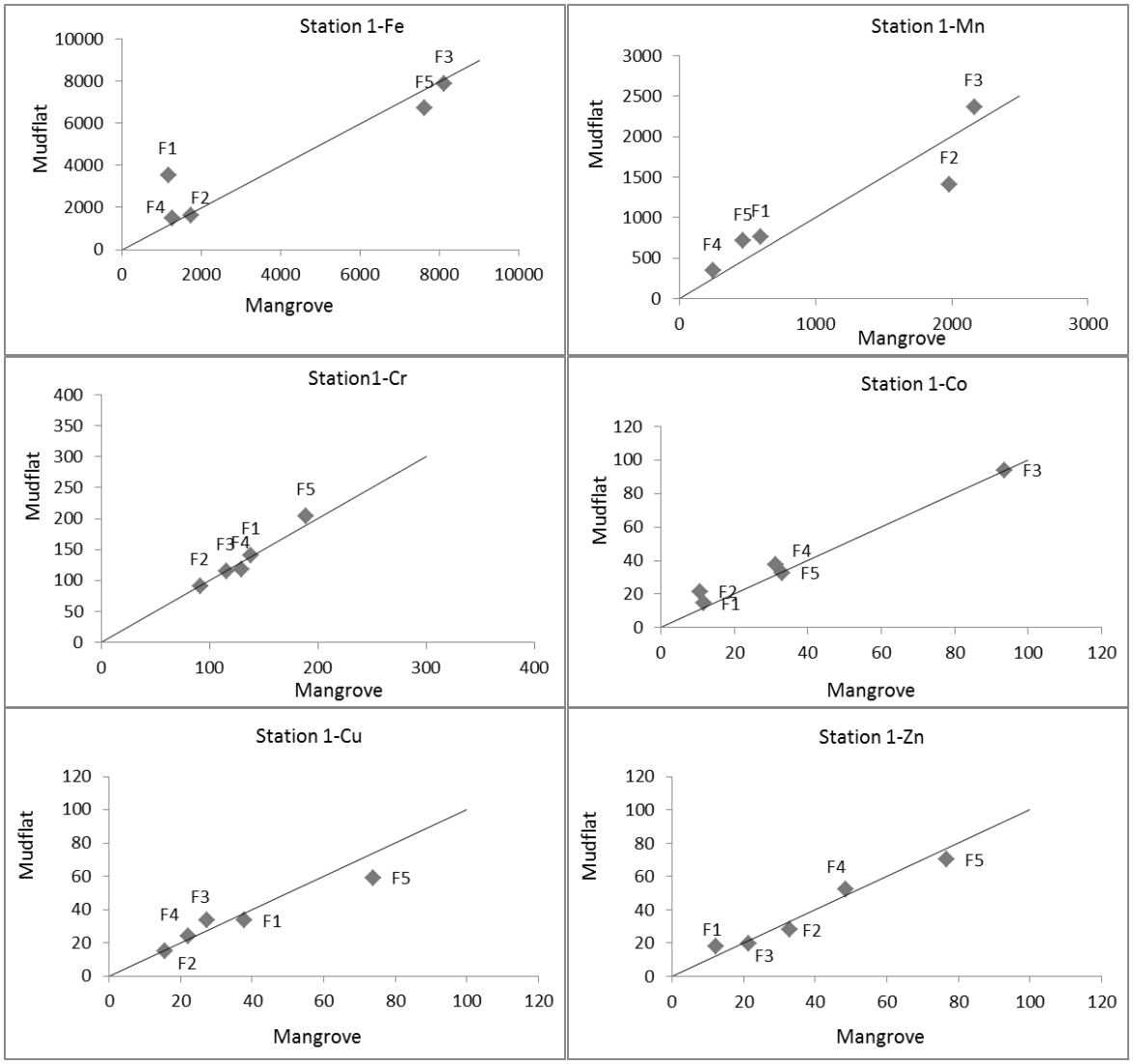


Figure 3.1.33: Isocon diagram of species of metals in mudflats versus mangroves of station 1 of the upper middle estuary.

Low pH values are often observed in mangrove sediments compared to un-vegetated mudflat sediments and are due to the microbial decomposition of mangrove litter and hydrolysis of tannin in mangrove plants, which releases organic acids (Clark et al., 1998; Tam and Wong, 1998). Additionally, the extensive mangrove root system leads to increased oxygen translocation into the sediment that facilitates pyrite oxidation leading to an increase in sediment acidity (Thibodeau and Nickerson, 1986). Thus, oxidation of organic matter may have occurred in mangrove sediments, which released the metals bound to organic matter as compared to mudflats, which have less oxygen percolation into the sediments. These released organic bound metals may have been bound to carbonates or diffused to the water column during tidal inundation where they may have interacted with the sediment particles of the mudflats through weak bonding reactions such as adsorption. The carbonate phase also tends

to adsorb metals when there is a reduction of Fe-Mn oxides and oxidation of organic matter in the aquatic system. Thus, in the upper middle estuary, most metals were noted in the exchangeable fraction in mudflats whereas due to less oxidizing conditions in the mudflats, most metals may have been retained in the organic/ sulfide fraction.

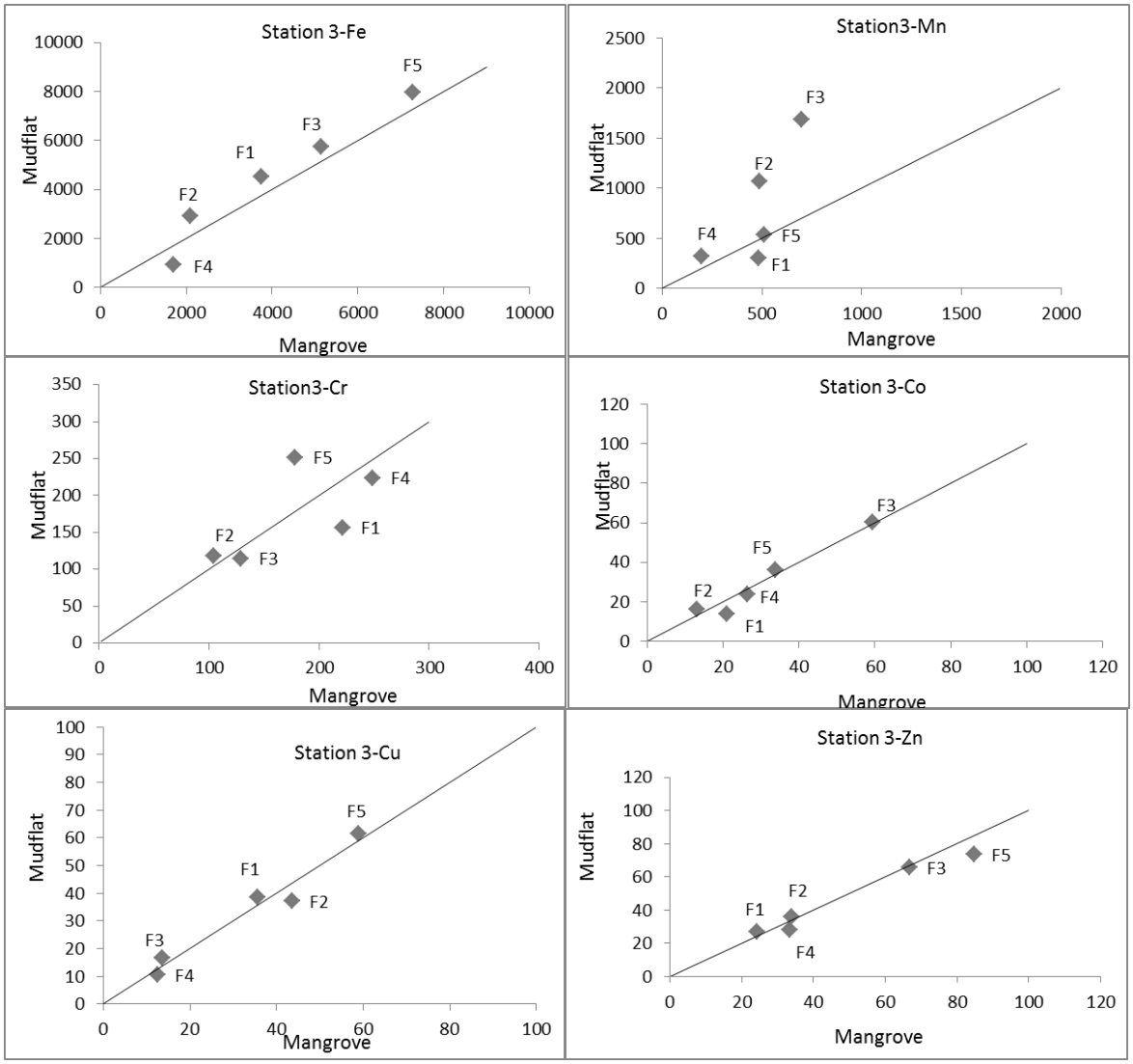


Figure 3.1.34: Isocon diagram of species of metals in mudflats versus mangroves at station 3 of the lower middle estuary.

At station 3, carbonate bound metals (Fe, Mn, Cr, Co and Zn) and Fe-Mn oxide bound metals (Fe, Mn and Cu) were enriched in the mudflats whereas organic matter/ sulfide bound metals (Fe, Cr, Co, Cu and Zn) was enriched in the mangroves (Figure 3.1.34). The exchangeable fraction was distributed in the mudflats for metals Fe, Cu and Zn and in mangrove for Mn, Co and Cr. In the lower middle estuary, higher percentages of silt and clay were recorded in

the mangrove sediments, which may have led to the rapid deposition and preservation of organic matter in the sediment. This might have led to compaction of the sediments with very little amount of oxygen to percolate into the sediments and consequently resulted in low oxidation of organic matter. Thus, most metals associated with the organic matter may have been either preserved or converted/associated with sulfides. However, the lower content of metals in the Fe-Mn oxide and carbonate bound fractions in the mangroves indicated that the metals may have been mobilized through redox changes and diffused from the sediments.

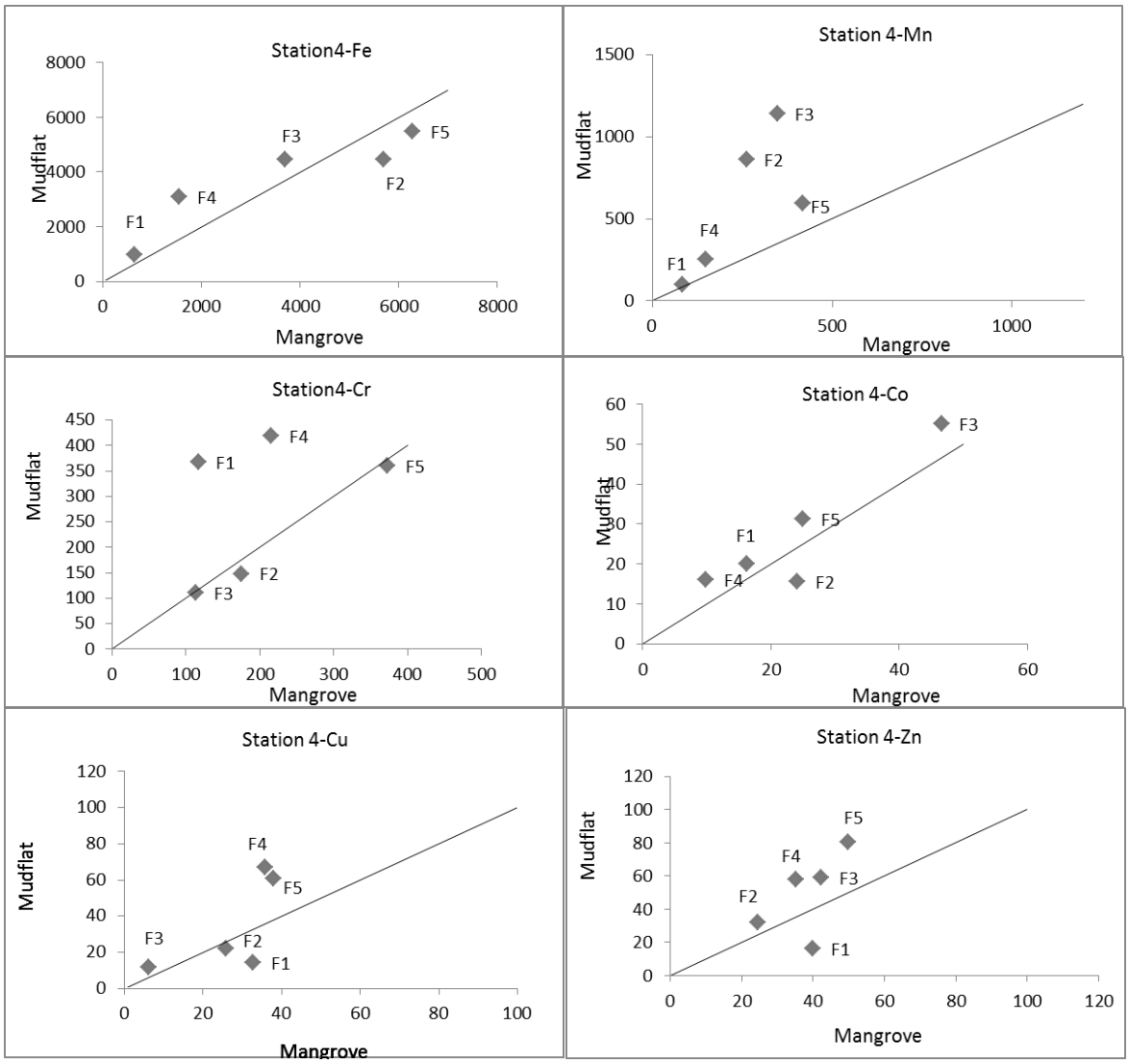


Figure 3.1.35: Isocon diagram of species of metals in mudflats versus mangroves at station 4 of the lower estuary.

The lower middle estuary is tidally influenced than the upper middle estuary. The intertidal flats are submerged and exposed for similar periods. As they are usually submerged during mid tide, when tidal currents tend to reach their maximum speeds, sediment movement is

mainly controlled by these currents, but wave action may also be a factor especially when the water is shallow during the low tide. Thus, the sediments are more disturbed physically as compared to the upstream regions which may cause mobilization of metals from the anoxic sediments and re-precipitated as oxides or loosely bound forms. The higher content of bulk Mn in the mudflats may have trapped the metals that were mobilized from the mangrove sediments.

At sampling location S4, exchangeable (Fe, Mn, Cr, and Co), Fe-Mn oxide bound metals (Fe, Mn, Co, Cu and Zn) and organic matter/ sulfide bound metals (Fe, Mn. Cr, Co, Cu and Zn) were enriched in the mudflats whereas carbonate bound metals (Fe, Cr, Co and Cu) was enriched in mangroves (Figure 3.1.35). In the mangrove sediments, the presence of calcareous material may have caused association of metals with the carbonates. Additionally the higher sand content in the mangroves that comprise larger quartz particles which have trigonal or hexagonal smooth crystal surfaces are unable to provide sufficient interaction area resulting in higher solubility of metals (Guven and Akinci, 2013). Thus, the coarse sediments may have provided low surface for retention of trace metals in loosely bound forms. The higher content of fine sediments and organic matter in the mudflat sediments of the lower estuary effectively trapped trace metals within the sediments. Thus, most metals were adsorbed onto the active surface of clay minerals and organic matter. Studies by Jingchun et al. (2010) found that mangrove sediments have higher salt content compared to mudflat and as salt contents in downstream sites were significantly higher than those in upstream sites of the estuary, which is attributed the salt accumulation in mangrove surface sediments due to evaporation and increased daily tidal inundation in downstream site. The relative high salinity in the lower estuary can inhibit the growth and activity of Sulfate reducing bacteria and thus affect the reduction of $SO4^{2-}$ and the decomposition of organic matter in sediment, resulting in metals bioavailability (Hou et al., 2013; Nizoli and Luiz-Silva, 2012). The high salinity in the lower estuary also enhanced in the content of major cations (e.g., Na, K, Ca, Mg) that compete for the sorption sites with heavy metals and decrease the binding of metals to humic acids (Du Laing et al., 2009).

Thus, the accumulation and bioavailability of metals within sediments depends upon various factors namely organic matter supply, sediment redox conditions, the rate of sulfate reduction, salinity and sediment particle size (Zhang et al., 2014). As sediment physicochemical parameters varied between vegetated and non-vegetated sediments along the

estuary, the partitioning and bioavailability of metals also changed. Studies by Almeida et al. (2005) and Jacob and Otte (2004) showed that sediments colonized by plants exhibit stronger oxidizing conditions than un-vegetated sediments. The surface sediment of mangroves may desiccate during low tide, become aerated by biological processes such as bioturbation or oxygen release from mangrove roots, resulting in oxidizing conditions (Clark et al., 1998). However, due to the high density of roots and a short period of flooding in the mangrove forest environment, the redox status of vegetated sediments may become the key limiting factor for bioavailability of metals in mangroves. In tidal mudflats, where sediments are not aerated by oxygen released from plant roots and higher moisture contents exist due to longer periods of tidal inundation, organic matter content become the important limiting factor for bioavailability of metals.

### 3.1. G Risk assessment

To understand the risk of metals to the sediment-associated benthic organisms, the total metal content in the bioavailable fractions were compared with sediment quality values (SQV) using SQuiRT (screening quick reference table) (Table 3.1.11).

Table 3.1.11: Screening Quick Reference table for metals in marine sediments (Buchman, 1999)

| Metal | Threshold Effect level (TEL) | Effects range level (ERL) | Probable Effects level (PEL) | Effects Range Median (ERM) | Apparent Effects Threshold (AET) |
|---|---|---|---|---|---|
| **Fe** | NA | NA | NA | NA | 22 % (Neanthes) |
| **Mn** | NA | NA | NA | NA | 260 (Neanthes) |
| **Cr** | 52.30 | 81.00 | 160 | 370 | 62 (Neanthes) |
| **Co** | NA | NA | NA | NA | 10 (Neanthes) |
| **Ni** | 15.9 | 20.9 | 42.8 | 51.6 | 110 (Echinoderm larvae) |
| **Cu** | 18.7 | 34 | 108 | 270 | 390 (Microtox and Oyster Larvae) |
| **Zn** | 124 | 150 | 271 | 410 | 410 (Infaunal community) |
| **Sediment guidelines** | | | | | |
| **Threshold Effects Level** | Maximum concentration at which no effects are observed | | | | |
| **Effects Range low** | 10th percentile values in effects | | | | |
| **Probable Effects Level** | Lower limit of the range of concentrations at which adverse effects are always observed | | | | |
| **Effects Range Median** | 50th percentile value in effects | | | | |
| **Apparent Effects Level** | Concentration above which biological indicator effects always observed | | | | |

In the mangroves, the concentration of Fe in the bioavailable fractions and bulk metals at all four stations fell below the Apparent Effects Threshold (AET) indicating no toxicity risk to biota. Mn showed higher concentrations in the bulk sediment as well as in bioavailable fractions than AET with relatively higher values in the upper middle estuary and Cumbharjua canal sediments (Table 3.1.12). Cr concentrations were also higher than the AET in the bulk sediments but lower in the bioavailable fractions. The concentration of Co in the bulk sediments were higher than AET at all four locations, however, Co in the bioavailable fractions was higher than the AET only at upper middle estuary and Cumbharjua canal and posed a toxicity risk. Cu in bulk sediments was greater than the ERL in cores S1, S2 and S3 and greater than TEL at S4 whereas bioavailable Cu was greater than TEL only in core S1. The concentration of Zn at all four mangrove cores was greater than TEL in the bulk sediments whereas bioavailable Zn concentrations did not pose any toxicity risk.

Average concentrations of bulk metals, bioavailable fractions and exchangeable and carbonate bound fraction of Fe, Mn, Cr, Co, Cu and Zn of mudflat sediments are presented in table 3.1.13. In mudflats, the concentration of Fe in the bulk sediments and bioavailable fractions fell below the AET and thus posed no toxicity risk. Mn concentrations in the bulk and bioavailable fractions were greater than the AET with higher values in core M1. Cr concentrations in the bulk sediments were greater than the AET; however, bioavailable Cr did not pose any toxicity risk. Co in the bulk and bioavailable fractions were higher than the AET and may pose considerable risk to biota. Cu concentrations in the bulk sediments were greater than the ERL whereas bioavailable Cu was greater than the TEL in core M1. Zn concentrations in the bulk sediments were greater than the TEL; however, bioavailable Zn did not pose any risk to biota.

Table 3.1.12: Average concentrations of bulk metals, bioavailable fractions and exchangeable and carbonate bound fraction of Fe, Mn, Cr, Co, Cu and Zn of mangrove sediments.

| Mangrove | | Bulk (ppm) | Bioavailable fraction (ppm) | Exchangeable + Carbonate (%) |
|---|---|---|---|---|
| Fe | S1 | 108400 (10.84 %) | 9418 (0.94%) | 0.02 |
| | S2 | 145300 (14.53 %) | 8399 (0.84%) | 0.02 |
| | S3 | 105400 (10.54 %) | 6908 (0.69%) | 0.08 |
| | S4 | 91500 (9.15 %) | 3943 (0.39%) | 0.15 |
| Mn | S1 | 5181*(>AET)* | 4993 *(>AET)* | 47.33 *(High risk)* |
| | S2 | 5122*(>AET)* | 5327*(>AET)* | 27.52 (*Medium risk)* |
| | S3 | 2138*(>AET)* | 1864*( >AET)* | 41.46 *(High risk)* |
| | S4 | 1153*(>AET)* | 844 *(>AET)* | 23.77(*Medium risk)* |
| Cr | S1 | 274 *(>AET)* | 26.75 | 1.07 |
| | S2 | 271*(>AET)* | 23.35 | 1.17 |
| | S3 | 318*(>AET)* | 41.01 | 1.5 |
| | S4 | 336*(>AET)* | 25.04 | 1.38 |
| Co | S1 | 21.75*(>AET)* | 14.73*(>AET)* | 4.65 |
| | S2 | 22.85*(>AET)* | 15.13*(>AET)* | 5.18 |
| | S3 | 23.23*(>AET)* | 8.98 | 7.49 |
| | S4 | 19.98*(>AET)* | 9.67 | 11.86 *(Medium risk)* |
| Cu | S1 | 45.90*(>ERL)* | 27.82 *(>TEL)* | 2.91 |
| | S2 | 36.26 *(>ERL)* | 15.83 | 2.69 |
| | S3 | 42.11*(>ERL)* | 15.6 | 2.4 |
| | S4 | 26.92 *(>TEL)* | 6.59 | 5.6 |
| Zn | S1 | 144*(>TEL)* | 33.21 | 2.05 |
| | S2 | 104*(>TEL)* | 20.91 | 2.61 |
| | S3 | 127*(>TEL)* | 22.9 | 2.76 |
| | S4 | 79.63*(>TEL)* | 18.54 | 7.76 |

Risk assessment code was also used to evaluate the toxicity of the labile phases (exchangeable + carbonate bound) of Fe, Mn, Cr, Co, Cu and Zn in sediments. In the mangrove cores, Fe concentrations in the labile phases posed no risk to the organisms. Mn, however, posed a medium risk in the lower estuary and canal sediments and a high risk in the upper middle and lower middle estuary. Cr in the labile fractions posed a low risk to the biota at all the four locations. Labile Co concentrations posed medium risk in the lower estuary.

The concentrations of labile Cu and Zn fell in the low risk category at all four mangrove cores.

Table 3.1.13: Average concentrations of bulk metals, bioavailable fractions and exchangeable and carbonate bound fraction of Fe, Mn, Cr, Co, Cu and Zn of mudflat sediments.

| Mudflat | | Bulk sediments | Bioavailable Fraction (ppm) | Exchangeable+ Carbonate % |
|---|---|---|---|---|
| Fe | M1 | 10.50 | 9433 (0.94%) | 0.05 |
| | M3 | 10.61 | 6771 (0.68%) | 0.08 |
| | M4 | 10.44 | 4907 (0.49%) | 0.24 |
| Mn | M1 | 5341*(>AET)* | 4875 *(>AET)* | 38.89 *(High risk)* |
| | M3 | 3652*(>AET)* | 3375 *(>AET)* | 35.37 *(High risk)* |
| | M4 | 2665*(>AET)* | 2349*(>AET)* | 32.73*(High risk)* |
| Cr | M1 | 262*(>AET)* | 25.63 | 1.03 |
| | M3 | 369*(>AET)* | 36.53 | 0.97 |
| | M4 | 342*(>AET)* | 37.07 | 2.39 |
| Co | M1 | 25.93*(>AET)* | 16.74 *(>AET)* | 7.33 |
| | M3 | 18.99*(>AET)* | 11.45 *(>AET)* | 6.50 |
| | M4 | 28.10*(>AET)* | 10.67 *(>AET)* | 8.20 |
| Cu | M1 | 46.48*(>ERL)* | 30.35 *(>TEL)* | 2.99 |
| | M3 | 39.74*(>ERL)* | 13.99 | 2.25 |
| | M4 | 41.25*(>ERL)* | 9.48 | 2.26 |
| Zn | M1 | 136*(>TEL)* | 32.61 | 2.25 |
| | M3 | 124*(>TEL)* | 21.98 | 3.34 |
| | M4 | 129*(>TEL)* | 22.38 | 3.72 |

In the mudflat cores, concentration of labile Mn fell in the high risk category at all three mudflat cores whereas labile Cr, Cu and Zn fell in the low risk category and labile Fe concentrations fell in the no risk category.

Thus, the sources and level of input of Mn, Cr and Co should be continuously monitored to understand the risk to the estuarine biota.

### 3.2 Seasonal Study

### 3.2. A Mangroves

#### 3.2. A.1 Sediment components: pH, sand, silt, clay and TOC.

The range and average values of sediment components in mangrove sediments in the premonsoon, monsoon and postmonsoon seasons are presented in table 3.2.1(a).

The pH of the mangrove sediments in the Zuari estuary during premonsoon, monsoon and postmonsoon ranged from 6.54 to 7.22 (average 6.79), 6.05 to 6.85 (average 6.51) and 6.32 to 7.00 (average 6.68) respectively. Sand content in the estuary ranged from 0.97 % to 29.98 % (average 9.57 %) during the premonsoon, 0.77 % to 30.04 % (average 9.23 %) during the monsoon and 0.47 % to 35.57 % (average 10.51 %) during the postmonsoon. The silt content in the estuary varied between 37.56 % and 56.15 % (average 44.18 %) during the premonsoon, 8.48 % and 53.79 % (average 37.30 %) during the monsoon and 34.24 % and 46.38 % (average 39.01 %) during the postmonsoon. The dominant sediment size fraction was clay ranging from 25.97 % to 60.52 % (average 46.26 %) during the premonsoon, 19.38 % to 89.84 % (average 53.47 %) during the monsoon and 27.52 % to 64.54 % (average 50.49 %) during the postmonsoon. The TOC content in the mangrove surface sediments during the premonsoon, monsoon and postmonsoon ranged from 1.88 % to 2.60 % (average 2.26 %), 1.16 % to 3.06 % (average 2.27 %) and 1.46 % to 2.70 % (average 2.30 %) respectively. Average silt was high during the premonsoon, clay during the monsoon, and sand and TOC during the postmonsoon.

In the spatial distribution of sediment components, near neutral pH was noted in the estuary sediments. The pH of the sediments at S1, S2 and S3 was low during monsoon followed by higher values during premonsoon season and postmonsoon (Figure 3.2.1). Highest sand content was noted in the lower estuary for all three seasons. Sand percentage decreased from the upper middle estuary to the lower middle estuary followed by as large increase towards the lower estuary. Considerable amount of sand was also noted in the Cumbharjua canal. Highest silt content was noted in the Cumbharjua canal for all three seasons whereas lowest values were noted in the upper middle estuary. The silt content increased from the upper middle estuary to the lower estuary. Highest clay content was noted in the upper middle estuary during the monsoon season. The clay content in the estuary decreased from the upper middle estuary to the lower estuary.

Table 3.2.1: Range and average values of sediment components and bulk metals in mangrove sediments in the in the premonsoon, monsoon and postmonsoon seasons.

| | | | Premonsoon | | Monsoon | | Postmonsoon | |
|---|---|---|---|---|---|---|---|---|
| | | | Average | Range | Average | Range | Average | Range |
| (a) | Sediment components | pH | 6.79 | 6.54 - 7.22 | 6.51 | 6.05- 6.85 | 6.68 | 6.32- 7.00 |
| | | Sand (%) | 9.57 | 0.97-29.98 | 9.23 | 0.77-30.04 | 10.51 | 0.47-35.57 |
| | | Silt (%) | 44.18 | 37.56-56.15 | 37.30 | 8.48-53.79 | 39.01 | 34.24-46.38 |
| | | Clay (%) | 46.26 | 25.97-60.52 | 53.47 | 19.38-89.84 | 50.49 | 27.52-64.54 |
| | | TOC (%) | 2.26 | 1.88-2.60 | 2.27 | 1.16-3.06 | 2.30 | 1.46-2.70 |
| (b) | Bulk metals | Al (%) | 9.78 | 8.73-10.97 | 9.54 | 5.87-11.34 | 10.40 | 8.11-11.22 |
| | | Fe (%) | 10.93 | 9.79-12.68 | 13.44 | 9.52-19.05 | 7.67 | 6.98-9.08 |
| | | Mn (ppm) | 3734 | 2286-4664 | 5325 | 1847-8983 | 5134 | 3331-6440 |
| | | Cr (ppm) | 353 | 264-542 | 242 | 147-305 | 274 | 246-300 |
| | | Co (ppm) | 22.5 | 17.00-29.50 | 16.94 | 10.00-24.50 | 18.44 | 15.75-21.25 |
| | | Ni (ppm) | 43.19 | 35.50-46.00 | 79.56 | 26.75-118.25 | 50.25 | 32.25-59.25 |
| | | Cu (ppm) | 39.25 | 30.00-48.25 | 113 | 74.25-174.25 | 108 | 101-117 |
| | | Zn (ppm) | 128 | 118-142 | 123 | 95.25-181 | 123 | 117-133 |

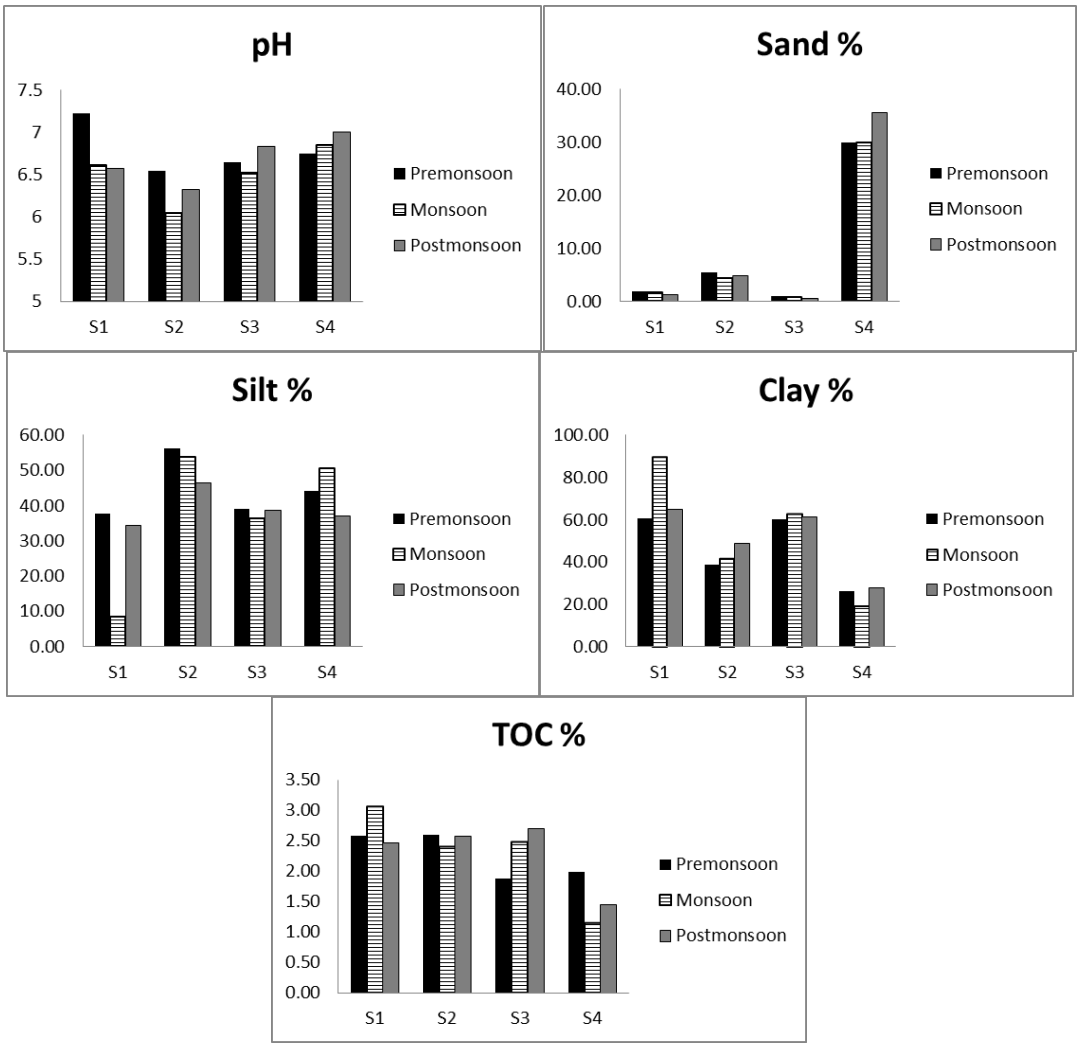


Figure 3.2.1: Spatial distribution of sediment component at stations in mangroves S1, S2, S3 and S4 in the premonsoon, monsoon, and postmonsoon.

Highest TOC content was noted in the upper middle estuary during the monsoon season. TOC percentage decreased from the upper middle estuary towards the lower estuary in the premonsoon and monsoon season. TOC increased from the upper middle estuary to the lower middle estuary during the postmonsoon season but with lowest values in the lower estuary. The distribution of sediment components indicated that the higher sand content was due to the strong hydrodynamics in the lower estuary in all three seasons. The Cumbharjua canal tends to accumulate higher silt content during all three seasons whereas higher clay and TOC accumulated in the upper middle estuary during the monsoon season. The large percentage of silt in the Cumbharjua canal may have brought through the runoff from the Mandovi and

deposited in the canal. Similarly, a large amount of organic matter accumulated in the upper middle estuary along with clay during the monsoon season due to the increase in fluvial runoff as a result of high rainfall and runoff.

### 3.2. A.2 Geochemistry of metals

The concentration of bulk metals in the mangrove sediments during premonsoon, monsoon and postmonsoon are presented in table 3.2.1(b). The percentage of Al during the premonsoon, monsoon and postmonsoon season varied from 8.73 % to 10.97 % (average 9.78 %), 5.87 % to 11.34 % (average 9.54 %) and 8.11 % to 11.22 % (average 10.40 %) respectively. The concentrations of Fe ranged from 9.79 % to 12.68 % (average 10.93 %) during the premonsoon, 9.52 % to 19.05 % (average 13.44 %) during the monsoon and 6.98 % to 9.08 % (average 7.67 %) during the postmonsoon. Mn content ranged from 2286 ppm to 4664ppm (average 3734 ppm) in the premonsoon, 1847 ppm to 8983 ppm (average 5325 ppm) in monsoon and 3331 ppm to 6440 ppm (average 5134 ppm) in the postmonsoon. Cr concentrations varied from 264 ppm to 542 ppm (average 353.13 ppm) in the premonsoon season, 147 ppm to 305 ppm (average 242 ppm) in the monsoon and 246 ppm to 300 ppm (average 274 ppm) in the postmonsoon season. The concentrations of Co in the mangrove sediments ranged from 17.00 ppm to 29.50 ppm (average 22.50 ppm) during the premonsoon, 10.00 ppm to 24.50 ppm (average 16.94 ppm) in the monsoon and 15.75 ppm to 21.25 ppm (average 18.44 ppm) in the postmonsoon. Ni concentrations varied from 35.50 ppm to 46.00 ppm (average 43.19 ppm) in premonsoon, 26.75 ppm to 118.25 ppm (average 79.56 ppm) in monsoon and 32.25 ppm to 59.25 ppm (average 50.25 ppm) in postmonsoon. Cu concentrations varied from 30.00 ppm to 48.25 ppm (average 39.25 ppm) in the premonsoon, 74.25 ppm to 174 ppm (average 113 ppm) in monsoon and 101 ppm to 117 ppm (average 108 ppm) in postmonsoon. Zn content in the mangrove sediments ranged from 118 ppm to 115 ppm (average 128 ppm) in premonsoon, 95.25 ppm to 181 ppm (average 123 ppm) in the monsoon and 117 ppm to 133 ppm (average 123 ppm) in the postmonsoon. Highest average concentrations of Cr, Co and Zn were noted during the premonsoon, Fe, Mn, Ni and Cu during the monsoon and Al during the postmonsoon.

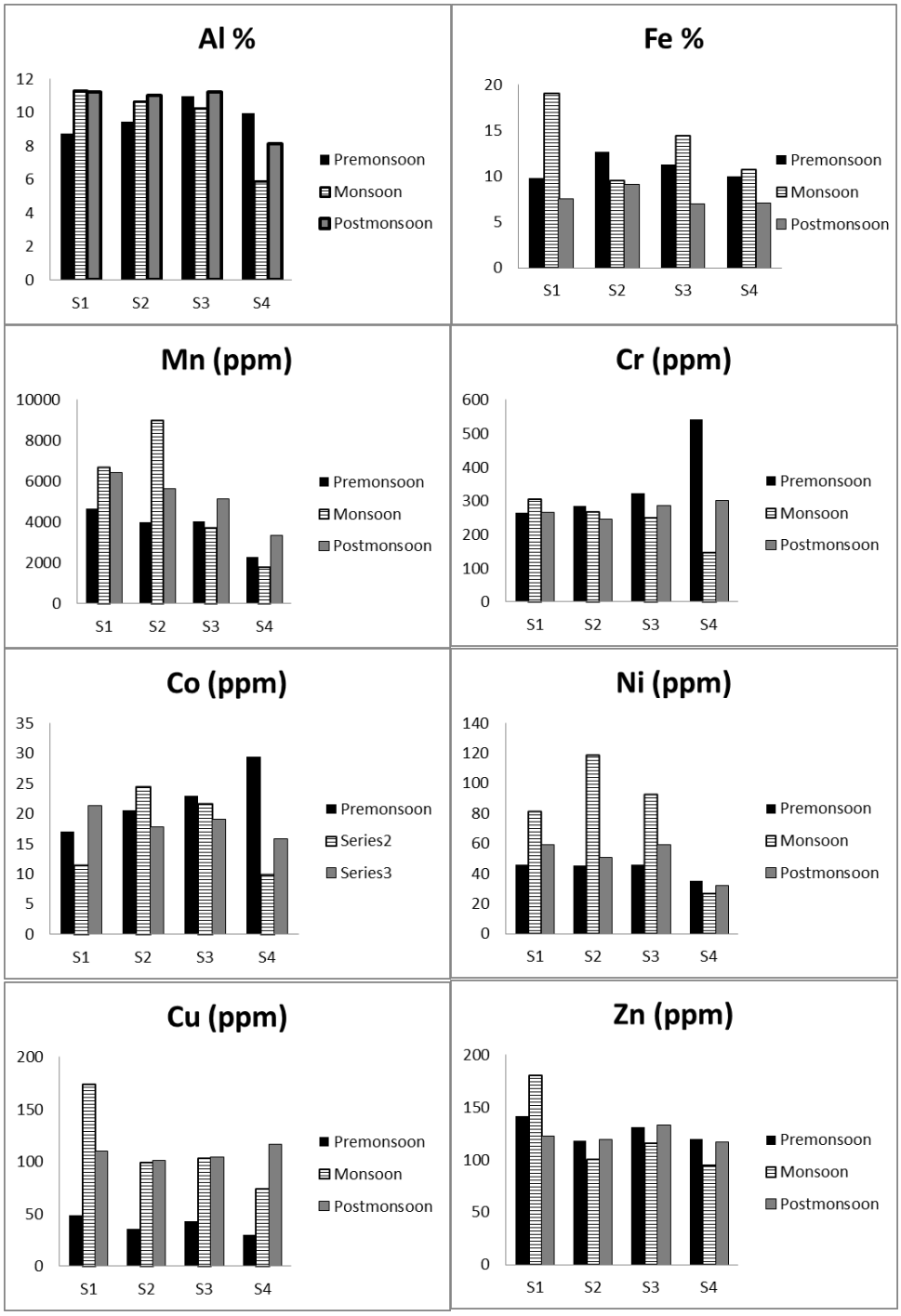


Figure 3.2.2: Spatial distribution of bulk metals at mangrove stations S1, S2, S3 and S4 in the premonsoon, monsoon and postmonsoon.

From the spatial distribution of metals in the mangroves of the Zuari estuary during the three seasons (Figure 3.2.2), it was observed that during the premonsoon season, the concentrations of Cr and Co increased along with sand from the upper middle to lower estuary. Fe along with silt exhibited similar distribution pattern with higher value in the Cumbharjua canal. Ni,

Cu and Zn showed decrease along with clay and Mn, during the premonsoon season from the upper middle to lower estuary with highest values in the upper middle estuary indicating their association with clay and co-precipitation with Mn oxides. Following premonsoon, concentration of most metals (Al, Fe, Mn, Ni, and Cu) increased, during the monsoon. The highest concentrations of Cr, Cu and Zn along with clay, TOC Al and Fe, decreased from the upper middle estuary towards the lower estuary during monsoon indicating source from the catchment area and the role of aluminosilicates, TOC and Fe oxides that favoured the retention of metals in sediments in the upstream region. Mn and Ni exhibited similar spatial distribution trend with peak values in the Cumbharjua canal. In the postmonsoon season, Co, Ni, Zn along with clay, TOC, Al and Mn exhibited similar distribution with overall decreasing trend from the upper middle estuary towards the lower estuary with enrichment in the lower middle estuary. Cr and Cu increased along with sand from the upper middle to lower estuary indicating their association with coarse sediments. Fe and silt exhibited similar spatial distribution pattern with peak values in the Cumbharjua canal.

It is thus apparent that metals show different associations with different seasons in the Zuari estuary mangrove sediments. During the pre-monsoon (dry) season, the water in the estuarine system remains well mixed and the intrusion of salt water is felt as far as 65 km upstream (Qasim and Sengupta, 1981). In natural settings, flocculation of clay minerals occurs dominantly in estuaries where fluvial (approximately 0 psu) waters are mixed with marine waters (approximately 30 psu) (Sutherland et al., 2015). Fe and Mn are known to precipitate at lower salinity through the formation of oxyhydroxides. Early removal of metals from solution occurs on changes of physicochemical properties of water in the upstream, through processes of flocculation and adsorption onto the active surfaces of clay minerals and Fe-Mn oxyhydroxides that are deposited to the sediments. Thus most trace metals (Ni, Cu and Zn) might have adsorbed on these oxides and clay particles and deposited in the upper middle estuary. Cr and Co along with sand were enriched in the lower estuary and may have been derived from local sources. Fe in the Cumbharjua canal either may have associated with the silt sized particle or formed large clusters that fall in the silt size range.

During the monsoon season, the estuary becomes stratified and a salt wedge is formed which extends up to about 12 km in the Zuari estuary. Heavy precipitation and land runoff in the monsoon season bring about large changes in physicochemical properties of the estuarine waters and the estuary becomes freshwater dominated. The large influx of terrestrial runoff

adds considerable suspended material to the estuary. Also abundant ore material is being flushed into the estuary that is stored on the banks in the upstream region for loading onto barges (Kessarkar et al., 2013). Since small rivers are originating from monsoon-dominated and/or mountainous regions, their total TOC contribution to the estuarine system must be substantial (Shynu et al., 2015). Thus high amount of aluminosilicates, Fe-Mn oxides and organic matter in the estuary many have trapped the trace metals (Cr, Cu and Zn) in the upper middle estuary. The monsoon season is followed by a recovery period during the postmonsoon season wherein there is a reduction in fresh water influx. Higher accumulation of trace metals, Co, Ni and Zn were related to the high content of fine sediments, organic matter and Mn oxides in the upper middle estuary that were brought during the monsoons. Cr and Cu were found to be enriched in the lower estuary and may be products of local discharges.

### 3.2.B Mudflats

#### 3.2.B.1 Sediment components: pH, sand, silt, clay and TOC

The range and average values of sediment components and metals in the mudflats along the Zuari estuary in premonsoon, monsoon and postmonsoon are presented in table 3.2.2.

The pH of the mudflat sediments during the premonsoon, monsoon and postmonsoon season ranged from 6.72 to 7.21 (average 6.93), 6.95 to 7.46 (average 7.21) and 6.75 to 7.05 (average 6.93) respectively. The percentage of sand varied from 1.90 % to 9.65 % (average 4.66 %) during the premonsoon, 3.93 % to 6.98 % (average 5.16 %) in the monsoon and 0.40 % to 3.57 % (average 1.83 %) in the postmonsoon. Silt varied from 36.54 % to 45.35 % (average 41.37 %) in the premonsoon, 32.58 % to 50.45 % (average 40.78 %) in monsoon and 36.27 % to 43.29 % (average 40.39 %) in the postmonsoon. Clay dominated the mudflat sediments ranging from 45.00 % to 61.56 % (average 53.97 %) in premonsoon, 42.57 % to 62.83 % (average 54.06 %) in monsoon and 55.20 % to 60.16 % (average 57.79 %) in postmonsoon. TOC exhibited minor seasonal variations ranging from 2.12 % to 2.75 % (average 2.45 %) in premonsoon, 2.11 % to 3.03 % (average 2.60 %) in monsoon and 2.23 % to 2.76 % (average 2.51 %) in postmonsoon.

Table 3.2.2 : Range and average values of sediment components and bulk metals in the mudflat sediments in the premonsoon, monsoon and postmonsoon seasons.

| | | | Premonsoon | | Monsoon | | Postmonsoon | |
|---|---|---|---|---|---|---|---|---|
| | | | Average | Range | Average | Range | Average | Range |
| (a) | Sediment components | pH | 6.93 | 6.72-7.21 | 7.21 | 6.95-7.46 | 6.93 | 6.75-7.05 |
| | | Sand (%) | 4.66 | 1.90-9.65 | 5.16 | 3.93-6.98 | 1.83 | 0.40-3.57 |
| | | Silt (%) | 41.37 | 36.54-45.35 | 40.78 | 32.58-50.45 | 40.39 | 36.27-43.29 |
| | | Clay (%) | 53.97 | 45.00-61.56 | 54.06 | 42.57-62.83 | 57.79 | 55.20-60.16 |
| | | TOC (%) | 2.45 | 2.12-2.75 | 2.60 | 2.11-3.03 | 2.51 | 2.23-2.76 |
| (b) | Bulk metals | Al (%) | 10.29 | 10.12-10.51 | 10.38 | 8.65-11.58 | 10.93 | 10.29-11.45 |
| | | Fe (%) | 10.91 | 10.56-11.52 | 13.21 | 9.53-15.56 | 7.79 | 7.44-8.18 |
| | | Mn (ppm) | 4384 | 2747-5985 | 4892 | 3746-6251 | 5472 | 4243-6422 |
| | | Cr (ppm) | 335 | 306-385 | 235 | 176-271 | 262 | 242-296 |
| | | Co (ppm) | 26.50 | 19.50-32.25 | 15.00 | 6.75-19.75 | 18.75 | 14.50-23.00 |
| | | Ni (ppm) | 42.67 | 38.50-48.25 | 80.50 | 72.50-89.25 | 68.08 | 60.25-83.50 |
| | | Cu (ppm) | 41.42 | 37.50-48.50 | 122 | 97.50-166 | 111 | 99.50-120 |
| | | Zn (ppm) | 136 | 126-150 | 124 | 108-155 | 118 | 99.75-136 |

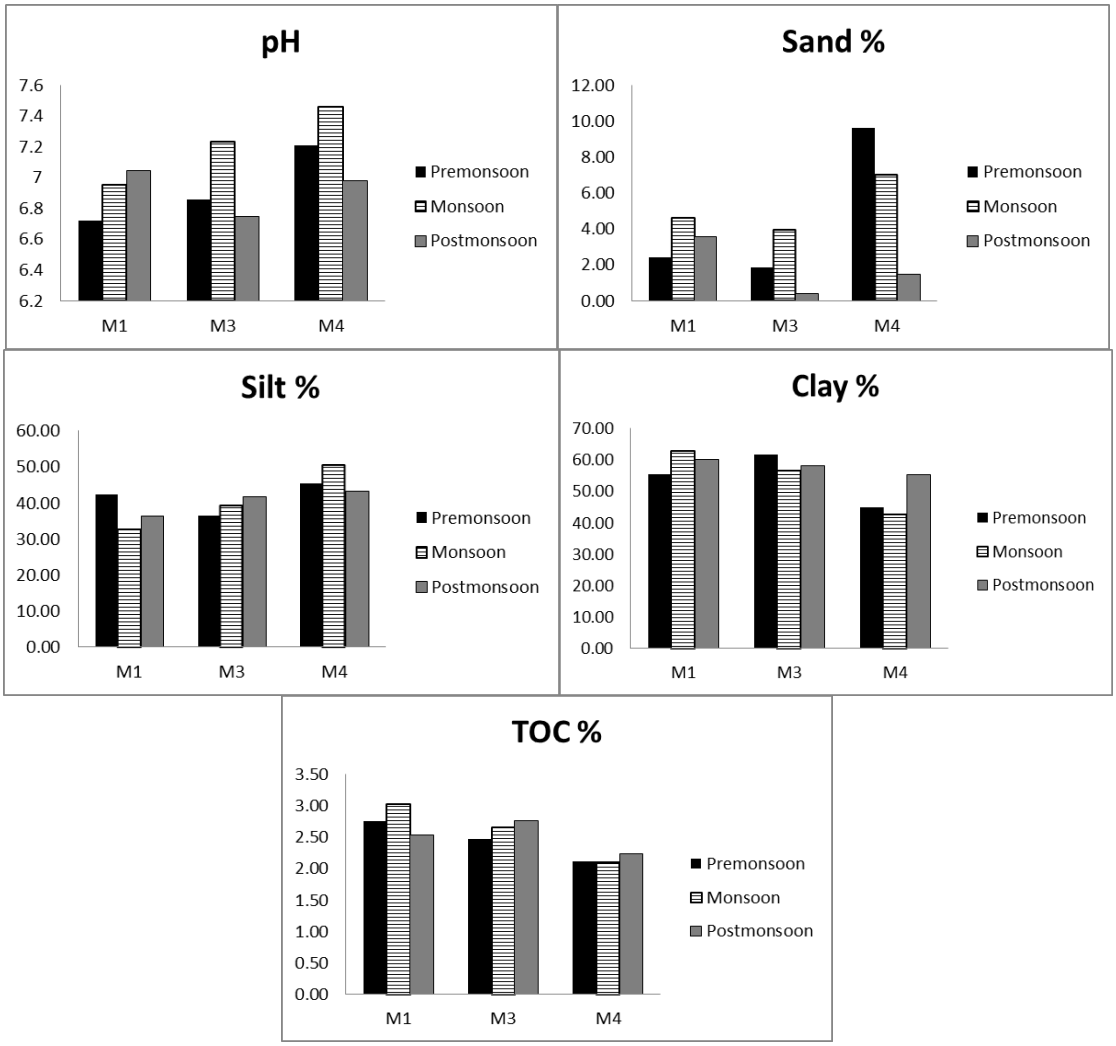


Figure 3.2.3: Spatial distribution of sediment components at stations M1, M3 and M4 in the premonsoon, monsoon and postmonsoon.

The spatial distribution of sediment components in the mudflat sediments (Figure 3.2.3) indicated that pH increased from the upper middle estuary to the lower estuary in the premonsoon and monsoon season whereas higher pH were noted in the upper middle estuary in the postmonsoon season. Sand content gradually increased towards the lower estuary in the premonsoon and monsoon season owing to strong hydrodynamics but showed lower percentage in the postmonsoon season. Silt content increased towards the lower estuary in monsoon and postmonsoon seasons. In premonsoon season, silt was low in the lower middle estuary. Clay exhibited higher percentage in the lower middle estuary during the premonsoon whereas gradually decreased in clay content was observed from the upper middle estuary to the lower estuary during the monsoon and postmonsoon. TOC was enriched in the upper

middle estuary mudflats in the premonsoon and monsoon, which decreased towards the lower estuary whereas higher TOC was noted in the lower middle estuary in the postmonsoon season.

### 3.2. B.2 Geochemistry of metals

The concentration of Al in mudflat sediments of the Zuari estuary ranged from 10.12 % to 10.51 % (average 10.29 %) in the premonsoon, 8.65 % to 11.58 % (average 10.38 %) in the monsoon and 10.29 % to 11.45 % (average 10.93 %) in the postmonsoon (Table 3.2.2(b)). Fe concentrations ranged from 10.56 % to 11.52 % (average 10.91 %) in premonsoon, 9.53 % to 15.56 % (average 13.21 %) in monsoon and 7.44 % to 8.18 % (average 7.79 %) in postmonsoon. Mn content in the mudflat sediment varied from 2747 ppm to 5985 ppm (average 4384 ppm) in premonsoon, 3746 ppm to 6251 ppm (average 4892 ppm) in monsoon and 4243 ppm to 6422 ppm (average 5472 ppm) in postmonsoon. Cr concentrations in the estuarine mudflats ranged from 306 ppm to 385 ppm (average 335 ppm) in premonsoon, 176 ppm to 271 ppm (average 235 ppm) in monsoon and 242 ppm to 296 ppm (average 262 ppm) in postmonsoon. Co concentrations varied from 19.50 ppm to 32.25 ppm (average 26.50 ppm) in premonsoon, 6.75 ppm to 19.75 ppm (average 15.00 ppm) in monsoon and 14.50 ppm to 23.00 ppm (average 18.75 ppm) in postmonsoon. Ni concentrations varied from 38.50 ppm to 48.25 ppm (average 42.67 ppm) in premonsoon, 72.50 ppm to 89.25 ppm (average 80.50 ppm) in monsoon and 60.25 ppm to 83.50 ppm (average 68.08 ppm) in postmonsoon. Cu content in sediments ranged from 37.50 ppm to 48.50 ppm (average 41.42 ppm) in premonsoon, 97.50 ppm to 166 ppm (average 122 ppm) in monsoon and 99.50 ppm to 120 ppm (average 111 ppm) in postmonsoon. Zn concentrations varied from 126 ppm to 150 ppm (average 136 ppm) in premonsoon, 108 ppm to 155 ppm (average 124 ppm) in monsoon and 99.75 ppm to 136 ppm (average 118 ppm) in postmonsoon. Highest average concentrations of Cr, Co and Zn were noted in the premonsoon, Fe, Ni and Cu in the monsoon and Al and Mn in postmonsoon.

When the spatial distribution of metals namely Cr, Co and Zn in the mudflat sediments (Figure 3.2.4) of premonsoon season are considered, they varied similar to sand, silt and Al distributions. These metals concentration decreased from the upper middle estuary to the lower middle estuary followed by higher value in the lower estuary indicating that input of Cr, Co and Zn was from the upstream regions of the estuary as well as from local point sources in the lower estuary. Cu co-varied with Fe, Mn and TOC with highest values in the

upper middle estuary indicating that Cu was co-precipitated along with Fe-Mn oxides and organic matter. Ni showed increase towards the lower estuary.

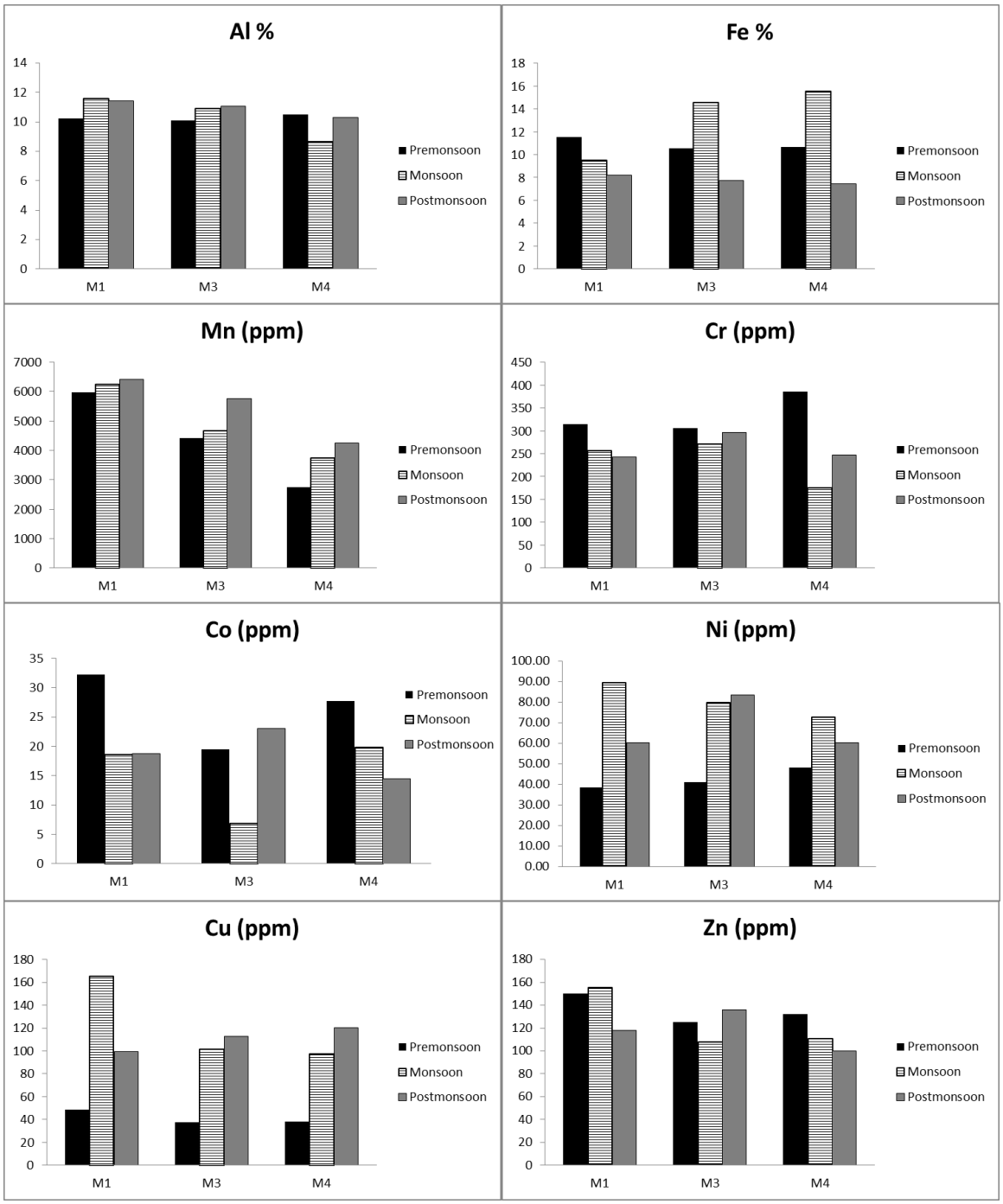


Figure 3.2.4: Spatial distribution of bulk metals at stations M1, M3 and M4 in the premonsoon, monsoon and postmonsoon.

Following premonsoon, most metals (Al, Fe, Mn, Ni, Cu and Zn) concentrations considerably increased. In monsoon, the spatial distribution of Cr, Ni, Cu and Zn co-varied with clay, TOC, Al and Mn whereas decreasing trend towards the lower estuary was noted with highest concentration in the upper middle estuary. Fe exhibited similar distribution to silt with increasing trend from the upper middle estuary to the lower estuary. The spatial distribution Co was noted to be similar to the distribution of sand where low content was noted in the lower middle estuary and high values were noted in the lower estuary. In the postmonsoon season, trace metal distribution of Cr, Co, Ni and Zn co-varied along with the distributions of TOC with peak values in the lower middle estuary whereas the distribution of Cu was similar to silt with higher concentration in the lower estuary. Al, Fe and Mn exhibited similar distribution pattern to clay with a gradual decrease from the upper middle estuary to the lower estuary.

The metal distribution showed seasonal differences in the mudflat sediments of the Zuari estuary. In the premonsoon season, most trace metals Cr, Co, Ni, Cu and Zn are enriched in the upper middle estuary sediments. This enrichment was due to the removal of metals during early estuarine mixing of fluvial and seawater. Further, enrichment of metals towards the upstream region of the estuary must be due to the proximity of the sampling location to the metal sources namely mining and ore processing units located in the upper reaches of the estuary, which could be a contributory factor for metals. Additionally, sediment grain size, organic matter and hydrous Fe-Mn oxides played a considerable role in the adsorption and deposition of metals to the sediments. In the monsoon, trace metals Co, Cr, Ni, Cu and Zn were enriched in the upper middle estuarine sediments along with fine sediments, organic matter and Mn oxides possible due to the large influx of fresh sedimentary material during the monsoon land runoff and may be altering the elemental budget in the estuarine sediments (Joseph and Srivastava, 1993). Significant amount of suspended /fine sediments and organic matter are added to the estuary that favors binding of metals, during this season. In the postmonsoon season, Cr, Co, Ni and Zn were enriched in the lower middle estuary along with organic matter suggests that these metals may be associated with sewage or industrial effluents. Dessai et al. (2009) made a similar observation, with higher enrichment of metals in the postmonsoon season in the middle estuary. Most metals showed low concentrations in the lower estuary. During the postmonsoon, the river discharge is negligible and saltwater intrudes progressively into the estuarine channel (Shetye et al., 2007). The absence of estuarine circulation and saltwater intrusion suppress turbulence and effectively removes fine

suspended sediments from the channel. Rao et al. (2011) reported that the turbidity maximum occurs in the bay region of Zuari estuary due to resuspension fine sediments from the marginal tidal flats and the combined the effect of wind-generated and ebb currents at neap tide and their interaction with shallow bottom may have eroded and re-suspended sediments from the shallow bathymetry.

### 3.2. C Geoaccumulation index

#### 3.2. C.1 Mangroves

The geoaccumulation index was computed for metals, Fe, Mn, Cr, Co, Ni, Cu and Zn (Table 3.2.3). It was noted that in premonsoon, Igeo values of Mn and Cr fell in class 2 (Igeo 1-2) of moderately polluted sediments, Fe in class 1(Igeo 0-1) of unpolluted to moderately polluted sediments and Co, Ni, Cu and Zn in class 0 (Igeo <0) of unpolluted sediments. In the monsoon season, Igeo values of Fe, Mn, Ni and Cu have shown considerable increase as compared to premonsoon season whereas Cr, Co and Zn showed a decrease. Mn fell in class 3 (Igeo 2-3) of moderately to strongly polluted sediments, Fe, Cr, Ni and Cu values fell in class1 (Igeo 0-1) of unpolluted to moderately polluted sediments and Co and Zn fell in class 0 (Igeo < 0) of unpolluted sediments. In the postmonsoon season, Fe, Mn, Ni, and Cu values showed decrease as compared to monsoon season whereas Cr and Co Igeo values have showed an increase. Mn fell in class 3 (Igeo 2-3) of moderately to strongly polluted sediments, Cr fell in class 2 (Igeo1-2) of moderately polluted sediments, Fe and Cu fell in class 1 (Igeo 0-1) of unpolluted to moderately polluted sediments and Co, Ni and Zn fell in class 0 (Igeo<0) of unpolluted sediments.

Table 3.2.3: Geoaccumulation index of metals in mangrove sediments in premonsoon, monsoon and postmonsoon.

| | **Igeo-Mangrove** | | | | | | |
|---|---|---|---|---|---|---|---|
| | Fe | Mn | Cr | Co | Ni | Cu | Zn |
| **Premonsoon** | 0.63 | 1.55 | 1.39 | -0.34 | -0.80 | -0.78 | -0.16 |
| **Monsoon** | 0.93 | 2.06 | 0.84 | -0.75 | 0.09 | 0.74 | -0.21 |
| **Postmonsoon** | 0.11 | 2.01 | 1.02 | -0.63 | -0.58 | 0.68 | -0.21 |

#### 3.2. C.2 Mudflats

Considerable seasonal variation was noted in the Igeo values in the mudflat sediments (Table 3.2.4). In premonsoon season, Igeo values of Mn and Cr fell in class 2 (Igeo 1-2) of moderately polluted sediments, Fe in class 1 (Igeo 0-1) of unpolluted to moderately polluted

sediments and Co, Ni, Cu and Zn in class 0 (Igeo<0) of unpolluted sediments, similar to mangrove sediments. In the monsoon season, Fe, Mn, Ni, and Cu Igeo values significantly increased as compared to premonsoon season whereas Cr, Co and Zn decreased. Mn fell in class 2 (Igeo 1-2) of moderately polluted sediments, Fe, Cr, Ni, and Cu fell in class 1 (Igeo 0-1) of unpolluted to moderately polluted sediments and Co and Zn in class 0 (Igeo<0) of unpolluted sediments.

Table 3.2.4 Geoaccumulation index of metals in mudflat sediments in premonsoon, monsoon and postmonsoon.

| | **Igeo-Mudflats** | | | | | | |
|---|---|---|---|---|---|---|---|
| | Fe | Mn | Cr | Co | Ni | Cu | Zn |
| **Premonsoon** | 0.62 | 1.78 | 1.31 | -0.10 | -0.81 | -0.70 | -0.07 |
| **Monsoon** | 0.90 | 1.94 | 0.80 | -0.93 | 0.10 | 0.85 | -0.20 |
| **Postmonsoon** | 0.14 | 2.10 | 0.96 | -0.60 | -0.14 | 0.72 | -0.27 |

In postmonsoon, Mn, Cr and Co Igeo values increased as compared to monsoon season whereas Fe, Ni, Cu and Zn values decreased. Igeo value of Mn fell in class 3 (Igeo 2-3) of moderately to strongly polluted sediments, Fe, Cr and Cu fell in class 1 (Igeo 0-1) of unpolluted to moderately polluted sediments and Co and Ni in class 0 (Igeo <0) of unpolluted sediments.

The considerable increase in Igeo values in the monsoon season was due to the increase in the terrestrial runoff from the catchment area which adds considerable amount of trace metals of anthropogenic origin into the estuary.

### 3.2. D Speciation of metals

### 3.2. D.1 Mangroves

#### 3.2. D.1a Iron

The concentration Fe in the mangrove sediments of the Zuari estuary varied in the order of abundance F5>F3>F4>F1>F2 in premonsoon, monsoon and post monsoon season. The concentration of Fe in the residual phase varied from 63122 ppm to 85063 ppm (average 76718 ppm) in premonsoon, 58010 ppm to 92243 ppm (average 76959 ppm) in monsoon and 68060 ppm to 91495 ppm (average 80454 ppm) in postmonsoon. Fe in the reducible fraction varied from 4403 ppm to 8453 ppm (average 6833 ppm) in premonsoon, 5948 ppm to 6465 ppm (average 6221 ppm) in monsoon and 4243 ppm to 6288 ppm (average 5381 ppm) in

postmonsoon. Fe content in the oxidisable fraction varied from 185 ppm to 750 ppm (average 566 ppm) in premonsoon, 374 ppm to 2154 ppm (average 1279 ppm) in monsoon and 62.50 ppm to 555 ppm (average 329 ppm) in postmonsoon. The concentrations of Fe n the exchangeable phase ranged from 7.30 ppm to 113 ppm (average 52.33 ppm) in premonsoon, 2.10 ppm to 89.20 ppm (average 43.91 ppm) in monsoon and 5.73 ppm to 101 ppm (average 61.59 ppm) in postmonsoon. The least concentration of Fe was associated with the carbonate fraction with concentrations ranging from 0.53 ppm to 1.68 ppm (average 1.24 ppm) in premonsoon, 0.45 ppm to 6.78 ppm(average 2.81 ppm) in monsoon and 0.48 ppm to 87.13 ppm (average 23.28 ppm) in post monsoon. Highest average concentrations of reducible Fe was noted in the premonsoon, oxidisable Fe in monsoon, and exchangeable, carbonate and residual Fe in the post monsoon. Overall, highest bioavailable Fe (F1+F2+F3+F4) was noted in the monsoon season (7547 ppm) followed by premonsoon (7452 ppm) and postmonsoon (5795 ppm).

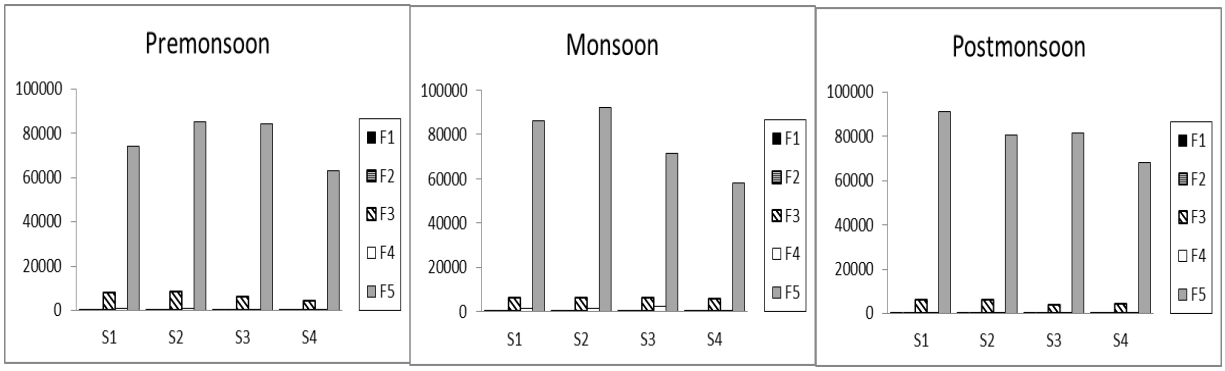


Figure 3.2.5: Spatial distribution of Fe speciation in mangrove sediments in the premonsoon, monsoon and postmonsoon.

The spatial distribution of Fe in the five fractions (Figure 3.2.5) revealed that the bioavailable Fe (sum of the first four fractions) was negligible in concentration as compared to the residual fraction at all four mangrove sites. However, among bioavailable phases, higher Fe in the Fe-Mn oxide bound fraction was noted at S1 and S2 in the premonsoon season as compared to monsoon and postmonsoon seasons. Residual Fe during the premonsoon increased from the upper middle estuary to the lower middle estuary followed by low concentrations in the lower estuary whereas gradual decrease was noted in monsoon and postmonsoon season towards the mouth of the estuary. Residual Fe was enriched at S2 in premonsoon and monsoon season indicating that the significant amount of Fe was supplied to the Zuari estuary, from the Mandovi estuary through the Cumbharjua canal, more

prominently during the monsoon season as the water flows from Mandovi to Zuari through this canal.

### 3.2. D.1b Manganese

Significant amount of Mn was available in the bioavailable phases of the mangrove sediments. The concentration of Mn in the mangrove sediments of the Zuari estuary varied in the order of abundance F3>F2>F5>F1>F4 in premonsoon, F3>F1>F5>F2>F4 in monsoon and F3>F5>F2>F1>F4 in postmonsoon. Mn content in the reducible phase was high in all three seasons and ranged from 543 ppm to 2258 ppm (average 1330 ppm) in premonsoon, 470 ppm to 4418 ppm (average 1925 ppm) in monsoon and 1188 ppm to 3220 ppm (average 2119 ppm) in postmonsoon. Mn in the carbonate phase varied from 496 ppm to 1641 ppm (average 967 ppm) in premonsoon, 238 ppm to 800 ppm (average 475 ppm ) in monsoon and 335 ppm to 668 ppm (average 521 ppm) in postmonsoon. Considerable amount of Mn was available in the exchangeable phase ranging from 116 ppm to 613 ppm (average 368 ppm) in premonsoon, 50.10 ppm to 1546 ppm (average 736 ppm) in monsoon and 35.08 ppm to 782 ppm (average 461 ppm) in postmonsoon. Least bioavailable Mn was associated with the oxidisable phase in all three seasons with concentrations ranging from135 ppm to 233 ppm (average 178 ppm) in premonsoon, 31.48 ppm to 828 ppm (average 358 ppm) in monsoon and 62.50 ppm to 555 ppm (average 329 ppm) in postmonsoon. Residual Mn varied seasonally ranging from 463 ppm to 595 ppm (average 511 ppm) in premonsoon, 368 ppm to 810 ppm (average 530 ppm) in monsoon and 603 ppm to 650 ppm (average 619 ppm) in postmonsoon. Overall, highest bioavailable Mn was noted in the monsoon (3493 ppm) followed by postmonsoon (3431 ppm) and premonsoon (2845 ppm).

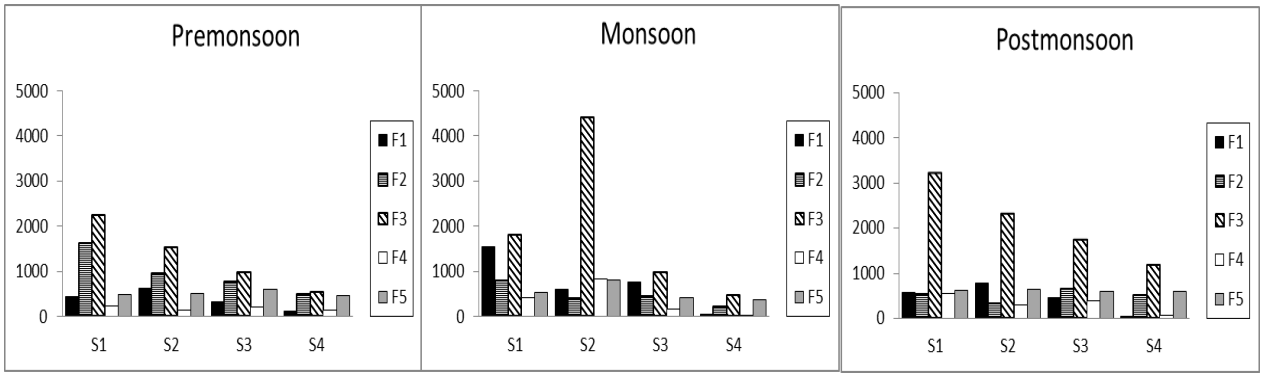


Figure 3.2.6 Spatial distribution of Mn speciation in mangrove sediments in the premonsoon, monsoon and postmonsoon.

The spatial distribution of Mn in the five fractions is presented in figure 3.2.6. The concentration of Mn in the bioavailable fractions exhibited significant variations across the three seasons. Exchangeable Mn exhibited a decreasing trend from the S1 to S4 with peak values at S2 in the premonsoon and postmonsoon seasons. However, in the monsoon season, there was a considerable increase in exchangeable Mn at S1 and S3. Carbonate bound Mn showed a decreasing trend from S1 to S4 during the premonsoon season followed by lower concentrations during the monsoon season and enrichment at S3 and S4 in postmonsoon season. Most seasonal variability was noted for the Fe-Mn oxide fraction. The concentration of reducible Mn decreased from S1 to S4 in the premonsoon and postmonsoon, with relatively higher values during the postmonsoon. In monsoon, lower concentrations were noted at S1 and S4 whereas enrichment at S2 was noted. Oxidisable Mn concentrations were very low in premonsoon season, followed by increase at S1 and S2 in the monsoon and increase at S1 and S3 in postmonsoon. Residual Mn exhibited little variation with seasons.

The upstream regions of the Zuari estuary have high Mn content due to the ore bearing landmass (Zingde et al., 1976) and storage of ores on banks for transportations. Leachates from the stored ore enter into the estuarine waters and are removed to the sediments as oxides through processes of precipitate and flocculation of encountering saline waters in the estuary. Thus, most Mn is removed in the upstream regions of the estuary resulting in enrichment in sediments. In the monsoon season, due to increase in fresh water input to the estuary, the Mn oxides formed in the sediments may undergo partial dissolution resulting in lower concentrations in the Fe-Mn oxide fraction and enrichment in the labile fractions (exchangeable and carbonate bound). Further, when there is heavy influx of fresh water from the river, the estuarine sediments may be exchanging part of the exchangeable phase of the metals of the water (Ouseph, 1987). A large amount of Mn enters into the estuary through run off and accumulates in the sediments from anthropogenic sources. This was also reported earlier. Additionally, the enrichment of reducible Mn in the Cumbharjua canal indicated large contribution of Mn from the Mandovi estuary to the Zuari estuary through the canal. In the postmonsoon season, due to decreasing fluvial discharge and with intrusion of sea water, the Mn re-precipitates as oxides in the estuary.

### 3.2. D.1c Chromium

Cr was less associated with the bioavailable phase and exhibited little spatial variability in all three seasons. The abundance of Cr in the five fractions varied in the order of abundance

F5>F4>F3>F1>F2 in premonsoon, monsoon and postmonsoon seasons. Most Cr was associated with the residual fraction ranging from 153 ppm to 240 ppm (average 193 ppm) in premonsoon, 171 ppm to 236 ppm (average 206 ppm) in monsoon and 195 ppm to 257 ppm (average 220 ppm) in postmonsoon. However, among the bioavailable phases, considerable amount of Cr was associated with the oxidisable phase varying from 12.08 ppm to 25.60 ppm (average 16.85 ppm) in premonsoon, 7.28 ppm to 13.23 ppm (average 11.31 ppm ) in monsoon and 8.10 ppm to 14.00 ppm (average 11.81 ppm) in postmonsoon. Cr in the reducible phase ranged from 9.80 ppm to 11.95 ppm (average 10.68 ppm) in premonsoon, 9.08 ppm to 12.30 ppm (average 11.13 ppm) in monsoon and 9.13 ppm to 10.78 ppm (average 9.93 ppm) in postmonsoon. Low concentrations of Cr was found in the exchangeable phase that varied from 0.95 ppm to 2.38 ppm (average 1.91 ppm) in premonsoon, 0.60 ppm to 0.83 ppm (average 0.68 ppm) in monsoon and 0.73 ppm to 1.33 ppm (average 1.06 ppm) in postmonsoon. Negligible concentration was noted in the carbonate bound fraction ranging from 1.03 ppm to 1.65 ppm (average 1.32 ppm) in premonsoon, 0.18 ppm to 0.68 ppm (average 0.33 ppm) in monsoon and 0.15 ppm to 0.73 ppm (average 0.36 ppm) in postmonsoon. Highest concentrations of exchangeable, carbonate bound and oxidisable Cr was noted in premonsoon, reducible Cr in monsoon and residual Cr in postmonsoon. Overall, highest bioavailable Cr was noted in premonsoon (30.77 ppm), followed by monsoon (23.45 ppm) and postmonsoon (23.15 ppm).

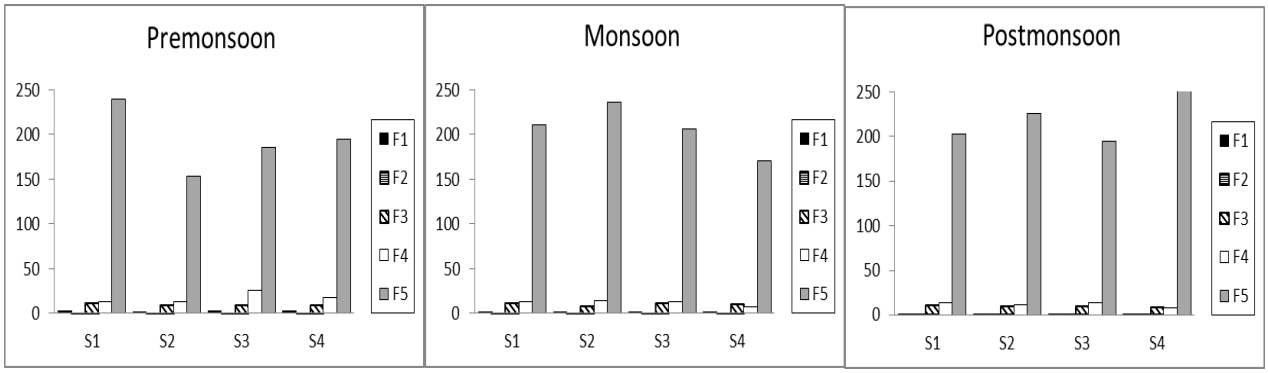


Figure 3.2.7: Spatial distribution of Cr speciation in mangrove sediments in the premonsoon, monsoon and postmonsoon.

The spatial distribution of bioavailable Cr across all three seasons showed little variations (Figure 3.2.7). Cr in the residual phase was highest in the upper estuary followed by the lower estuary and with lowest concentrations in the Cumbharjua canal during premonsoon. In

monsoon, residual Cr concentrations increased in the Cumbharjua canal and lower middle estuary and decreased in the lower estuary. In postmonsoon, the concentration of residual Cr was noted to increase considerably in the lower estuary.

As large Cr is bound in the mineral lattice form, minor amount of Cr is available for mobility in the estuarine mangrove sediments. It was noted that during premonsoon season, most Cr was supplied from the upstream regions of the estuary whereas enrichment in the lower estuary indicated that a small fraction of Cr might be supplied from local sources like harbor, barge building, etc. In the monsoon, enrichment of Cr in the Cumbharjua canal indicated input of considerable amount of Cr from the Mandovi estuary to the Zuari estuary. The decrease in the lower estuary suggested that Cr might have been re-suspended under influence of strong wind induced waves and may have deposited in the lower middle estuary. In the postmonsoon season, increase in the Cr in the lower estuary may be due to increasing marine influx that transports Cr into the estuary, from harbor.

### 3.2. D.1d Cobalt

The concentration of bioavailable Co in mangrove sediments was considerably low as compared to the residual fraction in all three seasons. The abundance of Co varied in the order of F5>F3>F4>F2>F1 in premonsoon, F5>F4>F3>F2>F1 in monsoon, and postmonsoon. The concentration of Co in the residual fraction varied from 26.48 ppm to 35.78 ppm (average 31.61 ppm) in premonsoon, 17.48 ppm to 35.95 ppm (average 28.81 ppm) in monsoon and 27.55 ppm to 36.40 ppm (average 32.27 ppm) in postmonsoon. The concentration range for reducible Co was from 4.48 ppm to 9.75 ppm (average 7.48 ppm) in premonsoon, 6.55 ppm to 11.43 ppm (average 6.82 ppm) in monsoon and 4.93 ppm to 9.33 ppm (Average 7.61 ppm) in postmonsoon. The Co associated with the organic matter/ sulfide bound fraction varied from 1.05 ppm to 2.88 ppm (average 1.98 ppm) in premonsoon, 7.28 ppm to 13.23 ppm (average 11.31 ppm) in monsoon and 8.10 ppm to 14.00 ppm (average 11.81 ppm) in postmonsoon. Smaller quantity of Co was found in the labile fractions in all three seasons. Carbonate bound Co varied from 1.43 ppm to 2.08 ppm (average 1.64 ppm) in premonsoon, 1.40 ppm to 2.43 ppm (average 1.94 ppm) in monsoon and 1.13 ppm to 1.78 ppm (average 1.44 ppm) in postmonsoon. Least Co content was found in the exchangeable fraction ranging from 0.60 ppm to 2.20 ppm (average 1.43 ppm) in premonsoon, 0.88 ppm to 1.13 ppm (average 1.01 ppm) in monsoon and 0.65 ppm to 1.60 ppm (average 1.12 ppm) in postmonsoon. Highest average Co content in the exchangeable was noted in the premonsoon,

carbonate bound Co in the monsoon season and reducible, oxidisable, and residual Co in the postmonsoon season. Overall, bioavailability of Co was high in the monsoon (22.88 ppm) followed by postmonsoon (21.99 ppm) and premonsoon (12.53 ppm) seasons.

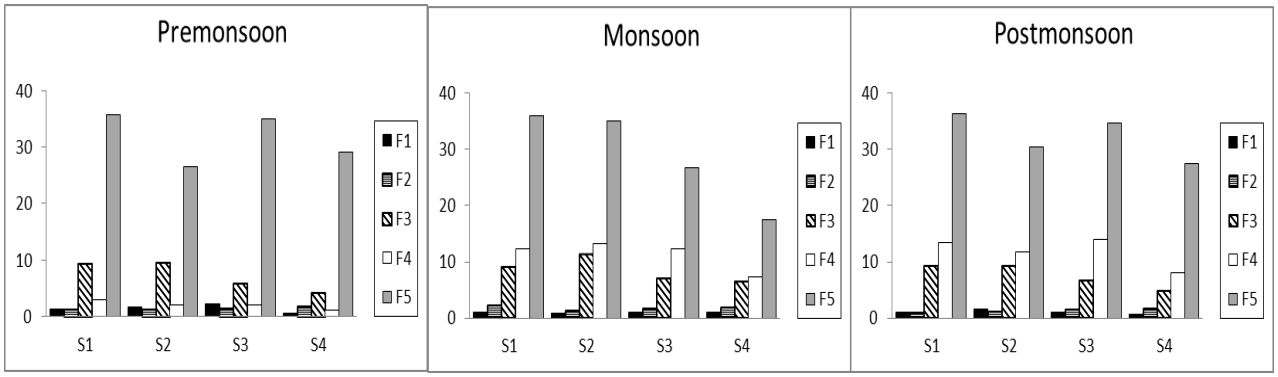


Figure 3.2.8: Spatial distribution of Co speciation in mangrove sediments in the premonsoon, monsoon, and postmonsoon.

In the spatial distribution of Co in the five fractions, large seasonal variability was observed in mangrove sediments (Figure 3.2.8). Exchangeable and carbonate bound Co maintained low concentrations in all the three seasons at each mangrove location. However, relatively higher exchangeable concentrations were noted in the premonsoon. Fe-Mn bound Co exhibited a decreasing trend from S1 to S4 with peak values at S2 in all three seasons. Co in the organic matter/ sulfide bound fraction exhibited large seasonal variations. Low carbonate bound Co concentrations were noted in the premonsoon season. However, considerable increase in oxidisable Co was observed in monsoon and postmonsoon seasons. The concentration of residual Co at S1 was relatively constant in all the three seasons whereas other stations showed variations. Residual concentrations were low during premonsoon at S2 and monsoon and postmonsoon seasons at S4.

Most bioavailable Co in the mangrove sediments was associated with the Fe-Mn oxide and organic matter/ sulfide bound phases. Similar enrichment of organic matter bound Mn in the monsoon season indicated that the chemistry of Co and Mn in the estuary are closely related and may be possibly linked to the same anthropogenic source.

### 3.2. D.1e Copper

Cu in the sediments of the Zuari estuary showed little seasonal variations in the bioavailable fractions. The abundance of Cu in the five fraction varied in the order of F5>F4>F3>F2>F1 in premonsoon, F5>F4>F3>F1>F2 in monsoon and F5>F4>F1>F3>F1 in postmonsoon. Large amount of Cu was associated with the residual fraction ranging from 49.50 ppm to 146 ppm (average 77.78 ppm) in premonsoon, 69.88 ppm to 202 ppm (average 115 ppm) in monsoon and 56.40 ppm to 89.08 ppm (average 68.69 ppm) in postmonsoon. Among the bioavailable fractions, Cu was mainly associated with the organic matter/sulfide fractions with concentrations ranging from 4.60 ppm to 18.58 ppm (average 11.65 ppm) in premonsoon, 6.28 ppm to 48.95 ppm (average 18.91 ppm) in monsoon and 8.58 ppm to 18.95 ppm (average 13.66 ppm) in postmonsoon. Cu content in the Fe-Mn oxide bound fraction varied from 1.10 ppm to 2.60 ppm (average 1.72 ppm) in premonsoon, 2.43 ppm to 5.33 ppm (average 3.79 ppm) in monsoon and 2.20 ppm to 2.80 ppm (average 2.64 ppm) in postmonsoon. Carbonate bound Cu ranged from 0.78 ppm to 1.53 ppm (average 1.07 ppm) in premonsoon, 1.23 ppm to 1.60 ppm (average 1.47 ppm) in monsoon and 1.43 ppm to 1.75 ppm (average 1.57 ppm) in postmonsoon. The concentration of exchangeable Cu varied from 0.65 ppm to 1.33 ppm (average 1.01 ppm) in monsoon, 1.10 ppm to 4.08 ppm (average 2.59 ppm) in monsoon and 2.00 ppm to 5.18 ppm (average 3.72 ppm) in postmonsoon. Highest concentrations of exchangeable and carbonate bound Cu was noted in the postmonsoon and Fe-Mn oxide bound, organic matter/sulfide bound and residual Cu in the monsoon. In general, elevated concentrations of bioavailable Cu were noted in the monsoon (26.76 ppm) followed by postmonsoon (21.59 ppm) and least in the premonsoon (15.44ppm).

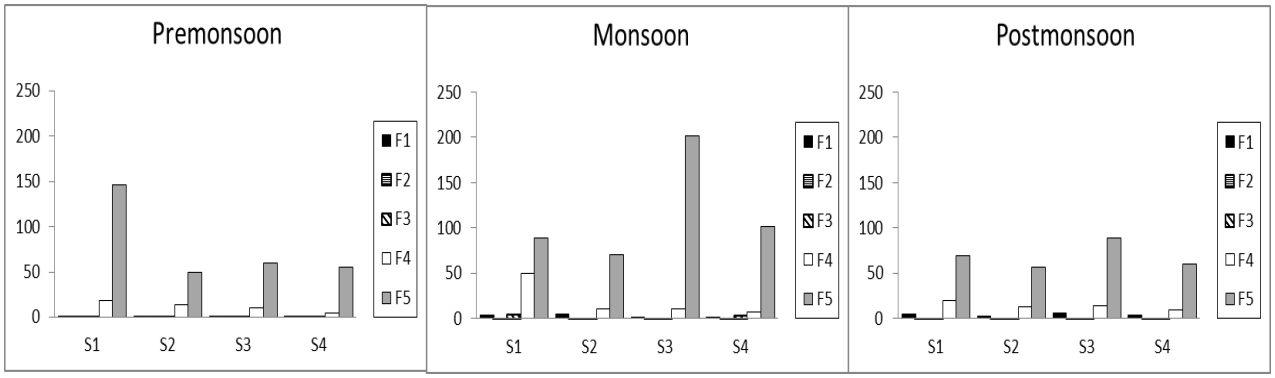


Figure 3.2.9: Spatial distribution of Cu speciation in mangrove sediments in the premonsoon, monsoon and postmonsoon.

The spatial distribution of Cu in the five fractions (Figure 3.2.9) indicated little variability in the distribution of bioavailable as compared to the residual phase. However, the concentration of Organic matter/sulfide bound Cu showed minor enrichment in the monsoon season at station S1. Residual Cu was high at S1 in premonsoon but decreased in the monsoon with enrichment at S3 and S4, and lower values in the postmonsoon.

The low concentration of Cu in the bioavailable phase indicated its low mobility in the sediments. However, in the monsoon, Cu readily bound to the organic matter due to its strong affinity towards humic/ fulvic acids. Copper is known to form stable Cu complexes with organic ligands with high stability constants (Morillo et al., 2004). Cu enrichment in the residual phase in monsoon was attributed to the high terrestrial weathered material brought to the estuary from the monsoonal run off to the estuarine sediments.

**3.2. D.1f Zinc**

The abundance of Zn in the five fractions varied in the order of F5>F3>F4>F2>F1 in premonsoon, monsoon and postmonsoon. The residual fraction accounted for major amount of Zn in the sediments of the mangroves ranging from 60.38 ppm to 95.48 ppm (average 80.22 ppm) in premonsoon, 58.65 ppm to 102.88 ppm (average 80.59 ppm) in monsoon and 67.58 ppm to 116.50 ppm (average 85.78 ppm) in postmonsoon. The Fe-Mn oxide bound fraction accounted for most of the bioavailable Zn in the sediments and ranged from 14.98 ppm to 19.50 ppm (average 17.03 ppm) in premonsoon, 10.75 ppm to 38.78 ppm (average 22.66 ppm) in monsoon and 12.90 ppm to 28.83 ppm (average 17.70 ppm) in postmonsoon. Considerable amount of Zn was associated with the organic matter/ sulfide bound fraction with concentrations ranging from 2.98 ppm to 9.20 ppm (average 6.03 ppm) in premonsoon, 5.33 ppm to 17.98 ppm (average 9.28 ppm) in monsoon and 5.43 ppm to 8.80 ppm (average 6.94 ppm) in post monsoon. Low concentrations of Zn was associated with the carbonate bound and exchangeable fractions. The concentration of carbonate bound Zn varied from 1.88 ppm to 2.60 ppm (average 2.07 ppm) in premonsoon, 0.65 ppm to 2.60 ppm (average 1.54 ppm) in monsoon, and 1.63 ppm to 3.33 ppm (average 2.53 ppm) in postmonsoon. Exchangeable Zn ranged from 0.50 ppm to 1.60 ppm (average 0.82 ppm) in premonsoon, 0.45 ppm to 1.58 ppm (average 1.03 ppm) in monsoon and 0.45 ppm to 1.08 ppm (average 0.85 ppm) in postmonsoon. Highest concentrations of exchangeable, Fe-Mn oxide, organic matter/ sulfide bound Zn was noted in the monsoon season and carbonate bound and residual

Zn in postmonsoon season. Overall, high bioavailable Zn was found in the monsoon (34.50 ppm) followed by postmonsoon (28.02 ppm) and premonsoon (25.95 ppm).

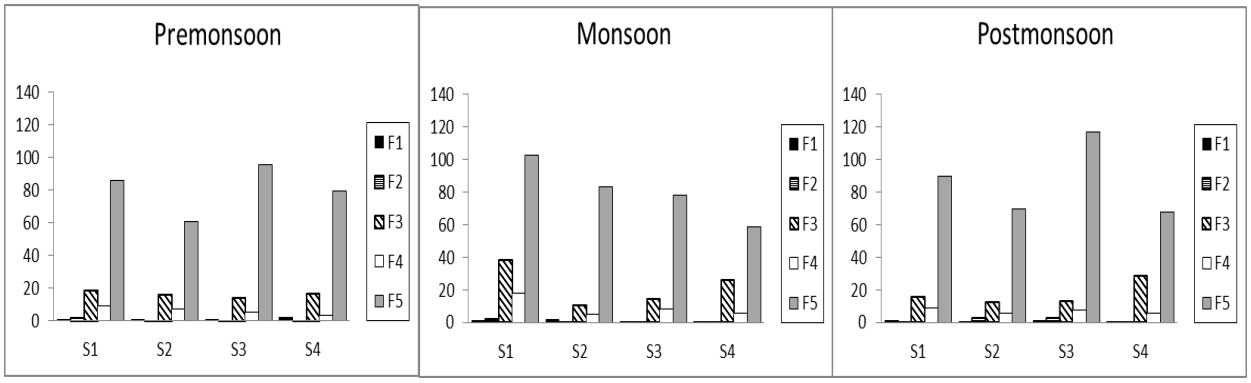


Figure 3.2.10: Spatial distribution of Zn speciation in mangrove sediments in the premonsoon, monsoon and postmonsoon.

The spatial distribution of Zn in the five fractions revealed that the exchangeable and carbonate bound fraction maintained very low concentrations in all three seasons (Figure 3.2.10). The Fe-Mn oxide fractions were constant in all four stations during the premonsoon. However, during the monsoon season, an increase in the Fe-Mn oxide bound Zn at stations S1 and S4 and during postmonsoon at station S4 was noted. The organic matter/ sulfide bound Zn showed high values in the monsoon season at station S1. Residual Zn considerably increased at stations S1 and S2 during monsoon and high at station S3 during premonsoon and postmonsoon.

Zn is known to complex with humic/fulvic acid and adsorb on Fe-Mn oxyhydroxides in the aquatic environment. The large influx of monsoonal runoff facilitated binding of Zn to particulate matter and was removed to the sediments increasing the concentrations. Most mineral bound Zn tends to settle in the upstream areas upon entering the estuary.

### 3.2. D.2 Mudflats

### 3.2. D.2a Iron

The percentage abundance of Fe in the five fractions varied in the order of F5>F3>F4>F1>F2 in the premonsoon, monsoon and postmonsoon seasons. The dominant fraction of Fe was the residual fraction with concentrations ranging from 51215 ppm to 76233 ppm (average 64343 ppm) in premonsoon, 74648 ppm to 84248 ppm (average 77883 ppm) in monsoon and 76668 ppm to 88073 ppm (average 81171 ppm) in postmonsoon. Fe in the bioavailable phase was

most abundant in the Fe-Mn oxide bound fraction with concentrations ranging from 4750 ppm to 8285 ppm (average 6140 ppm) in premonsoon, 6183 ppm to 6345 ppm (average 6247 ppm) in monsoon and 4385 ppm to 6043 ppm (average 5012 ppm) in postmonsoon. Considerable amount of Fe was associated with oxidisable phase ranging from 154 ppm to 1125 ppm (average 597 ppm) in premonsoon, 1534 ppm to 3421 ppm (average 2456 ppm) in monsoon and 303 ppm to 513 ppm (average 417 ppm) in postmonsoon. Low concentrations of Fe were associated with the exchangeable phase ranging from 20.60 ppm to 88.70 ppm (average 54.12 ppm) in premonsoon, 5.28 ppm to 48.93 ppm (21.30 ppm) in monsoon and 7.18 ppm to 104.48 ppm (average 40.21 ppm) in postmonsoon. The carbonate bound Fe ranged from 0.48 ppm to 17.83 ppm (average 7.16 ppm) in premonsoon, 0.63 ppm to 0.78 ppm (average 0.73 ppm) in monsoon and 0.35 ppm to 34.3 ppm (average 1.53 ppm) in postmonsoon. Highest average concentration of exchangeable and carbonate bound Fe was noted in premonsoon, reducible and oxidisable Fe in monsoon and residual Fe in postmonsoon. In general, highest bioavailable Fe was noted during the monsoon season (8724 ppm) followed by premonsoon (6798 ppm) and postmonsoon (5471 ppm).

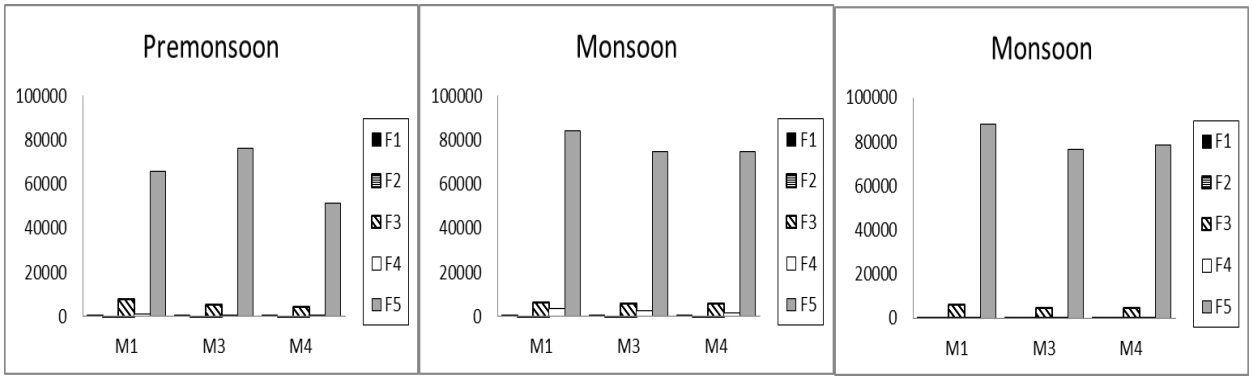


Figure 3.2.11: Spatial distribution of Fe speciation in mudflat sediments in the premonsoon, monsoon and postmonsoon.

The spatial variation of Fe in the five fractions showed that bioavailable Fe concentration was very low as compared to the residual fraction (Figure 3.2.11). However, Fe in the reducible phase exhibited a decreasing trend from M1 to M4 in premonsoon and monsoon seasons. Fe in the residual fraction was low at M1 and M4 during the premonsoon whereas residual Fe at M1 and M4 increased during monsoon and post monsoon. During monsoon season, a large amount of terrestrial Fe is added which is transported and deposited in the estuary. The concentration of residual Fe at M3 was almost constant in all three seasons indicating that the

intensive estuarine mixing at the lower middle estuary facilitates largely uniform sedimentation processes.

### 3.2. D.2b Manganese

Mn in mudflat sediments exhibited large seasonal variability with the five fractions of sediments. The concentration of Mn varied in the order of abundance F3>F2>F5>F1>F4 in premonsoon, F3>F1>F2>F5>F4 in monsoon and F3>F2>F5>F4>F1 in postmonsoon. Most bioavailable Mn was associated with the reducible fraction in all the three seasons ranging from 1110 ppm to 2703 ppm (average 2042 ppm) in premonsoon, 975 ppm to 2203 ppm (average 1536 ppm) in monsoon and 1785 ppm to 3083 ppm (average 2310 ppm) in postmonsoon. Mn in the carbonate bound fraction ranged from 780 ppm to 1450 ppm (average 1096 ppm) in premonsoon, 538 ppm to 728 ppm (average 607 ppm) in monsoon and 608 ppm to 893 ppm (709 ppm) in postmonsoon. Exchangeable Mn concentrations varied from 83.83 ppm to 764 ppm (average 385 ppm) in premonsoon, 270 ppm to 1020 ppm (average 613 ppm) in monsoon and 130 ppm to 475 ppm (average 314 ppm) in postmonsoon. Least bioavailable Mn was associated with the oxidisable phase with concentrations ranging from 189 ppm to 378 ppm (average 307 ppm) in premonsoon, 183 ppm to 458 ppm (average 287 ppm) in monsoon and 303 ppm to 513 ppm (average 417 ppm) in postmonsoon. The concentration of Mn in the residual phase ranged from 483 ppm to 620 ppm (average 539 ppm) in premonsoon, 400 ppm to 608 ppm (average 502 ppm) in monsoon and 583 ppm to 670 ppm (average 613 ppm) in postmonsoon. Highest concentration of carbonate bound metals was noted in the premonsoon, exchangeable metals in the monsoon and reducible, oxidisable, and residual Mn in the postmonsoon. Overall, highest bioavailable Mn was noted in the premonsoon (3830 ppm), followed by postmonsoon (3750 ppm) and monsoon season (3042 ppm).

In the spatial distribution of Mn in the five fractions, the concentration of Mn in the exchangeable fraction decreased from M1 to M4 in the premonsoon and monsoon (Figure 3.2.12), however with an increase in exchangeable Mn in the monsoon season at M1, M3 and M4. In the postmonsoon season, exchangeable Mn concentrations decreased but relatively higher concentration at station M3 compared to M2 and M4. Carbonate bound Mn was highest in premonsoon, decreased during the monsoon followed by minor increase in the postmonsoon. Most carbonate bound Mn was enriched at M3 in the premonsoon and postmonsoon season. Fe-Mn oxide bound Mn exhibited large variations among all the five

fractions. Reducible Mn showed a decreasing trend from M1 to M4 in premonsoon and postmonsoon whereas during monsoon, lower value at M3 was noted than M1 and M4. Oxidisable and residual Mn exhibited little seasonal variations.

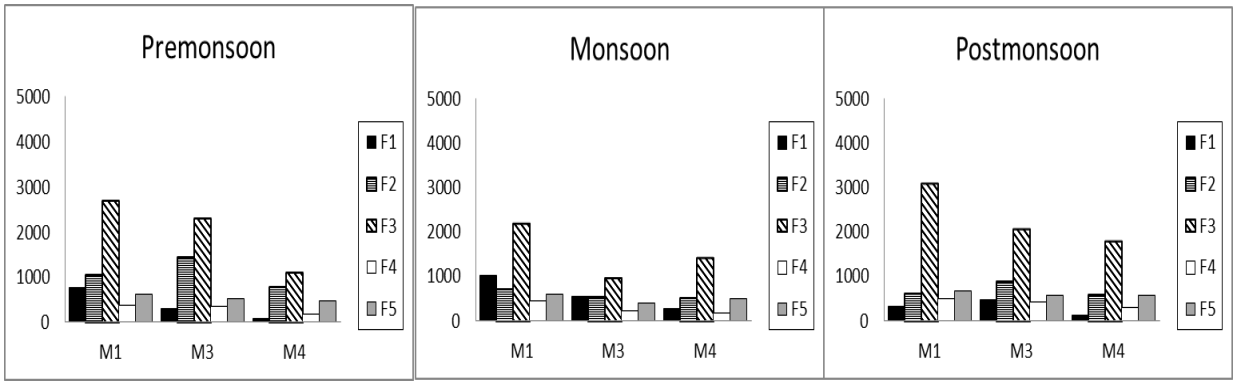


Figure 3.2.12: Spatial distribution of Mn speciation in mudflat sediments in the premonsoon, monsoon and postmonsoon.

In all three seasons, Mn was enriched in the upper middle estuary in the Fe-Mn oxide form due to the proximity of Mn sources in the upstream regions of the estuary and removal as oxides from solution during early estuarine mixing. Lower concentrations of reducible Mn was noted in the monsoon season may be due to redox changes in the sediment and mobilization of Mn which may have adsorbed to other sediment components or diffused to the water column. However, during the postmonsoon, due to sea water intrusion, the solubilized Mn gets re-precipitated as oxides on encountering waters of high salinity.

### 3.2. D.2c Chromium

In the mudflat sediments of the Zuari estuary, large quantity of Cr was associated with the residual phase with low concentrations in the bioavailable fractions in all the three seasons. The abundance of Cr in the five fractions varied in the order of F5>F4>F3>F1>F2 in premonsoon, monsoon and postmonsoon seasons. Residual Cr concentrations varied from 185 ppm to 193 ppm (average 190 ppm) in premonsoon, 182 ppm to 203 ppm (average 190 ppm) in monsoon and 206 ppm to 212 ppm (average 208 ppm) in postmonsoon. The concentration of Cr in the oxidisable phase ranged from 11.90 ppm to 23.83 ppm (average 18.44 ppm) in premonsoon, 11.75 ppm to 13.48 ppm (average 12.42 ppm) in monsoon and 12.28 ppm to 14.25 ppm (average 12.96 ppm) in postmonsoon. Reducible Cr concentrations varied from 10.78 ppm to 11.93 ppm (average 11.23 ppm) in premonsoon, 10.33 ppm to

11.88 ppm (average 11.09 ppm) in monsoon and 8.98 ppm to 10.25 ppm (average 9.50 ppm) in postmonsoon. Negligible concentration of Cr was noted in the exchangeable and carbonate bound phases. The concentration of Cr in the exchangeable fraction ranged from 0.68 ppm to 3.65 ppm (average 2.13 ppm) in premonsoon, 0.58 ppm to 0.98 ppm (average 0.78 ppm) in monsoon and 0.78 ppm to 0.80 ppm (average 0.78 ppm) in postmonsoon. Least Cr concentrations were noted in the carbonate bound fraction ranging from 0.90 ppm to 1.70 ppm (average 1.33 ppm) in premonsoon, 0.25 ppm to 0.30 ppm (average 0.27 ppm) in monsoon and 0.35 ppm to 0.60 ppm (average 0.43 ppm) in postmonsoon. Highest concentration of exchangeable, carbonate, reducible and oxidisable Cr was noted in the premonsoon and residual in the postmonsoon. Overall, bioavailable Cr was highest in the premonsoon season, followed by monsoon and least in postmonsoon.

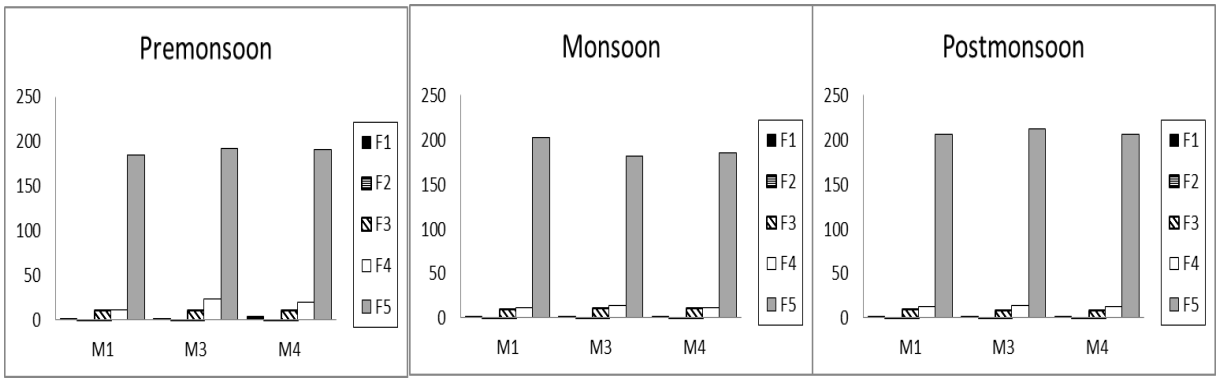


Figure 3.2.13: Spatial distribution of Cr speciation in mudflat sediments in the premonsoon, monsoon and postmonsoon.

The spatial distribution of Cr showed that Cr was low in the bioavailable fractions in all three seasons (Figure 3.2.13). However, oxidisable Cr was marginally high in the premonsoon season. The concentration of Cr in the residual fraction in premonsoon, was almost constant in all the three mudflat locations. However, during monsoon an increase in Cr in the upper middle estuary was noted whereas during postmonsoon, concentrations at M1, M3 and M4 considerably increased.

Cr was largely bound to the detrital fraction of sediments with little seasonal variation in the distribution in mudflats. However, slightly higher bioavailable Cr in the premonsoon, suggest anthropogenic addition of Cr from mining activities in the upstream regions of the estuary. The decrease of bioavailable Cr in the monsoon was probably due to dilution by addition of

sediment material. Residual Cr was noted to increase in the upper middle estuary during monsoon season, which may have been transported from the runoff from the upstream regions of the estuary.

### 3.2. D.2d Cobalt

The abundance of Co in the mudflat sediments varied in the order of F5>F3>F4>F1>F2 in premonsoon, F5>F4>F3>F2>F1 in monsoon and postmonsoon. Co was mainly available in the residual fraction with concentrations ranging from 30.00 ppm to 32.48 ppm (average 31.38 ppm) in premonsoon, 25.53 ppm to 36.33 ppm (average 23.39 ppm) in monsoon and 32.50 ppm to 37.05 ppm (average 33.74 ppm) in postmonsoon. Bioavailable Co was mainly associated with the oxidisable and reducible fractions. The concentration of Co in the organic matter/sulfide bound fraction ranged from 1.15 ppm to 3.73 ppm (average 2.30 ppm) in premonsoon, 11.75 ppm to 13.45 ppm (average 12.44 ppm) in monsoon and 12.28 ppm to 14.25 ppm (average 12.96 ppm) in postmonsoon. Fe-Mn oxide bound Co concentrations varied from 5.75 ppm to 9.15 ppm (average 7.13 ppm) in premonsoon, 7.53 ppm to 8.48 ppm (average 7.91 ppm) in monsoon and 5.68 ppm to 8.68 ppm (average 6.97 ppm) in postmonsoon. Low concentrations of Co were associated with the carbonate and exchangeable fractions in all three seasons. Carbonate bound Co ranged from 1.88 ppm to 2.43 ppm (average 2.08 ppm) in premonsoon, 1.73 ppm to 2.00 ppm (average 1.86 ppm) in monsoon and 1.78 ppm to 2.00 ppm (average 1.86 ppm) in postmonsoon. Co concentrations in the exchangeable fraction ranged from 1.65 ppm to 2.88 ppm (average 2.23 ppm) in premonsoon, 0.83 ppm to 1.58 ppm (average 1.18 ppm) in monsoon and 0.93 ppm to 1.18 ppm (average 1.08 ppm ) in postmonsoon. Highest average concentrations of exchangeable and carbonate bound Co was noted in the premonsoon, Fe-Mn oxide bound Co in the monsoon and organic matter/ sulfide bound and Residual Co in the postmonsoon. Overall, highest bioavailable Co was noted in the monsoon (23.39 ppm) followed by postmonsoon (22.94 ppm) and least in premonsoon (13.74 ppm).

From the spatial distribution of Co in the five fractions, significant seasonal variation was noted in the bioavailable fractions (Figure 3.2.14). Relatively higher concentrations of exchangeable Co were noted in the premonsoon season than monsoon and postmonsoon season. Carbonate bound Co showed little seasonal variation. Fe-Mn oxide bound Co increased at M3 and M4 in the monsoon season. Organic matter/ sulfide bound fraction was low in the premonsoon season and showed marked increase during the monsoon and

maintained higher concentrations during the postmonsoon. Residual concentrations also showed significant variations with an increase in the monsoon season at M1 and decrease at M3 and M4.

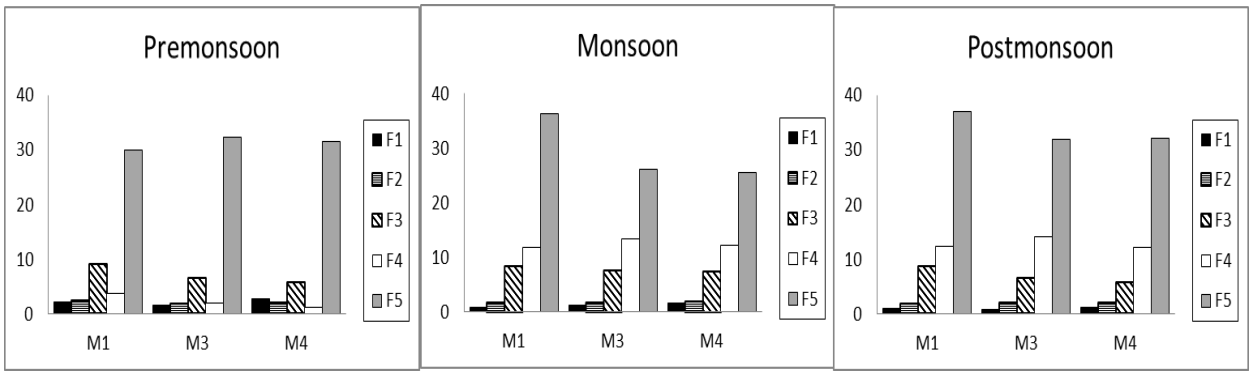


Figure 3.2.14: Spatial distribution of Co speciation in mudflat sediments in the premonsoon, monsoon and postmonsoon.

In the premonsoon season, higher exchangeable concentrations may be attributed to anthropogenic inputs. The decrease of exchangeable Co in the monsoon season was possibly due to diffusion of Co to the water column from sediments and also the Co ions must have interacted with the Fe-Mn oxides and deposited to the sediments. High organic matter bound Co in the monsoon season was probably due to the high influx of terrestrial matter into the estuary through runoff and the affinity of Co to humic/ fulvic substances.

### 3.2. D.2e Copper

The abundance of Cu in the mudflats varies in the order of F5>F4>F3>F2>F1 in premonsoon, F5>F4>F3>F1>F2 in monsoon and F5>F4>F1>F3>F2 in postmonsoon. The residual fraction was the dominant phase for Cu with concentrations ranging from 60.23 ppm to 64.50 ppm (average 62.07 ppm) in premonsoon, 90.33 ppm to 222 ppm (average 135 ppm) in monsoon and 66.30 ppm to 70.28 ppm (average 68.11 ppm) in postmonsoon. The organic matter/ sulfide bound fraction was the major portion of the bioavailable fraction of Cu which ranged from 5.60 ppm to 26.53 ppm (average 13.91 ppm) in premonsoon, 6.35 ppm to 54.18 ppm (average 25.62 ppm) in monsoon and 8.50 ppm to 20.10 ppm (average 14.69 ppm) in postmonsoon. Cu in the Fe-Mn oxide bound fraction ranged from 1.45 ppm to 3.28 ppm (average 2.11 ppm) in premonsoon and 2.58 ppm to 5.75 ppm (average 3.79 ppm) in monsoon and 2.18 ppm to 3.13 ppm (average 2.77 ppm) in postmonsoon. Low concentration

of Cu was associated with the exchangeable fraction ranging from 0.28 ppm to 1.15 ppm (average 0.77 ppm) in premonsoon, 1.23 ppm to 4.35 ppm (average 2.34 ppm) in monsoon and 3.10 ppm to 5.05 ppm (average 3.93 ppm) in postmonsoon. Concentrations of Cu in the carbonate bound fraction varied from 0.80 ppm to 1.65 ppm (average 1.18 ppm) in premonsoon, 1.08 ppm to1.98 ppm (average 1.43 ppm) in monsoon and 3.10 ppm to 5.05 ppm (average 3.93 ppm) in postmonsoon,. Highest concentrations of exchangeable and carbonate Cu were noted in the postmonsoon season whereas Fe-Mn oxide, organic matter/ sulfide bound and residual Cu were high in monsoon. Overall, bioavailable Cu concentrations were highest during monsoon (33.18 ppm) followed by postmonsoon (22.94 ppm) and premonsoon (17.96 ppm).

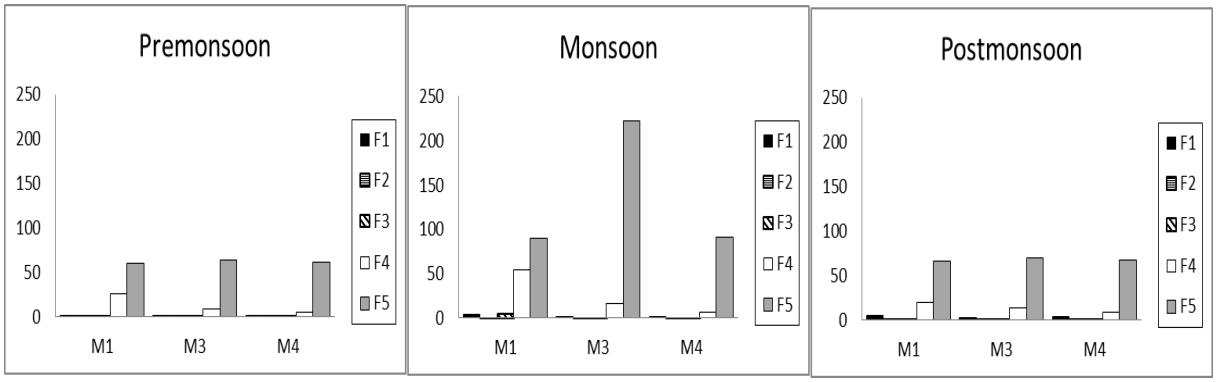


Figure 3.2.15: Spatial distribution of Cu speciation in mudflat sediments in the premonsoon, monsoon and postmonsoon.

The spatial distribution of Cu in the three seasons indicated significant variations in the distribution of bioavailable Cu and residual phase (Figure 3.2.15). Cu in the exchangeable, carbonate and Fe-Mn oxide fractions maintained low concentrations in all three seasons. However, organic matter/ sulfide bound Cu increased in the monsoon season more prominently at stations M1 and M3 followed by decrease in postmonsoon. The residual fraction showed significant enrichment in the monsoon season especially at station M3.

It was noted that bioavailable Cu increased in the monsoon season due to increase in the oxidisable fraction. High organic matter influx into the estuary during the monsoon resulted in increased binding ability of Cu to organic matter. Additionally, increased influx of weathered material to the estuary during the monsoon led to increase in residual Cu concentrations.

### 3.2. D.2f Zinc

The concentration of Zn in sediments varied in the order of F5>F3>F4>F2>F1 in premonsoon, monsoon and postmonsoon seasons. Major amount of Zn was associated with the residual fraction which ranged from 61.53 ppm to 82.33 ppm (average 70.63 ppm) in premonsoon, 71.40 ppm to 118.45 ppm (average 91.92 ppm) in monsoon and 79.85 ppm to 84.75 ppm (average 81.92 ppm) in postmonsoon. The Fe-Mn oxide bound fraction accounted for most quantity of the bioavailable fraction with concentrations varying from 13.85 ppm to 23.75 ppm (average 17.32 ppm) in premonsoon, 15.53 ppm to 29.33 ppm (average 20.66 ppm) in monsoon and 12.98 ppm to 15.90 ppm (average 14.38 ppm) in postmonsoon. Considerable amount of Zn was present in the organic matter/ sulfide bound fraction ranging from 2.98 ppm to 10.83 ppm (average 6.24 ppm) in premonsoon, 7.55 ppm to 16.30 ppm (average 11.91 ppm) in monsoon and 6.88 ppm to 8.48 ppm (average 7.76 ppm) in postmonsoon. Low concentration of Zn was associated with the carbonate bound and exchangeable fractions. Zn in the carbonate bound fraction varied from 1.35 ppm to 1.80 ppm (average 1.61 ppm) in premonsoon, 1.38 ppm to 1.98 ppm (average 1.61 ppm) in monsoon and 1.23 ppm to 3.45 ppm (average 2.48 ppm) in postmonsoon. Least concentrations of Zn were found in the exchangeable fraction and ranged from 0.43 ppm to 1.80 ppm (average 1.22 ppm) in premonsoon, 0.68 ppm to 1.13 ppm (average 0.85 ppm) in monsoon and 0.95 ppm to 1.58 ppm (average 1.23 ppm) in postmonsoon. Highest Zn concentrations for exchangeable and carbonate bound Zn were noted in postmonsoon and Fe-Mn oxide, organic matter/ sulfide bound and residual Zn in monsoon season. Overall, the sediments had higher concentration of Zn in the monsoon season (average 35.03 ppm) followed by premonsoon (26.38 ppm) and postmonsoon (25.85 ppm).

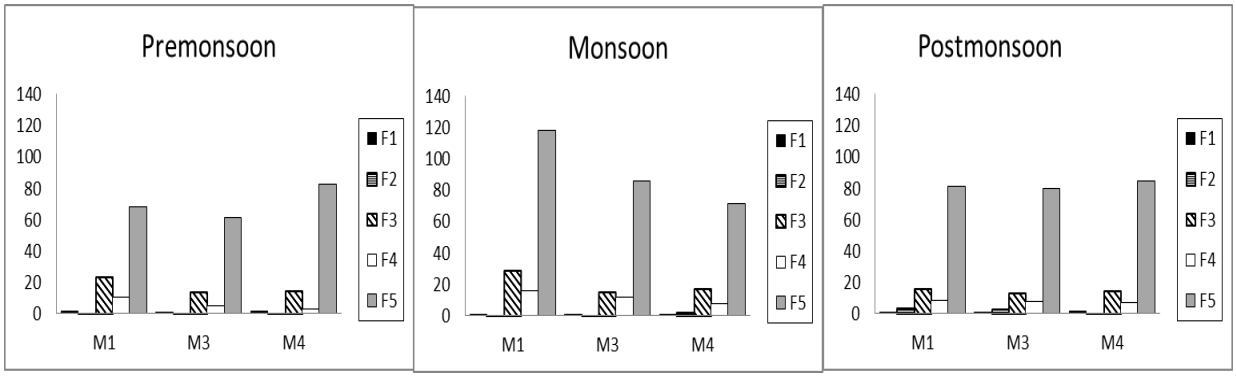


Figure 3.2.16: Spatial distribution of Zn speciation in mudflat sediments in the premonsoon, monsoon and postmonsoon.

The spatial distribution of Zn exhibited low concentrations for exchangeable and carbonate bound fraction in all the three seasons (Figure 3.2.16). Fe-Mn oxide bound Zn showed minor enrichment in the monsoon season. Significant increase was also noted for organic matter / sulfide bound Zn in monsoon season at all three mudflat locations. The residual fraction of Zn showed marked increase in monsoon season more prominently at M1 and M3. This variation was due to the large influx of terrestrial matter in the estuary that aided in binding of metals.

From the results described above, it was noted that the bioavailable concentration of metals in mangroves (Fe, Mn, Co, Cu and Zn) and mudflats (Fe, Co, Cu and Zn) was high during the monsoon season. However, most residual metals showed enrichment in the postmonsoon season for mangroves (Fe, Mn, Cr, Co and Zn) as well as mudflats (Fe, Mn, Cr and Co). Among the bioavailable fractions of metals in the surface sediments, most seasonal variations was observed in the Fe-Mn oxide bound and organic/sulfide bound fractions. A seasonal effect is apparent mainly for Mn and Co, which show large similarity and thus may be related to the same anthropogenic source.

The Zuari estuary is affected by several human activities such as mining, boating barge/ shipbuilding and land reclamation etc. through which considerable amount of material is added to the estuary overtime. In addition, high rainfall in the Western Ghats leads to active drainage, permitting strong to very strong hydrolytic action on parent rocks (Kessarkar et al., 2013) which wash off into the tributaries of river and estuary. Mining and associated industries also elevate the level of metals in the estuary.

An increase in the concentrations of few metals in the sediments during premonsoon and post-monsoon periods indicated that these metals were mobilized from the over-flooding of metal rich wastewater into the estuary during high rainfall and by reworking of the sediments (Ansari et al., 2000). Further, geochemical processes facilitated the metal dispersion and mobilization in estuarine sediments after, large-scale sediment-water movement during the monsoon period. In monsoon, the metals released by from the basin, mining effluents, and other anthropogenic sources, are drained into the Zuari estuary mainly through surface and subsurface discharges increasing bioavailable metal concentrations. Heavy rainfall during the monsoon would have flushed Fe–Mn oxides stored on the surface, associated with some

transition metals Co, Ni, Cu, Zn in particular (Kabata-Pendias and Pendias, 2001) and the Fe–Mn oxides along with their leachates transported to the estuary (Kessarkar et al., 2013).

Further, in postmonsoon, the subsurface discharge might have contributed substantial detrital metals to the estuary. In Goa, 52% of monsoon rainfall accounts for the surface runoff while 16 % accounts for charging the ground water (Ghosh, 1985). The ground water discharges into estuary from the laterites, that contain water reservoirs in them and sustain several springs, could be significant in the non-monsoon seasons (Chachadi, 2009; Anand et al., 2014). Subramaniam (1981) found that the effluence of the leaky laterites sustains the high discharges from rivers and tributaries, all along their course, especially in postmonsoon season. Additionally, discharges of fresh water from the Selaulim dam in the upstream region and subsurface flow contributes to the Zuari estuarine system in dry seasons (Shetye et al., 2007, Subramaniam, 1981). Thus, the ground water from the lateritic rocks could add minerals resulting in higher residual bound metals to the estuary in the postmonsoon season.

Moreover, geomorphology and drainage type combined with sedimentation processes played a substantial role on distribution of metals bound to sediments. Therefore, the monsoon hydrography and physico-chemical parameters of the estuary play a major role in regulating the concentrations and behavior of the metals in the estuarine system.

### 3.2. E Risk assessment

The average bioavailable concentrations of metals Fe, Mn, Cr, Co, Cu and Zn (Table 3.2.5) were compared with the Sediment quality values of the SQuiRT proposed by Buchman (1999).

Table 3.2.5: Concentrations of metals in the bioavailable fraction of mangrove and mudflat sediments expressed in ppm (except for Fe, which is expressed in percentage)

| | | | Fe | Mn | Cr | Co | Cu | Zn |
|---|---|---|---|---|---|---|---|---|
| (a) | Mangrove | Premonsoon | 0.75 | 2845(>AET) | 30.77 | 12.53(>AET) | 15.44 | 25.95 |
| | | Monsoon | 0.75 | 3493(>AET) | 23.45 | 22.88(>AET) | 26.76(>TEL) | 34.5 |
| | | Postmonsoon | 0.58 | 3431(>AET) | 23.15 | 21.99(>AET) | 21.59(>TEL) | 28.02 |
| (b) | Mudflats | Premonsoon | 0.68 | 3830(>AET) | 33.12 | 13.74(>AET) | 17.96 | 26.38 |
| | | Monsoon | 0.87 | 3042(>AET) | 24.56 | 23.39(>AET) | 33.18(>TEL) | 35.03 |
| | | Postmonsoon | 0.55 | 3750(>AET) | 23.68 | 22.94(>AET) | 22.94(>TEL) | 25.85 |

In the mangroves and mudflat sediments, bioavailable Mn and Co concentrations were higher than the Apparent Effects Threshold in all three seasons and can cause adverse effects on biota, whereas bioavailable concentrations of Cu in monsoon and postmonsoon were greater than the Threshold Effect Level and can pose considerable risk to biota. Moreover, higher concentrations during monsoon can cause significant toxicity to the sediment dwelling organisms.

Table 3.2.6: Risk assessment code calculated form Mangrove and mudflat sediments with reference to the labile fraction (exchangeable +carbonate) expressed in percentage.

| | | | Fe | Mn | Cr | Co | Cu | Zn |
|---|---|---|---|---|---|---|---|---|
| (a) | Mangroves | Premonsoon | 0.07 | 38.90 | 1.45 | 7.02 | 2.45 | 2.75 |
| | | Monsoon | 0.05 | 32.15 | 0.445 | 6.07 | 3.35 | 2.21 |
| | | Postmonsoon | 0.10 | 24.55 | 0.59 | 4.81 | 5.84 | 3.02 |
| (b) | Mudflats | Premonsoon | 0.10 | 33.74 | 1.55 | 9.58 | 2.37 | 2.90 |
| | | Monsoon | 0.02 | 34.47 | 0.49 | 5.86 | 2.53 | 2.03 |
| | | Postmonsoon | 0.05 | 23.61 | 0.53 | 5.35 | 6.00 | 3.44 |

The Risk assessment code calculated for the metals in the mangrove and mudflat sediments (Table 3.2.6) revealed that concentrations of labile Mn (exchangeable + carbonate) posed high risk in the premonsoon and monsoon seasons and medium risk in the postmonsoon season. The decrease in labile Mn in postmonsoon was probably due to dilution by seawater with higher salinity and conversion of labile Mn to oxide form.

### 3.3 Sediment collection in premonsoon of 2015, after mining ban

Sediment cores of 10 cm each were collected in the premonsoon season of 2015 to evaluate the concentration of metals in sediments following the mining ban imposed in 2012 to understand the changes in bioavailability. Further, efforts were made to assess the bioaccumulation of metals in mangrove pneumatophores and sediment associated biota relative to the bulk, bioavailable and labile metal content in sediments of the Zuari estuary. Four mangrove (S1, S2, S3 and S4) and three mudflat (M1, M2 and M4) cores collected were analyzed at 2 cm interval and the average data was considered for data interpretations. The sediments were analyzed for pH, sediment component, organic carbon, bulk metals and metal concentration in various sediment fractions.

### 3. 3.A Mangroves

#### 3.3. A.1 Sediment components

The range and average values of sediment components are presented in table 3.3.1(a).

The data revealed that the pH values recorded varied between 6 and 7. Near neutral pH was noted in the lower estuarine sediments whereas the sediments towards the upstream regions of the estuary and the Cumbharjua canal were weakly acidic in nature. The sediments of the estuarine mangroves were characterized by the fine size. Higher clay was noted in the upper middle estuary (80 %) which decreased towards the lower estuary (48 % at station S4) due to changes in hydrodynamics. Highest silt percentage was noted in the Cumbharjua canal (28.53 %) and sand in the lower estuary (27.96 %). The lower estuary is subjected to high hydrodynamics due to turbulence by waves causing resuspension of the finer sediments which are carried in suspension thus retaining the larger sediment size fractions at the lower estuary. High total organic carbon (TOC) content was noted in the lower middle estuarine (4.67 %) sediments. Organic matter is supplied to the estuarine environments from both external (terrestrial, domestic and municipal sewage) and internal (algal and microbial mats) sources. Benthic invertebrates and soil microorganisms may also contribute significant amounts of organic carbon to sediments (Reddy and DeLaune, 2008).

Table 3.3.1: Range and average values of sediment components and metals in bulk sediment (a, b) in cores of the present study- 2015 and in 2011 (c , d) collected at mangroves S1, S2, S3 and S4 respectively.

| | | | S1 | | S2 | | S3 | | S4 | |
|---|---|---|---|---|---|---|---|---|---|---|
| | | Parameters | Average | Range | Average | Range | Average | Range | Average | Range |
| (a) | Sediment components (2015) | pH | 6.66 | 6.5-6.8 | 6.05 | 6.0-6.2 | 6.22 | 6.0-6.4 | 6.99 | 6.8-7.2 |
| | | Sand (%) | 2.81 | 2-4 | 5.42 | 4-6 | 4.37 | 2-6 | 27.96 | 8-48 |
| | | Silt (%) | 17.19 | 12-20 | 28.53 | 26-31 | 26.51 | 22-32 | 23.36 | 18-27 |
| | | Clay (%) | 80.00 | 77-85 | 66.24 | 64-68 | 69.12 | 62-72 | 48.68 | 30-70 |
| | | TOC (%) | 2.36 | 1.99-2.56 | 2.49 | 2.12-2.97 | 4.67 | 3.79-5.37 | 1.5 | 0.50-2.34 |
| (b) | Metals in bulk sediment (2015 ) | Fe (%) | 9.92 | 9.6 -10.5 | 10.79 | 10.1- 11.7 | 9.47 | 9.1 -9.8 | 9.19 | 8.2- 9.7 |
| | | Mn (ppm) | 6155 | 5625 - 6725 | 3800 | 1200 - 6325 | 1595 | 775 - 2750 | 2990 | 1725 - 4075 |
| | | Cr (ppm) | 276 | 266 -285 | 273 | 266 -281 | 254 | 240 -269 | 260 | 236 -272 |
| | | Co (ppm) | 56.7 | 54-59 | 57.00 | 52 – 62 | 49.5 | 48 - 52 | 37.90 | 33 - 42 |
| | | Ni (ppm) | 150 | 144- 152 | 154 | 143- 160 | 129 | 125- 135 | 96.85 | 74- 115 |
| | | Cu (ppm) | 131 | 128 -133 | 119 | 112 -124 | 122 | 119 -125 | 99.05 | 90 -112 |
| | | Zn (ppm) | 143 | 137 -157 | 128 | 123 -138 | 145 | 126 -191 | 149 | 135 -157 |
| (c) | Sediment components (2011) | pH | 6.92 | | 6.34 | | 6.57 | | 6.87 | |
| | | Sand (%) | 0.98 | | 6.63 | | 0.86 | | 37.24 | |
| | | Silt (%) | 39.59 | | 57.09 | | 40.38 | | 32.07 | |
| | | Clay (%) | 59.42 | | 36.28 | | 58.76 | | 30.68 | |
| | | TOC (%) | 2.6 | | 2.49 | | 1.92 | | 1.66 | |
| (d) | Metals in bulk sediment (2011) | Fe (%) | 10.35 | | 12.51 | | 10.68 | | 9.91 | |
| | | Mn (ppm) | 5295 | | 4780 | | 3000 | | 1630 | |
| | | Cr (ppm) | 261 | | 247.2 | | 306 | | 395 | |
| | | Co (ppm) | 18.05 | | 21.85 | | 25.55 | | 19.4 | |
| | | Ni (ppm) | 40.95 | | 42.40 | | 46.4 | | 32.95 | |
| | | Cu (ppm) | 43.30 | | 33.55 | | 44.35 | | 31.95 | |
| | | Zn (ppm) | 153 | | 105 | | 130 | | 98.7 | |

### 3.3. A.2 Geochemistry of metals

The range and average values of metals Fe, Mn, Cr, Co, Ni, Cu and Zn in bulk sediments are presented in table 3.3.1(b)**.**

Substantial spatial variations were noted in the distribution of metals. Highest average concentrations of Fe, Co and Ni were noted in the Cumbharjua canal, followed by the upper middle estuary which progressively decreased towards the lower estuary. Mn, Cr, and Cu were enriched in the upper middle estuary and Zn in the lower estuary. The distribution of Co and Ni in the Cumbharjua canal sediments may have been influenced by Fe oxyhydroxides and silt. The enrichment of Cr and Cu in the upper middle estuary may have been influenced by Mn oxyhydroxides and clay. Zn enrichment in the lower estuary may have been influence by pH of the sediments

A comparison of the average values of sediment components and metal concentrations was attempted with the data of mangrove sediments collected in the year 2011 of the upper 10 cm of the cores at the same sampling locations before the mining ban was imposed (Table 3.3.1 c and d). It was observed that the silt fraction of the sediments at all the locations has considerably decreased which was compensated by an increase in the clay fraction. The trace metals concentrations have significantly increased in recent times. Mn, Cr, Co, Ni and Cu showed higher values at site S1; Cr, Co, Ni, Cu and Zn in core S2; Co, Ni, Cu and Zn at S3, and Mn, Co, Ni, Cu and Zn at S4. However, Fe concentrations at all sampling locations were lower as compared to 2011.

Table 3.3.2: Paired-samples t-test for the comparison of means of sediment components and metals in cores S1, S2, S3 and S4 with respect to year 2011before mining ban and 2015 after mining ban.

| | Pairs of variables | Difference of means | T | df | Sig. (2-tailed) |
|---|---|---|---|---|---|
| S1 | $Sand_{2011}$ - $Sand_{2015}$ | -1.82 | -3.49 | 4.00 | 0.03 |
| | $Silt_{2011}$ - $Silt_{2015}$ | 22.40 | 9.15 | 4.00 | 0.00 |
| | $Clay_{2011}$ - $Clay_{2015}$ | -20.58 | -9.11 | 4.00 | 0.00 |
| | $TOC_{2011}$ - $TOC_{2015}$ | 0.23 | 2.16 | 4.00 | 0.10 |
| | $Fe_{2011}$ - $Fe_{2015}$ | 0.43 | 1.54 | 4.00 | 0.20 |
| | $Mn_{2011}$ - $Mn_{2015}$ | -860 | -2.37 | 4.00 | 0.08 |
| | $Cr_{2011}$ - $Cr_{2015}$ | -15.05 | -2.53 | 4.00 | 0.06 |
| | $Co_{2011}$ - $Co_{2015}$ | -38.65 | -15.26 | 4.00 | 0.00 |

| | Pairs of variables | Difference of means | T | df | Sig. (2-tailed) |
|---|---|---|---|---|---|
| | $Ni_{2011}$ - $Ni_{2015}$ | -109 | -90.13 | 4.00 | 0.00 |
| | $Cu_{2011}$ - $Cu_{2015}$ | -87.25 | -32.14 | 4.00 | 0.00 |
| | $Zn_{2011}$ - $Zn_{2015}$ | 10.44 | 1.34 | 4.00 | 0.25 |
| S2 | $Sand_{2011}$ - $Sand_{2015}$ | 1.40 | 1.25 | 4.00 | 0.28 |
| | $Silt_{2011}$ - $Silt_{2015}$ | 28.56 | 8.53 | 4.00 | 0.00 |
| | $Clay_{2011}$ - $Clay_{2015}$ | -29.96 | -11.36 | 4.00 | 0.00 |
| | $TOC_{2011}$ - $TOC_{2015}$ | 0.00 | -0.02 | 4.00 | 0.98 |
| | $Fe_{2011}$ - $Fe_{2015}$ | 1.72 | 4.69 | 4.00 | 0.01 |
| | $Mn_{2011}$ - $Mn_{2015}$ | 980 | 1.79 | 4.00 | 0.15 |
| | $Cr_{2011}$ - $Cr_{2015}$ | -26.15 | -2.21 | 4.00 | 0.09 |
| | $Co_{2011}$ - $Co_{2015}$ | -35.15 | -26.54 | 4.00 | 0.00 |
| | $Ni_{2011}$ - $Ni_{2015}$ | -111 | -24.26 | 4.00 | 0.00 |
| | $Cu_{2011}$ - $Cu_{2015}$ | -85.75 | -28.31 | 4.00 | 0.00 |
| | $Zn_{2011}$ - $Zn_{2015}$ | -22.74 | -4.44 | 4.00 | 0.01 |
| S3 | $Sand_{2011}$ - $Sand_{2015}$ | -3.51 | -4.00 | 4.00 | 0.02 |
| | $Silt_{2011}$ - $Silt_{2015}$ | 13.87 | 7.85 | 4.00 | 0.00 |
| | $Clay_{2011}$ - $Clay_{2015}$ | -10.36 | -4.81 | 4.00 | 0.01 |
| | $TOC_{2011}$ - $TOC_{2015}$ | -2.75 | -7.63 | 4.00 | 0.00 |
| | $Fe_{2011}$ - $Fe_{2015}$ | 1.20 | 4.40 | 4.00 | 0.01 |
| | $Mn_{2011}$ - $Mn_{2015}$ | 1405 | 5.08 | 4.00 | 0.01 |
| | $Cr_{2011}$ - $Cr_{2015}$ | 51.65 | 4.60 | 4.00 | 0.01 |
| | $Co_{2011}$ - $Co_{2015}$ | -23.95 | -26.23 | 4.00 | 0.00 |
| | $Ni_{2011}$ - $Ni_{2015}$ | -82.25 | -32.05 | 4.00 | 0.00 |
| | $Cu_{2011}$ - $Cu_{2015}$ | -77.90 | -58.72 | 4.00 | 0.00 |
| | $Zn_{2011}$ - $Zn_{2015}$ | -15.10 | -1.13 | 4.00 | 0.32 |
| S4 | $Sand_{2011}$ - $Sand_{2015}$ | 9.28 | 1.00 | 4.00 | 0.37 |
| | $Silt_{2011}$ - $Silt_{2015}$ | 8.71 | 1.70 | 4.00 | 0.16 |
| | $Clay_{2011}$ - $Clay_{2015}$ | -18.00 | -1.97 | 4.00 | 0.12 |
| | $TOC_{2011}$ - $TOC_{2015}$ | 0.16 | 0.49 | 4.00 | 0.65 |
| | $Fe_{2011}$ - $Fe_{2015}$ | 0.72 | 2.45 | 4.00 | 0.07 |
| | $Mn_{2011}$ - $Mn_{2015}$ | -1360 | -2.46 | 4.00 | 0.07 |
| | $Cr_{2011}$ - $Cr_{2015}$ | 135 | 3.10 | 4.00 | 0.04 |
| | $Co_{2011}$ - $Co_{2015}$ | -18.50 | -3.26 | 4.00 | 0.03 |
| | $Ni_{2011}$ - $Ni_{2015}$ | -63.90 | -6.74 | 4.00 | 0.00 |
| | $Cu_{2011}$ - $Cu_{2015}$ | -67.10 | -11.07 | 4.00 | 0.00 |
| | $Zn_{2011}$ - $Zn_{2015}$ | -50.36 | -7.81 | 4.00 | 0.00 |

The paired sample t-test (Table 3.3.2) conducted on the means of the four cores with respect to the years 2011 and 2015, support the observations made in table 3.3.1 (c and d), with significantly higher mean values of trace metal concentrations in 2015 indicated by negative t-values. Positive t-values of Fe indicated higher mean values in the year 2011 before mining ban, which decreased in the year 2015. The decrease in Fe content may be due to the reduced input from iron ore mining activities and transportation from the catchment area of the Zuari. Positive t values were also obtained for silt at all the locations. It was reported previously that Iron was associated with the larger grain sized sediments such as magnetic iron minerals in the Mandovi-Zuari estuarine system (Dessai et al., 2009; Veerasingam et al., 2015; Noronha-D'Mello and Nayak, 2015). The increase in trace metal concentrations may be due to the increase in the clay fraction, which has a higher adsorption capacity than the larger grain size fractions. In the recent years, sand mining has increased in the Zuari estuary, which caused resuspension and settling of the fine sediments with time. This must have helped in remobilization of trace metals, which later deposited in the calm mangrove sediments. Additionally, discharges from ship building industries and sewage release on the shores of the Zuari River may have also contributed to the enhancement of trace metal concentrations in the Zuari estuary. Kessarkar et al. (2013), however, suggested that suspended particulate matter from fluvial sources could be the dominant source of trace metals in the Zuari estuary.

### 3.3. B Mudflats

The distribution of various sediment components and metals in the three sediments cores M1, M3 and M4 of 10 cm each collected in 2015 from mudflats of the Zuari estuary are presented below.

### 3.3. B.1 Sediment components

The range and average values of the sediment components in mudflat sediments is presented in table 3.3.3 (a). The results revealed that the mudflat sediments were characterized by near neutral pH and high mud fraction. The dominant grain size fraction was clay and was high in the lower middle estuary (73.12 %), followed by silt that was abundant in the upper middle estuary (31.19 %) and least was sand that showed higher percentage in the lower estuary (6.63 %). The presence of coarser sediments in the lower estuary indicated strong hydrodynamic conditions operated in

the area whereas higher finer sediments in the middle estuary indicated calmer depositional conditions. TOC was abundant in the upper middle estuary (2.41 %) among the mudflats and was associated with the higher silt content. The lower estuary is known for higher wave and tidal dynamics that is responsible for facilitating the deposition of coarser sediments (Chen, 1992) and carrying finer sediments towards the middle estuary during the flood tide.

### 3.3. B.2 Geochemistry of metals

The distribution of metals in the mudflat sediments exhibited considerable spatial variations. From table 3.3.3(b), Mn, Co and Ni showed high concentrations in the upper middle estuary, Cr and Cu were enriched in the lower middle estuarine sediments, and Fe and Zn showed high concentrations in the lower estuary. The high silt and TOC content in the upper middle estuary mudflat along with the high Mn content may have influenced the enrichment of Co and Ni. The enrichment of Cr and Cu in the sediments of the lower middle estuarine mudflat might have influenced by the high clay content. Further, the enrichment of Zn in the lower estuary can be attributed to the high Fe content in the sediments along with pH and to some extent the sand content.

A comparison of average values of sediment components and metal concentration of 2011 and 2015 datasets revealed that the concentrations of trace metals along with clay in the estuarine sediments had considerably increased whereas Fe concentration along with silt and organic matter had decreased (Table 3.3.3). In core M1, metal concentrations of Mn, Cr, Co, Ni, Cu and Zn along with sand, clay were higher in 2015 as compared to 2011 whereas Fe along with silt and TOC were higher in 2011. In core M3, Co Ni, Cu and Zn concentrations along with sand and clay were higher in 2015 whereas Fe, Mn and Cr along with silt and TOC showed higher average values in 2011. In core M4, Fe, Mn, Co Ni, Cu, Zn and clay were higher in 2015 whereas Cr, sand, silt and TOC were higher in 2011.

Table 3.3.3 Range and average values of sediment components and metals in bulk sediment (a, b) in cores of the present study- 2015 and in 2011 (c , d) collected at mudflats M1, M3 and M4 respectively.

| | | M1 | | M3 | | M4 | |
|---|---|---|---|---|---|---|---|
| | | Average | Range | Average | Range | Average | Range |
| (a)Sediment components | | | | | | | |
| (2015) | pH | 6.91 | 6.83-7.03 | 6.81 | 6.60-7.14 | 6.99 | 6.87-7.11 |
| | Sand (%) | 3.34 | 2.52-4.86 | 1.70 | 0.90-2.50 | 6.63 | 1.77-14.39 |
| | Silt (%) | 31.19 | 27.72-33.41 | 25.18 | 20.56-34.30 | 23.07 | 11.69-30.89 |
| | Clay (%) | 65.47 | 63.27-67.42 | 73.12 | 64.80-77.42 | 70.30 | 58.08-82.16 |
| | TOC (%) | 2.41 | 2.31-2.46 | 1.91 | 0.73-2.4 | 2.07 | 1.64-2.34 |
| (b)Metals in bulk sediments | | | | | | | |
| (2015) | Fe (%) | 9.90 | 9.55-10.29 | 9.90 | 9.57-10.43 | 10.26 | 9.98-10.69 |
| | Mn (ppm) | 6400 | 6250-6700 | 2910 | 1725-3725 | 4235 | 3300-5225 |
| | Cr (ppm) | 270 | 259-280 | 281 | 276-291 | 268 | 261-277 |
| | Co (ppm) | 55.70 | 52.00-59.00 | 51.40 | 48.00-56.75 | 45.25 | 42.50-47.25 |
| | Ni (ppm) | 145 | 142-148 | 138 | 133-144 | 122 | 114-131 |
| | Cu (ppm) | 129 | 126-133 | 130 | 124-134 | 120 | 117-125 |
| | Zn (ppm) | 140 | 136-150 | 138 | 133-145 | 146 | 140-151 |
| (c) Sediment components | | | | | | | |
| (2011) | pH | 6.75 | | 6.85 | | 7.14 | |
| | Sand (%) | 1.80 | | 0.98 | | 7.57 | |
| | Silt (%) | 41.43 | | 33.08 | | 44.63 | |
| | Clay (%) | 56.78 | | 65.94 | | 47.80 | |
| | TOC (%) | 2.82 | | 2.45 | | 2.11 | |
| (d)Metals bulk sediments | | | | | | | |
| (2011) | Fe (%) | 10.21 | | 11.18 | | 10.05 | |
| | Mn (ppm) | 5473 | | 4383 | | 2772 | |

| | | | | |
|---|---|---|---|---|
| | Cr (ppm) | 264 | 371 | 342 |
| | Co (ppm) | 32.10 | 21.90 | 28.45 |
| | Ni (ppm) | 44.40 | 43.30 | 42.35 |
| | Cu (ppm) | 47.95 | 40.95 | 40.65 |
| | Zn (ppm) | 136 | 133 | 128 |

Table 3.3.4: Paired-samples t-test for the comparison of means of sediment components and metals in cores M1, M3 and M4 with respect to years 2011 before mining ban and 2015 after mining ban.

| | Pairs of variables | Difference of means | t | Df | Sig. (2-tailed) |
|---|---|---|---|---|---|
| M1 | $Sand_{2011}$ - $Sand_{2015}$ | -1.54 | -2.51 | 4.00 | 0.07 |
| | $Silt_{2011}$ - $Silt_{2015}$ | 10.24 | 6.47 | 4.00 | 0.00 |
| | $Clay_{2011}$ - $Clay_{2015}$ | -8.69 | -6.82 | 4.00 | 0.00 |
| | $TOC_{2011}$ - $TOC_{2015}$ | 0.42 | 8.12 | 4.00 | 0.00 |
| | $Fe_{2011}$ - $Fe_{2015}$ | 0.31 | 0.70 | 4.00 | 0.52 |
| | $Mn_{2011}$ - $Mn_{2015}$ | -927 | -8.25 | 4.00 | 0.00 |
| | $Cr_{2011}$ - $Cr_{2015}$ | -5.65 | -0.41 | 4.00 | 0.70 |
| | $Co_{2011}$ - $Co_{2015}$ | -23.60 | -22.92 | 4.00 | 0.00 |
| | $Ni_{2011}$ - $Ni_{2015}$ | -101 | -49.99 | 4.00 | 0.00 |
| | $Cu_{2011}$ - $Cu_{2015}$ | -80.75 | -44.37 | 4.00 | 0.00 |
| | $Zn_{2011}$ - $Zn_{2015}$ | -4.12 | -1.30 | 4.00 | 0.26 |
| M3 | $Sand_{2011}$ - $Sand_{2015}$ | -0.72 | -1.97 | 4.00 | 0.12 |
| | $Silt_{2011}$ - $Silt_{2015}$ | 7.90 | 2.26 | 4.00 | 0.09 |
| | $Clay_{2011}$ - $Clay_{2015}$ | -7.18 | -2.06 | 4.00 | 0.11 |
| | $TOC_{2011}$ - $TOC_{2015}$ | 0.53 | 1.62 | 4.00 | 0.18 |
| | $Fe_{2011}$ - $Fe_{2015}$ | 1.27 | 4.27 | 4.00 | 0.01 |
| | $Mn_{2011}$ - $Mn_{2015}$ | 1473 | 3.03 | 4.00 | 0.04 |
| | $Cr_{2011}$ - $Cr_{2015}$ | 90.40 | 3.77 | 4.00 | 0.02 |
| | $Co_{2011}$ - $Co_{2015}$ | -29.50 | -18.85 | 4.00 | 0.00 |
| | $Ni_{2011}$ - $Ni_{2015}$ | -94.55 | -47.22 | 4.00 | 0.00 |
| | $Cu_{2011}$ - $Cu_{2015}$ | -89.15 | -49.61 | 4.00 | 0.00 |
| | $Zn_{2011}$ - $Zn_{2015}$ | -5.67 | -1.33 | 4.00 | 0.25 |
| M4 | $Sand_{2011}$ - $Sand_{2015}$ | 0.94 | 0.38 | 4.00 | 0.72 |
| | $Silt_{2011}$ - $Silt_{2015}$ | 21.56 | 7.03 | 4.00 | 0.00 |
| | $Clay_{2011}$ - $Clay_{2015}$ | -22.50 | -5.89 | 4.00 | 0.00 |
| | $TOC_{2011}$ - $TOC_{2015}$ | 0.04 | 0.43 | 4.00 | 0.69 |
| | $Fe_{2011}$ - $Fe_{2015}$ | -0.21 | -0.46 | 4.00 | 0.67 |
| | $Mn_{2011}$ - $Mn_{2015}$ | -1463 | -3.52 | 4.00 | 0.02 |
| | $Cr_{2011}$ - $Cr_{2015}$ | 74.40 | 4.48 | 4.00 | 0.01 |
| | $Co_{2011}$ - $Co_{2015}$ | -16.80 | -14.45 | 4.00 | 0.00 |
| | $Ni_{2011}$ - $Ni_{2015}$ | -79.40 | -20.81 | 4.00 | 0.00 |
| | $Cu_{2011}$ - $Cu_{2015}$ | -79.05 | -34.11 | 4.00 | 0.00 |
| | $Zn_{2011}$ - $Zn_{2015}$ | -17.39 | -5.02 | 4.00 | 0.01 |

Furthermore, the observations of the compared average values was supported by the results of the paired sample t-test where negative t-values of the variables indicated increase in trace metal concentrations in recent times and positive t-values indicated a significant decrease (Table 3.3.4). The increase in trace metals in the estuary may be related to sand mining operations that might have re-suspended the sediments causing the metals to interact with suspended matter and clay and were re-deposited to sediments. Additionally, anthropogenic inputs and their deposition to the sediments was facilitated by adsorption onto clay particles or formation of coating on sand particles. However, a significant decrease in Fe and silt (M1 and M3) indicated reduction in Fe inputs to the estuary in recent times.

### 3.3.C Geoaccumulation index

#### 3.3.C.1 Mangroves

Table 3.3.5: Geoaccumulation index of metals in sediments of core mangrove S1, S2, S3 and S4.

| | Fe | Mn | Cr | Co | Ni | Cu | Zn |
|---|---|---|---|---|---|---|---|
| **S1** | 0.49 | 2.27 | 1.03 | 0.99 | 0.74 | 0.95 | 0.00 |
| **S2** | 0.61 | 1.40 | 1.02 | 1.00 | 0.77 | 0.82 | -0.16 |
| **S3** | 0.42 | 0.19 | 0.91 | 0.80 | 0.51 | 0.86 | 0.00 |
| **S4** | 0.37 | 1.16 | 0.95 | 0.40 | 0.09 | 0.55 | 0.06 |

Geo-accumulation index (Muller, 1979) was computed to assess the level of metal contamination of sediments (Table 3.3.5). There was significant contamination of Mn and Cr in the estuary which varied spatially. Overall, higher Igeo values for all metals except for Zn were noted in the upper middle estuary and Cumbharjua canal. On comparing Igeo values with earlier study based on collection in 2011 (Noronha-D'Mello and Nayak, 2015), mangrove sediments that were previously significantly polluted by Fe, Mn and Cr in 2011 showed lower index for Fe in the present study and Igeo values of Mn increased at locations S1 and S4 and decreased at S2 and S3. Igeo values of Cr were similar to previously reported values at S1 and S2, however, Igeo values decreased at locations S3 and S4 than previously reported. This indicated that there was a substantial reduction of Fe and Cr inputs to the Zuari estuary due to ban on mining in the catchment area.

### 3.3. C.2 Mudflats

Table 3.3.6: Geoaccumulation index of metals in sediments of core mudflat M1, M3 and M4.

| | Fe | Mn | Cr | Co | Ni | Cu | Zn |
|---|---|---|---|---|---|---|---|
| **M1** | 0.48 | 2.33 | 1.00 | 0.96 | 0.69 | 0.93 | -0.03 |
| **M3** | 0.48 | 1.14 | 1.06 | 0.85 | 0.61 | 0.95 | -0.05 |
| **M4** | 0.53 | 1.70 | 0.99 | 0.67 | 0.43 | 0.83 | 0.03 |

The Geoaccumulation index of mudflat sediments revealed that there was significant amount of Mn and Cr in the sediments (Table 3.3.6). On comparing with the Igeo values of mudflat sediments collected in the premonsoon season of 2011, Igeo values of Fe at the three mudflat stations decreased after the imposition of the mining ban. Igeo values of Mn at M1 and M4 increased whereas Mn at M3 decreased in recent times. Igeo value of Cr at M1 increased whereas at M3 and M4 it decreased in recent times. The Igeo values of Co, Ni, Cu and Zn increased after the imposition of the mining ban. Thus, there was considerable remobilization of Mn, Co, Ni, Cu and Zn in the sediments in recent times due increased human activities like sand mining. Additionally, enhanced anthropogenic input in recent years must have contributed to the increase of index.

### 3.3.D Speciation of metals

#### 3.3.D.1 Mangroves

The average values of bioavailability of metals in the sediments carried out through sequential extraction within the five geochemical phases viz. exchangeable (F1), Carbonate (F2), Fe-Mn oxide/reducible (F3), organic matter and sulfide bound/ oxidisable (F4) and residual (F5) for cores S1, S2, S3 and S4 in the present study (a) and 2011 (b) are presented in table 3.3.7.

The metal data collected in the pre-mining ban period (2011) was compared with the post mining ban period (2015) using the isocon diagram for each of the analyzed metals and is illustrated in figure 3.3.1.

Table 3.3.7 Concentration of metals in various sediment fractions, bioavailable and Labile (Exchangeable + carbonate) fractions of mangrove cores S1, S2, S3 and S4 in present study 2015 (a) and 2011 (b).

| **(a)** | | Exchangeable | Carbonate | Fe-Mn oxide | Organic matter/ Sulfide | Residual | Sum of Bioavailable fractions | Exchangeable + Carbonate | |
|---|---|---|---|---|---|---|---|---|---|
| | | (ppm) | (ppm) | (ppm) | (ppm) | (ppm) | (ppm) | (%) | (ppm) |
| Fe | S1 | 3.56 | 10.91 | 6053 | 3170 | 83805 | 9236 | 0.02 | 14.47 |
| | S2 | 4.86 | 15.48 | 5464 | 2368 | 95122 | 7852 | 0.02 | 20.34 |
| | S3 | 3.22 | 34.34 | 4537 | 7990 | 69751 | 12564 | 0.05 | 37.56 |
| | S4 | 1.99 | 17.55 | 5623 | 1089 | 77083 | 6732 | 0.02 | 19.54 |
| Mn | S1 | 518 | 1849 | 2838 | 489 | 557 | 5696 | 37.97 | 2369 |
| | S2 | 590 | 765 | 1592 | 218 | 499 | 3165 | 35.09 | 1355 |
| | S3 | 371 | 345 | 313 | 66.00 | 329 | 1094 | 50.33 | 715 |
| | S4 | 158 | 1025 | 1047 | 107 | 614 | 2337 | 39.41 | 1183 |
| Cr | S1 | 7.79 | 0.94 | 8.26 | 14.73 | 305 | 31.71 | 2.59 | 8.73 |
| | S2 | 5.53 | 2.42 | 11.14 | 21.06 | 301 | 40.13 | 2.32 | 7.95 |
| | S3 | 8.75 | 0.91 | 8.40 | 12.39 | 213 | 30.45 | 4.08 | 9.66 |
| | S4 | 7.92 | 3.00 | 6.26 | 16.23 | 248 | 33.41 | 3.88 | 10.92 |
| Co | S1 | 1.72 | 4.02 | 8.87 | 4.71 | 40.20 | 19.31 | 9.64 | 5.74 |
| | S2 | 2.05 | 3.15 | 9.20 | 4.22 | 37.99 | 18.61 | 9.17 | 5.20 |
| | S3 | 2.69 | 4.19 | 6.21 | 5.34 | 40.56 | 18.42 | 11.69 | 6.88 |
| | S4 | 0.86 | 3.73 | 6.09 | 2.69 | 36.97 | 13.36 | 9.10 | 4.59 |
| Ni | S1 | 0.79 | 1.63 | 8.59 | 7.91 | 96.77 | 18.91 | 2.08 | 2.42 |
| | S2 | 1.92 | 1.70 | 10.43 | 7.90 | 92.59 | 21.95 | 3.16 | 3.62 |
| | S3 | 1.96 | 1.80 | 7.08 | 8.52 | 85.25 | 19.35 | 3.64 | 3.76 |
| | S4 | 1.81 | 1.94 | 6.58 | 3.52 | 76.28 | 13.84 | 4.21 | 3.75 |
| Cu | S1 | 3.67 | 1.07 | 1.38 | 16.29 | 65.64 | 22.40 | 5.38 | 4.74 |
| | S2 | 3.67 | 0.43 | 1.39 | 15.84 | 57.21 | 21.32 | 5.20 | 4.10 |
| | S3 | 6.39 | 0.36 | 0.37 | 22.45 | 55.58 | 29.57 | 7.91 | 6.75 |
| | S4 | 0.19 | 1.58 | 1.30 | 9.57 | 73.11 | 12.63 | 2.08 | 1.77 |
| Zn | S1 | 5.38 | 3.32 | 24.03 | 14.06 | 107 | 46.78 | 5.68 | 8.70 |
| | S2 | 5.12 | 1.88 | 16.63 | 10.55 | 83.35 | 34.17 | 5.97 | 7.00 |
| | S3 | 6.69 | 3.50 | 21.63 | 17.05 | 87.13 | 48.86 | 7.60 | 10.19 |
| | S4 | 2.87 | 4.12 | 30.28 | 9.20 | 103 | 46.46 | 4.68 | 6.99 |

| **(b)** | Core | Exchangeable (ppm) | Carbonate (ppm) | Fe-Mn oxide (ppm) | Organic/Sulfide (ppm) | Residual (ppm) | Bioavailable Fraction (ppm) |
|---|---|---|---|---|---|---|---|
| Fe | S1 | 15.84 | 5.69 | 7921 | 902 | 76452 | 8844 |
| | S2 | 14.88 | 3.50 | 8326 | 1280 | 89240 | 9624 |
| | S3 | 64.51 | 5.03 | 5650 | 955 | 77690 | 6674 |
| | S4 | 76.68 | 7.38 | 3887 | 184 | 62464 | 4154 |
| Mn | S1 | 562 | 1945 | 2362 | 268 | 485 | 5136 |
| | S2 | 609 | 717 | 2717 | 228 | 612 | 4270 |
| | S3 | 338 | 666 | 984 | 248 | 516 | 2235 |
| | S4 | 130 | 350 | 411 | 174 | 471 | 1064 |
| Cr | S1 | 1.62 | 0.91 | 11.43 | 13.27 | 198 | 27.22 |
| | S2 | 0.87 | 1.37 | 10.86 | 11.26 | 169 | 24.35 |
| | S3 | 2.16 | 0.95 | 11.54 | 24.07 | 177 | 38.70 |
| | S4 | 1.38 | 1.49 | 10.99 | 14.27 | 177 | 28.12 |
| Co | S1 | 1.00 | 1.32 | 9.71 | 3.16 | 34.19 | 15.19 |
| | S2 | 1.27 | 1.19 | 11.51 | 2.19 | 27.12 | 16.16 |
| | S3 | 2.14 | 1.21 | 5.89 | 2.31 | 33.93 | 11.55 |
| | S4 | 1.32 | 2.25 | 4.77 | 1.20 | 27.37 | 9.54 |
| Cu | S1 | 1.30 | 1.56 | 2.91 | 21.82 | 82.52 | 27.59 |
| | S2 | 1.13 | 1.11 | 2.06 | 11.27 | 69.12 | 15.56 |
| | S3 | 0.88 | 0.83 | 1.23 | 10.34 | 56.39 | 13.28 |
| | S4 | 1.36 | 1.21 | 0.74 | 4.38 | 44.24 | 7.68 |
| Zn | S1 | 0.67 | 1.95 | 22.06 | 9.75 | 80.95 | 34.42 |
| | S2 | 0.87 | 1.56 | 15.24 | 6.72 | 69.00 | 24.38 |
| | S3 | 1.22 | 2.18 | 14.66 | 5.87 | 87.08 | 23.93 |
| | S4 | 6.23 | 1.54 | 12.78 | 2.80 | 57.82 | 23.35 |

Iron was mainly associated with the residual fraction of sediments at all the four studied sites of the estuary (69751 ppm to 95122 ppm) which accounted to 85% to 92 %. Fe in the bioavailable fractions (F1+F2+F3+F4) was low in all cores. On comparing bioavailability of Fe in the post mining ban period (2015) with pre-mining ban (2011) Fe in the exchangeable fraction decreased at all stations and Fe-Mn oxide decreased at stations S1, S2 and S3 in the post mining ban period (Figure 3.3.1). Considerable increase of Fe in organic/sulfide bound and carbonate fraction was

noted in the present study as compared to 2011. Increased Fe in the organic/sulfide phase in recent times suggested the association of Fe with organic matter and/or sulfides probably in the absence of fresh Fe input from mining. Also, organic matter decay by microorganisms must have facilitated Fe immobilization.

Cr in the Zuari estuary was mainly associated with the residual phase (213 ppm to 385 ppm) that accounted to 87 % to 91 %. Highest bioavailable Cr concentrations was noted in core S2 followed by S4, S1 and S3. Bioavailable concentrations of Cr at S1, S2, and S4 were higher in the post-mining ban period than pre-mining ban (Figure 3.3.1). The increase in bioavailable concentrations at S1, S2 and S4 was due to increase of exchangeable, organic matter and carbonate bound Cr.

Considerable amount of Co was associated with the residual phase as compared to other phases (36.97 ppm to 40.56 ppm that accounted to 67 % to 73 %) with considerable quantity in bioavailable phases. Most bioavailable Co concentration was noted in sediments of S1 followed by S2, S3, and S4 and was mainly associated with the Fe-Mn oxide phase. Comparison of bioavailability of Co in the pre-mining ban with the present results showed that Co bioavailability had significantly increased in recent times due to increase in organic bound, carbonate, and exchangeable fractions.

Ni in the Zuari estuary was also largely associated with residual fraction (76.28 ppm to 96.77 ppm that accounted to 81 % to 85 %) that consists essentially of detrital silicate minerals. Highest average concentration of bioavailable Ni was noted at S2 followed by S3, S1 and S4 and was mainly associated with the Fe-Mn oxide bound and organic matter/ sulfide bound phases.

Cu was also mainly associated with the residual phase (55.58 ppm to 73.11 ppm that accounted to 65% to 85 %) in the Zuari estuary with considerable quantity in the bioavailable phases. Higher average bioavailable Cu concentration was noted in S3 followed by S1, S2 and S4 with high concentrations in the organic matter/sulfide bound phase. The bioavailability of Cu increased in recent times at S2, S3, and S4 when compared with pre-mining ban results mainly due to the increase in the organic bound and exchangeable fractions.

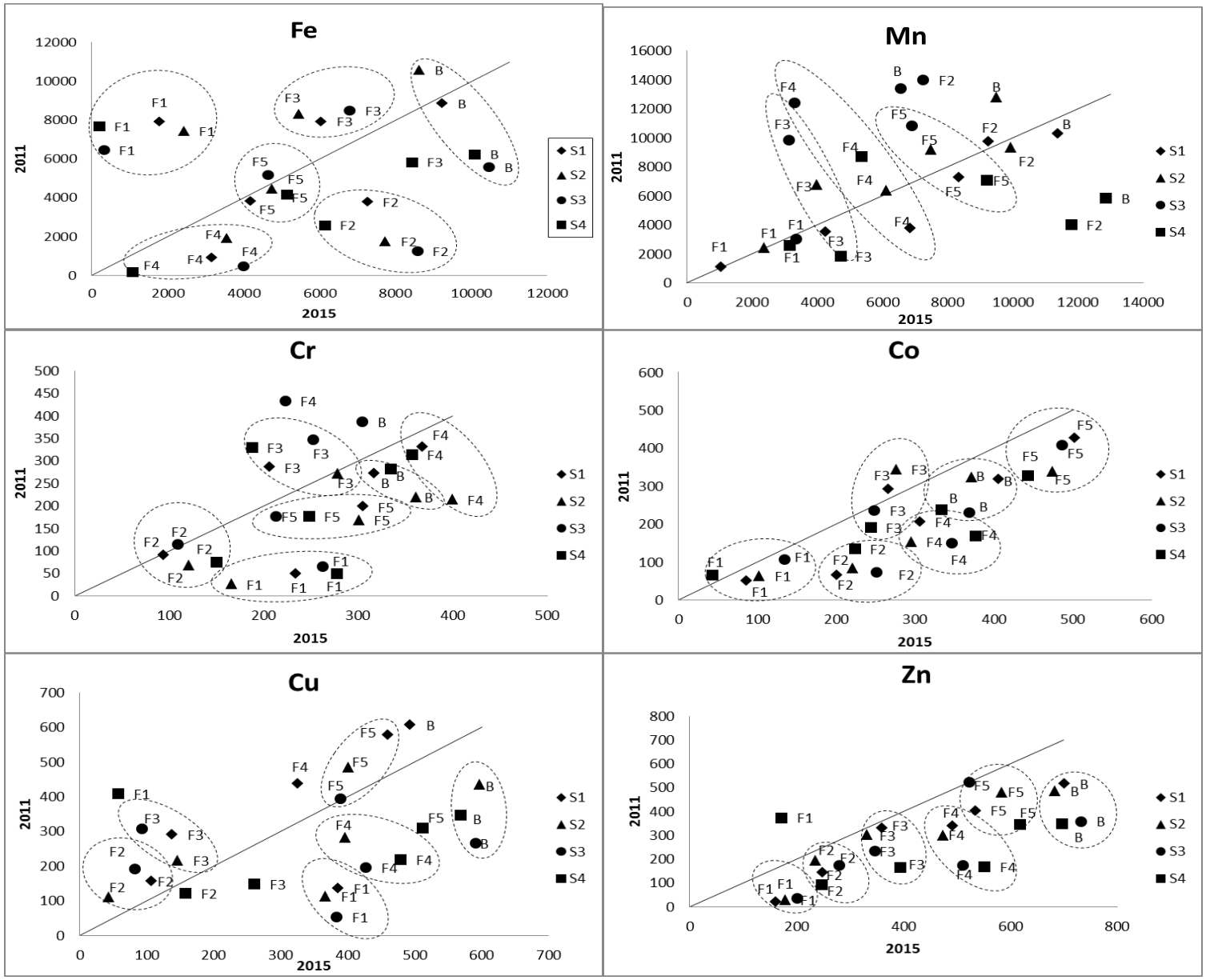


Figure 3.3.1 : Isocon diagram of Fe, Mn, Cr, Co, Cu and Zn in the exchangeable (F1), Carbonate (F2), Fe-Mn oxide bound (F3), Organic matter/ sulfide bound (F4), Residual (F5) and total bioavailable (B) fraction of sediments of cores S1, S2, S3 and S4 in 2011 and 2015.

Much of the Zn was associated with the residual phase of the sediments (83.35 ppm to 107 ppm that accounted to 64 % to 71 %) with considerable quantity in the bioavailable phases. The bioavailability of Zn had considerably increased in recent times when compared with 2011 speciation data, and was attributed to increase in the organic, Fe-Mn oxides, carbonate bound, and exchangeable fractions of Zn.

Manganese displayed spatial variability in its distribution in the five phases. A large quantity of Mn (1094 ppm to 5696 ppm that accounted for 77 % to 91 %) was associated with the bioavailable fractions of the mangrove sediments. Highest average concentration of Mn in the bioavailable phases was noted in core S1 followed by cores S2, S4 and S3. Mn in core S1, S2 and S4 was mainly associated with the reducible phase (F3) as it easily forms oxides. The comparison of Mn speciation data with earlier reported data based on sample collection in 2011 pre-mining ban period showed that bioavailable concentrations of Mn at S1 and S4 have increased in recent times. Increased concentrations of reducible Mn led to higher bioavailable Mn concentrations in S1 whereas exchangeable, carbonate and reducible Mn led to higher concentrations of bioavailable Mn at S4 than previously reported. Concentrations of bioavailable Mn at S2 and S3 have considerably decreased in recent years, after the ban on mining.

Mn in the reducible phase acts as a redox sensitive element that generally undergoes a change in mobility with respect to different physicochemical conditions. The high Mn concentrations associated with the reducible fraction in cores S1, S2 and S4 raised concerns over their potential mobility and subsequent bioavailability due to dredging or sand mining. Concentration of Mn in core S3 was mainly associated with the exchangeable and carbonate fractions, though, the concentrations in the exchangeable fraction was low as compared to cores S1 and S2 in the estuary. The concentration of bioavailable Mn in S3 and S4 was relatively lower compared to cores S1 and S2.

Overall, there was a considerable increase in the bioavailable fractions of most metals in recent times, which may be attributed to resuspension due to dredging of sediments and sand mining activities, which must have caused mobilization of metals that interact with the organic and inorganic components and are redeposited onto the surface sediments. Additionally, increase in

human activities in the catchment area must have contributed in the increase of metals. Increase in industrialization, shipbuilding, and transport activities in and around the estuary and domestic sewage discharges release considerable amount of organic matter and other metal contaminants in dissolved and particulate form. The elevated levels of Mn in the bioavailable fractions particularly in the exchangeable fraction were indicative of high mobility and potential toxicity to sediment dwelling organisms.

### 3.3. D.1a Risk assessment

To understand the risk of metals to the sediment-associated benthic organisms, the metal content in the bioavailable fractions (Table 3.3.7(a)) were compared with sediment quality values (SQV) using screening quick reference table (SQuiRT) proposed by Buchman (1999). The concentration of bioavailable Fe in all four stations fell below the Apparent Effects Threshold (AET) and Cr and Zn concentrations were below Threshold Effects Level (TEL) indicating no toxicity risk to biota. Concentration of bioavailable Ni and Cu at station S1, S2 and S3 fell between TEL and Effects Range Level (ERL) whereas Ni and Cu concentrations at S4 fell below TEL. Bioavailable Co concentrations were higher than AET at all stations and bioavailable Mn concentrations were well above AET at all locations in the estuary. Thus, bioavailable concentration of Co, Ni, and Cu suggests their potential toxicity to biota and concentrations of Mn indicated high toxicity to the sediment dwelling organisms. On comparing with the 2011 metal speciation concentrations, higher bioavailable concentrations in 2015 of Fe (S1, S3, S4), Mn (S1, S4), Cr (S1, S2, S4), Co (S1, S2, S3, S4), Cu (S2, S3, S4) and Zn (S1, S2, S3, S4) indicated the decrease in sediment quality in recent times and increased risk to sediment biota.

Risk assessment code was also used to evaluate the toxicity of the labile phases (exchangeable+ carbonate bound) of metals in sediments based on criteria described by Perin et al. (1985). The concentrations of labile Fe (Table 3.3.7(a)) were below 1 % and therefore pose no risk to sediment associated biota. However concentrations of labile Cr, Co, Ni, Cu and Zn were between 1 % and 10 % and posed a low risk and concentrations of labile Co at S3 posed medium toxicity risk (between 11 and 30 %). Labile Mn at S1, S2 and S4 (between 31 and 50 %) posed a high risk whereas at S3 fell in a very high risk category (>50 %). Thus, the concentrations of Mn in the sediments can cause detrimental effects to the associated biota including the mangroves. The

sequential extraction of metals therefore provided an insight on the potential bioavailability and mobility of sediment-bound metals, thus serving to predict the fate of heavy metals in the sediments.

### 3.3. D.2 Mudflats

The average values of metal concentrations in the five sedimentary fractions of the mudflat cores M1, M3 and M4 collected in 2015 is presented in table 3.3.8 (a) and that was compared with previously obtained data in 2011 (b). In addition, the metal data collected in the pre-mining ban period (2011) was compared with the post mining ban period (2015) using the isocon diagram for each of the analyzed metals and is illustrated in figure 3.3.2.

Iron was mainly associated with the residual fraction of the sediments at all three studied sites (81634 ppm to 85613 ppm) and accounted for 90 % to 92 %. Bioavailability of Fe was low at all locations as compared to residual Fe, however, among locations higher content of bioavailable Fe was noted in M1 followed by M3 and M4. Among the bioavailable fractions Fe was mainly associated with the Fe-Mn oxide bound fraction followed by organic/ sulfide bound fraction, carbonate and least in exchangeable fraction. A comparison of bioavailable Fe content with pre-mining ban concentration showed that bioavailable Fe content had increased post-mining ban and was attributed to increase in organic/ sulfide bound Fe and to some extent Fe-Mn oxide bound and carbonate bound Fe. Fe in the organic matter/ sulfide bound fraction and carbonate bound fraction had increased at M1, M3 and M4 whereas Fe-Mn oxide bound Fe increased at M3 and M4 in recent times. The significant increase in organic matter/ sulfide bound Fe during post mining ban indicated that organic matter might have played a significant role to bind Fe when there was a reduction of inputs of detrital mining Fe ore particles.

Chromium in the sediments was noted to be present mainly in the residual form (234 ppm to 293 ppm) which accounted for 85 % to 89 %. Bioavailability of Cr was mainly due to Cr content in the organic/ sulfide fraction followed by exchangeable and Fe-Mn oxide bound fractions. Higher bioavailable Cr was noted in M4 followed by M1 and M3. When 2015 bioavailable Cr concentrations was compared with 2011 data, it was noted that the bioavailability of Cr had significantly increased at M1 and M4 in recent times

Table 3.3.8: Concentration of metals in various sediment fractions, bioavailable fraction and Exchangeable + carbonate fractions of mudflat cores M1, M3 and M4 in present study (a) and 2011 (b).

| **(a)** | | Exchangeable | Carbonate | Fe-Mn oxide | Organic/ Sulfide | Residual | Bioavailable fraction | Exchangeable + Carbonate | |
|---|---|---|---|---|---|---|---|---|---|
| | | ppm | ppm | ppm | ppm | ppm | ppm | % | ppm |
| Fe | M1 | 5.14 | 12.41 | 6303 | 3407 | 83308 | 9727 | 0.02 | 17.55 |
| | M3 | 2.90 | 19.95 | 6643 | 2800 | 85613 | 9466 | 0.02 | 22.84 |
| | M4 | 1.45 | 66.31 | 5692 | 1716 | 81634 | 7475 | 0.08 | 67.76 |
| Mn | M1 | 437 | 1722 | 3098 | 527 | 555 | 5784 | 34.07 | 2159 |
| | M3 | 381 | 927 | 1251 | 195 | 480 | 2754 | 40.58 | 1308 |
| | M4 | 263 | 1410 | 1751 | 232 | 510 | 3656 | 39.81 | 1673 |
| Cr | M1 | 9.60 | 1.49 | 8.28 | 15.88 | 293 | 35.24 | 3.37 | 11.08 |
| | M3 | 11.86 | 0.74 | 9.71 | 11.56 | 250 | 33.87 | 4.45 | 12.60 |
| | M4 | 9.64 | 5.39 | 7.01 | 18.19 | 234 | 40.23 | 5.52 | 15.03 |
| Co | M1 | 2.07 | 4.47 | 9.19 | 5.01 | 39.70 | 20.73 | 10.83 | 6.53 |
| | M3 | 1.83 | 3.64 | 7.35 | 3.93 | 40.05 | 16.75 | 9.63 | 5.47 |
| | M4 | 1.23 | 4.11 | 6.55 | 3.30 | 47.05 | 15.17 | 8.53 | 5.33 |
| Ni | M1 | 0.85 | 1.56 | 8.79 | 8.23 | 95.26 | 19.42 | 2.10 | 2.41 |
| | M3 | 1.34 | 1.36 | 7.90 | 7.27 | 97.32 | 17.87 | 2.34 | 2.70 |
| | M4 | 2.21 | 2.51 | 7.15 | 5.60 | 91.73 | 17.46 | 4.29 | 4.71 |
| Cu | M1 | 3.33 | 0.63 | 1.82 | 19.62 | 60.12 | 25.39 | 4.66 | 3.96 |
| | M3 | 5.09 | 1.21 | 1.26 | 15.65 | 67.54 | 23.20 | 6.94 | 6.30 |
| | M4 | 3.26 | 1.59 | 1.02 | 14.50 | 68.23 | 20.37 | 5.44 | 4.85 |
| Zn | M1 | 4.51 | 2.46 | 23.70 | 27.43 | 91.50 | 58.10 | 4.88 | 6.97 |
| | M3 | 4.08 | 2.63 | 22.84 | 11.90 | 107 | 41.43 | 4.53 | 6.70 |
| | M4 | 4.49 | 3.58 | 26.76 | 11.55 | 112 | 46.36 | 5.03 | 8.06 |

| **(b)** (2011) | Core | Exchangeable (ppm) | Carbonate (ppm) | Fe-Mn oxide (ppm) | Organic/Sulfide (ppm) | Residual (ppm) | Bioavailable Fraction (ppm) |
|---|---|---|---|---|---|---|---|
| Fe | M1 | 34.40 | 5.25 | 7514 | 1336 | 64872 | 8889 |
| | M3 | 52.08 | 10.39 | 5350 | 515 | 76392 | 5929 |
| | M4 | 98.37 | 28.97 | 4640 | 241 | 60110 | 5008 |
| Mn | M1 | 756 | 1471 | 2424 | 346 | 666 | 4997 |
| | M3 | 339 | 1222 | 1883 | 343 | 529 | 3787 |
| | M4 | 116 | 859 | 1189 | 229 | 577 | 2392 |
| Cr | M1 | 1.45 | 0.86 | 11.16 | 12.07 | 194 | 25.53 |
| | M3 | 1.72 | 1.18 | 10.04 | 22.82 | 243 | 35.75 |
| | M4 | 3.64 | 1.56 | 10.85 | 20.92 | 189 | 36.97 |
| Co | M1 | 1.72 | 2.33 | 9.23 | 3.73 | 31.59 | 17.00 |
| | M3 | 1.67 | 1.66 | 5.99 | 2.08 | 32.39 | 11.40 |
| | M4 | 2.49 | 1.53 | 5.47 | 1.56 | 32.80 | 11.04 |
| Cu | M1 | 1.17 | 1.57 | 3.26 | 23.32 | 56.39 | 29.31 |
| | M3 | 0.89 | 0.74 | 1.45 | 9.38 | 62.78 | 12.44 |
| | M4 | 0.33 | 1.08 | 1.21 | 6.05 | 61.92 | 8.66 |
| Zn | M1 | 0.98 | 1.31 | 19.81 | 10.87 | 68.46 | 32.96 |
| | M3 | 1.51 | 2.01 | 13.48 | 4.81 | 66.41 | 21.81 |
| | M4 | 1.58 | 2.23 | 14.10 | 3.48 | 84.54 | 21.39 |

Cobalt was also associated with the residual fraction (39.70 ppm to 47.05 ppm) which accounted for 66 % to 76 %. Among the four bioavailable fractions, the Fe-Mn oxide fraction accounted for most bioavailability of Co followed by organic matter/sulfide and carbonate bound Co with least concentrations in the exchangeable fraction. Higher bioavailability of Co was noted in the upper middle estuary mudflat which decreased toward the lower estuary. Comparison of bioavailability of Co with the previous study in 2011 revealed increased values in recent times at all stations. Increase in the organic matter/ sulfide bound, carbonate bound Co at M1, M3 and M4 were noted whereas Fe-Mn oxide bound Co increased at M3 and M4 and exchangeable Co at M1 and M3.

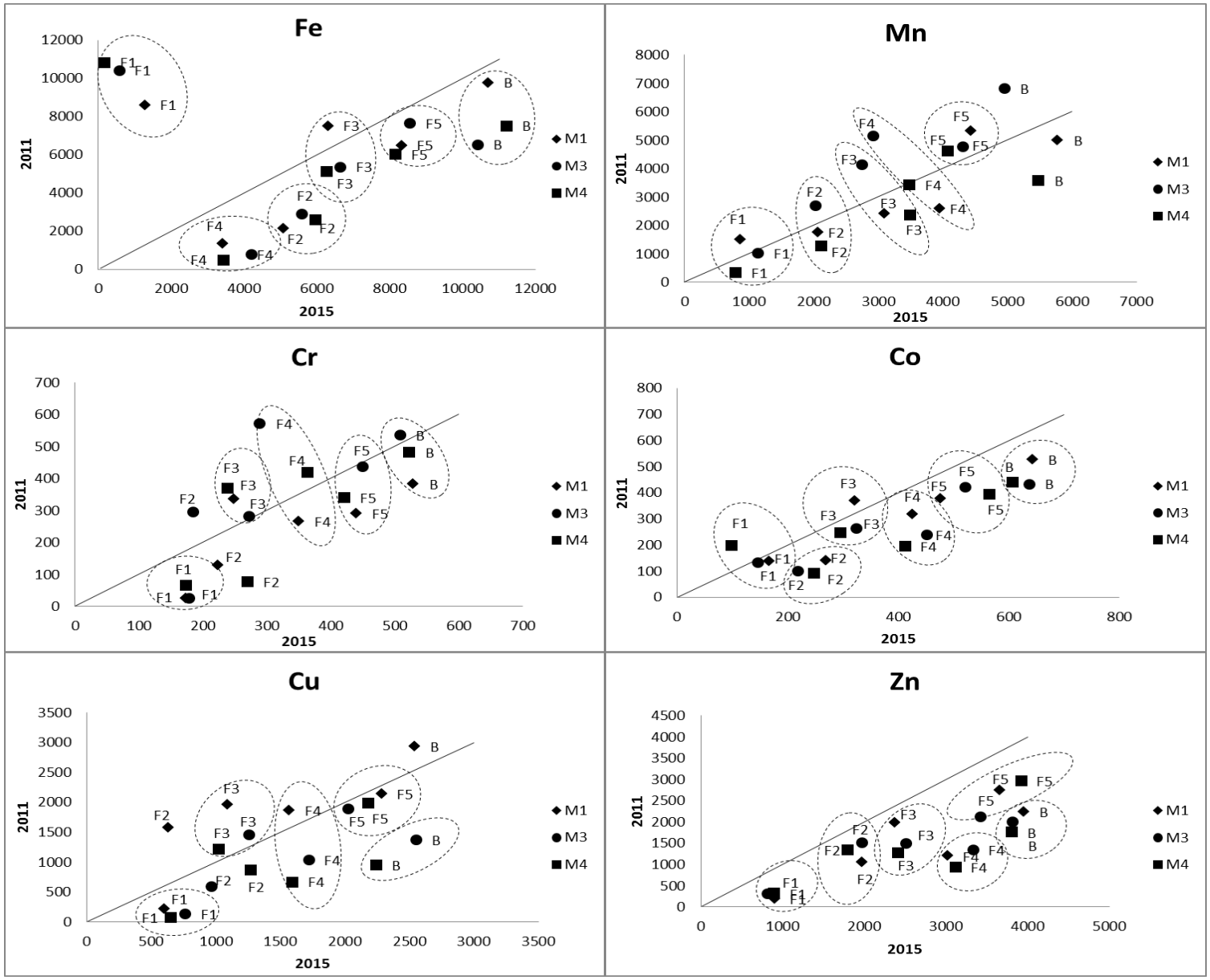


Figure 3.3.2 : Isocon diagram of Fe, Mn, Cr, Co, Cu and Zn in the exchangeable (F1), Carbonate (F2), Fe-Mn oxide bound (F3), Organic matter/ sulfide bound (F4), Residual (F5) and total bioavailable (B) fraction of sediments of cores M1, M3 and M4 in 2011 and 2015.

The residual fraction of the sediments was a major repository for Ni (91.73 ppm to 97.32 ppm) which accounted for 83 % to 84 %. Bioavailability of Ni was low at all there mudflat stations, however, the Fe-Mn oxide and organic matter/ sulfide phase had higher Ni concentrations than the carbonate and exchangeable fractions. Among stations higher bioavailable Ni was noted in M1 followed by M3 and M4.

Speciation of Cu in the sediments revealed that large amount of Cu was associated with the residual fraction of sediments (60.12 ppm to 68.23 ppm) which accounted for 70 % to 77 %. The organic matter/ sulfide bound Cu accounted for most bioavailability of Cu. Overall higher bioavailable Cu concentrations were noted in M1 followed by M3 and M4. The comparison of Cu speciation data with previous study in 2011 indicated higher bioavailable concentrations at M3 and M4 in recent times. In addition, Cu in the exchangeable fractions was enriched at M1, M3 and M4 whereas organic matter/sulfide bound and carbonate bound Cu was enriched at M3 and M4 in recent times.

Zinc in was present chiefly in the residual fractions the mudflat sediments (91.50 ppm to 112 ppm) which accounted for 63 % to 72 %. Considerable amount of Zn was associated with the bioavailable fractions in the Fe-Mn oxide and organic matter/ sulfide bound fractions. In general higher bioavailable Zn was noted in M1 followed by M4 and M3. When the speciation of Zn data was compared with the previous data of 2011, it was observed that the bioavailability of Zn had increased two fold in recent times due to increase in concentrations in all four bioavailable fractions.

High concentrations of Mn in the mudflat sediments were associated with the bioavailable fraction (2754 ppm to 5784 ppm) that accounted for 85 % to 91 % of the total Mn. Highest concentrations of bioavailable Mn was noted in M1 followed by M4 and M3. Manganese was mainly associated with the Fe-Mn oxide and carbonate bound fractions and significant concentrations were also present in the exchangeable and organic matter/ sulfide bound fractions. Comparison of bioavailable Mn with previously analyzed data of 2011 indicated that there was significant input of Mn in the upper middle estuary and lower estuary in recent times.

Higher concentration of bioavailable Mn in the upper middle estuary indicated that most anthropogenic Mn was removed on encountering saline waters during early estuarine mixing. Elevated concentrations in the lower estuary mudflats may be due to precipitation of Mn as oxides due to remobilization. Part of the Mn must have been incorporated into carbonates, which are higher in the lower estuary mudflats. Thus, elevated Mn concentrations in the sediments were indicative of high anthropogenic inputs of Mn and the probable to cause toxicity to biota.

As metals Fe, Cr, Co, Ni, Cu, and Zn had high percentage concentrations in the residual phase, it can be inferred that these metals are potentially less mobile and pose a lower toxicity risk as the distribution of these metals in the sediments are more strongly associated with clastic material. High Mn concentrations in the bioavailable fractions could be potentially toxic. A comparison of bioavailability of metals in post-mining ban period with pre-mining ban revealed elevated concentration of metals in the bioavailable fractions in the post-mining ban period. This increase might be due to remobilization of metals due to sand mining. Additionally, anthropogenic inputs into estuary from the catchment area must have contributed. Shipbuilding industries and jetties located along the banks of the estuary release considerable amount of metals as leachates to the waters, which are ultimately deposited to the sediments. In addition, industrial, agricultural, and domestic discharges release considerable amount of organic matter to the estuary, which adsorb metals and are deposited to the sediments. As the discharges of the mining activities and its effects in the catchment area had considerably reduced, role of other factors such as organic matter, hydrous oxides, pH that were suppressed earlier due to large influx of mining material are now accentuated in the distribution of metals.

### 3.3. D.2a Risk assessment

The concentration of metals in the bioavailable fraction of the mudflat sediments (Table 3.3.8(a)) were compared with the sediment quality values of SQuiRT. Bioavailable concentrations of Fe, Cr and Zn in the mudflat sediments were below the AET in all cores and thus posed no toxicity to sediment biota. Bioavailable concentrations of Ni and Cu were greater than the TEL but may not have any toxicity effects. The concentration of bioavailable Mn and Co were above the AET in all mudflat cores, which can cause adverse biological effects. When the bioavailable metal concentrations of 2015 were compared with 2011 bioavailable metal concentrations, the increase

in Fe (M1, M2, M3), Mn (M1 and M4), Cr (M1 and M4), Co (M1, M3 and M4), Cu (M3 and M4) and Zn (M1, M3 and M4) concentration indicated that the sediment quality has decreased over times due to remobilization or anthropogenic inputs.

RAC was computed for the labile fraction of metals in the sediments. The concentrations of labile Mn fell in the high risk category of RAC ranging from 31 % to 50 %. However, the concentrations of labile Fe, Cr, Co, Ni, Cu and Zn fell in the low risk category ranging from 1 % to 10 % in all mudflat cores except for Co in M1 that showed labile concentration of 10.83 % which borderlines the medium risk category.

Thus, the concentrations of Mn and other metals in the estuary should be continuously monitored to assess their concentrations and potential toxicity to biota. Anthropogenic activities in the catchment area of the estuary can release significant amount of metals that settle to the sediments which act a repository for pollutants. The metals may be continued to be stored in the sediments or can be mobilized due to changes in redox conditions, bioturbation or dredging. The mobilized metals undergo a phase change from solid to solution, which can either be re-precipitated or diffuse to the water column. These metals may be mobilized in the estuary or are taken up by biota, which undergo bioaccumulation and biomagnification and then transferred in the food chain to higher organisms.

# *Chapter 4*

# *Bioaccumulation of metals*

## 4.1 Bioaccumulation of metals in mangrove pneumatophores

The mangrove species *Avicennia officinalis* was present at sampling locations S1, S2 and S3 whereas *Sonnertia alba* was present at sampling location S4 (Table 4.1.1). The families of Avicinnaceae and Sonnertiaceae have evolved distinct morphological changes to deal with anoxic sediments and possess aerial roots called pneumatophores that enable gaseous exchange and oxygenation for respiration in an anoxic environment. Different mangrove species have different ability to alter sediment physico-chemical properties and affect the organic matter content of mangrove sediment (Lacerda et al., 1995).

Table 4.1.1: Mangrove species identified at the four mangrove sampling locations.

| Mangrove | Mangrove species |
|---|---|
| S1 | *Avicennia Officinalis* |
| S2 | *Avicennia Officinalis* |
| S3 | *Avicennia Officinalis* |
| S4 | *Sonnertia Alba* |

The concentration of metals in pneumatophores is presented in table 4.1.2. The abundance of metals in mangrove pneumatophores varied in the order Fe>Mn>Zn>Cu>Cr>Ni>Co at locations S1 and S3. At the other two locations namely S2 and S4, Co was higher than Ni. Metals Fe, Mn, Cu, and Zn are considered as essential elements for mangrove growth, however higher concentrations of these elements might have negative effect on the plants. Concentration of metals in *A. officinalis* pneumatophores was found to be higher than that in *S. alba*.

Table 4.1.2: Concentration of metals in mangrove pneumatophores expressed in ppm.

| Mangrove | Fe | Mn | Cr | Co | Ni | Cu | Zn |
|---|---|---|---|---|---|---|---|
| **S1** | 4015 | 1045 | 10.15 | 3.65 | 4.75 | 16.85 | 52.16 |
| **S2** | 2610 | 525 | 7.05 | 3.10 | 2.10 | 11.50 | 37.97 |
| **S3** | 3580 | 955 | 7.90 | 3.40 | 4.05 | 10.10 | 38.93 |
| **S4** | 840 | 75 | 3.90 | 2.70 | 2.40 | 7.80 | 14.42 |

Metal concentrations in the mangrove pneumatophores were compared with the metal concentrations in the sediments (Table 4.1.3). Fe ranged from 91900 ppm to 107900 ppm in bulk sediments, 6732 ppm to 12564 ppm in the bioavailable fractions and 14.47 ppm to 37.56 ppm in the labile fractions whereas in pneumatophores it varied from 840 ppm to 4015 ppm. Mn, on the other hand, ranged from 1595 ppm to 6155 ppm in the bulk sediments, 1094 ppm to 5696 ppm in the bioavailable fractions and 715 ppm to 2369 ppm in the labile fraction of sediments whereas in the pneumatophore it varied from 75 ppm to 1045 ppm. Cr concentration in the bulk sediments ranged from 254 ppm to 276 ppm, 30.45 ppm to 40.13 ppm in the bioavailable and 7.95 ppm to 10.92 ppm in the labile fraction whereas the concentration in the pneumatophores varied from 3.90 ppm to 10.15 ppm. The concentration of Co in the sediments varied from 37.90 ppm to 57.00 ppm in bulk, 13.36 ppm to 19.31 ppm in bioavailable and 4.59 ppm to 6.88 ppm in the labile fraction whereas Co in pneumatophores ranged from 2.70 ppm to 3.65 ppm. Ni concentration varied from 96.85 ppm to 154 ppm in the bulk, 13.84 ppm to 21.95 ppm in the bioavailable and 2.42 ppm to 3.76 ppm in the labile fraction of the sediments whereas Ni in mangrove pneumatophores ranged from 2.10 ppm to 4.75 ppm. The concentration of Cu in the sediments ranged from 99.05 ppm to 131 ppm in the bulk, 12.63 ppm to 29.57 ppm in the bioavailable and 1.77 ppm to 6.75 ppm in the labile fraction whereas in pneumatophore, Cu concentration varied from 7.80 ppm to 16.85 ppm. Zn concentration in the sediments ranged from 128 ppm to 149 ppm in bulk, 34.17 ppm to 48.86 ppm in the bioavailable and 6.99 ppm to 10.19 ppm in labile whereas Zn concentrations in pneumatophores ranged from 14.42 ppm to 52.16 ppm.

Large amount of Fe and Mn were present in the bulk sediments, bioavailable, and labile fractions of the sediments as compared to Cr, Co, Ni, Cu, and Zn. The concentration of metals in the pneumatophores showed that Fe and Mn were higher as compared to Cr, Co, Ni, Cu, and Zn. Thus, Fe and Mn possibly were taken up in large quantities due to their high availability in the sediments, mainly in the bioavailable and labile fractions. Additionally, the range of Cu and Zn concentrations in the mangrove pneumatophores were higher than their respective labile fractions, which reflect the accumulation affinity for Cu and Zn by the mangrove plants.

Table 4.1.3: Concentration of metals Fe, Mn, Cr, Co, Ni, Cu and Zn determined in bulk sediments, bioavailable and labile fractions in the 2015 post-mining ban collection expressed in ppm.

| | | Fe | Mn | Cr | Co | Ni | Cu | Zn |
|---|---|---|---|---|---|---|---|---|
| Bulk | S1 | 99200 | 6155 | 276 | 56.70 | 150 | 131 | 143 |
| | S2 | 107900 | 3800 | 273 | 57.00 | 154 | 119 | 128 |
| | S3 | 94700 | 1595 | 254 | 49.50 | 129 | 122 | 145 |
| | S4 | 91900 | 2990 | 260 | 37.90 | 96.85 | 99.05 | 149 |
| Bioavailable | S1 | 9236 | 5696 | 31.71 | 19.31 | 18.91 | 22.40 | 46.78 |
| | S2 | 7852 | 3165 | 40.13 | 18.61 | 21.95 | 21.32 | 34.17 |
| | S3 | 12564 | 1094 | 30.45 | 18.42 | 19.35 | 29.57 | 48.86 |
| | S4 | 6732 | 2337 | 33.41 | 13.36 | 13.84 | 12.63 | 46.46 |
| Labile | S1 | 14.47 | 2369 | 8.73 | 5.74 | 2.42 | 4.74 | 8.70 |
| | S2 | 20.34 | 1355 | 7.95 | 5.20 | 3.62 | 4.10 | 7.00 |
| | S3 | 37.56 | 715 | 9.66 | 6.88 | 3.76 | 6.75 | 10.19 |
| | S4 | 19.54 | 1183 | 10.92 | 4.59 | 3.75 | 1.77 | 6.99 |

The bioconcentration factor (BCF) was calculated to assess the metals accumulation in pneumatophores relative to the environmental loadings and estimate chemical residuals in the plants (MacFarlane et al., 2007; Mountouris et al., 2002). The calculated BCF values with respect to bulk, bioavailable, and labile metal concentrations in sediments are presented in table 4.1.4.

The BCF values that were calculated using bulk concentrations for all metals were below 0.5 at all locations, except for Mn at S3 (0.6). The bioavailable BCF values were greater than bulk BCF for all metals. High BCF values of bioavailable Zn and Cu were noted at S1 (1.12 and 0.75 respectively) and S2 (1.11 and 0.54 respectively) as compared to other metals. However, bioavailable Mn (0.87) and Zn (0.80) showed high BCF for sampling location S3. At site S4, Cu (0.62) showed higher bioavailable BCF value as compared to other metals. Further, BCF values of labile sediment fractions (Exchangeable + carbonate bound fractions) revealed very high values for Fe (276), Ni (1.97), Cu (3.56) and Zn (6.00) at S1; Fe (128), Cu (2.81) and Zn (5.42) at S2; Fe (95.33), Cu (1.50) and Zn (3.82) at S3 and Fe (43.01), Cu (4.42) and Zn (2.07) at S4. Thus, Fe, Cu, and Zn were more bioaccumulated in the mangrove pneumatophores as compared

to other metals and Fe was hyper-accumulated with respect to the labile sediment fraction. Kathiresan et al. (2014) reported earlier high Fe accumulation in mangrove plant tissues.

Table 4.1.4: Bioconcentration factors in pneumatophores calculated using the bulk and bioavailable metals at sampling locations S1, S2, S3 and S4.

| | **Fe** | **Mn** | **Cr** | **Co** | **Ni** | **Cu** | **Zn** |
|---|---|---|---|---|---|---|---|
| **BCF- Bulk sediments** | | | | | | | |
| **S1** | 0.04 | 0.17 | 0.04 | 0.06 | 0.03 | 0.13 | 0.37 |
| **S2** | 0.02 | 0.14 | 0.03 | 0.05 | 0.01 | 0.10 | 0.30 |
| **S3** | 0.04 | 0.60 | 0.03 | 0.07 | 0.03 | 0.08 | 0.27 |
| **S4** | 0.01 | 0.03 | 0.01 | 0.07 | 0.02 | 0.08 | 0.10 |
| | | | | | | | |
| **BCF- Bioavailable** | | | | | | | |
| | Fe | Mn | Cr | Co | Ni | Cu | Zn |
| **S1** | 0.43 | 0.18 | 0.32 | 0.19 | 0.25 | 0.75 | 1.12 |
| **S2** | 0.33 | 0.17 | 0.18 | 0.17 | 0.10 | 0.54 | 1.11 |
| **S3** | 0.28 | 0.87 | 0.26 | 0.18 | 0.21 | 0.34 | 0.80 |
| **S4** | 0.12 | 0.03 | 0.12 | 0.20 | 0.17 | 0.62 | 0.31 |
| | | | | | | | |
| **BCF-Labile** | | | | | | | |
| | Fe | Mn | Cr | Co | Ni | Cu | Zn |
| **S1** | 277.47 | 0.44 | 1.16 | 0.64 | 1.97 | 3.56 | 6.00 |
| **S2** | 128.35 | 0.39 | 0.89 | 0.60 | 0.58 | 2.81 | 5.42 |
| **S3** | 95.33 | 1.33 | 0.82 | 0.49 | 1.08 | 1.50 | 3.82 |
| **S4** | 43.01 | 0.06 | 0.36 | 0.59 | 0.64 | 4.42 | 2.07 |

The role of Fe is well known in the formation of chlorophyll, protein synthesis and root growth (Jones et al., 1991) whereas Mn is involved in photosynthesis, respiration, and lignin and amino acid biosynthesis, and activation of several enzymes (Mukhopadhyay and Sharma, 1991). Furthermore, oxygen released by the pneumatophores of mangrove plant creates an oxidant geochemical microenvironment which helps to oxidize soluble $Fe^{2+}$ and $Mn^{2+}$ to insoluble $Fe(OH)_3$ and $MnO_2$ in sediments (Silva et al., 1990). Following this, oxide-hydroxides of Fe and Mn strongly co-precipitate with other metals and additionally form of iron plaques on root surfaces of the mangroves (Bartlett, 1961; Lacerda, 1997). The higher content of iron and manganese in the pneumatophores could be possibly involved in the oxidant geochemical reaction occurring in the mangrove sediments and their uptake by root tissues and subsequent

accumulation in other plant tissues as suggested by Kathiresan et al. (2014). Copper is an essential micronutrient required in the mitochondria and chloroplast reactions, enzyme systems related to photosystem II electron transport, cell wall lignification, carbohydrate metabolism, and protein synthesis (Verkleij and Schat, 1990). Zinc is also an essential micro-nutrient of numerous enzyme systems, respiration enzyme activators, and the biosynthesis of plant growth hormones (Ernst et al., 1992). Thus possibly essential elements viz. Fe, Mn, Zn and Cu were more bio-accumulated compared to Co, Cr and Ni. Cr, Ni and Co are considered as non-essential elements and toxic to plant growth (Bonanno and Giudice, 2010; He et al., 2014). Between the two species, *Avicennia officinalis* accumulated higher metal concentrations in pneumatophore tissues. Similar observation was made earlier by Sarangi et al. (2002) wherein metal concentrations in five mangrove species were studied and *A. officinalis* accumulated highest concentrations of metals analyzed. *A. officinalis* tends to manage the uptake of essential metals to fulfil metabolic requirements while restricting the uptake of non-essential metals to avoid toxicity (Chakraborty et al., 2013). The low accumulation of metals in *S. alba* pneumatophores than *A. officinalis* is likely due to physiological differences and variations that exist in accumulation strategies of different plant species (Defew et al., 2005). The variations in metal accumulation between the two species and location in the estuary might be due to the metal need of the specific tissues, variation in salinity, the amount/quantity of metals deposition in the mangrove sediments and seawater intrusion during high tide as observed by Edu et al. (2015). In addition, the plant species, types of plant components, physiological age of tissue and seasons likewise, have significant influence on metal accumulation ability of the plants (Jones, 1998). Thus, the effects of biological and physical phenomena, such as tidal inundation, salinity changes, wind and waves that allow the processes of bioturbation, re-suspension and erosion and affect the metal concentrations in sediments (Bellucci et al., 2002), may have a large influence on the uptake and accumulation ability of metals by the mangrove plants.

The labile fraction of the sediments is anthropogenically influenced and is easily available to biota. High uptake and accumulation of labile Fe, Cu and Zn by the mangrove plants suggest their potential phytoremediation ability and thus act as long term sinks for metals. Phytoextraction of contaminants from sediments requires translocation from root to other plant

parts and hyper-accumulation of contaminants requires species tolerant to high concentrations of bioavailable metals (MacFarlane et al., 2007).

Pearson's correlation of metal concentrations in pneumatophores versus average metal concentrations of bulk sediments, bioavailable fraction and labile fraction was computed. Statistically significant correlation ($p<0.005$, $n=7$) was obtained for the data set of bulk sediments and bioavailable fraction. For core S1, $r=0.98$; $p=0.0001$ was obtained for metals in pneumatophore with bulk sediments and $r=0.94$; $p=0.0014$ for metals in pneumatophores with bioavailable fraction. For core S2 pneumatophores with bulk, $r=0.99$; $p=0.00004$ and pneumatophores with bioavailable, $r=0.98$; $p=0.0001$ values were obtained. For core S3, pneumatophore with bulk, $r=0.97$; $p=0.0003$ and pneumatophore with bioavailable, $r=0.98$; $p=0.00007$ and for S4, pneumatophores with bulk, $r=1.00$; $p=0.0000001$ and pneumatophore with bioavailable, $r=0.97$, $p=0.0004$ values were obtained. Hence, the strong correlation indicated that pneumatophores are able to accumulate metals in accordance to the metal content deposited in the underlying sediments. Pneumatophores are perennial organs that have a longer duration of accumulation of trace elements as they contain high concentrations of tannins compared to other tissue types, which provides a greater ability to bind trace metals (Silva et al., 1990; Zheng et al., 1997; Ismail, 2002). Nath et al. (2014) found a strong positive relationship between metals in sediments and pneumatophores that suggest the potential use of pneumatophore tissues as a bio-indicator of estuarine contamination. Pearson's correlation test showed no significant correlation with respect to the labile fraction of sediments, i.e. $r=0.09$; $p=0.84$ for core S1; $r=0.04$; $p=0.93$ for core S2; $r=0.14$; $p=0.76$ for core S3, and, $r= -0.73$; $p=0.88$ for S4. The poor correlation of metal concentrations in pneumatophores and metals in the labile fraction may be due to the low concentration of metals in the labile fraction of sediments and their subsequent uptake, translocation and storage in other plant parts such as root, bark and leaves.

Thus, mangrove plants accumulated Fe, Mn, Cu and Zn in their pneumatophores tissues and exhibited differences in accumulation of metal with respect to location and species due the spatial variation in sediment characteristics, quantity of metals deposited in the sediments, their bioavailability and differences in plant species and tissue physiology.

## 4.2 Bioaccumulation of metals in sediment associated biota

Sediments are sinks for heavy metals in estuarine/marine environments and play a key role in the transmission and deposition of metals (Bastami et al., 2015). Sediments may contain higher than average abundances of metals due to input from anthropogenic activities, which may cause the formation of the more bioavailable forms of the metals. Benthic organisms can take up the bioavailable fraction of metals from the sediments and accumulate them in their tissues that can cause toxicity. Such effects can significantly affect the trophic structure of a biological community. The metals deposited in the sediments at the water-sediment interface are important to the fauna as compared with subsurface sediments since most fauna live above the reduced zone in sediments. Therefore, the composition of surface sediments has a significant influence on the living conditions of marine organisms. Thus, establishing a correlation between metal form and concentrations in sediments and their uptake by biota is important to understand the impact of sediment contaminants in the food chain in estuarine environments (Birch et al., 2014).

The molluscs are a diverse and species–rich phyla of the animal kingdom wherein gastropods make up more than 80 % of the species and bivalves constituting a major part (15 %) of the rest (Oehlmann and Schulte-Oehlmann, 2003). They are common, macroscopic, ecologically and commercially important on a global scale as food and as non-food resources (Palpandi and Kesavan, 2012). Molluscs are in direct contact with the ambient medium (water or sediment) due to the lack of an exoskeleton and can assimilate contaminants not only from the diet via the gastro-intestinal tract but also from ambient water or sediment via the integument and respiratory organs resulting in greater contaminant accumulation potential. They are being successfully applied as biological indicators due to their effective accumulation of organic and metallic pollutants in their tissues at concentrations several orders of magnitude above those observed in the field environment (Elder and Collins, 1991; Bryan et al., 1983). Bivalves and gastropod molluscs are also considered as useful biomonitors of certain metals. Most metals are generally concentrated many times higher within an organism’s soft tissue, rather than the shell (Kesavan et al., 2013). The objective of the present study was to estimate the heavy metal concentrations such as Fe, Mn, Cr, Co, Ni, Cu, and Zn, in the soft tissues of molluscs collected from different locations along the Zuari estuary and explore the potential of using these molluscs as a

bioindicator for metal accumulation. The different species collected from the sedimentary environments are listed in table 4.2.1.

Table 4.2.1: Sediment associated biota collected from the intertidal environments of the Zuari estuary.

| Sample | Subenvironment | Species | Phyllum | Class |
|---|---|---|---|---|
| S2 | Mangrove | *Neritina (Dostia)* | Mollusca | Gastropoda |
| M3 | Mudflat | *Telescopium telescopium* | Mollusca | Gastropoda |
| | | *Crassostrea sp.* | Mollusca | Bivalvia |
| | | *Muricidae sp.* | Mollusca | Gastropoda |
| | | *Neritina (Dostia)* | Mollusca | Gastropoda |
| M4 | Mudflat | *Cerithidea quadrata* | Mollusca | Gastropoda |
| | | *Telescopium telescopium* | Mollusca | Gastropoda |
| | | *Crassostrea sp.* | Mollusca | Bivalvia |

In Zuari estuary, one gastropod species *Neritina (Dostia) violacea* was collected from the Cumbharjua canal mangrove S2, two gastropods *Telescopium telescopium and Muricidae sp.* and one bivalve belonging to genus *Crassostrea* was collected from M3 mudflat and three gastropods *Neritina (Dostia) violacea, Cerithidea quadrata* and *Telescopium telescopium* and bivalves belonging to genus *Crassostrea* were collected at M4 mudflat (Table 4.2.1).

The concentration of metals Fe, Mn, Cr, Co, Ni, Cu, and Zn determined in bulk sediments, bioavailable and labile fractions in the year 2015 post-mining ban collection (Table 4.2.2) was used for comparison and calculation of various indices. Highest bulk metal concentration of Fe, Co and Ni were noted in S2, Cr and Cu in M3 and Mn and Zn in M4. Metals in the bioavailable fractions showed greater abundance for Co and Ni at S2, Fe and Cu at M3 and Mn, Cr and Zn at M4. The labile fraction of metals showed higher content of Co and Cu at M3 and Fe, Mn, Cr, Ni and Zn at M4. Overall, abundance of metals in the sediments decreased in the order of Bulk sediments> bioavailable> labile.

Table 4.2.2: Concentration of metals Fe, Mn, Cr, Co, Ni, Cu and Zn determined in bulk sediments, bioavailable and labile fractions in the 2015 post-mining ban collection and Apparent effects threshold (AET) in sediments for Benthic invertebrate and Oysters (Gries and Waldow, 1996).

| | | Fe Ppm | Mn Ppm | Cr Ppm | Co Ppm | Ni Ppm | Cu ppm | Zn ppm |
|---|---|---|---|---|---|---|---|---|
| Bulk sediments | S2 | 107945 | 3800 | **273** | 57.00 | **154** | 119 | 128 |
| | M3 | 99015 | 2910 | **281** | 51.40 | 138 | 130 | 138 |
| | M4 | 102595 | 4235 | **268** | 45.25 | 122 | 120 | 146 |
| Bioavailable | S2 | 7852 | 3165 | 40.13 | 18.61 | 21.95 | 21.32 | 34.17 |
| | M3 | 9466 | 2754 | 33.87 | 16.75 | 17.87 | 23.20 | 41.43 |
| | M4 | 7475 | 3656 | 40.23 | 15.17 | 17.46 | 20.37 | 46.36 |
| Labile | S2 | 20.34 | 1355 | 7.94 | 5.20 | 3.62 | 4.10 | 7.00 |
| | M3 | 22.85 | 1308 | 12.60 | 5.47 | 2.70 | 6.30 | 6.71 |
| | M4 | 67.76 | 1673 | 15.03 | 5.34 | 4.72 | 4.85 | 8.07 |
| Benthic AET | | NA | NA | 260 | NA | >140 | 530 | 410 |
| Oyster AET | | NA | NA | NA | NA | NA | 390 | 1600 |

The concentrations of metals in bulk, bioavailable, and labile fractions were compared with the Apparent effects threshold (AET) of benthic invertebrates and oysters. The AETs are concentrations of specific metals of concern in sediments above which a significant adverse biological effect always occurs. The concentration of Cr in bulk sediments was above the AET for benthic invertebrates at S2, M3, and M4; and concentration of Ni at S2 was above the AET for benthic in vertebrates when compared to the standard values available (Gries and Waldor, 1996).

The concentration of metals in the benthic organisms was observed to vary spatially and among the different species (Table 4.2.3). Overall, the organisms showed significantly higher concentrations of Fe, Mn, Cu and Zn in their tissues whereas Cr, Co and Ni were accumulated in lesser amounts.

Table 4.2.3: The concentration of metals in tissues of the sediment associated biota in mangrove S2 and mudflats M3 and M4.

| | | **Fe** ppm | **Mn** Ppm | **Cr** ppm | **Co** Ppm | **Ni** ppm | **Cu** ppm | **Zn** ppm |
|---|---|---|---|---|---|---|---|---|
| **S2** | *Neritina (Dostia) violacea* | **2276** | **517** | 11.43 | 17.68 | **22.67** | **23.67** | **190** |
| **M3** | *Telescopium telescopium* | **2640** | **782** | 7.12 | 6.67 | 8.67 | **213** | **237** |
| | *Crassostrea sp.* | **939** | **170** | 4.15 | 4.79 | 5.39 | **341** | **804** |
| | *Muricidae sp.* | **1183** | **166** | 13.01 | 7.33 | ND | **1994** | **556** |
| **M4** | *Neritina (Dostia) violacea* | **2095** | **440** | 8.17 | 13.53 | 12.98 | **23.35** | **161** |
| | *Crassostrea sp.* | **1348** | **74.91** | 4.49 | 3.65 | 1.30 | **207** | **1525** |
| | *Cerithidea quadrata* | **978** | **414** | 5.94 | 10.68 | 12.78 | **74.57** | **69.75** |
| | *Telescopium telescopium* | **517** | **1229** | 3.53 | 6.17 | 9.00 | **161** | **409** |

ND- Not detectable

Highest concentrations of Fe (2640 ppm) were found in tissues of *T. telescopium* at M3, Mn (1229 ppm) in *T. Telescopium* of M4, Cr (13.01 ppm) and Cu (1994 ppm) in *Muricidae sp.* of M3, Co (17.68 ppm) and Ni (22.67 ppm) in *N. violacea* of S2 and Zn (1525 ppm) in *Crassostrea sp.* of M4. The concentration of metals varied in the order Fe>Mn>Zn>Cu>Ni>Co>Cr in *N. violacea* at S2. At M3, metals varied in the order of Fe>Mn>Zn>Cu>Ni>Cr>Co in *T. Telescopium*, Fe>Zn>Cu>Mn>Ni>Co>Cr in *Crassostrea sp.* and Fe>Cu>Zn>Mn>Cr>Co>Ni in *Muricidae sp.* At M4, metals concentrations varied in the order of Fe>Mn>Zn>Cu>Co>Ni>Cr in *N. violacea*, Zn>Fe>Cu>Mn>Cr>Co>Ni in *Crassostrea sp.*, Fe>Mn>Cu>Zn>Ni>Co>Cr in *C. quadrata*, Mn>Fe>Zn>Cu>Ni>Co>Cr in *T. telescopium. N. violacea* of the Cumbharjua canal S2 accumulated higher content of metals Fe, Mn, Cr, Ni, Co, Cu and Zn than the same species collected from the mudflat of the lower middle estuary. *T. telescopium* of M3 accumulated higher

content of Fe, Cr, Co and Cu whereas *T. telescopium* of M4 had higher content of Mn, Ni and Zn in its tissues. *Crassostrea* sp. of M3 had higher concentration of Mn, Co, Ni, and Cu in their tissues whereas Fe, Cr and Zn were higher in *Crassostrea sp.* of M4.

The concentration of metals in the biota was compared with the concentration of metals in the bulk sediments, bioavailable, and labile fractions. The concentration of Fe ranged from 99015 ppm to 107945 ppm in the bulk sediments, 7475 ppm to 9466 ppm in the bioavailable fraction and 20.34 ppm to 67.76 ppm in the labile fraction of the sediments whereas Fe in the tissues of the molluscs ranged from 517 ppm to 2640 ppm, highest being in *T. telescopium* at M3. Mn concentrations in the sediments ranged from 2910 ppm to 4235 ppm in the bulk sediments, 2754 ppm to 3656 ppm in the bioavailable fraction and 1308 ppm to 1673 ppm in the labile fraction while Mn in the mollusc's tissues varied from 74.91 ppm to 1229 ppm, highest being in *T. telescopium* at M4. The concentration of Cr varied from 268 ppm to 281 ppm in the bulk sediments, 33.87 ppm to 40.23 ppm in the bioavailable fraction and 7.94 ppm to 15.03 ppm in the labile fraction whereas Cr in the molluscs tissues ranged from 3.53 ppm to 13.01 ppm, highest being in *Muricidae sp*. at M3. Co concentration in the sediments ranged from 45.25 ppm to 57.00 ppm in the bulk sediments, 15.17 ppm to 18.61 ppm in the bioavailable fraction and 5.20 ppm to 5.47 ppm in the labile fraction while Co in molluscs tissues varied from 3.65 ppm to 17.68 ppm, highest being in *N. violacea* at S2. Ni concentration in the sediments varied from 122 ppm to 154 ppm in the bulk sediments, 17.46 ppm to 21.95 ppm in the bioavailable fraction of sediments and 2.70 ppm to 4.72 ppm in the labile fraction whereas Ni in the mollusc's tissues varied from 1.30 ppm to 22.67 ppm, highest being in *N. violacea* at S2. Cu in the sediments ranged from 119 ppm to 130 ppm in the bulk sediments, 20.37 ppm to 23.20 ppm in the bioavailable fraction and 4.10 ppm to 6.30 ppm in the labile fraction whereas Cu in the tissues ranged from 23.35 ppm to 1994 ppm, highest being in *Muricidae sp*. at M3. Zn concentration in the sediments ranged from 128 ppm to 146 ppm in bulk sediments, 34.17 ppm to 46.36 ppm in bioavailable fraction and 6.71 ppm to 8.07 ppm in the labile fraction whereas Zn in molluscs tissues varied from 69.75 ppm to 1525 ppm, highest being in *Crassostrea sp.* at M4.

Overall, Fe and Mn concentrations were highest in the mollusc's tissues, which may have been due to its high bioavailability in the sediments resulting in increased uptake by biota. Cu and Zn

concentrations were higher in the mollusc's tissues than the sediments, which indicated that Cu and Zn were, taken up in large amounts and were bioaccumulated in the organism tissues. Cr, Co, and Ni were taken up in low concentrations by the organisms due to their low bioavailability in the sediments.

The Biota Sediment Accumulation Factor (BSAF) of metals was calculated which described the bioaccumulation of the sediment-associated metals into tissues of ecological receptors. The BSAF values (Table 4.2.4) with respect to the bulk sediments showed that *T.telescopium, Crassostrea sp*. and *Muricidae sp.* at M3, and *Crassostrea sp.* and *T. telescopium* at M4 showed values greater than 1.00 for Cu. Further, all the sampled organisms at the three locations, except for *C. quadrata* at M4, exhibited values greater than 1.00 for Zn. The BSAF values for Fe, Mn, Cr, Co and Ni were less than 1.00 for all collected biota samples. Higher BSAF values were noted with respect to the bioavailable metal concentrations as compared to the bulk metal concentrations. Cu and Zn showed high BSAF values ranging from 1.00 to 85.96 in the species collected at the three locations. Fe, Mn, Cr, Co and Ni exhibited BSAF values less than 1.00, except for Ni for *N. violacae* (1.03) at S2. BSAF values were also calculated using the labile fraction of the sediments. The BSAF values varied from less than 1.00 to as high as 317. The BSAF values of Fe, Zn and Cu were greater than 1.00 for all species at the three locations in addition to Cr, Co and Ni for some species. *N. violacea* at S2 showed BSAF values greater than 1.00 for Fe, Cr, Ni, Cu, and Zn. At M3, *T. telescopium* exhibited BSAF values greater than 1.00 for Fe, Co, Ni, Cu and Zn, *Crassostrea sp.* for Fe, Ni, Cu and Zn, and *Muricidae sp.* for Fe, Cr, Co, Cu and Zn. At station M4, *N. violacea* exhibited BSAF values greater than 1.00 for Fe, Co, Ni, Cu and Zn, *Crassostrea sp*. for Fe, Cu and Zn, *C. quadrata* and *T. telescopium* for Fe, Co, Ni, Cu and Zn. From the computed BSAF values, it is clear that *Crassostrea sp.* and *Muricidae sp.* accumulated large amount of Cu and Zn.

Table 4.2.4: Biota Sediment Accumulation Factor (BSAF) calculated relative to concentrations of bulk metals, bioavailable metals and labile metals.

| | Station | Organism | Fe | Mn | Cr | Co | Ni | Cu | Zn |
|---|---|---|---|---|---|---|---|---|---|
| BSAF-Bulk metals | S2 | *N.violacea* | 0.02 | 0.14 | 0.04 | 0.3 | 0.15 | 0.20 | **1.49** |
| | M3 | *T. telescopium* | 0.03 | 0.27 | 0.03 | 0.1 | 0.06 | **1.63** | **1.72** |
| | | *Crassostrea sp.* | 0.01 | 0.07 | 0.01 | 0.0 | 0.04 | **2.62** | **5.82** |
| | | *Muricidae sp.* | 0.01 | 0.06 | 0.05 | 0.1 | -- | **15.33** | **4.03** |
| | M4 | *N. violacea* | 0.02 | 0.10 | 0.03 | 0.3 | 0.11 | 0.20 | **1.10** |
| | | *Crassostrea sp.* | 0.01 | 0.02 | 0.02 | 0.0 | 0.01 | **1.73** | **10.47** |
| | | *C. quadrata* | 0.01 | 0.10 | 0.02 | 0.2 | 0.10 | 0.62 | 0.48 |
| | | *T. telescopium* | 0.01 | 0.29 | 0.01 | 0.1 | 0.07 | **1.34** | **2.81** |
| BSAF-Bioavailable | S2 | *N.violacea* | 0.29 | 0.16 | 0.28 | 0.9 | **1.03** | **1.11** | **5.57** |
| | M3 | *T. telescopium* | 0.28 | 0.28 | 0.21 | 0.4 | 0.49 | **9.16** | **5.73** |
| | | *Crassostrea sp.* | 0.10 | 0.07 | 0.12 | 0.2 | 0.30 | **14.72** | **19.40** |
| | | *Muricidae sp.* | 0.12 | 0.06 | 0.38 | 0.4 | -- | **85.96** | **13.42** |
| | M4 | *N.violacea* | 0.28 | 0.12 | 0.20 | 0.8 | 0.74 | **1.15** | **3.46** |
| | | *Crassostrea sp.* | 0.18 | 0.02 | 0.11 | 0.2 | 0.07 | **10.15** | **32.89** |
| | | *C. quadrata* | 0.13 | 0.11 | 0.15 | 0.7 | 0.73 | **3.66** | **1.50** |
| | | *T. telescopium* | 0.07 | 0.34 | 0.09 | 0.4 | 0.52 | **7.89** | **8.82** |
| BSAF-Labile | S2 | *N.violacea* | **112** | 0.38 | **1.44** | **3.4** | **6.26** | **5.78** | **27.20** |
| | M3 | *T. telescopium* | **116** | 0.60 | 0.57 | **1.2** | **3.21** | **33.74** | **35.37** |
| | | *Crassostrea sp.* | **41.09** | 0.15 | 0.33 | 0.8 | **2.00** | **54.20** | **120** |
| | | *Muricidae sp.* | **51.75** | 0.13 | **1.03** | **1.3** | -- | **317** | **82.89** |
| | M4 | *N. violacea* | **30.91** | 0.26 | 0.54 | **2.5** | **2.75** | **4.81** | **19.89** |
| | | *Crassostrea sp.* | **19.90** | 0.04 | 0.30 | 0.6 | 0.28 | **42.64** | **189** |
| | | *C.quadrata* | **14.44** | 0.25 | 0.40 | **2.0** | **2.71** | **15.37** | **8.64** |
| | | *T. telescopium* | **7.63** | 0.73 | 0.23 | **1.1** | **1.91** | **33.14** | **50.68** |

The metal pollution index (MPI) was calculated using the equation MPI= ($Cf_1$ x $Cf_2$ x $Cf_3$….x Cfn) $^{1/n}$ where $Cf_i$ is the concentration of metal in the sample and the results were presented in table 4.2.5. The MPI revealed that gastropods tend to accumulate more metals in their tissues than bivalves-*Crassostrea sp*.

Table 4.2.5 :Metal pollution index (MPI) for organism collected from the intertidal environments along the Zuari estuary.

| Sample location | Organism | MPI | N |
|---|---|---|---|
| **S2** | *N. violacea* | 81.69 | 7 |
| **M3** | *T. telescopium* | 88.62 | 7 |
| | *Crassostrea sp.* | 65.63 | 7 |
| | *Muricidae sp.* | 166 | 6 |
| **M4** | *N. violacea* | 65.10 | 7 |
| | *Crassostrea sp.* | 48.99 | 7 |
| | *C. quadrata* | 55.91 | 7 |
| | *T. telescopium* | 69.95 | 7 |

The analysis of the metals content in the tissues, along with BSAF and MPI of the mollucs revealed that the sediment-associated biota accumulated more Fe, Mn, Cu, and Zn over Cr, Co and Ni. Fe, Mn, Cu, and Zn are considered as essential elements whereas Cr, Co and Ni are non-essential but are required for metabolism in trace quantities and both essential and non-essential metals are taken up from water, sediment, or food, by the benthic organisms. Essential elements Fe, Mn, Cu, and Zn are important for the metabolism of the organism. Iron is associated with various enzymes in living systems such as peroxidase, catalase, cytochrome, oxidase, nitrogenase (Cole, 1983). Cu and Zn play an important role in the composition of approximately 90 enzymes in animal metabolism (Carvalho et al., 1993). Mn though available in high concentrations in the sediment bioavailable fractions and tissues, showed low BSAF values, which may indicate the slowing of Mn uptake after reaching the maximal level of this metal in the organisms

The enhanced accumulation of Fe, Mn, Zn, and Cu in organisms may be due to sequestration of metal cations in insoluble metal- rich granules and cellular metal detoxification/redistribution (Viarengo and Nott, 1993; Irato et al., 2003). The rates of metal uptake and excretion are affected by the biology of the organism, the permeability of the external surface, the nature of food, and the efficiency of the osmoregulational system present (Rainbow, 1995). The scrap metals from the boat metals and fishing vessels and paint residues (antifouling paints) from local boat jetties may be the source of zinc and copper to the sediment and which is taken up by the organism and

accumulated in the tissues (Palpandi and Kesavan, 2012). Fe in the labile fraction is directly related to anthropogenic metal inputs exhibited higher BSAF, which may be from leachates of mining ores. BSAF values for Mn were low which may be due to homoestasis (internal regulation) of metals by the organisms (Fasulo et al., 2008).

The differences between BSAF and MPI in the different molluscs species may be related to the differences in the detoxification mechanisms and/or metabolic activities (Azevedo et al., 2012). It is known that accumulation of metals in large concentrations can cause toxicity to the organism. However, the organisms have regulatory and detoxification mechanisms. Some metalloproteins are known by their function in detoxification such as Metallothioneins which are low-molecular-weight cytosolic proteins with a high cysteine content, showing a strong affinity towards certain essential and nonessential trace elements, such as Cu and Zn (Kägi and Schäffer, 1988) and, therefore, make them less toxic to other cellular constituents (HEATH, 1990). Zn and Cu are known as essential elements that activate many enzymatic systems. Zn especially has an important function since it is a component of metallothionein. This protein is very important in the detoxification of toxic metals through the dismutation of zinc-binding (Smirnov et al., 2005). Since molluscs have a limited ability to excrete pollutants, metabolize organic chemicals, and physiologically inactivate toxic metals by binding to metallothioneins, the molluscs tend to attain higher bioaccumulation factors for many metals (Berger et al., 1995, Oehlmann and Schulte-Oehlmann, 2003).

Thus, benthic invertebrates are important in the assessment of ecological risks of aquatic sites. One of the primary contaminant exposure pathways for these organisms is the consumption of contaminated food. Deposited sediments often act as a local sink for contaminants, which may increase the contaminant exposure for sediment associated biota that ingest sediment particles while foraging. These sediment benthic invertebrates are an important food source for fish and some terrestrial wildlife. Therefore, the concentrations of bioavailable contaminants in sediment revealed the food chain transfer and the potential toxicity of sediment contaminants (Jacobs, 1998). The metals in sediments are not always bioavailable, since their bioavailability depends on a series of factors such as pH, Eh, granulometry and organic matter content. Nonetheless,

metals in the environment are taken up by the organisms and can accumulate in tissues (HEATH, 1990).

Table 4.2.6: Pearson's correlation coefficient (*r*) and significance (*p*) of metals in tissues with bulk sediments, bioavailable and labile fraction of metals.

| Species | Sampling location | Metal correlation | r | *p* |
|---|---|---|---|---|
| *N. violacae* | S2 | Tissue/ bulk sediment | **0.98** | <0.05 |
| | | Tissue/bioavailable metals | **0.98** | <0.05 |
| | | Tissue/labile metals | 0.05 | >0.05 |
| | M4 | Tissue/ bulk sediment | **0.99** | <0.05 |
| | | Tissue/bioavailable metals | **0.96** | <0.05 |
| | | Tissue/labile metals | 0.06 | >0.05 |
| *T. telescopium* | M3 | Tissue/ bulk sediment | **0.97** | <0.05 |
| | | Tissue/bioavailable metals | **0.99** | <0.05 |
| | | Tissue/labile metals | 0.12 | >0.05 |
| | M4 | Tissue/ bulk sediment | 0.22 | >0.05 |
| | | Tissue/bioavailable metals | 0.59 | >0.05 |
| | | Tissue/labile metals | **0.90** | <0.05 |
| *Crassostrea sp.* | M3 | Tissue/ bulk sediment | 0.68 | >0.05 |
| | | Tissue/bioavailable metals | 0.65 | >0.05 |
| | | Tissue/labile metals | -0.15 | >0.05 |
| | M4 | Tissue/ bulk sediment | 0.58 | >0.05 |
| | | Tissue/bioavailable metals | 0.45 | >0.05 |
| | | Tissue/labile metals | -0.23 | >0.05 |
| *Muricidae sp.* | M3 | Tissue/ bulk sediment | 0.32 | >0.05 |
| | | Tissue/bioavailable metals | 0.24 | >0.05 |
| | | Tissue/labile metals | -0.30 | >0.05 |
| *C. quadrata* | M4 | Tissue/ bulk sediment | **0.93** | <0.05 |
| | | Tissue/bioavailable metals | **0.99** | <0.05 |
| | | Tissue/labile metals | 0.27 | >0.05 |

When Pearson's correlation of metals in tissue with metals in the bulk, bioavailable and labile fractions was computed (Table 4.2.6), *N. violacae* showed significant correlation of metals in

tissue with the bulk sediments and bioavailable fractions at locations S2 and M4. *T. telescopium* exhibited significant positive correlations of metals in tissue with metals in bulk sediments and bioavailable fraction at M3 and metals in sediments with labile fraction in M4. *C. quadrata* showed significant correlation of metals with the bulk sediment and bioavailable fractions. *Crassostrea sp.* and *Muricidae sp.* did not show any significant relation of metals in tissues with metals in sediments.

*N. violacae* exhibited consistency in its correlation of metals in tissue with bulk and bioavailable metals at both sample locations along with high MPI at S2 and M4, which may suggest its use as a bioindicator since it tends to accumulate metals relative to that available in the sediments. *T. telescopium* and *C. quadrata* also exhibited significant correlation of metals in tissue with bulk and bioavailable metals and showed high MPI suggesting their ability in biomonitoring of metals. The bivalve *Crassostrea* did not show any significant correlation of metals in tissues with sediments, along with lowest MPI at M3 and M4, *Muricidae sp*. exhibited poor correlation of metals in tissues with metals in sediments but with high MPI. Thus, gastropods *N. violacae*, *T. telescopium*, and *C. quadrata* can be used as potential bioindicators in the estuarine environment since they reflect the conditions of the local environment.

The bioaccumulation study showed that there were evidences of bioaccumulation of metals Fe, Cu and Zn in the biota of the Zuari estuary. However, information on the impact of pollutants on biota can only be obtained by applying long-term in situ biomonitoring assays (Bervoets et al., 2004) due to fluctuations in anthropogenic metal inputs and estuarine dynamics, physicochemical processes and changes in macrofauna community structure. Thus, long-term studies should be carried out to continuously monitor the estuarine quality and identify potential threats to the estuarine fauna.

# *Chapter 5*

# *Summary and Conclusions*

Mudflats and mangroves are important estuarine sub-environments, found in the inter-tidal zone of tropical and subtropical coasts. The mangrove and mudflats receive large contaminant inputs from catchments derived from run-off, anthropogenic leachates and discharges, as well as atmospheric and marine inputs. Consequently these environments have become important sinks for nutrients, organic and inorganic contaminants. Among these pollutants, metals have received significant attention due to their long-term effects on the environment. Metals originating from both natural and anthropogenic sources are discharged into estuarine system, which are transported and distributed in the aqueous phase and sediments. Physicochemical processes like adsorption and co-precipitation cause deposition of large quantity of metals to the sediment. Additionally, sediment parameters like sediment size, mineralogy, salinity, pH, organic matter content and oxidation–reduction potential are important parameters controlling the accumulation and the availability of metals in the sediment.

The Zuari estuary, located on the west coast of India is one of the major estuaries in Goa. Its catchment area is known for open cast iron and ferromanganese mines and is used to transport iron ores to the Mormugao harbor located at the mouth of the Zuari estuary. Mining in Goa has resulted in an environmental threat that was first felt in the year 1978 and as a consequence 287 mining concessions/leases were terminated and again in the year 2012, that led to a complete ban on mining. Several jetties, barge building and repairing industries, constructions and domestic waste discharges along the estuary release a large amount of organic and inorganic contaminants to the estuary. The Cumbharjua canal links the Zuari estuary to the adjacent Mandovi estuary and adds more mining material to the Zuari during the monsoons and ebb tide. These contaminants accumulate in the estuarine sediments over long periods and degrade the environmental quality and cause detrimental effect to the estuarine ecosystems. The estuarine sediments thus record the regional environmental changes and anthropogenic impacts. A geochemical investigation of estuarine sediment should illustrate the distribution, source, and enrichment of chemical elements in relation to sedimentary processes in the estuary. With this background the following objectives of the study were formulated:

1. To study the abundance and distribution of metals in sediments and to understand the role of physicochemical and geochemical parameters influencing the distribution of metals.

2. To study the concentration of metals in soft tissue of selected biota associated with sediments.

3. To establish a relation between bioavailability of metals in sediments and bioaccumulation of metals in biota.

To fulfil the above objectives, sediment grain size, total organic carbon, clay mineralogy, magnetic susceptibility parameters and bulk and clay metal chemistry and fractionation of metals was carried out on sediment cores, seasonal surface samples along with metal accumulation in biota. Four sampling locations in the Zuari estuary were selected from which one mudflat and mangrove from the upper middle estuary, lower middle estuary and lower estuary and one mangrove from the Cumbharjua canal were sampled. Furthermore, to understand the depositional environment, metal association and possible sources, statistical analysis of Pearson's correlation, principal component analysis and isocon diagrams were used. Pollution indices of enrichment factor, geoaccumulation index were used to know the metal contamination status of the estuary. Furthermore, geochemical speciation of metals into five fractions was carried out to understand the mobility and bioavailability of metals in the sediments. The contamination of metals in different sediment fractions was compared with sediment quality guidelines to determine the toxity risk to biota.

The sediment cores of approximately 40 cm were collected from mudflat and mangrove environments of the upper middle estuary, lower middle estuary and lower estuary and one mangrove from the Cumbharjua canal in 2011 during premonsoon season. In the mangrove environments, finer sediments, organic matter and metals were higher in the middle estuary and canal sediments while coarser sediments with fewer metal concentrations were seen in the lower estuary. The hydrodynamic conditions changed from lower estuary towards the upstream regions owing to mixing of riverine and sea water that led to finer sediment deposition in the middle estuary. Kaolinite, smectite, illite and traces of chlorite constituted the clay mineral assemblage

and had a minor influence on metal distributions. Magnetic susceptibility measurements indicated that there are substantial inputs of mining material into estuary mainly in the upper middle estuary and Cumbharjua canal. The variations in metal abundance were attributed to a difference in hydrodynamic conditions regulated by the tide, freshwater flow and geomorphology of the Zuari estuary. The results revealed that the estuary received material from natural weathering of rocks as well as from anthropogenic sources such as mining and industrial/domestic discharges.

In the upper middle estuary, trace metal distribution was influenced by adsorption onto Fe-oxides and flocculation in low salinity. In the Cumbharjua canal, there was substantial anthropogenic input of metals that was transported from the Mandovi estuary during periods of high rainfall and was accumulated in the sediments. The lower middle estuary mangrove showed little variations in metal distribution patterns and sediment grain size as metals associated with suspended matter may have been fully mixed and then deposited in this region. Hydrous Fe-oxides and aluminosilicates influenced the distribution patterns of metals in the sediments. Metals were less concentrated at the lower estuary mangrove, which was due to intensive tidal washing and dilution of metals by coarser sediments. However, the metals were associated with the finer sediments. Al, Fe and Mn distributions indicated lithogenic source. Correlation analysis of bulk metals with the clay minerals revealed that Cr was associated with chlorite in core S1 whereas Ni was associated with kaolinite and Zn was associated with smectite in core S2. Metals did not show significant association with the clay minerals in cores S3 and S4. Salinity played a significant role in the association of Ni with kaolinite whereas Zn may have replaced Al in the smectitic clays. Correlation analysis of magnetic susceptibility parameters and metals in the mangrove sediments indicated that the iron ore mined and transported from the catchment areas contributed ferrimagnetic particles to the sediments resulting in enhancement of magnetic susceptibility. Comparison of metals in the clay fraction with bulk metals in the mangrove sediments showed that most trace metals were enriched in the clay fraction. Fe and to some extent Co showed higher concentrations in the bulk suggesting their association with the larger sized sediments of sand and silt. Enrichment factor and Geo-accumulation index showed that Fe, Mn and Cr were enriched in the mangrove sediments. Fractionation of metals Fe, Mn, Cr, Co, Cu and Zn revealed that concentrations of bioavailable Mn pose a considerable risk to biota. Metals

Fe, Cr, Co, Cu and Zn were associated with the residual fraction of the sediments and thus have a major detrital control.

The mudflat cores collected from the upper middle estuary, lower middle estuary and lower estuary were also analyzed for sediment components, clay mineralogy, magnetic susceptibility and metal geochemistry and fractionation. The mudflat sediments along the estuary were dominated by silt and clay. The lower estuary sediments had higher percentage of coarse sediments whereas higher clay was noted in the lower middle estuary. This distribution of grain size was influenced by hydrodynamic conditions which are stronger towards the mouth and becomes calmer towards the upstream regions. Organic matter was higher in the upper middle estuary either due to the high content of finer sized sediments, inputs from sewage and wastewater or lower hydrodynamics. Clay mineralogy analysis of the mudflat sediments revealed that kaolinite was the most abundant clay mineral and was enriched in the upper middle estuary, whereas Smectite was high in the lower estuary and illite and chlorite was abundant in the lower middle estuary and their distribution varied due to estuarine dynamics, flocculation and stability properties of the clay minerals. Analysis of magnetic susceptibility parameters of the mudflat sediments indicated that the upper middle estuary contained higher amount of magnetic material than other regions of the estuary. Among metals, most were accumulated in the upper middle estuary than the mouth due to estuarine hydrodynamics, which increases towards the mouth under the influence of strong waves. In the upper middle estuary, metal distributions were influenced by Fe-Mn oxides and organic matter and less influenced by sediment grain size. Correlation analysis indicated that the metals were supplied from an anthropogenic source, as they do not show significant correlation with Al. In the lower middle estuary, the influence of sediment grain size and organic matter on metal distributions was noted to be negligible. However it was noted that the mudflat sediments were undergoing early diagenetic processes. The mudflat sediments of the lower estuary revealed that metal distributions were less affected by sediment components and the most metals were of detrital origin and associated with aluminosilicates. Poor correlation of bulk metals and clay minerals indicated the clay mineralogy had very little influence on metal distribution and was more influenced by other sediment components and physiochemical processes. The strong correlation between magnetic susceptibility and several heavy metal concentrations suggests a significant contribution to the

magnetism from anthropogenic sources and revealed the metals may have been preferentially adsorbed onto the exterior surface of Fe- oxides and precipitated to the sediments. The comparison of metal concentrations in the bulk sediments and clay fraction, however, revealed that most trace metals were enriched in the clay fraction of sediments and were associated with aluminosilicates except for Fe, which was higher in the bulk sediments suggesting its association with coarse sediments. Enrichment factor and Geoaccumulation indices revealed that the mudflats sediments were contaminated by Fe, Mn and Cr. Speciation of metals Fe. Mn, Cr, Co, Cu and Zn revealed that Fe, Cr, Co, Cu and Zn were associated with the residual phase and thus have low mobility and bioavailability. However, bioavailable concentrations of Mn in the sediments were considerably high indicating high potency for mobility and toxicity.

A comparison of mudflat and mangrove sediment components and metals was made using the isocon diagram which revealed that, the variability in the distribution of metals and sediment components within mudflats and mangroves increased towards the lower estuary and may be attributed to the geomorphic characteristics and the physical processes in the estuary. In the upper middle estuary, much of the sedimentary material is supplied and the narrow canal width and the low tidal current magnitude facilitated quick removal of material from the water column to the sediments. Fe-Mn oxyhydroxides and organic matter adsorbed trace metals in the mudflats whereas in the mangroves, organic matter played a significant role in metal accumulation. In the lower middle estuary, the relatively broader channel width that allows for an increased tidal magnitude and thus may cause resuspension and re-deposition of sediments. Metals in the mudflats were influenced by sand, clay Mn-oxides and whereas silt influenced metal distribution in mangroves. In the lower estuary, the broad width of the bay and the high energy conditions caused turbulence due to which much of the sediments are re-suspended and transported to calmer regions. Hydrodynamics played as significant role in the lower estuary and most metals were enriched in the mudflats sediments than mangroves due to higher fine sediments and Fe Mn oxides. In general, the sediments of the mudflats were influenced by physico-chemical processes whereas metals in the mangroves sediment were influenced by organic matter.

Differences in speciation of mudflat and mangrove sediments showed that the accumulation and bioavailability of metals within sediments depends organic matter supply, salinity and sediment

particle size. Due to the high density of roots and a short period of flooding in the mangrove forest environment, the redox conditions of vegetated sediments may be the main limiting factor for bioavailability in mangroves. In tidal mudflats, where sediments are not aerated by oxygen released from plant roots and higher moisture contents exist for longer periods of tidal inundation, organic matter content becomes the important limiting factor for bioavailability

Surface sediments were collected in the premonsoon, monsoon and postmonsoon season. Metals showed differential associations with different seasons in the Zuari estuary mangrove sediments. During the pre-monsoon (dry) season, with high salinity intrusion, hydrous Fe-Mn oxides played a role in the distribution of metals in the mangrove sediments. During the monsoon season, the stratification of the estuary and large land runoff bring about large changes in physicochemical properties of the estuarine waters and a large amount of material is transported into the estuary. In the postmonsoon, there is a reduction in fresh water influx, accumulation of trace metals, is related to fine sediments, organic matter and Mn oxides that were brought during the monsoons.

The metal distribution showed observable seasonal differences in the mudflat sediments of the Zuari estuary. In the premonsoon season, enrichment of most trace metals in the upper middle estuary sediments was due to the removal of metals during early estuarine mixing and proximity of the sampling location to the metal sources. The sediment grain size, organic matter and hydrous Fe-Mn oxides affected metal distributions. In the monsoon, trace metals were enriched in the upper middle estuarine sediments along with fine sediments, organic matter and Mn oxides due to the large influx of fresh sedimentary material from land runoff from the catchment area. In the post-monsoon season, trace metals were enriched in the lower middle estuary along with organic matter suggesting that these metals may be associated with increasing sewage effluxion. Most metals showed least concentrations in the lower estuary. Resuspension of sediments may have been a major process influencing metal distribution in the postmonsoon.

Sediments collected from the estuarine mangroves and mudflat environments of the Zuari estuary and adjoining Cumbharjua canal in 2015 premonsoon season were analyzed to assess concentration and bioavailability of metals in the estuarine environment after ban on mining. Following the ban on mining, Fe concentrations in sediments decreased in the estuary with silt

whereas trace metals Mn, Cr, Co, Ni, Cu and Zn increased with the clay fraction of sediments. Speciation studies revealed that Fe, Cr, Co, Ni, Cu and Zn were mainly of lithogenic origin, less mobile and bioavailable and posed low risk to biota associated with the sediments. The high content of Mn in the bioavailable fraction raised concerns over its potential mobility, bioavailability and subsequent toxicity.

In the mudflat sediments, the spatial variations of metals in the sediments were attributed to various hydrodynamic and physicochemical processes. A comparison of average values of sediment components and metal concentration of 2011 and 2015 datasets revealed that the concentrations of trace metals along with clay in the estuarine sediments had considerably increased whereas Fe concentration along with silt and organic matter had decreased. The increase in trace metals in the estuary may be related to anthropogenic inputs and their redistribution in the sediments was facilitated by adsorption onto clay particles or formed coating on sand particles. Additionally, resuspension of bottom sediments may have considerably influenced the metal distribution. Speciation of metals revealed that Fe, Cr, Co, Ni, Cu and Zn were concentrated in the residual phase indicating these metals are potentially less mobile and pose a lower toxicity risk. Concentrations of bioavailable Mn in the estuary posed a high risk to biota. A comparison of bioavailability of metals in post-mining ban period with pre-mining ban revealed elevated concentration of metals in the bioavailable fractions in the post-mining ban period and indicated increased anthropogenic inputs into estuary from the catchment area. Although the mining in the catchment area has been stopped, the leachates of ore stored on the river banks continue to enter into the estuary. In addition, input of metals from various sources, couples with resuspension of sediments due to sand mining has resulted in an increase in trace metal content in sediments in recent times.

Further, an attempt was made to assess bioaccumulation of metals in biota using mangrove pneumatophores and sediment associated molluscs. Mangrove plants accumulated Fe, Cu and Zn in their pneumatophores tissues and exhibited differences in accumulation of metal with respect to location and species due the spatial variation in sediment characteristics, quantity of metals deposited in the sediments, their bioavailability. Differences in plant species and tissue physiology may have contributed to the variations in bioaccumulation. The strong correlation of

metal content in sediment with metals in pneumatophores indicated that mangroves are able to accumulate metal in accordance to availability of metals in the underlying sediments.

Sediment associated biota was also assessed for metal bioaccumulation. It was found that Fe, Cu and Zn were preferentially bioaccumulated over other metals. The rates of metal uptake and excretion are affected by the biology of the organism, the permeability of the external surface, the nature of the food, and the efficiency of the osmoregulational system present. The difference in bioaccumulation ability in different molluscs species may be related to the differences in the detoxification mechanisms and/or metabolic activities. Gastropods *N.violacae, T.telescopium* and *C. quadrata* were identified as potential bioindicators in the estuarine environment since they reflect the conditions of the local sedimentary environment.

# *References*

Abdullah, A.R., Tahir, N.M., Loong, T.S., Hoque, T.M. and Sulaiman, A.H., 1999. The GEF/UNDP/IMO Malacca Straits demonstration project: sources of pollution. *Marine Pollution Bulletin,* 39, 229-233.

Akhil, P.S., Nair, M.P. and Sujatha, C.H., 2013. Core sediment biogeochemistry in specific zones of Cochin Estuarine System (CES). *Journal of Earth System Science,* 122, 1557-1570.

Alagarsamy, R., 2006. Distribution and seasonal variation of trace metals in surface sediments of the Mandovi estuary, west coast of India. *Estuarine, Coastal and Shelf Science,* 67, 333-339.

Albee, A.L., 1962. Relationships between mineral association, chemical composition and physical properties of chlorite series. *American mineralogist,* 47, 851.

Allan, J.E., Coey, J.M.D., Resende, M. and Fabris, J.D., 1988. Magnetic properties of iron-rich oxisols. *Physics and Chemistry of Minerals,* 15, 470-475.

Almeida, C.M., Mucha, A.P. and Vasconcelos, M.T., 2005. The role of a salt marsh plant on trace metal bioavailability in sediments, estimation by different chemical approaches. *Environmental Science and Pollution Research,* 5, 271–277.

Aloupi, M. and Angelidis, M.O., 2002. The significance of coarse sediments in metal pollution studies in the coastal zone. *Water, air and soil pollution,* 133,121-131.

Álvarez-Iglesias, P. and Rubio, B., 2009. Redox status and heavy metal risk in intertidal sediments in NW Spain as inferred from the degrees of pyritization of iron and trace elements. *Marine pollution bulletin,* 58, 542-551.

American Geological Institute, 1960. Glossary of Geology and Related Sciences with Supplement. *Am. Geol. Inst., Washington,* D.C., 2nd Ed., 371pp.

Amiard-Triquet, C. and Rainbow, P.S. (eds.), 2009. Environmental assessment of estuarine ecosystems: a case study. *CRC press.* pp 90.

Amundsen, P.A., Staldvik, F.J., Lukin, A.A., Kashulin, N.A., Popova, O.A. and Reshetnikov, Y.S., 1997. Heavy metal contamination in freshwater fish from the border region between Norway and Russia. *Science of the Total Environment,* 201, 211-224.

Anand, S.S., Sardessai, S., Muthukumar, C., Mangalaa, K.R., Sundar, D., Parab, S.G. and Kumar, M.D., 2014. Intra-and inter-seasonal variability of nutrients in a tropical monsoonal estuary (Zuari, India). *Continental Shelf Research,* 82, 9-30.

Andrews J.E., Brimblecombe, P., Jickells, T.D. and Liss, P.S., 2004. An Introduction to Environmental Chemistry, 2nd Edition, *Blackwell Publishing,* Oxford.

Anithamary, I., Ramkumar, T. and Venkatramanan, S., 2012. Distribution and accumulation of metals in the surface sediments of Coleroon river estuary, east coast of India. *Bulletin of environmental contamination and toxicology,* 88, 413-417.

Ansari, A.A., Singh, I.B. and Tobschall, H.J., 2000. Role of monsoon rain on concentrations and dispersion patterns of metal pollutants in sediments and soils of the Ganga Plain, India. *Environmental Geology,* 39, 221-237.

Azevedo, J.D.S., Hortellani, M.A. and Sarkis, J.E.D.S., 2012. Accumulation and distribution of metals in the tissues of two catfish species from Cananéia and Santos-São Vicente estuaries. *Brazilian Journal of Oceanography, 60*, 463-472.

Bartlett, R.J., 1961. Iron oxidation proximate to plant roots. *Soil Science*, 92, 372-379.

Bastami, K.D., Neyestani, M.R., Shemirani, F., Soltani, F., Haghparast, S. and Akbari, A., 2015. Heavy metal pollution assessment in relation to sediment properties in the coastal sediments of the southern Caspian Sea. *Marine pollution bulletin,* 92, 237-243.

Beeftink, W.G. and Rozema, J., 1988. The nature and functioning of salt marshes. In *Pollution of the North Sea,* Springer Berlin Heidelberg, 59-87.

Bellucci, L.G., Frignani, M., Paolucci, D. and Ravanelli, M., 2002. Distribution of heavy metals in sediments of the Venice Lagoon: the role of the industrial area. *Science of the Total Environment,* 295, 35-49.

Berger, B., Dallinger, R. and Thomaser, A., 1995. Quantification of metallothionein as a biomarker for cadmium exposure in terrestrial gastropods. *Environmental toxicology and chemistry,* 14, 781-791.

Bervoets, L., Meregalli, G., De Cooman, W., Goddeeris, B. and Blust, R., 2004. Caged midge larvae (Chironomus riparius) for the assessment of metal bioaccumulation from sediments in situ. *Environmental toxicology and chemistry,* 23, 443-454.

Bianchi, T.S., 2006. Biogeochemistry of Estuaries. *Oxford University Press,* Oxford, pp.720.

Birch, G.F., Melwani, A., Lee, J.H. and Apostolatos, C., 2014. The discrepancy in concentration of metals (Cu, Pb and Zn) in oyster tissue (Saccostrea glomerata) and ambient bottom sediment (Sydney estuary, Australia). *Marine pollution bulletin,* 80, 263-274.

Birch, G., Nath, B. and Chaudhuri, P., 2015. Effectiveness of remediation of metal-contaminated mangrove sediments (Sydney estuary, Australia). *Environmental Science and Pollution Research,* 22, 6185-6197.

Bird, E.C.F. and Barson, M.M., 1977. Measurement of physiographic changes on mangrove-fringed estuaries coastlines. *Marine Research in Indonesia,* 18, 73-80.

Biscaye, P.E., 1965. Mineralogy and sedimentation of recent deep sea clay in the Atlantic Ocean and adjacent seas and oceans. *Geological Society of America Bulletin,* 76, 803-832.

Bonanno, G. and Giudice, R.L., 2010. Heavy metal bioaccumulation by the organs of Phragmites australis (common reed) and their potential use as contamination indicators. *Ecological indicators,* 10, 639-645.

Boyle, D., Brix, K.V., Amlund, H., Lundebye, A.K., Hogstrand, C. and Bury, N.R., 2008. Natural arsenic contaminated diets perturb reproduction in fish. *Environmental science and technology*, 42, 5354-5360.

Bryan, G.W., Langston, W.J., Hummerstone, L.G., Burt, G.R. and Ho, Y.B., 1983. An assessment of the gastropod, Littorina littorea, as an indicator of heavy-metal contamination in United Kingdom estuaries. *Journal of the Marine Biological Association of the United Kingdom*, 63, 327-345.

Bubb, J.M., Rudd, T. and Lester, J.N., 1991. Distribution of heavy metals in the River Yare and its associated Broads III. Lead and zinc. *Science of the total environment*, 102, 189-208.

Buccolieri, A., Buccolieri, G., Cardellicchio, N., Dell'Atti, A., Di Leo, A. and Maci, A., 2006. Heavy metals in marine sediments of Taranto Gulf (Ionian Sea, southern Italy). *Marine chemistry*, 99, 227-235.

Buchman, M.F., 1999. NOAA screening quick reference tables. NOAA HAZMAT report, 99–111, Coastal Protection and Restoration Division, *National Oceanic and Atmospheric administration*, Seattle, WA, p 12.

Buddemeier, R.W., Smith, S.V., Swaney, D.P., Crossland, C.J. and Maxwell, B.A., 2008. Coastal typology: An integrative "neutral" technique for coastal zone characterization and analysis. *Estuarine, Coastal and Shelf Science*, 77, 197-205.

Bukhari, S.S., 1994. Studies on Mineralogy and Geochemistry of Bed and Suspended Sediment of Mandovi River and its Tributaries in Goa, West Coast of India (Ph.D. thesis). Department of Marine Sciences, *Goa University, Goa*, India, p. 240.

Bukhari, S.S. and Nayak, G.N., 1996. Clay minerals in identification of provenance of sediments of Mandovi estuary, Goa, west coast of India. *Indian journal of marine sciences*, 25, 341-345.

Bunt, J.S., 1992. How can fragile ecosystems best be conserved? In: Use and Misuse of the Seafloor, K.J. Hsü, J. Thiede, ed. Dahlem Workshop Reports, *Wiley and Sons*, Chichester, 229-242.

Burdige, D.J., 1993. The biogeochemistry of manganese and iron reduction in marine sediments. *Earth-Science Reviews,* 35, 249-284.

Burton, E.D., Phillips, I.R. and Hawker, D.W., 2005. Geochemical partitioning of copper, lead, and zinc in benthic, estuarine sediment profiles. *Journal of environmental quality,* 34, 263-273.

Caçador, I., Costa, A.L. and Vale, C., 2004. Carbon storage in Tagus salt marsh sediments. *Water, Air and Soil Pollution: Focus,* 4, 701-714.

Callender, E. and Bowser, C.J., 1980. Manganese and copper geochemistry of interstitial fluids from manganese nodule-rich pelagic sediments of the northeastern equatorial Pacific Ocean. *American journal of science,* 280, 1063-1096.

Cameron, W.M. and Pritchard, D.W., 1963. *Estuaries, The Sea,* 2, 306-324.

Campbell, P.G.C., Lewis, A.G., Chapman, P.M., Crowder, A.A., Fletcher, W.K., Imber, B., Luoma, S. N., Stokes, P.M. and Winfrey, M., 1988. Biologically Available Metals in Sediments, No. NRCC 27694, *National Research Council of Canada*, Ottawa, pp.298.

Carreira, R.S., Wagener, A.L., Readman, J.W., Fileman, T.W., Macko, S.A. and Veiga, A., 2002. Changes in the sedimentary organic carbon pool of a fertilized tropical estuary, Guanabara Bay, Brazil: an elemental, isotopic and molecular marker approach. *Marine Chemistry,* 79, 207-227.

Carvalho, C.E.V., Lacerda, L.D. and Gomes, M.P., 1993. Application of a model system for the study of transport and diffusion in complex terrain to the tract experiment. *Acta Limnoogica,* Brasiliense, 6, 222-229.

Casado-Martinez, M.C., Smith, B.D. and Rainbow, P.S., 2013. Assessing metal bioaccumulation from estuarine sediments: comparative experimental results for the polychaete Arenicola marina. *Journal of Soils and Sediments,* 13, 429-440.

Casado-Martinez, M.C., Smith, B.D., Luoma, S.N. and Rainbow, P.S., 2010. Metal toxicity in a sediment-dwelling polychaete: threshold body concentrations or overwhelming accumulation rates? *Environmental Pollution,* 158, 3071-3076.

Chachadi, A. G., 2009. Hydrogeology and water availability status in the state of Goa. In: Natural Resources of Goa: A Geological Perspective, Mascarenhas A. and Kalavampara, G. (eds.), *Geological Society of Goa,* Goa, 119-148.

Chakraborty, D., Bhar, S., Majumdar, J. and Santra, S.C., 2013. Heavy metal pollution and phytoremediation potential of Avicennia officinalis L. in the southern coast of the Hoogly estuarine system. *International Journal of Environmental Science,* 3, 2291-2303.

Chakraborty, P. (a), Chakraborty, S., Ramteke, D. and Chennuri, K., 2014. Kinetic speciation and bioavailability of copper and nickel in mangrove sediments. *Marine pollution bulletin,* 88, 224-230.

Chakraborty, P. (b), Ramteke, D., Chakraborty, S. and Nath, B.N., 2014. Changes in metal contamination levels in estuarine sediments around India–an assessment. *Marine pollution bulletin,* 78, 15-25.

Chan, L.S., Yeung, C.H., Yim, W.S. and Or, O.L., 1998. Correlation between magnetic susceptibility and distribution of heavy metals in contaminated sea-floor sediments of Hong Kong Harbour. *Environmental Geology,* 36, 77-86.

Chen, W. Y., 1992. Sediment transport and sediment dynamic environment of the mudflat with reference to the northern bank of Hangzhou Bay and southern bank of Changjiang Estuary (in Chinese with an English abstract). *Acta Oceanologia Sinica,* 13, 813–821.

Chester, R. and Jickells, T., 2012. The transport of material to the oceans: The fluvial pathway. *Marine Geochemistry,* 11-51.

Cheung, M.S. and Wang, W.X., 2008. Analyzing biomagnification of metals in different marine food webs using nitrogen isotopes. *Marine Pollution Bulletin,* 56, 2082–2088.

Choque, L.F.C., Ramos, O.E.R., Castro, S.N.V., Aspiazu, R.R.C., Mamani, R.G.C., Alcazar, S.G.F., Sracek, O. and Bhattacharya, P., 2013. Fractionation of heavy metals and assessment of contamination of the sediments of Lake Titicaca. *Environmental monitoring and assessment,* 185, 9979-9994.

Clark, M.W., McConchie, D., Lewis, D.W. and Saenger, P., 1998. Redox stratification and heavy metal partitioning in Avicennia-dominated mangrove sediments: a geochemical model. *Chemical Geology,* 149, 147–171.

Collier, R. and Edmond, J., 1984. The trace element geochemistry of marine biogenic particulate matter. *Progress in oceanography,* 13, 113-199.

Dallinger, R., 1993. Strategies of metal detoxification in terrestrial invertebrates. In: Dallinger, R. and Rainbow, P.S. (eds.) *Ecotoxicology of Metals in Invertebrates Lewis Publisher,* Boca Raton, FL. 246-332.

Dalrymple, R.W., Zaitlin, B.A. and Boyd, R., 1992. A conceptual model of estuarine sedimentation. *Journal of Sedimentary Petrology,* 62, p.116.

Dang, D.H., Lenoble, V., Durrieu, G., Omanović, D., Mullot, J.U., Mounier, S. and Garnier, C., 2015. Seasonal variations of coastal sedimentary trace metals cycling: Insight on the effect of manganese and iron (oxy) hydroxides, sulphide and organic matter. *Marine pollution bulletin,* 92, 113-124.

d'Anglejan, B., Ramesh, R. and Lucotte, M., 1990. Metal-rich coatings on residual sand deposits in the St. Lawrence upper estuary. *Science of the Total Environment,* 97, 395-406.

da Silva, G.S., do Nascimento, A.S., de Sousa, E.R., Marques, E.P., Marques, A.L.B., Corrêa, L.B. and Silva, G.S., 2014. Distribution and Fractionation of Metals in Mangrove Sediment from the Tibiri River Estuary on Maranhão Island. *Revista Virtual de Química,* 6, p.323.

Dearing, J.A., Bird, P.M., Dann, R.J.L. and Benjamin, S.F., 1997. Secondary ferrimagnetic minerals in Welsh soils: a comparison of mineral magnetic detection methods and implications for mineral formation. *Geophysical Journal International,* 130, 727-736.

Defew, L.H., Mair, J.M. and Guzman, H.M., 2005. An assessment of metal contamination in mangrove sediments and leaves from Punta Mala Bay, Pacific Panama. *Marine Pollution Bulletin,* 50, 547-552.

Deloffre, J., Lafite, R., Lesueur, P., Lesourd, S., Verney, R. and Guézennec, L., 2005. Sedimentary processes on an intertidal mudflat in the upper macrotidal Seine estuary, France. *Estuarine, Coastal and Shelf Science,* 64, 710-720.

Deloffre, J., Verney, R., Lafite, R., Lesueur, P., Lesourd, S. and Cundy, A.B., 2007. Sedimentation on intertidal mudflats in the lower part of macrotidal estuaries: sedimentation rhythms and their preservation. *Marine Geology,* 24, 19-32.

Dessai, D.V.G. and Nayak, G.N., 2007. Seasonal distribution of surface sediments and hydrodynamic conditions in Zuari Estuary, Goa, central west coast of India. *Journal of Indian Association of Sedimentologists,* 26, 25 - 32.

Dessai, D.V. and Nayak, G.N., 2009. Distribution and speciation of selected metals in surface sediments, from the tropical Zuari estuary, central west coast of India. *Environmental monitoring and assessment,* 158, 117-137.

Dessai, D.V., Nayak, G.N. and Basavaiah, N., 2009. Grain size, geochemistry, magnetic susceptibility: proxies in identifying sources and factors controlling distribution of metals in a tropical estuary, India. *Estuarine, Coastal and Shelf Science,* 85, 307-318.

Dhanakumar, S., Murthy, K.R., Solaraj, G. and Mohanraj, R., 2013. Heavy-metal fractionation in surface sediments of the Cauvery River Estuarine Region, southeastern coast of India. *Archives of environmental contamination and toxicology,* 65, 14-23.

Dragun, Z., Roje, V., Mikac, N. and Raspor, B., 2009. Preliminary assessment of total dissolved trace metal concentrations in Sava River water. *Environmental Monitoring and Assessment,* 159, 99-110.

Du Laing, G., Bogaert, N., Tack, F.M., Verloo, M.G. and Hendrickx, F., 2002. Heavy metal contents (Cd, Cu, Zn) in spiders (Pirata piraticus) living in intertidal sediments of the river Scheldt estuary (Belgium) as affected by substrate characteristics. *Science of the Total Environment,* 289, 71-81.

Du Laing, G., Rinklebe, J., Vandecasteele, B., Meers, E. and Tack, F.M.G., 2009. Trace metal behavior in estuarine and riverine floodplain soils and sediments: a review. *Science of the Total Environment,* 407, 3972-3985.

Edu, E.A.B., Edwin-Wosu, N.L. and Inegbedion, A., 2015. Bio-Monitoring of Mangal Sediments and Tissues for Heavy Metal Accumulation in the Mangrove Forest of Cross River Estuary. Doi:10.5567/ECOLOGY-IK.2015.46.52.

Edzwald, J.K. and O'Melia, C.R., 1975. Clay distributions in recent estuarine sediments. *Clays and Clay minerals,* 23, 39-44.

Elder, J.F. and Collins, J.J., 1991. Freshwater molluscs as indicators of bioavailability and toxicity of metals in surface-water systems. *In Reviews of environmental contamination and toxicology,* Springer New York. pp. 37-79.

Ernst, W.H.O., Verkleij, J.A.C. and Schat, H., 1992. Metal tolerance in plants. *Acta Botanica,* Neerlandica, 41, 229-248.

Evans, R.D., Andrews, D. and Cornell, R.J., 1988. Chemical fractionation and bioavailability of cobalt-60 to benthic deposit-feeders. *Canadian Journal of Fisheries and Aquatic Sciences,* 45, 228-236.

Eyre, B., 1993. Nutrients in the sediments of a tropical north-eastern Australian estuary, catchment and nearshore coastal zone. *Marine and Freshwater Research,* 44, 845-866.

Faragallah, H.M. and Khalil, M.K., 2009. Chemical Fractionation of Copper and Manganese in the Sediment of Alexandria Two Bays, Egypt. *Global Journal of Environmental Research,* 3, 61-67.

Farias, C.O., Hamacher, C., Wagener, A.D.L.R., Campos, R.C.D. and Godoy, J.M., 2007. Trace metal contamination in mangrove sediments, Guanabara Bay, Rio de Janeiro, Brazil. *Journal of the Brazilian Chemical Society,* 18, 1194-1206.

Fasulo, S., Mauceri, A., Giannetto, A., Maisano, M., Bianchi, N. and Parrino, V., 2008. Expression of metallothionein mRNAs by in situ hybridization in the gills of Mytilus galloprovincialis, from natural polluted environments. *Aquatic toxicology,* 88, 62-68.

Fendorf, S.E., 1995. Surface reactions of chromium in soils and waters. *Geoderma,* 67, 55-71.

Fernandes, L.L. and Nayak, G.N., 2014. Characterizing metal levels and their speciation in intertidal sediments along Mumbai coast, India. *Marine pollution bulletin,* 79, 371-378.

Fernandes, L., Nayak, G.N., Ilangovan, D. and Borole, D.V., 2011. Accumulation of sediment, organic matter and trace metals with space and time, in a creek along Mumbai coast, India. *Estuarine, Coastal and Shelf Science,* 91, 388-399.

Fernandes, M.C. and Nayak, G.N., 2015. Speciation of metals and their distribution in tropical estuarine mudflat sediments, southwest coast of India. *Ecotoxicology and environmental safety*, 122, 68-75.

Fernandes, O.A., 2009. Physiography and general geology of Goa. In: A. Mascarenhas, G. Kalavampara (eds), Natural resources of Goa: a geological perspective. *Published by Geological Society of Goa*, 11–23.

Ferreira, G.A., Machado, A.L.S. and Zalmin, I.R., 2004. Temporal and spatial variation on heavy metal concentrations in the bivalve Perna perna (Linnaeus, 1758) on the northern coast of Rio de Janerio state, Brazil. *Brazilian Archives of Biology and Technology,* 47, 319-327.

Feuillet, J.P. and Fleischer, P., 1980. Estuarine circulation: controlling factor of clay mineral distribution in James River estuary, Virginia. *Journal of Sedimentary Research*, 50(1).

Filipek, L.H., Chao, T.T. and Carpenter, R.H., 1981. Factors affecting the partitioning of Cu, Zn and Pb in boulder coatings and stream sediments in the vicinity of a polymetallic sulfide deposit. *Chemical Geology*, 33, 45-64.

Folk, R.L., 1974. In Petrology of sedimentary rocks. Austin, Texas: Hemphill. pp 182.

Förstner, U., Ahlf, W., Calmano, W., Kersten, M., and Schoer, J., 1990. Assessment of mobilityin sludges and solid wastes. In: Broeckaert, J.A.C., Gucer, S. and Adams, F. (eds.), Metal speciation in the environment. NATO ASI Series G, *Ecological Sciences,* 23, Springer, Berlin. 1–41.

Frey, R.W. and Howard, J.D., 1986. Mesotidal estuarine sequences: a perspective from the Georgia Bight. *Journal of Sedimentary Research,* 56.

Furukawa, K. and Wolanski, E., 1996. Sedimentation in mangrove forests. *Mangroves and salt marshes*, 1, 3-10.

Furukawa, K., Wolanski, E. and Mueller, H., 1997. Currents and sediment transport in mangrove forests. *Estuarine, Coastal and Shelf Science,* 44, 301-310.

Fytianos, K. and Lourantou, A., 2004. Speciation of elements in sediment samples collected at lakes Volvi and Koronia, N. Greece. *Environment International*, 30, 11-17.

Gao, X., Chen, S., and Long, A. 2008. Chemical speciation of 12 metals in surface sediments from the northern South China Sea under natural grain size. *Marine Pollution Bulletin,* 56, 770–797.

Ghosh, T.K., 1985. Groundwater potential evaluation of an area in Goa by remote sensing methods. Proc. Earth Resources for Goa's Development, *Geological Society of India,* Hyderabad, 419-421.

Gokul, A.R., Srinivasan, M.D., Gopalakrishnan, K. and Vishwanathan, L.S., 1985. Stratigraphy and structure of Goa. In: Earth Resources for Goa's Development. *Geological Survey of India,* Hyderabad, 1-13.

Grant, J.A., 1986. The isocon diagram- a simple solution to Gresen's equation for metasomatic alteration. *Economic. Geology,* 81, 1976-1982.

Greim, H. and Snyder, R. (eds.), 2008. Toxicology and risk assessment: a comprehensive introduction. *John Wiley and Sons,* 1-18.

Gries, T.H. and Waldow, K.H., 1996. Progress re-evaluating Puget Sound apparent effects thresholds (AETs). Volume I: Amphipod and Equinoderm Larval AETs. Olympia: Washington Department of Ecology. *Washington Department of Natural Resources*.

Gupta, S.K. and Singh, J., 2011. Evaluation of mollusc as sensitive indicator of heavy metal pollution in aquatic system: a review. *IIOAB journal,* 2, 49-57.

Gutierrez, M., 2000. Trace element concentration patterns in sediments of the lower Rio Conchos, Mexico. *Water, air and soil pollution,* 121, 259-270.

Guven, D.E. and Akinci, G., 2013. Effect of sediment size on bioleaching of heavy metals from contaminated sediments of Izmir Inner Bay. *Journal of Environmental Sciences,* 25, 1784-1794.

Guyot, J.L., Jouanneau, J.M., Soares, L., Boaventura, G.R., Maillet, N. and Lagane, C., 2007. Clay mineral composition of river sediments in the Amazon Basin. *Catena,* 71, 340-356.

Haese, R.R., Wallmann, K., Dahmke, A., Kretzmann, U., Müller, P.J. and Schulz, H.D., 1997. Iron species determination to investigate early diagenetic reactivity in marine sediments. *Geochimica et Cosmochimica Acta,* 61, 63-72.

Harbison, P.A.T., 1986. Mangrove muds—a sink and a source for trace metals. *Marine Pollution Bulletin,* 17, 246-250.

Hayes, M.O. 1975. Morphology of sand accumulation in estuaries. In: L.E. Cronin (Editor), *Estuarine research,* Vol. 2, *Academic press,* New York, 3-22.

HEATH, A.G., 1990. Water pollution and fish Physiology. 2. ed. Boca Raton; Boston: CRC Press. p. 245.

He, B., Li, R., Chai, M. and Qiu, G., 2014. Threat of heavy metal contamination in eight mangrove plants from the Futian mangrove forest, China. *Environmental geochemistry and health,* 36, 467-476.

He, C., Bartholdy, J. and Christiansen, C., 2012. Clay mineralogy, grain size distribution and their correlations with trace metals in the salt marsh sediments of the Skallingen barrier spit, Danish Wadden Sea. *Environmental Earth Sciences,* 67, 759-769.

Hedges, J.I., Keil, R.G. and Benner, R., 1997. What happens to terrestrial organic matter in the ocean?. *Organic geochemistry,* 27, 195-212.

Horowitz, A. J., 1991. A Primer on Sediments – Trace Element Chemistry, Lewis Publ., Michigan, U.S.A., pp 136.

Horowitz, A.J. and Elrick, K.A., 1987. The relation of stream sediment surface area, grain size and composition to trace element chemistry. *Applied Geochemistry,* 2, 437-451.

Hou, D., He, J., Lü, C., Ren, L., Fan, Q., Wang, J. and Xie, Z., 2013. Distribution characteristics and potential ecological risk assessment of heavy metals (Cu, Pb, Zn, Cd) in water and sediments from Lake Dalinouer, China. *Ecotoxicology and environmental safety,* 93, 135-144.

Huerta-Diaz, M.A. and Morse, J.W., 1992. Pyritization of trace metals in anoxic marine sediments. *Geochimica et Cosmochimica Acta,* 56, 2681-2702.

Huu, H.H. H., Rudy, S. and Van Damme, A., 2010. Distribution and contamination status of heavy metals in estuarine sediments near Cau Ong harbor, Ha Long Bay, Vietnam. *Geology Belgica,* 13, 37 – 47.

Ip, C.C., Li, X.D., Zhang, G., Wai, O.W. and Li, Y.S., 2007. Trace metal distribution in sediments of the Pearl River Estuary and the surrounding coastal area, South China. *Environmental Pollution,* 147, 311-323.

Irato, P., Santovito, G., Cassini, A., Piccinni, E. and Albergoni, V., 2003. Metal accumulation and binding protein induction in Mytilus galloprovincialis, Scapharca inaequivalvis, and Tapes philippinarum from the Lagoon of Venice. *Archives of environmental contamination and toxicology,* 44, 476-484.

Ismail, S., 2002. Assessment of heavy metal pollution in mangrove habitat of Karachi and vicinity. Unpublished PhD thesis, *Botany Department, Karachi University*, p. 174.

Jacob, D.L. and Otte, M.L., 2004. Long-term effects of submergence and wetland vegetation on metals in a 90-year old abandoned Pb, Zn mine tailings pond. *Environmental Pollution,* 130, 337–345.

Jacobs, B., 1998. Biota Sediment Accumulation Factors for Invertebrates: Review and Recommendations for the Oak Ridge Reservation. BJC/OR-112, Bechtel Jacobs Company LLC, Oak Ridge, Tennessee.

Jarvis, I.J. and Jarvis, K., 1985. Rare earth element geochemistry of standard sediments: a study using inductively coupled plasma spectrometry. *Chemical Geology,* 53, 335-344.

Jaud, M., Grasso, F., Le Dantec, N., Verney, R., Delacourt, C., Ammann, J., Deloffre, J. and Grandjean, P., 2016. Potential of UAVs for Monitoring Mudflat Morphodynamics (Application to the Seine Estuary, France). *ISPRS International Journal of Geo-Information,* 5, 50.

Jenne, E.A., 1968. Controls on Mn, Fe, Co, Ni, Cu, and Zn concentrations in soils and water: the significant role of hydrous Mn and Fe oxides. *Advances in chemistry series,* 73, 337-387.

Jennerjahn, T.C. and Ittekkot, V., 1997. Organic matter in sediments in the mangrove areas and adjacent continental margins of Brazil. 1. Amino acids and hexosamines. *Oceanolica Acta*, 20, 359-369.

Jingchun, L., Chongling, Y., Spencer, K.L., Ruifeng, Z. and Haoliang, L., 2010. The distribution of acid-volatile sulfide and simultaneously extracted metals in sediments from a mangrove forest and adjacent mudflat in Zhangjiang Estuary, China. *Marine Pollution Bulletin*, 60, 1209-1216.

Jones, J.B., 1998. Plant nutrition manual. New York: CRC Press.

Jones, J.B., Wolf, B. and Mills, H.A., 1991. Plant analysis hand book: a practical sampling, preparation, analysis and interpretation guide. New York: Micro Macro Publishing.

Kabata-Pendias, A. and Pendias, H., 2001. Trace elements in soils. 3rd Ed. Boca Raton, London, New York, CRC Press. pp. 413.

Kagi, J.H. and Schaeffer, A., 1988. Biochemistry of metallothionein. *Biochemistry*, 27, 8509-8515.

Karlin, R., 1990. Magnetite diagenesis in marine sediments from the Oregon continental margin. Journal of Geophysical Research: *Solid Earth*, 95, 4405-4419.

Kathiresan, K., 2002. Greening the blue mud. *Revista de biología tropical*, 50, 869-874.

Kathiresan, K. and Bingham, B.L., 2001. Biology of mangroves and mangrove ecosystems. *Advances in marine biology*, 40, 81-251.

Kathiresan, K., Saravanakumar, K. and Mullai, P., 2014. Bioaccumulation of trace elements by Avicennia marina. *Journal of Coastal Life Medicine*, 2, 888-894.

Kennedy, V.H., Sanchez, A.L., Oughton, D.H. and Rowland, A.P., 1997. Use of single and sequential chemical extractants to assess radionuclide and heavy metal availability from soils for root uptake. *Analyst*, 122, 89R-100R.

Kesavan, K., Murugan, A., Venkatesan, V. and Kumar, V., 2013. Heavy metal accumulation in molluscs and sediment from Uppanar Estuary, southeast coast of India. *Thalassas*, 29, 15-21.

Kessarkar, P.M., Shynu, R., Rao, V.P., Chong, F., Narvekar, T. and Zhang, J., 2013. Geochemistry of the suspended sediment in the estuaries of the Mandovi and Zuari rivers, central west coast of India. *Environmental monitoring and assessment*, 185, 4461-4480.

Kessarkar, P.M., Suja, S., Sudheesh, V., Srivastava, S. and Rao, V.P., 2015. Iron ore pollution in Mandovi and Zuari estuarine sediments and its fate after mining ban. *Environmental monitoring and assessment*, 187, 1-17.

Kim, J.H., Gibb, H.J. and Howe, P.D., 2006. Cobalt and inorganic cobalt compounds, Issue 69 of Concise international chemical assessment document. *World Health Organization*, pp 88.

Kjerfve, B. and Magill, K.E., 1989. Geographic and hydrodynamic characteristics of shallow coastal lagoons. *Marine geology*, 88, 187-199.

Klinkhammer, G., Elderfield, H., Greaves, M., Rona, P. and Nelsen, T., 1986. Manganese geochemistry near high-temperature vents in the Mid-Atlantic Ridge rift valley. *Earth and planetary science letters*, 80, 230-240.

Kolay, A.K., 2007. Soil genesis, classification survey and evaluation (Vol. 2). Atlantic Publishers and Dist.

Korfali, S.I. and Jurdi, M.S., 2011. Speciation of metals in bed sediments and water of Qaraaoun Reservoir, Lebanon. *Environmental monitoring and assessment*, 178, 563-579.

Krumgalz, B.S., Fainshtein, G. and Cohen, A., 1992. Grain size effect on anthropogenic trace metal and organic matter distribution in marine sediments. *Science of the total environment*, 116, 15-30.

Krupadam, R.J., Smita, P. and Wate, S.R., 2006. Geochemical fractionation of heavy metals in sediments of the Tapi estuary. *Geochemical Journal*, 40, 513-522.

Kumar, A. and Ramanathan, A.L., 2015. Speciation of selected trace metals (Fe, Mn, Cu and Zn) with depth in the sediments of Sundarban mangroves: India and Bangladesh. *Journal of Soils and Sediments*, 15, 2476-2486.

Lacerda, L.D., 1997. Trace metals in mangrove plants: why such low concentrations? In: Kjerfive B, Lacerda LD, Drop ES, editors. Mangrove ecosystem studies in Latin America and Africa. Paris, France: *UNESCO*, 171-178.

Lacerda, L.D., Ittekkot, V. and Patchineelam, S.R., 1995. Biogeochemistry of Mangrove Soil Organic Matter: a Comparison Between Rhizophora and Avicennia Soils in South-eastern Brazil. *Estuarine, Coastal and Shelf Science,* 40, 713-720.

Lacerda, L.D., Rezende, C.E., Aragon, G.T. and Ovalle, A.R., 1991. Iron and chromium transport and accumulation in a mangrove ecosystem. *Water, Air and Soil Pollution*, 57, 513-520.

Lee, S.V. and Cundy, A.B., 2001. Heavy metal contamination and mixing processes in sediments from the Humber Estuary, Eastern England. *Estuarine, Coastal and Shelf Science*, 53, 619-636.

Lim, W.Y., Aris, A.Z. and Zakaria, M.P., 2012. Spatial variability of metals in surface water and sediment in the Langat river and geochemical factors that influence their water-sediment interactions. *The Scientific World Journal*, Doi: http://dx.doi.org/10.1100/2012/652150.

Linden, O. and Jernelov, A., 1980. The mangrove swamp-an ecosystem in danger. *Ambio*, 9, 81-88.

Liu, J., Zhu, R., Roberts, A.P., Li, S. and Chang, J.H., 2004. High-resolution analysis of early diagenetic effects on magnetic minerals in post-middle-Holocene continental shelf sediments from the Korea Strait. *Journal of Geophysical Research: Solid Earth*, 109, 1-15.

Liu, W.X., Li, X.D., Shen, Z.G., Wang, D.C., Wai, O.W.H. and Li, Y.S., 2003. Multivariate statistical study of heavy metal enrichment in sediments of the Pearl River Estuary. *Environmental Pollution,* 121, 377-388.

Li, X., Shen, Z., Wai, O.W. and Li, Y.S., 2000. Chemical partitioning of heavy metal contaminants in sediments of the Pearl River Estuary. *Chemical Speciation and Bioavailability,* 12, 17-25.

Lopez-Sanchez, J.F., Rubio, R., Samitier, C. and Rauret, G., 1996. Trace metal partitioning in marine sediments and sludges deposited off the coast of Barcelona (Spain). *Water Research,* 30, 153-159.

Loring, D.H. and Hill, S., 1992. Factors controlling the Bioavailability of Heavy Metals in sediments: report for ICES working group on Biological contaminants. *ICES, Copenhagen,* 70.

Luoma, S.N., 1983. Bioavailability of trace metals to aquatic organisms—a review. *Science of the total environment,* 28, 1-22.

Luoma, S.N., Rainbow, P.S. and Luoma, S., 2008. Metal contamination in aquatic environments: science and lateral management. *Cambridge University Press,* pp. 141-150.

Lu, S.G., Bai, S.Q. and Xue, Q.F., 2007. Magnetic properties as indicators of heavy metals pollution in urban topsoils: a case study from the city of Luoyang, China. *Geophysical Journal International,* 171, 568-580.

MacFarlane, G.R. and Burchett, M.D., 2002. Toxicity, growth and accumulation relationships of copper, lead and zinc in the grey mangrove Avicennia marina (Forsk.) Vierh. *Marine Environmental Research,* 54, 65–84.

MacFarlane, G.R., Koller, C.E. and Blomberg, S.P., 2007. Accumulation and partitioning of heavy metals in mangroves: a synthesis of field-based studies. *Chemosphere,* 69, 1454-1464.

Machado, W., Silva-Filho, E.V., Oliveira, R.R. and Lacerda, L.D., 2002. Trace metal retention in mangrove ecosystems in Guanabara Bay, SE Brazil. *Marine Pollution Bulletin,* 44, 1277–1280.

Mahara, Y. and Kudo, A., 1981. Interaction and mobility of cobalt-60 between water and sediments in marine environments possible effects by acid rain. *Water Research,* 15, 413-419.

Maher, B.A., 1988. Magnetic properties of some synthetic sub-micron magnetites. *Geophysical Journal International,* 94, 83-96.

Maher, B.A. and Taylor, R.M., 1988. Formation of ultrafine-grained magnetite in soils. *Nature,* 336, 368-370.

Marchand, C., Lallier-Verges, E., Baltzer, F., Albéric, P., Cossa, D. and Baillif, P., 2006. Heavy metals distribution in mangrove sediments along the mobile coastline of French Guiana. *Marine chemistry,* 98, 1-17.

Marchand, C., Fernandez, J.M., Moreton, B., Landi, L., Lallier-Verges, E. and Baltzer, F., 2012. The partitioning of transitional metals (Fe, Mn, Ni, Cr) in mangrove sediments downstream of a ferralitized ultramafic watershed (New Caledonia). *Chemical Geology,* 300, 70-80.

Massolo, S., Bignasca, A., Sarkar, S.K., Chatterjee, M., Bhattacharya, B.D. and Alam, A., 2012. Geochemical fractionation of trace elements in sediments of Hugli River (Ganges) and Sundarban wetland (West Bengal, India). *Environmental monitoring and assessment,* 184, 7561-7577.

Mathé, P.E., Rochette, P. and Colin, F., 1997. The origin of magnetic susceptibility and its anisotropy in some weathered profiles. *Physics and Chemistry of the Earth,* 22, 183-187.

Mattigod, S.V., Gibali, A.S. and Page, A.L., 1979. Effect of ionic strength and ion pair formation on the adsorption of nickel by kaolinite. *Clays and Clay Minerals,* 27, 411-416.

McLean, J.E. and Bledsoe, B.E., 1992. Behavior of metals in soils. USEPA Ground Water Issue. EPA/540/S-92/018. 1-25.

McNally, W. H. and Mehta, A. J., 2004. Sediment Transport and Deposition in Estuaries (Sample Chapter). In Encyclopedia of Life Support Systems (EOLSS): *Coastal Zones and Estuaries*, Retrieved from http://www.eolss.net/sample-chapters/c09/E2-06-01-04.pdf.

Meade, R.H., 1972. Transport and deposition of sediments in estuaries. *Geological Society of America Memoirs,* 133, 91-120.

Meng, X., Xia, P., Li, Z. and Liu, L., 2016. Mangrove forest degradation indicated by mangrove-derived organic matter in the Qinzhou Bay, Guangxi, China, and its response to the Asian monsoon during the Holocene climatic optimum. *Acta Oceanologica Sinica,* 35, 95-100.

Michael H.C., 2010. In: Encyclopedia of Earth. Monosson Cleveland C, editor. Washington DC: National Council for Science and the Environment. *Heavy metal*.

Misra, A. and Vethamony, P., 2015. Assessment of the land use/land cover (LU/LC) and mangrove changes along the Mandovi–Zuari estuarine complex of Goa, India. *Arabian Journal of Geosciences,* 8, 267-279.

Mistch, W.J., Gosselink, J.G., Anderson, C.J. and Zhang, L., 2009. Wetland Ecosystems. *John Wiley and Sons, Inc.*, Hoboken, New Jersey.

Morillo, J., Usero, J. and Gracia, I., 2004. Heavy metal distribution in marine sediments from the southwest coast of Spain. *Chemosphere,* 55, 431-442.

Morse, J.W. and Luther, G.W., 1999. Chemical influences on trace metal-sulfide interactions in anoxic sediments. *Geochimica et Cosmochimica Acta,* 63, 3373-3378.

Mountouris, A., Voutsas, E. and Tassios, D., 2002. Bioconcentration of heavy metals in aquatic environments: the importance of bioavailability. *Marine Pollution Bulletin,* 44, 1136-1141.

Mukhopadhyay, M.J. and Sharma, A., 1991. Manganese in cell metabolism of higher plants. *The Botanical Review*, 57, 117-149.

Muller, G., 1979. Schwermetalle in den Sedimentation des Rheins– Ver-anderungen seit 1971. *Umschau*, 79, 778–783.

Murty, C.S., Das, P.K., Nair, R.R., Veerayya, M. and Varadachari, V.V.R., 1976. Circulation and sedimentation processes in and around the Aguada Bar conservative and non-conservative. *Indian Journal of Marine Sciences,* 5, 7-17.

Nair, C. K., 1992. Chemical partitioning of trace metals in sediments of a tropical estuary. Thesis submitted to *The Cochin University of Science and Technology,* pp 4.

Nath, B., Birch, G. and Chaudhuri, P., 2014. Assessment of sediment quality in Avicennia marina-dominated embayments of Sydney Estuary: the potential use of pneumatophores (aerial roots) as a bio-indicator of trace metal contamination. *Science of the Total Environment,* 472, 1010-1022.

Nayak, G. N., 2002. Impact of mining on environment in Goa. New Delhi: *International Publishers,* p.112

Nizoli, E.C. and Luiz-Silva, W., 2012. Seasonal AVS–SEM relationship in sediments and potential bioavailability of metals in industrialized estuary, southeastern Brazil. *Environmental geochemistry and health,* 34, 263-272.

Noronha-D'Mello, C.A. and Nayak, G.N., 2015. Geochemical characterization of mangrove sediments of the Zuari estuarine system, West coast of India. *Estuarine, Coastal and Shelf Science,* 167, 313-325.

Oehlmann, J. and Schulte-Oehlmann, U., 2003. Molluscs as bioindicators. *Trace Metals and other Contaminants in the Environment,* 6, 577-635.

Okoro, H.K., Fatoki, O.S., Adekola, F.A., Ximba, B.J. and Snyman, R.G., 2012. A review of sequential extraction procedures for heavy metals speciation in soil and sediments. *Open Access Scientific Reports,* 181(1).

Oldfield, F., 1999. Environment magnetism: The range of applications In Walden, J., Smith, J.P. and Oldfield, F. (eds.) Environmental magnetism, a practical guide, *Quaternary research association, Technical Guide,* 6, 212-222.

Ouseph, P.P., 1987. Heavy metal pollution in the sediments of Cochin estuarine system. Proc. of National Sem. *Estuarine Management,* 123-127.

Palpandi, C. and Kesavan, K., 2012. Heavy metal monitoring using Nerita crepidularia-mangrove mollusc from the Vellar estuary, Southeast coast of India. *Asian Pacific Journal of Tropical Biomedicine,* 2, S358-S367.

Panda, D., Subramanian, V. and Panigrahy, R.C., 1995. Geochemical fractionation of heavy metals in Chilka Lake (east coast of India)—a tropical coastal lagoon. *Environmental Geology,* 26, 199-210.

Pardo, R., Barrado, E., Lourdes, P. and Vega, M., 1990. Determination and speciation of heavy metals in sediments of the Pisuerga River. *Water Research,* 24, 373-379.

Pathak, M.C., Kotnala, K.L. and Prabaharan, N., 1988. Effects of bridge piers on a tropical estuary in Goa, India. *Journal of coastal Research,* 475-481.

Pedersen, T.F. and Price, N.B., 1982. The geochemistry of manganese carbonate in Panama Basin sediments. *Geochimica et Cosmochimica Acta,* 46, 59-68.

Pejrup, M., 1988. The triangular diagram used for classification of estuarine sediments: a new approach. In: deBoer, P.L., van Gelder, A., and Nio, S.D. (eds.), Tide-influenced Sedimentary Environments and Facies. *Dordrecht: D. Reidel Publishing Company,* pp 289-300.

Pempkowiase, J., Sikora, A., and Biernacka, E., 1999. Speciation of heavy metals in marine sediments versus their bioaccumulation by mussels. *Chemosphere,* 39, 313–321.

Perin, G., Craboledda, L., Lucchese, M., Cirillo, R., Dotta, L., Zanetta, M.L. and Oro, A.A., 1985. Heavy metal speciation in the sediments of Northern Adriatic Sea. A new approach for environmental toxicity determination. In: Lakkas, T.D., (ed). *Heavy Metals in the Environment, CEP Consultants Edinburg,* 454-456.

Peters, C. and Dekkers, M.J., 2003. Selected room temperature magnetic parameters as a function of mineralogy, concentration and grain size. *Physics and Chemistry of the Earth,* Parts A/B/C, 28, 659-667.

Petersen, W., Willer, E. and Willamowski, C., 1997. Remobilization of trace elements from polluted anoxic sediments after resuspension in oxic water. *Water, Air and Soil Pollution,* 99, 515–522.

Pickering, W.F., 1986. Metal ion speciation—soils and sediments (a review). *Ore Geology Reviews,* 1, 83-146.

Prajith, A., Rao, V.P. and Chakraborty, P., 2016. Distribution, provenance and early diagenesis of major and trace metals in sediment cores from the Mandovi estuary, western India. *Estuarine, Coastal and Shelf Science,* 170, 173-185.

Prajith, A., Rao, V.P. and Kessarkar, P.M., 2015. Magnetic properties of sediments in cores from the Mandovi estuary, western India: Inferences on provenance and pollution. *Marine pollution bulletin,* 99, 338-345.

Pritchard, D.W., 1952. Estuarine hydrography. In: H.E. Landsberg (Editor), Advances in Geophysics. *Academic Press,* New York, 1, 243-280.

Pritchard, D.W., 1967. What is an estuary: physical viewpoint. *American Association for the Advancement of Science,* 83, 3-5.

Pugliese Andrade, G.R., de Azevedo, A.C., Cuadros, J., Souza, V.S., Correia Furquim, S.A., Kiyohara, P.K. and Vidal-Torrado, P., 2014. Transformation of Kaolinite into Smectite and Iron-Illite in Brazilian Mangrove Soils. *Soil Science Society of America Journal*, 78, 655-672.

Qasim, S.Z. and Gupta, R.S., 1981. Environmental characteristics of the Mandovi-Zuari estuarine system in Goa. *Estuarine, Coastal and Shelf Science,* 13, 557-578.

Qi, S., Leipe, T., Rueckert, P., Di,, Z. and Harff, J., 2010. Geochemical sources, deposition and enrichment of heavy metals in short sediment cores from the Pearl River Estuary, Southern China. *Journal of Marine Systems,* 82, S28-S42,

Rainbow, P.S., 1995. Biomonitoring of heavy metal availability in the marine environment. *Marine Pollution Bulletin,* 31, 183-192.

Rainbow, P.S., 2002. Trace metal concentrations in aquatic invertebrates: why and so what? *Environmental Pollution,* 120, 497-507.

Rao, V.P. and Rao, B.R., 1995. Provenance and distribution of clay minerals in the sediments of the western continental shelf and slope of India. *Continental Shelf Research,* 15, 1757-1771.

Rao, V.P., Shynu, R., Kessarkar, P.M., Sundar, D., Michael, G.S., Narvekar, T., Blossom, V. and Mehra, P., 2011. Suspended sediment dynamics on a seasonal scale in the Mandovi and Zuari estuaries, central west coast of India. *Estuarine, Coastal and Shelf Science,* 91, 78-86.

Rao, V.P., Shynu, R., Singh, S.K., Naqvi, S.W.A. and Kessarkar, P.M., 2015. Mineralogy and Sr–Nd isotopes of SPM and sediment from the Mandovi and Zuari estuaries: Influence of weathering and anthropogenic contribution. *Estuarine, Coastal and Shelf Science,* 156, 103-115.

Rauret, G., 1998. Extraction procedures for the determination of heavy metals in contaminated soil and sediment. *Talanta,* 46, 449-455.

Reddy, K.R. and DeLaune, R.D., 2008. Biogeochemistry of wetlands: science and applications. *Crc Press*.

Rezaie-Boroon, M.H., Toress, V., Diaz, S., Lazzaretto, T., Tsang, M. and Deheyn, D.D., 2013. The geochemistry of heavy metals in the mudflat of Salinas de San Pedro Lagoon, California, USA. *Journal of Environmental Protection,* 4, 12-25. Doi: 10.4236/jep.2013.41002.

Robinson, G.D., 1982. Trace metal adsorption potential of phases comprising black coatings on stream pebbles. *Journal of Geochemical Exploration*, 17, 205-219.

Roden, E.E. and Zachara, J.M., 1996. Microbial reduction of crystalline iron (III) oxides: Influence of oxide surface area and potential for cell growth. *Environmental Science and Technology,* 30, 1618-1628.

Rojas, N. and Silva, N., 2005. Early diagenesis and vertical distribution of organic carbon and total nitrogen in recent sediments from southern Chilean fjords (Boca del Guafo to Pulluche Channel)/Diagénesis temprana y distribución vertical de carbono orgánico y nitrógeno total en sedimentos recientes de los fiordos del sur de Chile (Boca del Guafo hasta canal Pulluche). Investigaciones Marinas. *Valparaiso,* 3, 3183.

Rolph, T.C., Vigliotti, L. and Oldfield, F., 2004. Mineral magnetism and geomagnetic secular variation of marine and lacustrine sediments from central Italy: timing and nature of local and regional Holocene environmental change. *Quaternary Science Reviews*, 23, 1699-1722.

Roussiez, V., Ludwig, W., Monaco, A., Probst, J.L., Bouloubassi, I., Buscail, R. and Saragoni, G., 2006. Sources and sinks of sediment-bound contaminants in the Gulf of Lions (NW Mediterranean Sea): a multi-tracer approach. *Continental Shelf Research*, 26, 1843-1857.

Rumisha, C., Elskens, M., Leermakers, M. and Kochzius, M., 2012. Trace metal pollution and its influence on the community structure of soft bottom molluscs in intertidal areas of the Dar es Salaam coast, Tanzania. *Marine pollution bulletin*, 64, 521-531.

Sandeep, K., Shankar, R. and Krishnaswamy, J., 2010. Assessment of suspended particulate pollution in the Bhadra River catchment, Southern India: an environmental magnetic approach. *Environmental Earth Sciences*, 62, 625-637.

Sangode, S.J., Suresh, N. and Bagati, T.N., 2001. Godavari source in the Bengal fan sediments: results from magnetic susceptibility dispersal pattern. *Current Science*-Bangalore, 80, 660-664.

Sarangi, R.K., Kathiresan, K. and Subramanian, A.N., 2002. Metal concentrations in five mangrove species of the Bhitarkanika, Orissa, east coast of India. *Indian Journal of Marine Sciences,* 31, 251-253.

Satyanarayana, D., and Sen Gupta, R., 1996. Present status of coastal pollution in India and future strategies. In: Qasim, S.Z. and Roonwal, G.S. (eds.), India's Exclusive Economic Zone, *Omega Scientific Pubs,* New Delhi, India. 158–169.

Schmidt, A., Yarnold, R., Hill, M. and Ashmore, M., 2005. Magnetic susceptibility as proxy for heavy metal pollution: a site study. *Journal of Geochemical Exploration,* 85, 109-117.

Schropp, S.J. and Windom, H.L. (eds.), 1988. A guide to the interpretation of metal concentrations in estuarine sediments. Tallahassee, Florida, USA: Florida Department of Environmental Regulation, *Coastal Zone Management Section,* p.44.

Seshan, B.R.R., Natesan, U. and Deepthi, K., 2010. Geochemical and statistical approach for evaluation of heavy metal pollution in core sediments in southeast coast of India. *International Journal of Environmental Science and Technology*, 7, 291-306.

Sharmin, S., Zakir, H.M. and Shikazono, N., 2010. Fractionation profile and mobility pattern of trace metals in sediments of Nomi River, Tokyo, Japan. *Journal of Soil Science and Environmental Management*, 1, 001-014.

Shazili, N.A.M., Yunus, K., Ahmad, A.S., Abdullah, N. and Rashid, M.K.A., 2006. Heavy metal pollution status in the Malaysian aquatic environment. *Aquatic Ecosystem Health and Management*, 9, 137-145.

Shetye, S.R., Shankar, D., Neetu, S., Suprit, K., Michael, G.S. and Chandramohan, P., 2007. The environment that conditions the Mandovi and Zuari estuaries. In: Shetye, S.R., Dileep Kumar, M. and Shankar, D., (eds.), The Mandovi and Zuari estuaries. NIO; Dona Paula, Goa, India, 29-38.

Shiyuan, X., Jing, T., Zhenlou, C., Zhongyuan, C. and Quanrong, L., 1997. Dynamic accumulation of heavy metals in tidal flat sediments of shanghai. *Oceanologia et Limnologia Sinica,* 5, p.8.

Shi, Z., 1992. Application of the 'Pejrup Approach' for the Classification of the Sediments in the Microtidal Dyfi Estuary, West Wales, U.K. *Journal of Coastal Research,* 8, 482-491.

Shynu, R., Rao, V.P., Kessarkar, P.M. and Rao, T.G., 2012. Temporal and spatial variability of trace metals in suspended matter of the Mandovi estuary, central west coast of India. *Environmental Earth Sciences,* 65, 725-739.

Shynu, R., Rao, V.P., Parthiban, G., Balakrishnan, S., Narvekar, T. and Kessarkar, P.M., 2013. REE in suspended particulate matter and sediment of the Zuari estuary and adjacent shelf, western India: Influence of mining and estuarine turbidity. *Marine Geology,* 346, 326-342.

Shynu, R., Rao, V.P., Sarma, V.V.S.S., Kessarkar, P.M. and ManiMurali, R., 2015. Sources and fate of organic matter in suspended and bottom sediments of the Mandovi and Zuari estuaries, western India. *Current Science,* 108, 226- 238.

Silva, C.A.R., Lacerda, L.D. and Rezende, C.E., 1990. Metals reservoir in a red mangrove forest. *Biotropica*, 339-345.

Singh, K.T., Nayak, G.N. and Fernandes, L.L., 2013. Geochemical evidence of anthropogenic impacts in sediment cores from mudflats of a tropical estuary, Central west coast of India. Soil and Sediment Contamination: *An International Journal,* 22, 256-272.

Singh, K.T., Nayak, G.N., Fernandes, L.L., Borole, D.V. and Basavaiah, N., 2014. Changing environmental conditions in recent past—Reading through the study of geochemical characteristics, magnetic parameters and sedimentation rate of mudflats, central west coast of India. *Palaeogeography, Palaeoclimatology, Palaeoecology*, 397, 61-74.

Smirnov, L.P., Sukhovskaya, I.V. and Nemova, N.N., 2005. Effects of environmental factors on low-molecular-weight peptides of fishes: a review. *Russian Journal of Ecology*, 36, 41-47.

Smith, I.C. and Carson, B.L., 1981. Trace metals in the environment, Ann Arbor, MI, *Ann Arbor Science publishers*.

Snedaker, S.C., 1984. Mangroves: A summary of knowledge with emphasis on Pakistan. In: Marine Geology and Oceanography of Arabian Sea and Coastal Pakistan, Haq, B.U. and Milliman, J.O., (eds). *Van Nostrand Reinhold Company*, New York, 255-262.

Spencer, K.L., Cundy, A.B. and Croudace, I.W., 2003. Heavy metal distribution and early-diagenesis in salt marsh sediments from the Medway Estuary, Kent, UK. *Estuarine, Coastal and Shelf Science*, 57, 43-54.

Spetter, C.V., Buzzi, N.S., Fernández, E.M., Cuadrado, D.G. and Marcovecchio, J.E., 2014. Assessment of the physicochemical conditions sediments in a polluted tidal flat colonized by microbial mats in Bahía Blanca Estuary (Argentina). *Marine pollution bulletin*, 91, 491-505.

Stumm, M., and J.J. Morgan. 1996. Aquatic chemistry. 3rd ed. *John Wiley and Sons*, New York.

Stutz, M. L. and O. H. Pilkey. 2002. Global distribution and morphology of deltaic barrier island systems. *Journal of Coastal Research,* 36, 694-707.

Subramaniam, A., 1981. Surface and groundwater resources in the northern part of Goa. *Proc. Earth resources for Goa's Development*, Panaji, Goa, 475-483.

Subramanian, V. and Mohanchandran, G., 1994. Deposition and Fluxes of Heavy Metals in the Sediments of three major Peninsular Estuaries. In: Dyer, K.R. and Orth, R.J. (eds), Changes in Fluxes in Estuaries, *Olsen and Olsen Pub.*, Denmark, 97-106.

Sundaray, S.K., Nayak, B.B., Lin, S. and Bhatta, D., 2011. Geochemical speciation and risk assessment of heavy metals in the river estuarine sediments—a case study: Mahanadi basin, India. *Journal of hazardous materials*, 186, 1837-1846.

Sun, Z., Mou, X., Tong, C., Wang, C., Xie, Z., Song, H., Sun, W. and Lv, Y., 2015. Spatial variations and bioaccumulation of heavy metals in intertidal zone of the Yellow River estuary, China. Catena, 126, 43-52.

Sutherland, B.R., Barrett, K.J. and Gingras, M.K., 2015. Clay settling in fresh and salt water. *Environmental Fluid Mechanics,* 15, 147-160.

Szefer, P., Ali, A.A., Ba-Haroon, A.A., Rajeh, A.A., Geldon, J. and Nabrzyski, M., 1999. Distribution and relationships of selected trace metals in molluscs and associated sediments from the Gulf of Aden, Yemen. *Environmental Pollution*, 106, 299-314.

Tam, N.F.Y. and Wong, Y.S., 1998. Variations of soil nutrient and nutrient and organic matter content in a subtropical mangrove ecosystem. *Water, Air and Soil Pollution,* 103, 245–261.

Tessier, A., Campbell, P.G. and Bisson, M., 1979. Sequential extraction procedure for the speciation of particulate trace metals. *Analytical chemistry*, 51, 844-851.

Thibodeau, F.R. and Nickerson, N.H., 1986. Differential oxidation of mangrove substrate by Avicennia germinans and Rhizophora mangle. *American Journal of Botany*, 73, 512–516.

Thomas, R.P., Ure, A.M., Davidson, C.M., Littlejohn, D., Rauret, G., Rubio, R. and López-Sánchez, J.F., 1994. Three-stage sequential extraction procedure for the determination of metals in river sediments. *Analytica Chimica Acta*, 286, 423-429.

Thomson, R. and Oldfield, F., 1986. Environmental magnetism. *Allen and Unwin*, London, pp. 227.

Thuy, H.T.T., Tobschall, H.J. and An, P.V., 2000. Trace element distributions in aquatic sediments of Danang–Hoian area, Vietnam. *Environmental Geology*, 39, 733-740.

Turekian, K.K., 1977. The fate of metals in the oceans. *Geochimica et Cosmochimica Acta*, 41, 1139-1144.

Turekian, K.K. and Wedepohl, K.H., 1961. Distribution of the elements in some major units of the earth's crust. *Geological Society of America Bulletin*, 72, 175–192.

Turki, A.J., 2007. Metal Speciation (Cd, Cu, Pb and Zn) in Sediments from Al Shabab Lagoon, Jeddah, Saudi Arabia. *Marine Sciences*, 18.

Turner, S. and Riddle, B. 2001. Estuarine Sedimentation and Vegetation – Management Issues and Monitoring Priorities. *Environment Waikato Internal Series* 2001/05. Document #: 686944.

Valle-Levinson, A. ed., 2010. Contemporary issues in estuarine physics. Cambridge *University Press.*

Vanbroekhoven, K., Van Roy, S., Gielen, C., Maesen, M., Diels, L. and Seuntjens, P., 2006. Varying redox conditions changes metal behavior due to microbial activities. *In Geophysical Research Abstracts*, 8, 2292.

Veerasingam, S., Vethamony, P., Murali, R.M. and Fernandes, B., 2015. Depositional record of trace metals and degree of contamination in core sediments from the Mandovi estuarine mangrove ecosystem, west coast of India. *Marine pollution bulletin*, 91, 362-367.

Venkatramanan, S., Chung, S.Y., Ramkumar, T., Gnanachandrasamy, G. and Kim, T.H., 2015. Evaluation of geochemical behavior and heavy metal distribution of sediments: the case study of the Tirumalairajan river estuary, southeast coast of India. *International Journal of Sediment Research*, 30, 28-38.

Verkleij, J.A.C. and Schat, H., 1990. Mechanisms of metal tolerance in higher plants. Heavy metal tolerance in plants: *Evolutionary aspects,* 179-193.

Viarengo, A. and Nott, J.A., 1993. Mechanisms of heavy metal cation homeostasis in marine invertebrates. Comparative Biochemistry and Physiology Part C: *Comparative Pharmacology,* 104, 355-372.

Volvoikar, S.P. and Nayak, G.N., 2014. Factors controlling the distribution of metals in intertidal mudflat sediments of Vaitarna estuary, North Maharashtra coast, India. *Arabian Journal of Geosciences,* 7, 5221-5237.

Wahyudi, C. and Minagawa, M., 1997. Response of benthic foraminifera to organic carbon accumulation rates in the Okinawa Trough. *Journal of Oceanography,* 53, 411-420.

Walker, C.H., Sibly, R.M., Hopkin, S.P. and Peakall, D.B., 2012. Principles of ecotoxicology, CRC press.

Walkley, A. and Black, I.A., 1934. An examination of the degtjareff method for the determining organic matter and a proposed modification of the chromic acid titration method. *Soil Science,* 37, 29-38.

Wang, X.H. and Andutta, F.P., 2013. Sediment transport dynamics in ports, estuaries and other coastal environments. Intech. Open Access Publisher.

Waples, D.W., 2013. Organic facies. In: Geochemistry in Petroleum Exploration. Springer Science and Business Media, Springer Netherlands, p. 14.

Welle, B.A., Hirsch, A.C., Davis, L.E., Johnson, A.C., Hunt, G.J. and Eves, R.L., 2004. Origin of calcareous sediments in the Holocene Pigeon Creek tidal lagoon and tidal delta, San Salvador Island, Bahamas. *American Journal of Undergraduate Research,* 3, 1-8.

Wolanski, E., 1994. Physical oceanographic processes of the Great Barrier Reef. CRC Press.

Wolanski, E., 1995. Transport of sediment in mangrove swamps. *Hydrobiologia,* 295, 31-42.

Wolanski, E., Andutta, F. and Delhez, E., 2012. Estuarine hydrology. *In Encyclopedia of Lakes and Reservoirs,* Springer Netherlands, 238-249.

Wolanski, E., Mazda, Y. and Ridd, P.. 1992. Mangrove hydrodynamics. In: Robertson, A.I. and. Alongi, D.M., (eds.). Tropical mangrove ecosystem, *American Geophysical Union,* Washington D.C., 436-462.

Woodroffe, C. 1992. Mangrove sediments and geomorphology. In Robertson, A. I. and Alongi, D.M. (eds.), Tropical mangrove ecosystem, *American Geophysical Union,* Washington, 7-41.

Xue-Feng, H.U., Yan, D.U., Jian-Wei, F.E.N.G., Sheng-Qiong, F.A.N.G., Xiao-Jiang, G.A.O. and Shi-Yuan, X.U., 2013. Spatial and seasonal variations of heavy metals in wetland soils of the tidal flats in the Yangtze Estuary, China: Environmental implications. *Pedosphere,* 23, 511-522.

Yang, J., Cao, L., Wang, J., Liu, C., Huang, C., Cai, W., Fang, H. and Peng, X., 2014. Speciation of metals and assessment of contamination in surface sediments from Daya Bay, South China Sea. *Sustainability,* 6, 9096-9113.

Yang, S., Tang, M., Yim, W.W.S., Zong, Y., Huang, G., Switzer, A.D. and Saito, Y., 2011. Burial of organic carbon in Holocene sediments of the Zhujiang (Pearl River) and Changjiang (Yangtze River) estuaries. *Marine Chemistry,* 123, 1-10.

Yang Z., 1988, Mineralogical assemblages and chemical characteristic of clay from sediments of the Yellow, Yangtze and Pearl Rivers and their relationship to the climate environment in their sediment source areas. *Oceanologia et Limnologia Sinica,* 19, 336 - 346.

Young, L.B. and Harvey, H.H., 1992. The relative importance of manganese and iron oxides and organic matter in the sorption of trace metals by surficial lake sediments. *Geochimica et Cosmochimica Acta,* 56, 1175-1186.

Yuan, C.G., Shi, J.B., He, B., Liu, J.F., Liang, L.N. and Jiang, G.B., 2004. Speciation of heavy metals in marine sediments from the East China Sea by ICP-MS with sequential extraction. *Environment International,* 30, 769-783.

Yu, X., Yan, Y. and Wang, W.X., 2010. The distribution and speciation of trace metals in surface sediments from the Pearl River Estuary and the Daya Bay, Southern China. *Marine Pollution Bulletin,* 60, 1364-1371.

Yüzereroglu, T.A., Gök, G., Çogun, H.Y., Firat, Ö., Aslanyavrusu, S., Maruldal, O. and Kargi, F., 2010. Heavy metals in Patella caerulea (Mollusca, Gastropoda) in polluted and non-polluted areas from the Iskenderun Gulf (Mediterranean Turkey). *Environmental Monitoring and Assessment,* 167, 257–264. Doi: 10.1007/s10661-009-1047-x.

Zhang, C., Yu, Z.G., Zeng, G.M., Jiang, M., Yang, Z.Z., Cui, F., Zhu, M.Y., Shen, L.Q. and Hu, L., 2014. Effects of sediment geochemical properties on heavy metal bioavailability. *Environment international,* 73, 270-281.

Zhang, J., Huang, W.W. and Martin, J.M., 1988. Trace metals distribution in Huanghe (Yellow River) estuarine sediments. *Estuarine, Coastal and Shelf Science,* 26, 499-516.

Zheng, S., Zheng, D., Liao, B. and Li, Y., 1997. Tideland pollution in Guangdong Province of China and mangrove afforestation. *Forest Research,* 10, 639-646.

Zhong, A.P., Guo, S.H., Li, F.M., Gang, L.I. and Jiang, K.X., 2006. Impact of anions on the heavy metals release from marine sediments. *Journal of Environmental Sciences,* 18, 1216-1220.

Zhou, H.Y., Peng, X.T. and Pan, J.M., 2004. Distribution, source and enrichment of some chemical elements in sediments of the Pearl River Estuary, China. *Continental Shelf Research,* 24, 1857-1875.

Zhou, J., Ma, D., Pan, J., Nie, W. and Wu, K., 2008. Application of multivariate statistical approach to identify heavy metal sources in sediment and waters: a case study in Yangzhong, China. *Environmental Geology,* 54, 373-380.

Zingde, M.D., Singbal, S.Y.S., Moraes, C.F. and Reddy, C.V.G., 1976. Arsenic, copper, zinc and manganese in the marine flora and fauna of coastal and estuarine waters around Goa. *Indian Journal of Marine Sciences,* 5, 212-217.

Zvinowanda, C.M., Okonkwo, J.O., Shabalala, P.N. and Agyei, N.M., 2009. A novel adsorbent for heavy metal remediation in aqueous environments. *International Journal of Environmental Science and Technology,* 6, 425-434.